OCTOBER 1961

International Chemical Engineering

THE UNIVERSITY OF MICHIGAN
NOV 1 5 1962
ENGINEERING LIBRARY

A quarterly journal of translations from Russia Eastern Europe and Asia

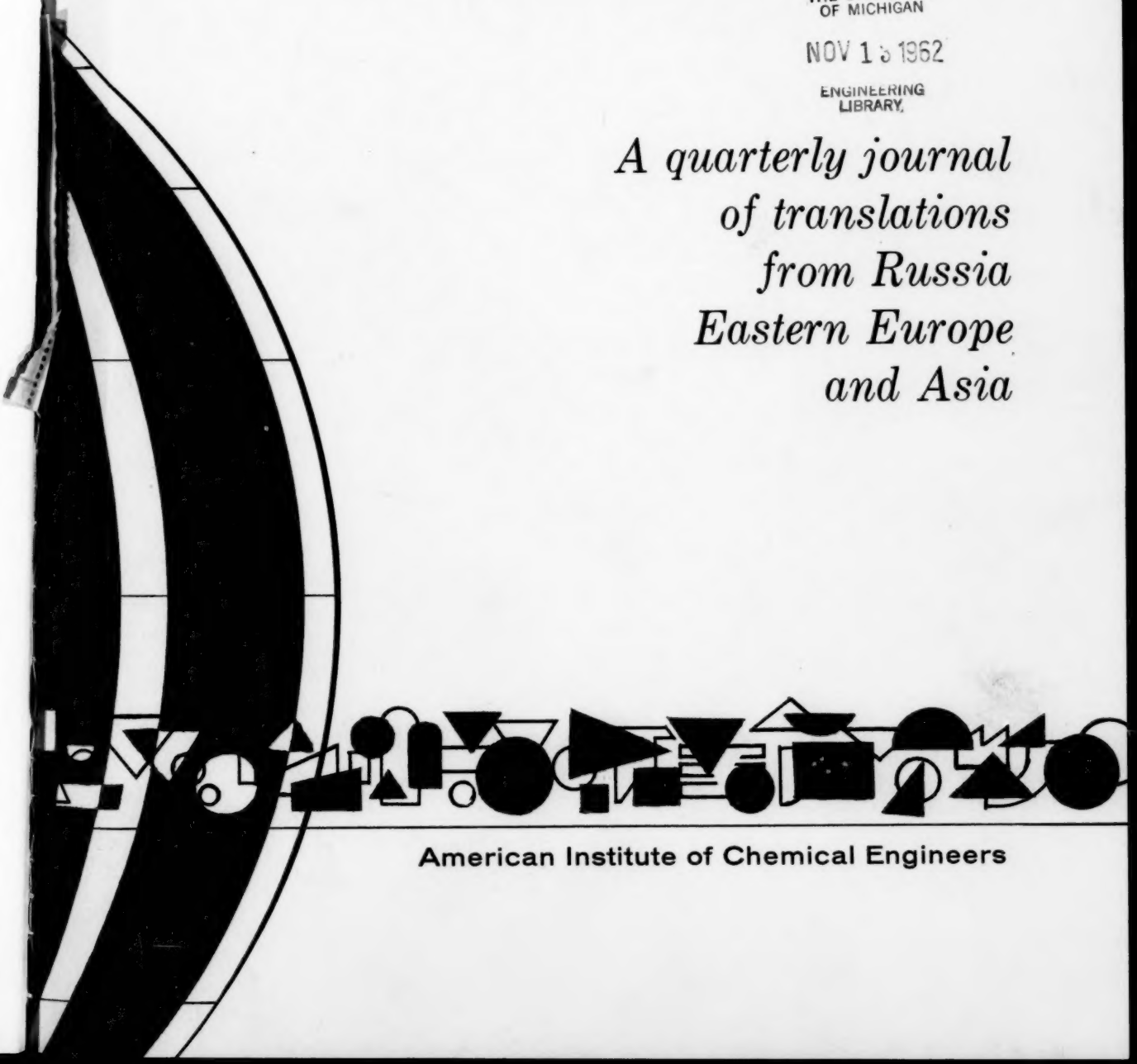

American Institute of Chemical Engineers

Publisher
F. J. Van Antwerpen

Editorial Director
Larry Resen

Editor
Waldo B. Hoffman

Assistant Editor
Renate U. Treibmann

OCTOBER 1961
Volume 1, No. 1

International Chemical Engineering

Advisory Board

Dr. RAYMOND F. BADDOUR, *Department of Chemical Engineering, Massachusetts Institute of Technology.*

Dr. HARDING BLISS, *Department of Chemical Engineering, Yale University, Editor A. I. Ch. E. Journal.*

Mr. D. M. BOYD, Jr., *Instrument Department, Universal Oil Products Co., Des Plaines, Illinois.*

Dr. MICHAEL J. DEUTCH, *consulting engineer, Washington, D. C.*

Dr. C. S. GROVE, Jr., *Director of Engineering Research, Syracuse University Research Institute.*

Dr. H. E. HOELSCHER, *Chairman, Department of Chemical Engineering, The John Hopkins University.*

Dr. C. J. HUANG, *Department of Chemical Engineering, University of Houston.*

Dr. J. J. MCKETTA, *Chairman, Department of Chemical Engineering, University of Texas.*

Dr. E. L. PIRET, *Principal Science Officer, American Embassy, Paris, France.*

Dr. F. M. TILLER, *Dean of Engineering, University of Houston.*

Dr. J. G. TOLPIN, *consultant, Chicago, Illinois, Professorial Lecturer, Northwestern University*

Dr. C. R. WILKE, *Head, Department of Chemical Engineering, University of California.*

Cover design by PAUL ARLT

INTERNATIONAL CHEMICAL ENGINEERING is published quarterly by the American Institute of Chemical Engineers, 345 East 47th Street, New York 17, New York. It is devoted in the main to selective translations of current chemical engineering literature from the Soviet Union, the countries of Eastern Europe, and Asia.

INTERNATIONAL CHEMICAL ENGINEERING is supported in large part by a grant from the National Science Foundation of the United States.

For transliteration of Russian, British Standard 2979 will be followed; for Chinese, the Wade-Giles system.

Subscription Prices—Per Year *(4 issues)*

United States $15.00

Canada $15.50

Pan America $16.50

Other Foreign $17.00

Subscriptions should be addressed to INTERNATIONAL CHEMICAL ENGINEERING, 345 East 47 Street, New York 17, New York.

Application to mail at second-class postage rates pending at New York, N. Y. and Ann Arbor, Michigan.

Table of contents

Vol. 1, No. 1 INTERNATIONAL CHEMICAL ENGINEERING October 1961

A. V. Agafonov, I. E. Gel'ms, and E. I. Rabinovich. **1** Choice of a catalyst for cracking residual petroleum fractions and an investigation of catalyst poisoning in the process, *Khim. i Tekh. Topliv i Masel 5 (1960)*, U.S.S.R.

C. S. Grove, Jr. and R. V. Jelinek, Syracuse University. **6** Status of crystallization in the Soviet Union, *(Review article)*, UNITED STATES.

A. I. Leonov **13** Influence of the gaseous medium on the course of physicochemical processes in semiconductor oxides at high temperatures, *Izvest. Akad. Nauk SSSR, Otdel. Khim. Nauk No. 9, 1529-1534 (1960)*, U.S.S.R.

V. A. Kargin, V. A. Kabanov, V. P. Zubov, and I. M. Papisov. **17** Polymerization of acetone, *Doklady Akad. Nauk SSSR 134, No. 5, 1098-1099 (1960)*, U.S.S.R.

Yu. A. Shlyapnikov, V. B. Miller, M. B. Neiman, E. S. Torsueva and B. A. Gromov. **19** Thermo-oxidative degradation of polypropylene: A study of the comparative effectiveness of some antioxidants, *Vysokomolekulyarnye Soedineniya 2, No. 9, 1409-1412 (1960)*, U.S.S.R.

G. D. Efremova and R. O. Koroleva. **22** The equilibrium solid-liquid-gas in the system melamine-ammonia-CO_2, *Zhurnal Fizicheskoi Khimii, Vol. 35, No. 4, (1961)*, U.S.S.R.

G. D. Efremova and G. G. Leont'eva. **24** The solubility of melamine in solutions of dicyandiamide in liquid ammonia, *Khimicheskaya Promyshlennost, No. 8, (1960)*, U.S.S.R.

G. P. Korneichuk, V. A. Roiter, V. Ya. Vol'fson, Ya. V. Zhigailo, and A. Z. Lyubiteleva. **26** Peculiarities of the catalytic oxidation of naphthalene: Investigation of the oxidation of naphthalene in deep beds of vanadia catalysts, *Ukrain. Khim. Zhur. 26, No. 4, 432-439 (1960)*, UKRAINE, U.S.S.R.

V. Ya. Vol'fson, G. P. Korneichuk, V. A. Roiter, and Ya. V. Zhigailo. **31** Peculiarities of the catalytic oxidation of naphthalene: Kinetics of the oxidation of naphthalene in deep beds of vanadia catalysts, *Ukrain. Khim. Zhur. 26, No. 5, 588-593 (1960)*, UKRAINE, U.S.S.R.

S. G. Lyubetskii, B. A. Dolgoplosk, and B. L. Erusalimskii. **35** Polymerization of ethylene under the influence of free radicals. Kinetics of ethylene polymerization in benzene and heptane solution, *Vysokomolekulyarnye Soedineniya 3, No. 5, 734-739 (1961)*, U.S.S.R.

M. S. Nemtsov. **39** Kinetic relationships in the reaction of olefins with sulfuric acid, *Khim. Prom. No. 8, 15-23 (1960)*, U.S.S.R.

A. G. Kasatkin, S. Z. Kagan, and V. G. Trukhanov. **50** Empirical equilibrium distribution equations for liquid-liquid systems, *Khim. Prom. No. 6, 50-54 (1960)*, U.S.S.R.

G. M. Panchenkov, Yu. M. Zhorov, and Yu. Yui-lin. **55** Kinetic aspects of the catalytic cracking of heavy distillate stocks, *Khim. i Tekhnol. Topliv i Masel 5, No. 11, 4-8 (1960)*, U.S.S.R.

G. M. Panchenkov and Yu. M. Zhorov. **58** A method for the determination of the rates and kinetic constants of complex chemical reactions in a flowing system, *Doklady Akad. Nauk SSSR 135, No. 5, 1172-1175 (1960)*, U.S.S.R.

G. M. Panchenkov, V. A. Skoblo, and Yu. M. Zhorov. **61** Determination of effective diffusion coefficients in porous sorbents, *Izvest. Vysshikh Ucheb. Zaved., Neft i Gaz 4, No. 1, 73-77 (1961)*, U.S.S.R.

L. Yu. Artyukh, L. A. Vulis, and V. P. Kashkarov. **64** Combustion of gas flowing at the surface of a plate, *Inzhener-Fiz. Zhur., 4, No. 3 (1961)*, KAZAKHSTAN, U.S.S.R.

continued on following page

N. I. Gel'pern and V. P. Kvasha. **68** Maintaining optimum temperature conditions in chemical reactors, *Khimicheskaya Promyshlennost, No. 1, 51-56 (1961)*, U.S.S.R. *(1961)*, U.S.S.R.

Yu. G. Zelinski and V. V. Kafarov. **74** Hydrodynamic conditions on open-grid (turbogrid) trays, *Khimicheskaya Promyshlennost, No. 2, 122-126 (1961)*, U.S.S.R. *122-126 (1961)*, U.S.S.R.

M. S. Furman, A. D. Shestakova, I. L. Arest-Yakubovich, and N. A. Lyubitsina. **79** Oxidation of n-butane in the liquid phase under pressure, *Khimicheskaya Promyshlennost, No. 1, 6-11 (1961)*, U.S.S.R.

N. B. Yanovskaya and K. K. Potapova. **85** Investigations of polyacrylonitrile fibers obtained at various drafts, *Izvest. Vysshikh Ucheb. Zaved., Tekhnol. Tekstil. Prom., No. 3 (16), 24-29 (1960)*, U.S.S.R.

P. V. Varentsov and M. S. Yufa. **88** The movement of a bed of solid particles in rotary kilns, *Khim. Mashinostroenie, No. 5, 22-26 (1959)*, U.S.S.R.

Ágnes Somogyi, Istvan Géczy, and János Dobó. **93** Graft copolymerization in the presence of benzoyl peroxide-dimethyl aniline with the aid of irradiation, *Magyar Tud. Akad. Kem. Oszt. Közl., 15, 18-28 (1961)*, HUNGARY

V. T. Slavyanskii, E. N. Krestnikova, and M. V. Proskuryakov. **99** Study of bubble formation in glass melting under vacuum, *Steklo i Keramika 16, No. 9, 25-29 (1959)*, U.S.S.R.

L. M. Mirzoeva. **106** Determination of solid phase concentration in a two-phase medium in upward motion in a vertical tube, *Izvest. Akad. Nauk Azerbaidzhan. SSR No. 9, 11-19 (1957)*, AZERBAIDZHAN, U.S.S.R.

F. Mihail, F. Gherghel, M. Stănescu, and S. Kornbaum. **110** Chlorination of low-pressure polyethylene and its compounding with polyvinyl chloride, *Revista de Chimie, 12, No. 5 (1961)*, ROMANIA.

Vendelín Macho **117** Effect of sulfur and some of its compounds on the Oxo process, *Chem. Zvesti 15, 181-190 (1961)*, CZECHOSLOVAKIA.

A. A. Berlin, L. I. Boguslavski, R. Kh. Burshtein, N. G. Matveeva, A. I. Sherle, and N. A. Shurmovskaya. **122** Some electrophysical properties of polymer complexes of tetracyanethylene with metals, *Doklady Akademii Nauk SSSR (Academy of Sciences, USSR. Reports), 136, No. 5, 1127-1129 (1961). Physical Chemistry*, U.S.S.R.

Ryszard Chudzikiewicz. **124** Factors affecting the degree of mixing of granular materials, *Przem. Chem. 40, 48-51 (1961)*, POLAND.

Yu. N. Vol'nov and B. V. Ozimov. **129** Reflection spectra and their application to the study of sorption processes, *Zhur. Vsesoyuz. Khim. Obshchestva im. D. I. Mendeleeva 5, No. 5, 591-591 (1960)*, U.S.S.R.

I. A. Uskov, Yu. G. Tarasenko, and T. A. Kusnitsyna. **132** Compounding of dissolved polymethylmethacrylate with fillers, *Vysokomolek. Soed. 3, No. 1, 37-40 (1961)*, UKRAINE, U.S.S.R.

135 List of journals currently received and monitored

Information retrieval follows page 136

EDITORIAL

THIS, the first issue of *International Chemical Engineering*, is the initial step in a program, encouraged, and supported in part by the National Science Foundation of the United States, to present selectively the most important current work in chemical engineering going on in the Soviet Union, Eastern Europe, and Asia.

An effort will be made in this quarterly journal to spotlight such areas of chemical engineering as are being particularly emphasized in the Soviet Bloc countries. Inevitably, certain individual issues of the journal will appear to be rather heavily concentrated in one or more particular areas—petrochemicals or catalysis, for instance. This will depend on the interest and quality of published Soviet Bloc work over any given period of time. However, in the long run, coverage will be as wide as possible, based on a rather broad definition of chemical engineering, embracing even certain fields which, in a more traditional view, might be looked on as "fringe areas." In this connection, we wish to appeal strongly to our readers for expression of their opinions and desires as to general areas of emphasis and selection of types of articles to be translated and published in *International Chemical Engineering*. Correspondence will be welcomed—and heeded.

Our intent is to cover current work in the countries involved. This does not, however, preclude the possibility of focusing attention on an isolated, heretofore untranslated article which is considered important and fruitful, even though it may be as much as two or three years old. This will not be the rule, we hasten to add.

On page 135 of this issue is a list of the journals now being received and monitored. This list is in process of continuous expansion, particularly by setting up regular exchanges of technical literature between Soviet Bloc institutions of learning and the A.I.Ch.E. We wish to ask again for help in evaluating this mass of technical literature on the part of interested chemical engineers who read the languages in question. We should also like to hear from public or private groups, both in the United States and abroad, which are involved in similar endeavors in this field. This with a view to the setting up of areas of mutual assistance and cooperation, as well as to avoid duplication of evaluation and translation effort.

Systems of notation and units, as well as editing style in general, present unusual difficulties in a journal which draws for its source material on a wide variety of journals published originally in eight or ten different languages. Every effort will be made to reduce these heterogeneous systems to standard American usage. In cases where this is not completely possible, differences will be explained in footnotes or in translator's remarks. Clarity will be the goal.

Starting with this issue, *International Chemical Engineering* will follow the new A.I.Ch.E. program of Information Retrieval, based on the concept coordination system of information storage and retrieval. See pages following page 136 for details and for key words and abstracts covering all articles in the issue.

W.B.H.

WE WISH TO THANK the following chemical engineers who have given of their time and effort in evaluation of material in the original languages. This has been extremely valuable in selection of articles for inclusion in this issue.

W. Begell, Roger & Royer, Inc., New York, N. Y.

Y. C. Chang, United States Steel Corp., Monroeville, Pa.

Kwang-Chu Chao, California Research Corp., Richmond, Calif.

Tsai-yen Chen, Yale University, New Haven, Conn.

D. S. Davies, Dorr-Oliver, Inc., Westport, Conn.

L. T. Fan, Kansas State University, Manhattan, Kans.

T. P. Forbath, American Cyanamid Co., New York, N. Y.

N. Gilbert, University of Cincinnati, Cincinnati, Ohio

Y. Y. Hsu, National Aeronautics and Space Administration, Lewis Research Center, Cleveland, Ohio

H. W. Hsu, Thermodynamics Laboratory, Lafayette, Ind.

L. Jacolev, Associated Technical Services, Inc., East Orange, N. J.

G. S. Lee, Arthur D. Little, Inc., Cambridge, Mass.

R. H. Newton, Herman C. Schutt, Boston, Mass.

B. Mandelik, Chemical Construction Corp., New York, N. Y.

G. Miskosza, DuPont of Canada Ltd.

G. T. Motock, Olin Mathieson Chemical Corp. New Haven, Conn.

H. L. Olin, University of Iowa, Iowa City, Iowa

L. C. Pan, Chemical Construction Corp., New York, N. Y.

S. Sacharuk, Olin Mathieson Chemical Corp., Salem, Mass.

D. Satas, Kendall Corp., Chicago, Ill.

R. C. Shen, U. S. Industrial Chemicals Corp., New York, N. Y.

J. H. Staib, Esso Research and Engineering Co., Linden, N. J.

G. C. Szego, Space Technology Laboratories, Los Angeles, Calif.

S. Szepe, Sinclair Research Laboratories, Harvey, Ill.

C. Wang, Tonawanda Laboratory, Linde Air Co., New York, N. Y.

R. E. C. Weaver, Tulane University, New Orleans, La.

C. Y. Wen, University of West Virginia, Morgantown, W. Va.

E. Y. Weissman, Case Institute of Technology, Cleveland, Ohio

H. H. Yang, Texas U. S. Chemical Co., Port Neches, Texas

A. V. Agafonov
I. E. Gel'ms
E. I. Rabinovich

USSR

Choice of a Catalyst for Cracking Residual Petroleum Fractions and an Investigation of Catalyst Poisoning in the Process*

Recent Russian work on the disposition of heavy petroleum fractions, plus an investigation of the key problem – poisoning by metals.

A special circumstance in the operating conditions of a catalyst in the cracking of a residual crude is an accelerated poisoning process under the combined action of temperature, water vapor, sulfur compounds, and resinous substances, a result of their content of metal-organic compounds.

Such poisoning is exhibited considerably more strongly with the use of powdered catalysts.

It is known that the high molecular weight hydrocarbons in the heavy portion of the crude, which in the catalytic cracking of a residual crude are the principal source of reformed products, have a low stability at the temperatures used for cracking. Under these conditions, there is no need for a large decrease in the activation energies of the selective splitting reactions which differentiate the catalytic process from thermal decomposition. In addition, the use of high-activity catalysts for this purpose involves a considerable increase in gas and coke formation. On the other hand, as a result of the intensive poisoning of the catalyst in the process of cracking the residual crude, the advantage of active silica-alumina catalysts for carrying out the secondary reactions such as redistribution of the hydrogen, cyclization, isomerization, etc., is lost rapidly, since it is precisely these reactions which are suppressed first.

The measure of the necessary activity for a catalyst employed in the cracking of a residual crude should be the attainment of good motor performance properties in the gasolines, together with a favorable gas composition and intensive conversion of the residual fractions.

Reserves of residual crude do not limit development of the catalytic cracking process. Therefore, installation of large plants is economically advantageous. However, in this case, there arises the necessity for large quantities of catalyst, and there is a great increase in the catalyst consumption necessary to maintain equilibrium activity. Processing of a residual crude, in view of the large deposition of coke, requires a highly effective process for burning off the coke, and the use of large quantities of steam for better evaporation and desorption of the products of reaction from the catalyst surface, and for the protection of the catalyst surface from poisoning by sulfur and metals. These conditions require the use of catalysts thermally stable in the presence of water vapor and sulfur compounds.

NATURAL CATALYSTS

The conditions listed above are satisfied by refractory high-alumina kaolinitic clays and kaolins, some varieties of which, merely after a simple thermal treatment, already possess sufficiently good stable catalytic properties.

The existance of plastic and cohesive properties in the majority of such clays has enabled the All-Union Scientific-Research Institute of the Petroleum Industry* to develop techniques for preparing stable powdered catalysts of the microspherical type by the spray drying of suitably prepared clay suspensions.

Sufficiently rich reserves for production of such catalysts are found in many regions of the country,

*On a process for catalytic cracking of residual crude, see: *Khim. i. Tekh. Topliv i Masel*, 4 (1959).

This article first published in *Khim. i Tekh. Topliv i Masel* 5, 6-12 (1960).

*Details of the technology for preparation of microspherical catalysts from kaolin clays were worked out at the Gor'kov experimental base of the All-Union Scientific-Research Institute for the Petroleum Institute by S. V. Kapatsinskii, E. I. Kislyakova, V. A. Burylov, et al.

Table 1

Properties of typical natural catalysts obtained by the thermal treatment of kaolin

Clays	Activity indices		Abrasion resistance index*	Bulk wt., g./cc.	Specific surface sq.m./g.	Specific pore volume cc./g.	Al_2O_3 content, wt.%
	activity index	stability index					
Pelletized catalysts							
Suvorov basic, grades SO, S1, S2.....	15–17	17–18	30–50***	1.05–1.1	25–30	0.04–0.06	42–43
Latnin basic, grade 1, L-1..	24–27	20–22	5–10	1.1–1.15	35–40	0.12–0.14	40–43
Troshkov, grade 1.....	26–29	24–27	10–15	1.1–1.12	70–80	0.15–0.17	38–43
Microspherical catalysts							
Suvorov (with addition of 20–25% Mayach)	11–15	14–15	19–25	1.0–1.05	25–30	0.04–0.06	36–38
Troshkov, grade 1.....	21–22**	20–21	22–24	1.1–1.15	60–70	0.13–0.15	34–36

*The abrasion index refers to testing of the pelletized catalysts with air-lift (TU-367-circulation), and of the microspherical catalysts under abrasion in a centrifugal grinding mill (TsM-57).

**In the case of calcining under special conditions, the activity index reaches 25–27 points.

***To assure high abrasion resistance, high-plasticity clays are required in the charge.

some of which are in the neighborhood of large petroleum refining centers.

For preparation of catalysts for the cracking of residual crude there have proven suitable, in the pure form or as composites, the clays of the very rich deposits in the central districts of the European part of the Russian Soviet Federative Socialist Republic (Suvorov, Latnin, Borovichi), the Tavtiman, Mayach, and certain other clays in Bashkir, the clays of the Mezhnikov deposit in the Urals, the very large-scale Troshkov deposits in the Irkutsk region, and many other deposits which have been little investigated as yet.

All of these deposits are far from uniform in the quality of the clay, which is separated into grades for production of catalysts, just as for production of refractory materials and ceramics. Considerable reserves of clay from the deposits mentioned above may be used without complicated purification methods for preparation of catalysts for the cracking of residual crudes. Only a few of these clays (of the higher grade) can be used to prepare catalysts for cracking of distillate crude.

In this category of clays belong, for example, the higher grades of the Troshkov kaolins.

Table 1 shows some characteristics of pilot-plant samples of natural catalysts prepared from various natural clays. The activity of the catalysts in this table is characterized by indices based on the cracking of a light crude, since this was considered more sensitive to changes in the physical and chemical properties of the natural catalysts.

INVESTIGATION OF CATALYST POISONING

The question of the poisoning of a cracking catalyst operating on a distillate crude has been the subject of a number of published papers (2, 3, 4, 5, 6). We have studied this question in its application to a concrete process for cracking a residual crude on a powdered catalyst.

Table 2 shows experimental data relating to the deactivation of the simplest type of natural microspherical catalyst prepared from Troshkov clay, in a process for cracking petroleum and semi-fuel oil. These data were obtained during prolonged testing in a pilot plant.* Characteristics of the material used as cracking stock are given briefly in Table 3.

In Table 2, in addition to the usual activity indices, which give only indirect characteristics for cracking of residual crude, are shown data from a number of direct control experiments in the cracking of petroleum as well as of a heavy distillate crude. These experiments were carried out under different conditions during various periods in the life of the catalyst. There are also shown the amount of metal deposited on the catalyst, and the change in its structure as a function of its specific surface and its porosity.

It is evident from the data in Table 2 that, as a result of only approximately 20 days of operation of a process for cracking petroleum or semi-fuel oil, with the given rate of replenishment of the system with fresh catalyst (an average of about 1.5% referred to the crude, including all forms of loss and sample taking), the state of the catalyst can be estimated as at equilibrium by the following criteria: by the amount of crude processed on the average per unit of catalyst employed in the process; by the

*The pilot plant work was carried out under the direction of N. A. Chepurov and R. N. Yudinson.

Table 2.

Deactivation of catalyst in petroleum and semi-fuel oil cracking (temperature, 450°C)

Feedstock for pilot-plant control experiments	Petroleum					Distillate	
Amount of feedstock (petroleum and semi-fuel oil) treated with the catalyst operating in the system, kg./kg.	4.5	14	17	36	37	0.0	43
Duration of catalyst operation in cracking of petroleum and semi-fuel oil, days	2.0	6.0	8.0	19.0	21**	0.0	34
Yield of cracking products in control experiments, % by wt. on crude							
Gas up to C_4, inclusive	4.9	4.9	4.5	3.1	2.8	8.3	5.4
Gasoline, C_5–200°C*	35.2	35.0	35.8	32.4	32.1	25.6	19.0
Fraction from 200–350°C	35.6	36.2	38.2	38.2	36.7	–	–
Residue above 500°C	2.2	1.2	0.6	1.6	0.9	–	–
Coke	8.0	8.2	7.9	9.7	$n \cdot 10^{-3}$	3.9	7.2
Gasoline: coke ratio	4.4	4.3	4.5	3.5	3.2	6.6	2.6
Composition of cracking gases, wt. % on gas							
H_2	2.9	5.4	5.1	9.0	6.8	1.3	13.1
CH_4	17.0	19.9	14.0	18.3	16.9	9.4	14.2
C_2	22.2	19.9	20.9	17.8	18.7	11.3	10.2
C_3	26.7	24.9	29.2	25.4	25.1	29.0	29.2
C_4	31.2	29.9	30.8	29.5	32.5	49.0	33.3
State of catalyst from laboratory index determination and analyses							
Activity index	18.7	11.1	9.7	6.0	7.7	21.5	7.7
Coke formation	2.1	2.9	3.7	3.4	3.5	2.2	3.4
Gasoline: coke ratio	8.9	3.8	2.6	1.8	2.2	9.8	2.3
Content on catalyst, wt. %							
V	0.015	0.091	0.065	0.16	0.15	0.007	0.15
Ni	0.012	0.055	0.065	0.10	0.06	10^{-3}	0.08
Co	–	0.001	0.0025	0.009	0.025	–	0.008
Specific surface, sq.m./g.	–	–	51.5	43.5	40.0	53	43
Specific porosity, cc./g.	–	–	0.12	–	–	0.125	0.13

*In the original petroleum, the content of gasoline fractions was about 23%.

**The petroleum was processed for 21 days, the semi-fuel oil longer.

indices established in the control experiments on cracking of petroleum; by the established level of the catalyst activity index, referred to cracking of a light crude; by the condition of the porous structure; and by the metal content determined.

A change in the parameters set forth in Table 2 may be considered a result of catalyst poisoning by metals and sulfur, together with the effects caused by heat and steam poisoning (decrease in surface and porosity).

Deposition of metals, as the sum of the three elements analyzed for, amounted to 0.22–0.27%, based on the weight of the catalyst. Heat and steam poisoning amounted to an insignificant decrease in the active surface from 53 to 43 cu.m./g., and a practically unchanged porosity.

The selectivity of the catalyst action changed sharply, which is characteristic of poisoning by metals as well as by sulfur. However, a comparison of the results of these experiments with laboratory tests on the artificial deposition of metals on a catalyst, that is, excluding the side action of sulfur compounds, showed that the main role in catalyst poisoning is played by the metals (Table 4).

The satisfactory correspondence between the de-

Table 3.

Properties of cracking stock

Indices	Petroleum	Semi-fuel oil
Density, d_4^{20}	0.872	0.927
Sulfur content, wt. %	1.78	2.29
Carbon residue, wt. %	5.37	7.71
Content of asphaltenes, wt. %	5.1	6.1
Silica gel tars, wt. %	21.5	24.0
Water-soluble chlorides, mg./l.	100	~160
Ash, wt. %	0.03	0.05
Content of vanadium	0.006	0.006
Content of nickel	–	0.0042
Spectroscopic analysis also detected	Na, Mg, Si, Ti, Ca, Ba, Al, Mn, Fe, Co, Cu, Zn, etc.	

Table 4.

Poisoning action of metals deposited artificially and in the cracking process

Properties	Method of depositing metals	
	Artificially from salt solution	In the cracking process
Content, wt. %:		
V	0.14	0.15–0.16
Ni	0.09	0.06–0.1
Co	None	0.025–0.009
Yield in cracking light feedstock, wt. %		
Gasoline (index)	7.9	7.7–6.0
Gas	4.8	3.8–4.0
Coke	5.3	3.5–3.4
Yield in cracking petroleum, wt. %		
Gasoline	23.3	25.2–27.2
Gas	5.2	7.6–7.2
Coke	16.7	13.4–11.3

Table 5.

Influence of metals deposited on the catalyst on some properties in cracking distillate crude and petroleum

Properties	Properties of crude cracked			
	Distillate		Petroleum	
	Pilot plant	Laboratory	Pilot plant	Laboratory
Total content of V, Ni, and Co in catalyst, wt. %	0.238	0.238	0.252	0.252
Ratio of coke yields on poisoned and fresh catalysts	1.85	1.55	1.2	1.2
Relative decrease in gasoline yield	1.35	2.8	1.1	1.25
Factor of decrease in gasoline: coke ratio	2.5	4.2	1.3	1.4
Factor of increase in hydrogen content of cracking gas	10	–	2.7	–

activation indices of the catalyst under artificial poisoning and the data obtained on poisoning in a process of petroleum cracking provides a basis for extrapolating certain laboratory test results also to the actual operating conditions of a process for cracking crude containing metals.

There should be noted the considerably lower degree of catalyst poisoning with an equal quantity of deposited metals in the cracking of residual crude, in comparison with the cracking of distillates, as illustrated by the series of indices set forth in Table 5.

STEAM TREATMENT

Attention should also be paid to the results of laboratory experiments on the role of water vapor carried in with the crude, and for treatment of the regenerated catalyst.

In Table 6 are shown the results of experiments to study the effects of treatment with steam at 750°C of catalysts with different quantities of metals previously deposited on them.

As can be seen from the data in the table, treatment of a poisoned catalyst with steam aids in

Table 6.

Action of steam on a microspherical catalyst made from Troshkov clay, with varying metal content

Properties	Initial catalyst		Same catalyst after deposition of:					
			0.06% V		0.1% V		0.95% V	
	Before steam treatment	After steam treatment	Before steam treatment	After steam treatment	Before steam treatment	After steam treatment	Before steam treatment	After steam treatment
Cracking of light standard crude in the testing unit								
Gasoline yield (index), %	21	20	14.6	20.2	11.4	13.3	13.9	13.0
Gas yield, %	8.2	6.0	5.6	6.1	4.0	3.0	6.2	3.6
Coke yield, %	2.7	1.0	2.4	1.5	3.5	1.6	4.8	1.4
Specific gravity of gas, g./l.	0.83	0.98	0.58	1.05	0.39	0.6	0.45	0.5
Gasoline: coke ratio	7.8	20	6.1	13.5	3.3	8.3	2.9	9.3
Cracking of petroleum in the testing unit								
Gasoline yield	35.4	34.3	30.1	34.9	–	–	30.6	31.3
Gas yield	11.7	7.6	10.1	7.0	–	–	10.5	6.5
Coke yield	10.9	8.1	11.2	8.4	–	–	12.8	8.9
Specific gravity of gas	0.89	0.98	0.77	1.11	–	–	0.61	0.68
Gasoline: coke ratio	3.2	4.3	2.7	4.2	–	–	2.4	3.5

restoration of the lost activity, and increases the selectivity of the catalyst.

The positive effect of steam on a catalyst contaminated with metals depends on the quantity and state of the metals deposited; the steam is specially effective in the initial stages of catalyst poisoning. It is natural that such an effect can be observed fully only for catalysts which are sufficiently stable under heat and steam poisoning. Such catalysts, in particular, are the high-alumina catalysts made from Troshkov clay. However, the effect of steam treatment of a catalyst poisoned with metals in the cracking process is not lasting. Therefore, continuous feeding of steam with the cracking stock, as in the treatment of a regenerated catalyst, is an important condition for the successful operation of a process for cracking residual crude.

Tests made during continuous investigation of a catalyst in a pilot plant in the cracking of petroleum and semi-fuel oil, and special laboratory tests, lead to the conclusion that a process for cracking residual crude on a microspherical natural catalyst can be based on standard indices determined by the equilibrium state of the catalyst. Such indices have also been recommended as a starting point for design calculations (1, 8).

For cracking of residual crude, more detailed studies were made of a microspherical catalyst made from Troshkov clay, and verification tests were also made on samples of catalysts from Tavtiman and Suvorov clays. A catalyst made from Suvorov clay, which was somewhat inferior to Troshkov clay in initial activity and strength, nevertheless gave better results in comparative stability.

ECONOMICS OF NATURAL CATALYSTS

Capital investment in the construction of an industrial catalyst plant is estimated at not more than 500 rubles per ton per year of catalyst production capacity. In addition, an investment is required in the open pit mining operation at the site of the clay deposits, which amounts to from 100 to 200 rubles per ton per year of catalyst production capacity. The total capital investment for production of a catalyst plus the necessary raw material base, as well as the production cost of such a simple natural catalyst, is many times lower than for production of a synthetic catalyst. Under conditions where it is necessary to adjust within a short period of time to a rapidly increasing flow of raw petroleum, this is extremely significant.

Calculations show that the use of natural catalysts instead of synthetic makes it possible to economize only in the capital investment for production of the catalyst, and that the cost of the initial charge is not less than 15 rubles per ton per year of crude destined for catalytic cracking.

An economic comparison of the operating indices of different catalysts is more complex, since in this case it is difficult to find a measure for evaluation of small changes in the balance and quality of the cracking products, as well as for changes in the operating characteristics of the plant which arise from a change of catalysts. However, in the case of the cracking of a residual crude on a microspherical natural or synthetic catalyst in their equilibrium states, no significant advantage was remarked for the synthetic catalyst. For this reason, the decisive influence on the economics of the process is the production cost of the catalyst.

CONCLUSIONS

1. The catalytic cracking of residual fractions of petroleum with natural microspherical catalysts may be based on standard indices, in spite of the poisoning of the catalyst by metals contained in the crude.

2. For the process, it is advantageous to use the simplest natural catalyst made from high-alumina clays with a kaolin base.

3. Production of such a catalyst is assured by a raw material base which extends over many regions of the Soviet Union.

4. The strongest effective factor in the poisoning of a catalyst in the process for cracking of residual forms of crude is the deposition of metals. However, the catalyst retains sufficient activity to carry out its catalytic functions in splitting off the high molecular weight portion of the raw material, and to perform its necessary role as heat and coke carrier.

5. For stable operation of the catalyst in the process of cracking a residual crude, an essential role is played by steam, whether fed into the reaction zone, or used for processing a catalyst after regeneration.

6. Use of a natural catalyst for cracking residual crude instead of a synthetic one shows a significant economic advantage.

LITERATURE CITED

1. Agafonov, A. V., Sukhanov, V. P., Rabinovich, E. I., Yudinson, R. N., Doklad na IV Mezhdunarodnom neftyanom kongresse (Transactions of the 4th World Petroleum Congress), III, p. 535 (1955).

2. Wunderlich, O. A., Prichard, J. J., Ivey, F. E., Jr., *Oil and Gas Journal*, 54, No. 24, p. 121 (1955).

3. Small, N. J., Kirkadly, P. H. S., Newton, A., Doklad na IV Mezhdunarodnom neftyanom kongresse (Transactions of the 4th World Petroleum Congress), III, p. 261 (1955).

4. McEvoy, J. E., Milliken, T. H., Mills, G. A., *Ind. & Eng. Chem.*, No. 5, p. 865-868 (1957).
5. Rothrock, J. J., Birkhimer, E. R., Leum, L. N., *Ind. & Eng. Chem.*, 49, No. 2, p. 272-276 (1957).
6. Conner, I. E., Jr., Rothrock, J. J., Birkhimer, E. R., Leum, L. N., *Ind. & Eng. Chem.*, 49, No. 2, p. 276-282 (1957).
7. Johnson, P. H., Eberline, C. R., Denton, R. V., *Ind. & Eng. Chem.*, 49, No. 8, p. 1255 (1955).
8. Agafonov, A. V., Manakov, N. Kh., Manshilin, V. V., et al., *Khim. i Tekh. Topliv i Masel*, No. 4, (1959).

C. S. Grove, Jr.
R. V. Jelinek

UNITED STATES

Status of Crystallization in the Soviet Union

The status of crystallization in the Soviet Union is on a par with that of the Western World. A review of theoretical and mathematical studies, plus an investigation of experimental studies which have led to industrial applications in the Soviet Union.

TSARIST Russia had an excellent competence in chemistry and chemical research which received international recognition. This excellence has continued in present day Soviet research in various areas of chemistry and chemical phenomena. Except in certain heavily emphasized chemical areas, theoretical and basic achievements have been more noteworthy than applied engineering counterparts.

There has been little distinction in Soviet education and research between basic sciences and engineering sciences, a fact more noticeable with respect to chemistry and chemical engineering than in other areas. While recent pronouncements of Soviet policy indicate an intent to differentiate between basic scientific research and applied engineering research, the distinction to date does not show a separation to the degree which is common in the Western World, especially the United States. A separation into discrete unit operations is very uncommon in Soviet educational institutions and also in Soviet literature. Accordingly, research in chemical engineering is reported in a variety of sources. For example, crystallization research is published in both basic and applied journals.

In general, Soviet scientists in the field of crystallization appear thoroughly familiar with Western techniques and research. The best Soviet research is excellent and makes good use of experimental and theoretical approaches. In crystallization, the leading research facility is the Institute of Crystallography, Academy of Sciences, Moscow. At this Institute competent scientists with good equipment produce many excellent research studies and publications. This Institute has no counterpart in the Western World.

Soviet chemical engineers and technologists appear to be slow in translating results of basic research into applied practices. This weakness is recognized in the USSR and efforts are being made to make more rapid application of basic research results for improvement of technical processes (2, 103, 116, and 117).

Shubnikov (99) specifically discusses the future development of crystallography in the light of resolutions adopted by the 21st Congress of the Communist Party of the Soviet Union. The following objectives were set: 1. discovery of the laws of formation of crystals; 2. study of the laws of atomic-molecular structure on the basis of methods developed by crystallography itself, and examination of the connection between structure and properties of crystals; 3. study of the laws of the interaction of a crystal with its medium and environment; and, 4. production and study of crystals possessing properties required by new technology and the introduction of such crystals into the national economy. In a previous paper, Shubnikov (100) pointed out that crystal formation problems are of great importance in science and technology. Modern solid state physics (piezo- and ferroelectricity, ferromagnetism, luminescence, photoelectricity, semiconduction, optics) is closely bound to a study and

This article was written specially for *International Chemical Engineering*. The authors are associated with Syracuse University, Syracuse, N. Y.

use of large uniform crystals. Crystal studies also contribute strongly to metallurgy, chemical, and ceramic industries as well as to virology.

GROWTH OF CRYSTALS

There are presently two principal theories of ideal crystal growth: 1. the Kossel-Strauskii molecular-kinetic theory of ideal perfect growth; and, 2. the Frank theory of ideal imperfect dislocation growth. The first theory ignores crystal imperfections and introduces a number of simplifying assumptions in analyzing growth processes. The second theory incorporates initial imperfections, mainly as screw dislocations, which gradually rise from the crystal faces and cause continuous growth in a spiral fashion. The Frank theory appears to be stressed more by the Soviet scientists.

Sheftal (94) has discussed the normal development of a crystal in favorable conditions and the complex abnormal development as influenced by unfavorable conditions due to the action of the medium. The manner in which the physical properties of crystals depend on growth conditions is determined by inclusions from the medium, by stresses caused by uneven distribution of inclusions, and by supersaturation. Good crystal growth comes from a favorable chemical environment, with good stirring to provide uniform material supply to the crystal surfaces, under carefully controlled temperature gradients.

Considerable work has been done on the effect of impurities on the production of crystallization nuclei in supercooled solutions. The papers of Kamenetskaya and Danilov (13, 15-17, 44-45) summarize the conclusions from these studies: 1. Crystallization centers from impure solutions at high degrees of supercooling which are determined by the surface tension at the crystal liquid interface; 2. the absence of much supercooling in practice is due to active insoluble particles and small amounts of surface-active impurities; 3. the mechanisms that determine the activity of insoluble and soluble impurities differ.

Detailed experimental and theoretical studies have been carried out on growth of crystals from melts. Landau (61) derived partial differential equations that describe impurity distribution in the melt at any time. Any method of controlling the impurity distribution in the crystal is highly important in the growth of semiconduction crystals and in subsequent commercial use. The rules of chemical crystallography apply to the growth of piezoelectric crystals. Rez (86) utilized these rules and determined eighteen distinct groups of substances which warrant detailed examination as piezoelectrolytics.

Intensive and extensive work has been carried out by Soviet scientists on crystallization of large single crystals from aqueous solutions. Chirkov (10) described five types of crystallization of isomorphic salts from aqueous solutions. Factors affecting crystal growth were determined by Sheftal (95) to the degree of association, the presence of admixtures, the crystallization pressure, the conditions of equilibrium, and the forms and solubilities of the crystals.

Sheftal and various co-workers (82, 96-97) have published extensively on growth of crystals, indicating not only their interest in these large crystals but also the importance placed by the Soviets on crystals for electronics and other commercial applications. The morphological peculiarities of the growth of silicon crystals were described by Shamba and Sheftal (93) for crystallization from the melt and from the gaseous phase. Conditions of crystallization as they affect structure and shape of crystals were determined for sucrose by Sheftal and Gavrilova (98).

The kinetics of salt crystallization, both theoretical and experimental, was reviewed by Todes (109). Various aspects of crystal growth were discussed: 1. isothermal crystallization of a supersaturated solution; 2. crystallization of seed crystals; 3. spontaneous formation of crystal nuclei; 4. high supersaturation; 5. crystallization in the diffusion field; 6. crystallization with turbulent stirring; and 7. crystallization by solvent evaporation. Some limited technical applications were considered. Gorskii (38) has applied the probability theory theoretically to derive the effect of various physical factors on the crystallization parameters of any substance.

Salli (89-90) developed a theory from kinetics on the growth and form of a new crystal phase separating from a supersaturated solution. Since the thickness of the stagnant layer on the surface of a growing crystal controls diffusion of new material to the crystal face, stirring improves the rate of crystal growth to a maximum dependent on the system. Utilizing theoretical concepts of many previous investigators, Chumakov (11) has described the growth of a large number of piezoelectric crystals from solvents.

Danilov and co-workers carried out extensive work and reported their results in a series of papers (18-21). Most of this work dealt with crystallization of organic substances from undercooled liquids. Krishtal (60), a former co-worker of Danilov, shows continued interest in his experimental and mathematical study of the relation of temperature to rate of crystal growth of meta-nitrobenzoldehyde and benzophenone.

Intense interest has been shown by Soviet

scientists in the mathematical and theoretical concepts of crystallization processes. Experimental verification is often difficult or lacking. Grigor'yev (39, 40) developed several excellent papers on crystallization in binary and ternary systems. A theoretical method based on the Kossel-Strauskii theory of crystal growth was developed by Ansheles (3) for determining the structural importance of crystal faces. He applied his theory to explain the mechanism of crystal growth in a diamond.

Nucleation was described theoretically by Lyubov and Roitburd (66), who studied the growth rate of nuclei in one-component systems. A mathematical analysis of fractional crystallization and precipitation of compounds of rare earth elements was presented by Serebrevnikov (92). Analysis of available data showed Figurovskii and Komarova (26) that crystallization proceeds by a chain mechanism.

An indefatigable Soviet worker in crystallization is Lemmlein (62). His theory shows that every concentration in a solution corresponds to a definite critical size of crystal particle that can exist in equilibrium with that solution. Lemmlein, Dukova and Chernov (63) discuss the dynamics of elementary growth processes and evaporation of some volatile organic crystals on the basis of screw or spiral dislocation. Microcine matography was used experimentally for recording this phenomenon. Kozlovskii (56-59) continued these studies on organic crystallization and described processes for spiral growth and solution of crystals.

Equations for the kinetics of crystallization of solutions and melts were derived by Skryabin (101). His theoretically computed curves coincide nicely with actual experimental curves for supersaturated potassium alum solutions and for melts of various metals.

The extent of Soviet work on growth of crystals indicates the importance attached to the unit operation of crystallization by their scientists. It is obvious that the need for practical application is well recognized, and in many cases practical application studies outstrip theoretical and basic investigations.

CRYSTAL SYSTEMS

The vast reaches of the Soviet empire contain large regions of natural mineral resources. Many of these have not been fully explored. Some of them are of great commercial value to the development of the Soviet economy. It is not surprising, therefore, to find an extensive literature on the crystallographic properties of many minerals. There is also a large body of information on crystal systems based on academic and industrial experimentation.

Extensive data on the crystal chemistry of the actinide elements have been collected, collated, and presented by Makarov (67). He shows by tables and test the relationships of crystal structures in actinides, especially thorium, uranium, plutonium, and neptunium. In this study, Makarov referenced Western work heavily, showing not only the up-to-date knowledge of non-Soviet studies but suggesting as well the dependence of the Soviets on such up-to-date knowledge.

The equilibrium distribution of isomorphic and isodimorphic components of various systems has been studied widely. Gorshtein and co-workers (33-37) investigated many systems of commercial importance. These investigations established experimentally a linear law of distribution which has a practical significance in fractionation and separation of multicomponent salt systems and mixed minerals.

Preparation of high quality potash fertilizers from potash minerals of the Carpathian mines is difficult because of the multimineral nature of the raw materials. Pozin and Muratova (83-84) showed that good quality potassium chloride could be obtained by proper crystallization methods.

Phase diagrams of various systems have been developed with implied commercial significance. Typical of these systems is the work of Goroschenko (30-32) on various sulfates of niobium and tantalum. Organic systems as well have been studied, viz., the work of Kitaigorodskii and Tungch'ai (51) on the phase diagram of p-dibromobenzene and p-diiodobenzene.

Among recent publications the following exemplify the diversity of studies on crystal systems: Stroganov, et al. (105) on the structure of the crystallohydrates of nickel chloride; Ivankina (43) on the structure of the crystalline lattice of solid solutions of alkali halide salts; Gagarinskii and Mashirev (27) on the crystallohydrates of zirconium tetrafluoride; and, Kost and Golder (54) on the crystalline structure and density of the cerium hydrides.

The quantum efficiency of the photoeffect in silver bromide crystals within the visible range was studied by Egorova (24). The polymorphic transformations of the superconducting compounds of bismuth were investigated by Zhuravlev et al. (118). They found that superconductivity was related to the crystallochemistry of the compounds. Zinc-selenide crystals of high purity were grown from the gaseous phase by Crucianu and Chistyakov (12) and the peculiarities of their structure were studied by x-ray diffraction techniques.

Recent Soviet publications reveal an increased study on the luminescence of various crystal systems. Lushchik and Lushchik (65) investigated the regularities in the emission spectra of alkali halide

phosphors. The dependence of infrared and visible luminescence intensity on temperature and X-ray irradiation in sodium chloride, potassium chloride and potassium bromide crystals was investigated by Ezhik and Shavlo (25). The mechanism of luminescence of alkali halide crystals activated by various other metal ions was studied by Lushchik (64). The phenomenon of electroluminescence in monocrystals of zinc sulfide and cuprous chloride was investigated by Oranovskii et al. (78), utilizing a specially arranged microscope field.

The practical significance of a study of crystal systems is recognized by Soviet investigators. Its importance in the expanding Soviet chemical and metallurgical industry is emphasized by the extent and diversity of these studies.

HABIT MODIFICATION OF CRYSTALS

Of great academic as well as industrial importance are the changes wrought in crystal properties, habits of crystals, and growth of crystals by the presence of admixtures in the solution ("mother liquor"). The inclusions in crystal faces and the interactions between admixtures and the pure material have been investigated less intensively than have the changes in habit.

Some of the organic colored substances have received much attention in these studies. Methylene blue was investigated by Slavnonva (102) in solutions of lead nitrate and barium nitrate. It was found that the controlling factors by which impurities enter the growing crystals depend on structural similarities between the components, surface adsorption properties, the nature of the impurity, and the tendency of the impurity to give adsorbed particles.

Detailed historical discussions of the effect of impurities on crystal growth and habit have been presented by Saratovkin (91) and Ansheles (4). They showed that both skeletal and antiskeletal growths can be achieved by controlling the nature of the system of the impurity and the pure compound.

Gordetskii and Saratovkin, studying cadmium iodide crystals, found that impurities play a large part in producing spiral growth on screw dislocations. According to Saratovkin (91) this type of effect produces dendritic growth during crystallization, both of metals and of organic and inorganic salts. Bliznakov and Kirkova (8) found that increasing the concentration of the impurity in the mother liquor increased its inclusion in the faces of the growing crystal. The dislocation brought about by impurities also can be achieved by irregular temperature distribution in a growing crystal, according to Indenbonn (42).

Small additions of surface-active substances to the solutions increased the rate of crystal growth and repressed the speed of nuclei formation in a study of hydrated tricalcium aluminate by Zaytseva and Smirnova (115). Mokiyevskii (76) found that changes in the crystal form and in the rate of crystallization were brought about in growing epsom salt by aniline and methylene blue. Some organics are repelled by the growing faces of crystals. Melik-Gaikazyon et al. (72) carried out confirming experiments on recrystallization of ammonium chloride in the presence of pectin.

Avakyan and Lashko (5) studied, by microscopic methods, the changes during crystallization of the eutectic of potassium chloride and potassium chromate in the presence of surfactants. All tested surfactants influence the process of eutectic crystallization by shifting the eutectic point. Oriented crystallization was proved in the hardening of hydrated calcium sulfate in the presence of surfactants by the work of Tekhonov and Borymaskaya (108). Dobrovniskaya and Eidel'man (22) studied the influence of crystallization conditions on the distribution of thallium in single crystals of sodium iodide.

The use of surfactants and organic substances to control grain size and brightness of electrodeposited metals is well known and important. Extensive studies of this phenomenon have been carried out by Soviet scientists. Aliev (1) has studied the effects of temperature and of iodine on the crystallization of selenium. Also typical of recent work is a study by Gorbunova and Lebedeva (28) on the influence of surfactants on the shape and texture of zinc deposits.

Consideration of the distribution of isomorphous impurities between the crystal and liquid phases in zone refining led Kirgentsev (50) to derive an equation for this distribution. The simplified equation related the distribution to relative concentrations of the impurity and the pure substance both in the melt and solid phases, as defined by a distribution coefficient.

The importance of changing crystallization processes by addition of impurities to the mother liquor or melt is recognized commercially. Stroitelev (106) has described a procedure for selecting the most effective admixtures in the growing of commercially valuable crystals. His article typifies the great interest and competence of Soviet investigators in this phase of crystal studies.

CRYSTALLIZATION METHODS AND EQUIPMENT

Methods for growing commercially valuable crystals have been developed both in the Western World and in the Soviet Union. In most cases the equipments are similar, since the laws of crystallization are universal and cannot be confined by

political boundaries. A knowledge of Western techniques and equipment has been used by Soviet engineers to increase their competence in crystallization.

Optical glasses for instrumentation in infrared and untraviolet regions are important. Common optical glasses cannot be used in these regions. Fluorite (calcium fluoride) has a high and uniform transmission over a wide wavelength range. Studies on the preparation of synthetic fluorite, as well as on fluorides of sodium and lithium, have been carried out by Stepanov and Feofilov (104), by Vasil' yeva (110) and by Kozlova (55).

Scintillation counters are used widely for studying nuclear radiation. Both organic and inorganic crystals have been developed as scintillators. Soviet physicists have used crystal scintillation counters for solving new problems and for developing new methods of detecting nuclear radiation (7, 23, 114).

Semiconductor crystals must be uniform and their quality must be predictable. The nature, amount and distribution of impurities present or deliberately introduced into such crystals determine their electrical properties. Excellent studies have been carried out by Petrov and Zemskov (80) on the growth of single crystals of germanium with uniform inclusions of radioactive indium, by Kokorish and Sheftal (53) on growing dislocation free germanium single crystals, and by Maslov, et al. (68) on growing monocrystals of germanium under molten salts and oxides.

Piezoelectric crystals have various important uses, for example in pressure transducers, in frequency stabilization, etc. The growth of large synthetic crystals of piezoelectric materials has been investigated by Rez and Tsinober (87), and by Butuzov and Bryatov (9). Ferroelectric crystals have been prepared and studied by Novosil'tsev et al. (77) and by Rez (86).

Standard industrial crystallizations are carried out in the chemical and food industries of the Soviet Union. Melnik (73), Yarmolinskii (112), Mircev and Sandera (74), and Sadovyi and Chubik (88) have conducted studies on the crystallization of sucrose from massecuites. Typical investigations on other standard chemicals have been made by Melik-Gaikazion and Ermolaev (71), by Belikovich and Lyskovich (6) and by Petrov and Treibus (81).

The effect of ultrasonics on the crystallization processes of metals, alloys, organics, and inorganics has been investigated widely and the results applied to industrial processes. Kapustin (46-48) is one of the most prolific investigators on the use of ultrasonics to improve crystallization processes. Other scientists who have contributed heavily to this ultrasonics field include Gudtsov (41), Vitovskii (111), Danilov and Chedzhmenov (14), Mazhul (70), Zaboleev-Zotov and Pogodin-Alekseev (113), and Kavalynaite (49).

The preparation of single crystals for luminescence has been described by Mizetskaya (75). Artificial rubies were grown in an apparatus designed according to Verneuil's technique. This apparatus was used by Petrov and Shashkov to grow silicon crystals (79).

Typical of commercial crystallizers are the following: for naphthalene, designed by Privalov (85); for mechanical crystallization, designed by Tamarin (107); for laboratory studies, developed by Matusevich (69). The application of high speed cinephotography (up to 5000 frames per second) was developed by Klassen-Neklyndova et al. (52) to study kinking under compression in crystals of cesium iodide and naphthalene.

Soviet research and industry use standard methods and equipment for studying and producing industrially important crystals. Their investigations are steady and continuing and lead to development of sound methods and practical equipment.

ACKNOWLEDGMENT

The authors gratefully acknowledge the help of Messrs. Walter Buckman, Cyril Geacintov, William Pettus and Miss Amy Paige in the collection of literature citations and of Mrs. Suzanne Treadwell Grove in editing the manuscript.

LITERATURE CITED

1. Aliev, M. I., *Trudy Azerbaidzhan. Ind. Inst.*, No. 19, 280-7 (1957).

2. Anonymous, *Khim. Mashinostroyenie*, No. 2, 1-3 (1959).

3. Ansheles, O. M., *Uchenye Zapiski Leningradskogo Gosudarstvennogo Universiteta im. A. A. Zhdanova*, No. 215, 84 (1959).

4. Ansheles, O. M., *Introduction to Crystallography*, Zhdanov State University, Leningrad (1952).

5. Avakyan, S. V. and Lashko, N. F., *Zhur. Fiz. Khim.*, 23, No. 6, 729-35 (1949).

6. Belikovich, B. A. and Lyskovich, A. B., *I. Franko L'vov State University.*

7. Belyayev, L. M., Vitovskii, B. V., and Dobrzhanskii, G. F., *Reports at the First Conference on Crystal Growth*, 5-10 March 1956, 197-206.

8. Bliznakov, G. and Kirkova, E., *Godishnik Safiskiya Univ. Fiz. Mat. Fak. Khim.*, 50, Pt. 1-7, 75-88 (1955/56) pub. 1958.

9. Butuzov, V. P. and Bryatov, L. V., *Reports at the First Conference on Crystal Growth*, 5-10 March 1956, 241-44.

10. Chirkov, S. K., *Zhur. Neorgan. Khim.*, 1, 2813-19 (1956).

11. Chumakov, A. A. and Koptsik, V. A., *Kristallografiya*, 4, 235-8 (1959).

12. Crucianu, E. and Chistyakov, Yu. D., *Kristallografiya*, 5, No. 3, 344-7 (1960).

13. Danilov, V. I., *Problems of Metal Science and Metal Physics, Symposium I*, 7, (1949).
14. Danilov, V. I. and Chedzhemenov, G. Kh., *Problemy Metalloved. i Fiz. Metal., Sbornik*, 4, 34-49 (1955) *Referat. Zhur., Khim.* (1956), Abstr. No. 57488.
15. Danilov, V. I. and Kamenetskaya, D. S., *Zhur. Eksperim. i Teor. Fiz.*, 19, 313-18 (1949).
16. Danilov, V. I. and Kamenetskaya, D. S., *Problems of Metal Science and Metal Physics, Symposium II*, 3, (1951).
17. Danilov, V. I. and Kamenetskaya, D. S., *Dokl. AN SSSR*, 68, No. 4, 677-80 (1949).
18. Danilov, V. I., Kozachkovskii, O. D. and Labkovskii, Ya. M., *Zhur. Eksperim i Teor. Fiz.*, 18, 886-92 (1948).
19. Danilov, V. I. and Krishtal, Yu. A., *Zhur. Eksperim. i Teor. Fiz.*, 19, 304-12 (1949).
20. Danilov, V. I. and Malkin, V. I., *Zhur. Fiz. Khim.*, 28, No. 10, 1837-44 (1954).
21. Danilov, V. I. and Ovsiyenko, D. Ye., *Zhur. Eksperim. i Teor. Fiz.*, 21, 879-86 (1951).
22. Dobrovniskaya, E. R. and Eidel'man, L. G., *Kristallografiya*, 5, No. 5, 734-7 (1960).
23. Dzhelopov, V. P., Golovin, B. M. and Saratov, V. I., *Dokl. AN SSSR.*, 99, 943 (1954).
24. Egorova, M. S., *Uchenye Zapiski Leningrad. Gosudarst. Pedagog. Inst. im. A. I. Gertsena*, 148, 209-10 (1958).
25. Ezhik, I. I. and Shavlo, S. T., *Izvest. Vysshikh Ucheb. Zavedenii, Fiz.* No. 3, 62-7 (1959).
26. Figurovskii, N. A. and Komarova, I. A., (M. V. Lomonosov State Univ., Moscow) *Zhur. Neorgan. Khim.*, 4, 522-9 (1959).
27. Gagarinskii, Yu. V. and Mashirev, V. P., *Izvest. Sibir. Otdel. Akad. Nauk SSSR*, No. 11, 50-6 (1959).
28. Gorbunova, K. M. and Lebedeva K. P. (Phys.-Chem. Inst., Moscow). *Zhur. Fiz. Khim.*, 33, 669-76 (1959).
29. Gorodetski, A. F. and Saratovkin, D. D., *Reports at the First Conference on Crystal Growth*, 5-10 March 1956, 151-8.
30. Goroshchenko, Ya. G., *Zhur. Neorgan. Khim.*, 1, 903 (1956).
31. Goroshchenko, Ya. G., *Zhur. Neorgan. Khim.*, 1, 909-14 (1956).
32. Goroshchenko, Ya. G., *Zhur. Neorgan. Khim.*, 1, 915-20 (1956).
33. Gorshtein, G. I., *Zhur. Neorgan. Khim.*, 3, No. 1, 51-8 (1958).
34. Gorshtein, G. I. and Silant'yeva, N. I., *Zhur. Obshch. Khim.*, 23, 1290-1302 (1953).
35. Gorshtein, G. I. and Silant'yeva, N. I., *Zhur. Obshch. Khim.*, 24, 29-36 (1954).
36. Gorshtein, G. I. and Silant'yeva, N. I., *Zhur. Obshch. Khim.*, 24, 201-3 (1954).
37. Gorshtein, G. I. and Silant'yeva, N. I., *Zhur. Obshch. Khim.*, 26, 1821-6 (1956).
38. Gorskii, F. K., *Sbornik Nauch. Rabot. Minsk. Med. Inst.*, 15, 308-27 (1955). *Referat. Zhur., Khim.*, (1956), Abstr. No. 74360.
39. Grigor'yev, A. T., *Dokl. AN SSSR*, 84, No. 5, 989-92 (1952).
40. Grigor'yev, A. T., *Dokl. AN SSSR*, 88, No. 2, 273 (1953).
41. Gudtsov, N. T., *Dokl. AN SSSR, Novogo Ser.*, 71, No. 2, 273 (1950).
42. Indenboon, V. L., *Kristallografiya*, 2, 594-603 (1957).
43. Ivankina, M. S., *Izvest. Vysshikh Ucheb. Zavedenii, Fiz.*, No. 1, 101-5 (1958).
44. Kamenetskaya, D. S., *Reports at the First Conference on Crystal Growth*, 5-10 March 1956, 33-38.
45. Kamenetskaya, D. S., *Problems of Metal Science and Metal Physics, Symposium III*, 371 (1952).
46. Kapustin, A. P., *Izvest. AN SSSR, Ser. Fiz.*, 14, 357-65 (1950).
47. Kapustin, A. P., *Zhur. Tekh. Fiz.*, 22, 765-72 (1952).
48. Kapustin, A. P., *Trudy Inst. Kristallogr. AN SSSR*, 10, 177-8 (1954)
49. Kavalynaite, V. E., *Primenenie Ul'traakustiki k Islledovan. Veshchestva*, No. 6, 167-70 (1958).
50. Kirgentsev, A. N. (Far Eastern Branch, Acad. Sci. USSR Vladivostock). *Zhur. Fiz. Khim.*, 33, 1422-9 (1959).
51. Kitaigorodskii, A. I. and Tung-ch'ai, Liang, (Inst. of Heteroorg, Cmpds. Acad. of Sci.) *Kristallografiya*, 5, No. 2, 221-29 (1960).
52. Klassen-Neklyndova, M. V., Cheruysheva, M. A., and Tomilovskii, G. E., *Kristallografiya*, 5, No. 4, 617-21 (1960).
53. Kokorish, E. Yu. and Sheftal, N. N., *Kristallografiya*, 5, No. 1, 150-52 (1960).
54. Kost, M. E. and Golder, G. A., *Zhur. Neorgan. Khim.*, 4, 1488-90 (1959).
55. Kozlova, O. G., *Trudy Vsesoyuz. Nauch. Issledovatel. Inst. Pezvoplichesk. Mineral. Syr'ya*, 2, No. 1, 107-16 (1958).
56. Kozlovskii, M. I. (M. V. Lomonosov State Univ. Moscow) *Kristallografiya*, 3, 209-13 (1958).
57. Kozlovskii, M. I. (M. V. Lomonosov State Univ. Moscow). *Kristallografiya*, 3, 236-7 (1958).
58. Kozlovskii, M. I. (M. V. Lomonosov State Univ. Moscow). *Kristallografiya*, 3, 483-7 (1958).
59. Kozlovskii, M. I. and Lemmlein, G. G., (M. V. Lomonosov State Univ. Moscow). *Kristallografiya*, 3, 351-7 (1958).
60. Krishtal, Yu. A., (Inst. Transport Eng. Dnepropetrovsk). *Nauch. Doklady Vysshei Shkoly Met.*, No. 4, 197-202 (1958).
61. Landau, A. I., *Reports at the First Conference on Crystal Growth*, 5-10 March 1956, 58-64.
62. Lemmlien, G. G., *Dokl. AN SSSR*, 89, No. 2, 283-6 (1953).
63. Lemmlein, G. G., Dukova, E. D. and Chernov, A. A., *Kristallografiya*, 2, 428-36 (1957).
64. Lushchik, Ch. B., *Izvest. Akad. Nauk Eston. SSR, Ser. Tekh. i Fiz.-Mat. Nauk*, 8, No. 4, 287-95 (1959).
65. Lushchik, N. E. and Lushchik, Ch. B., *Trudy Inst. Fiz. i Astron., Akad. Nauk Eston. SSR*, No. 6, 5-62 (1957).
66. Lyubov, B. Ya. and Roitburd, A. L., *Sbornik Trudov Inst. Met. i Fiz. Met. Tsentral. Nauch. Issledovatel. Inst. Chernoi Met.* 5, 91-123 (1958).
67. Makarov, Ye. S., *Crystal Chemistry of Simple Compounds of Uranium, Thorium, Plutonium, and Neptunium*, Consultants Bureau, Inc., New York (1959).
68. Maslov, V. N., Granovskii, Yu. V. and Samygin, V. D., *Zhur. Priklad, Khim.*, 32, 2574 (1959).
69. Matusevich, L. N., *Zavodskaya Laboratoriya*, 23, No. 6, 757-9 (1957).
70. Mazhul, M. M., *Uchenye Zapiski Beloruss. Univ.*, No. 32, 211-18 (1957). *Referat. Zhur. Met.*, (1957), Abstr. No. 24786.
71. Melik-Gaikazion, I. Ya. and Ermolaev, V. A., *Izvest. Vysshikh Ucheb. Zavedenii, Fiz.*, No. 5, 141-3 (1958).
72. Melik-Gaikazion, I. Ya., Saratovkin, D. D. and Kliss, A. G., *Izvest. Tomsk. Politekh. Inst.*, 95, 372-7 (1958).
73. Melnik, B. D., *Khim. Prom.* 9, 193-6 (1956).
74. Mircev, A. and Sandera, K., *Ref. Zhur. Khim.*, No. 1, 2782 (1958).
75. Mizetskaya, I. B., Trofimenko, A. P. and Fursenko, V. D.

Zhur. Neorgan. Khim., 3, 2236-9 (1958).

76. Mokiyevskii, V. A., *Kristallografiya*, 1, No. 4, 3-46 (1955).

77. Novosil'tsev, N. S., Khodakov, A. L., Sholokhovich, M. L., Fesenko, Ye. G. and Kramarov, O. P., *Izvest. AN SSSR, Ser. Fiz.*, 21, 295-304 (1957).

78. Oranovskii, V. E., Panasyuk, E. I. and Fedyushin, B. T., (P. N. Lebedev Physics Inst., Moscow). *Inzhener.-Fiz. Zhur. Akad. Nauk Beloruss. SSSR*, 2, No. 1, 39-45 (1959).

79. Petrov, D. A. and Shashkov, Yu. M., *Izvest. AN SSSR, Otd. Tekh. N.*, No. 5, 102-3 (1957).

80. Petrov, D. A. and Zemskov, V. S., *Reports at the First Conference on Crystal Growth*, 5-10 March 1956, 207-14.

81. Petrov, D. A. and Treibus, E. B., *Kristallografiya*, 5, No. 3, 429-34 (1960).

82. Popov, S. K. and Sheftal, N. N., *USSR Patent No. 108*, (October 25, 1957).

83. Pozin, M. Ye. and Muratova, M. I., *Zhur. Priklad. Khim., (USSR)*, 30, No. 9, 1446-50 (1957).

84. Pozin, M. Ye. and Muratova, M. I., *Zhur. Priklad. Khim., (USSR)*, 30, No. 9, 1451-54 (1957).

85. Privalov, V. Ye., *Koks i Khimiya*, No. 3, 46-9 (1959).

86. Rez, I. S., *Kristallografiya*, 5, No. 1, 54-9 (1960).

87. Rez, I. S. and Tsinober, L. I., *Reports at the First Conference on Crystal Growth*, 5-10 March 1956, 227-31.

88. Sadovyi, I. E. and Chubik, I. A., (Technol. Inst. Food Ind., Leningrad). *Izvest. Vysshikh Ucheb. Zavedenii, Pishchevaya Tekhnol.*, No. 4, 90-4 (1958).

89. Salli, I. V., *Nauchnye Zapiski Dnepropetrovskogo Gosudarstvenogo Universiteta SSSR*, 41, 37-42 (1953).

90. Salli, I. V., *Zhur. Eksperim. i Teor. Fiz.*, 25, 208-14 (1953).

91. Saratovkin, D. D., *Dendritic Crystallization*. Consultants Bureau, Inc., (trans.), New York 1959 (Original publisher: Metallurgizdat, 1953).

92. Serebrevnikov, V. V., *Uchenye Zapiski Tomsk. Gosudarst. Univ. im. V. V. Kuibysheva*, No. 29, 60-8 (1959).

93. Shamba, N. A. and Sheftal, N. N., *Kristallografiya*, 2, 441-4 (1957).

94. Sheftal, N. N., *Reports at the First Conference on Crystal Growth*, 5-10 March 1956, 5-25.

95. Sheftal, N. N., *Rost Kristallov, AN SSSR, Inst. Kristallog., Doklady Soveshchaniya*, 5-31 (1957).

96. Sheftal, N. N., *Tr. Inst. Kristallogr. AN SSSR*, 4, 231-3 (1948).

97. Sheftal, N. N., *Tr. Inst. Kristallogr. AN SSSR*, 3, 71 (1947).

98. Sheftal, N. N. and Gavrilova, I. V. (Akad. Sci. Moscow). *Proc. Intern. Soc. Sugar Cane Technologist*, 10, 282-6 (1959).

99. Shubnikov, A. V., *Kristallografiya*, 5, No. 1, 3-14 (1960).

100. Shubnikov, A. V., *Reports at the First Conference on Crystal Growth*, 5-10 March 1956, 3.

101. Skyrabin, A. K., *Zhur. Fiz. Khim.*, 31, No. 4, 780-91 (1957).

102. Slavnova, Ye. N., *Reports at the First Conference on Crystal Growth*, 5-10 March 1956, 117-25.

103. Spitsyn, V. I., *Zhur. Neorgan. Khim.*, 4, No. 6, 1227-32 (1959).

104. Stepanov, I. V. and Feofilov, P. P., *Reports at the First Conference on Crystal Growth*, 5-10 March 1956, 181-90.

105. Stroganov, E. V., Koshina, I. I., Andreev, S. N. and Kalyadir, A. B., *Vestnik Leningrad. Univ.*, 15, No. 4 *Ser. Fiz. i Khim.* No. 1, 130-7 (1960).

106. Stroitelev, S. A., *Izvest. Tomsk. Politekh. Inst.*, 95, 393-6 (1958).

107. Tamarin, V. M., *Koks i Khimiya*, No. 5, 38-43 (1958).

108. Tekhonov, V. A. and Borymskaya, E. P. *Nauch Zapiski L'vov Politekh. Inst.* No. 23, 47-55 (1953). *Referat. Zhur., Khim.* (1956), Abstr. No. 33271.

109. Todes, O. M., (Acad. Sci. USSR, Leningrad). *Freiberger Forschungsh.*, A 123, 341-63.

110. Vasil'yeva, M. A., *Reports at the First Conference on Crystal Growth*, 5-10 March 1956. 191-6.

111. Vitovskii, B. V., *Tr. Kristallogr. AN SSSR*, 1, No. 11, 221-2 (1955).

112. Yarmolinskii, M. B., *Trudy Vsesoyuz. Nauch.-Issledovatel. Inst. Sakharn. Prom.*, No. 2, 104-15 (1953).

113. Zaboleev-Zotov, V. V. and Pogodin-Alekseev, G. I., *Moskov. Vysshee Tekh. Uchilishche im. N. E. Baumana, Sbornik Statei*, 147-56 (1958).

114. Zavoyskii, Ye. K., Smolkin, G. Ye., Plakhov, A. G. and Butslov, M. M., *Dokl. AN SSSR*, 100, 241 (1955).

115. Zaytseva, N. G. and Smirnova, A. M., *Kolloidnyi Zhur.*, 20, No. 5, 636-9 (1958).

116. Zhavoronkov, N. M., *Izvest. AN SSSR, Otd. Khim. N.*, No. 11, 1277-83 (Nov. 1957).

117. Zhavoronkov, N. M. and Planovskii, A. N., *Chemical Engineering Around the World*, (E. L. Piret, ed.) American Institute of Chemical Engineers (1958) Ch. 36 (461-84).

118. Zhuravlev, N. N., Zhdanov, G. S. and Alekseevskii, N. E., *Vestnik Moskov. Univ., Ser. Mat., Mekh. Astron., Fiz. i Khim.*, 14, No. 3, 117-27 (1959).

A. I. Leonov

USSR

Influence of the Gaseous Medium on the Course of Physico-Chemical Processes in Semiconductor Oxides at High Temperatures

Results of a study of the reactivity of ZnO and Cr_2O_3 oxides with varying partial pressures of oxygen in the gaseous medium. There was observed a general dependence of reactivity, catalytic activity, and electrical conductivity of semi-conductor oxides on the composition of the gaseous medium.

In studies of reaction kinetics in the solid phase much attention is devoted to study of the stoichiometric upsets in chemical compounds on which the reactivity of the latter depends (1, 2). The gaseous medium is one of the factors causing the deviations from stoichiometric proportions in oxides. For example, after a lowering of the partial pressure of oxygen in the atmosphere, the former may pass partially from the oxide into the gaseous phase and an excess of metal atoms might be formed in the oxide. Physicochemical processes occur at a high rate in such a "defect" substance. A rise of the chemical reactivity of oxides is also possible as a result of chemical adsorption of oxygen and formation of nonstoichiometric surface compounds. Recently much interest has been attached to the study of the role of stoichiometric disturbance in the chemistry of solids at high temperatures. The results of some studies of the properties of refractory oxides ThO_2, Cr_2O_3, and ZrO_2 were published in 1957 (3), as well as those of UO_2 (4), these properties having been studied at temperatures up to 2,000° C in vacuum, or in argon, carbon monoxide, and other gaseous media.

In the present paper we present the results of a study of the reactivity of ZnO and Cr_2O_3 oxides depending on the partial pressure of oxygen in the gaseous medium. Our experimental data on reaction kinetics and the sintering of the oxides are compared with the existing data on the catalytic and the electrical properties of the oxides. A general dependence of reactivity, catalytic activity, and electrical conductivity of semiconductor oxides on the composition of the gaseous medium was observed.

This article first published in *Izvest. Akad. Nauk SSSR, Otdel. Khim. Nauk*, No. 9, 1529-1534 (1960). The author is associated with the Institute of Silicate Chemistry of the Academy of Sciences of the USSR.

EXPERIMENTAL PART

"Analytical grade" oxide specimens were used as the starting materials. Heating of the samples to 1,500° C was performed in a platinum furnace, while heating above 1,500° C was done in a molybdenum tube furnace. Air, argon, hydrogen, and metal vapors were used as the gaseous media. Partial pressures of oxygen in the gases used are shown in Table 1.

The quantitative determination of chemical compounds in the oxide mixtures after the heating was done by means of chemical phase analysis. The method of selective dissolution of ZnO in 1:1 hydrochloric acid solution at room temperature was used in the analysis of the $ZnO-Al_2O_3$ mixture (5); $ZnAl_2O_4$ and Al_2O_3 remained in the residue. During the analysis of the heated $MgO-Cr_2O_3$ mixture, the free MgO was dissolved in a 10% solution of ammonium nitrate with heating; $MgCr_2O_4$ and Cr_2O_3 remained in the residue. The determination of the amount of the dissolved components was made by means of a complexometric titration (6).

Table 1
Partial pressure of oxygen in gases at various experimental temperatures

Gaseous medium	P_{O_2}, atm.		
	1000°C	1500°C	1750°C
Air	0.21	0.21	0.21
Argon containing 0.4% O_2	4.0×10^{-3}	4.0×10^{-3}	4.0×10^{-3}
Hydrogen containing 2.3% H_2O	1.7×10^{-16}	1.1×10^{-12}	7.4×10^{-11}

The phase composition of the substances under study was also determined by means of x-ray and microscopic analyses. The sample sintering was described by the following indexes: linear shrinkage, porosity, bulk density, and specific gravity.

Reaction $ZnO + Al_2O_3 = ZnAl_2O_4$. ZnO and Al_2O_3 oxides were first heated for two hours at 1,000° C after which they were pulverized in a mortar to pass a 200 mesh sieve. The experiments were run at temperatures of 900, 950 and 1,000° C in argon containing 0.4% of oxygen, in purified argon, and in vapors of metallic zinc. Argon was freed of oxygen by passage through tubular furnaces filled with metallic magnesium shavings, at a temperature of 600° C. Experiments run in metallic zinc vapor were set up as follows. Zinc and the test sample were placed in a quartz test tube, as shown in Fig. 1. The test tube with its contents was placed in a furnace and heated. The zinc, located at the bottom of the test tube, vaporized, its vapor rose, condensed on the test tube walls and flowed downward. Zinc vapor with the pressure of several millimeters of mercury was thus present in the atmosphere during the experiment (above molten zinc at temperatures of 500-600° C). The experimental results are shown in Table 2.

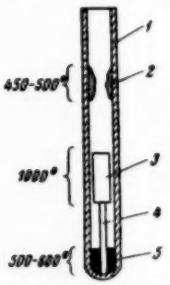

Fig. 1. Quartz test tube for running experiments in zinc vapors: 1) quartz test tube: 2) sublimed zinc; 3) sample; 4) support; 5) zinc.

As is evident from the data in Table 2, the formation of $ZnAl_2O_4$ occurred two or more times more intensively in purified argon or in zinc vapor than in argon containing 0.4% of oxygen.

According to the literature data (2), a deviation from the stoichiometric proportion in zinc oxide takes place with alteration of the atmospheric composition. Therefore it would be desirable to follow any changes in the metal-to-oxygen ratio in the oxide with changes in the oxygen partial pressure. However, such an analysis presents some difficulty, as the quantitative change of the composition is slight and takes place predominantly at the edges of the crystals and the aggregates. New methods of physicochemical analysis must be sought for the practical solution of this problem.

Table 2
Effect of the gaseous medium in the course of the reaction $ZnO + Al_2O_3 = ZnAl_2O_4$

Temp., °C	Duration, min.	Amount of $ZnAl_2O_4$ formed, %		
		Argon + 0.4% O_2	Purified argon	Metallic zinc vapor
900	60	5.5	12.0	23.0
950	60	20.0	60.5	59.5
1000	60	35.0	89.7	88.2

Reaction $MgO + Cr_2O_3 = MgCr_2O_4$. Many studies had been devoted to the examination of the reaction of formation of chrome spinelide (7) owing to the importance of this compound as a phase entering the compositions of chrome-magnesite refractories. The high rate of formation of $MgCr_2O_4$ was noted in these studies, as compared to the rate of $MgAl_2O_4$ formation, this being connected with the greater degree of mobility of chromium atoms, as compared to those of aluminum. These studies had been made in an air (oxidizing) atmosphere. A study of the kinetics of the formation reaction of $MgCr_2O_4$ in gaseous media with various partial pressures of oxygen is of technological importance, as the basic refractories in metallurgical furnaces are subjected to the action of a gaseous atmosphere with a variable concentration of oxygen.

In the experiments with the synthesis of chrome spinelide at 950° C and 1,000° C we used a finely dispersed (minus 200 mesh) composition I (see Table 3). At temperatures of 1,350° C and 1,500° C the experiments were run with the coarse-grained composition II (minus 95 mesh) owing to the high rate of formation of the chrome spinelide. The experimental results are shown in Table 3.

As can be seen in Table 3, the amount of chrome spinelide formed at 950 and 1,000° C increases with the increasing oxygen concentration in the gaseous phase. This is explained by the following reasons. Chromium forms a series of oxides with oxygen: CrO_3, Cr_5O_{13}, Cr_5O_{12} and Cr_2O_3, which exist under definite temperature range conditions (8). Cr_2O_3 is stable above 400° C. However, at elevated temperatures a chemical adsorption of oxygen is observed (9) as a result of which surface oxygen compounds of chromium with a raised valence of the latter are formed. At 1,350° C with a reduction of

Table 3.
Influence of the gaseous medium on the course of the reaction $MgO + Cr_2O_3 = MgCr_2O_4$

Temp., °C	Duration, min.	Amount of $MgCr_2O_4$ formed, %			Number of the Composition used
		Air	A + 0.4% O_2	H_2 + 2.3% H_2O	
950	30	67.0	53.6	35.0	I
1000	30	80.0	69.2	52.5	I
1350	60	82.5	51.7	85.0	II
1500	60	91.0	-	96.0	II

the oxygen partial pressure from 2.1×10^{-1} atm. (air) to 4×10^{-3} atm. (A + 0.4% O_2), the amount of $MgCr_2O_4$ formed declined from 82.5% to 51.7%, which fact may be connected with desorption of the superstoichiometric oxygen. However, a further reduction of oxygen pressure to about 10^{-13} atm. (hydrogen) led to an increased yield of magnesium chromite to 85%. Under high temperature conditions (1,350° C), a dissociation of chromium oxide occurs in hydrogen: $Cr_2O_3 = 2Cr + 1.5O_2$, as a result of which part of the oxygen passes into the gaseous phase and an excess of chromium atoms develops in the solid oxide. The dissociative activation manifests itself more distinctly with a rise in the temperature, as is evident from the experiments with $MgCr_2O_4$ synthesis at 1,500° C (Table 3) and the experiments on sintering of chromium oxide at 1,750° C (Table 4).

It is evident from the data in Table 4 that the greater shrinkage of chromium oxide specimens in argon took place owing to the reduction of porosity.

Table 4.
Sintering of chromium oxide (temperature 1,750°C; duration of heating 3 hours)

Sintering indexes	Atmosphere	
	Air	A + 0.4% O_2
Linear shrinkage, %	3.5	17.5
Bulk density, g./cm.^{3}	3.04	4.62
Density, g./cm.^{3}	5.38	5.37
Open porosity, %	38.60	1.40
True porosity, %	43.60	13.96

In specimens heated in air, no crystals were detected; the specimens were speckled with very small pores. Specimens heated in argon were coarsely crystalline and the crystal diameter reached 50 μ.

As indicated by these experiments, it is possible to activate the physicochemical processes in oxides at high temperatures by a change in the partial pressure of oxygen in the gaseous phase.

GENERAL NATURE OF THE INFLUENCE OF THE GASEOUS MEDIUM ON THE REACTIVITY, THE CATALYTIC ACTIVITY AND THE ELECTRICAL CONDUCTIVITY OF SEMICONDUCTOR OXIDES

The theory (10-13), according to which the electronic processes which develop in a semiconductor and which determine its electrical and magnetic properties also determine its reactivity and catalytic activity, has been recognized widely at present. It was interesting, therefore, to compare our experimental data on the interaction between the gaseous phase and the kinetics of the chemical reactions, sintering, and recrystallization of oxides with the data on the electrical conductivity and catalytic activity of these oxides, as affected by the gaseous medium composition.

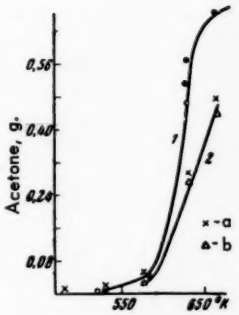

Fig. 2. Yield of acetone in 2 hours as a function of temperature: 1) in pure nitrogen; 2) in a mixture of gases (N_2 + 0.4% O_2) owing to the dehydrogenation reaction; a) based on the amount of acetone; b) based on the amount of hydrogen. From Myasnikov and Pshezhetskii.

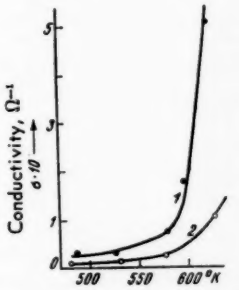

Fig. 3. Change of the conductivity of ZnO with temperature in the reaction zone: 1) in pure nitrogen; 2) in a gas mixture (N_2 + 0.4% O_2). According to Myasnikov and Pshezhetskii.

Zinc Oxide. The intensity of the progress of the reaction $ZnO + Al_2O_3 = ZnAl_2O_4$ at temperatures of 900, 950 and 1,000° C increases by a factor of 2 or more in argon or in zinc vapor in comparison with its progress in argon containing 0.4% of oxygen, as indicated in Table 2. Myasnikov and Pshezhetskii (14) had studied the connection between the catalytic and the semiconductor properties of zinc oxide. They studied the electrical conductivity of zinc oxide in parallel with its catalytic activity in the reaction of dehydrogenation of isopropyl alcohol, which leads to formation of acetone (ZnO electrical conductivity was measured during the reaction). The experiments were run in pure nitrogen and hydrogen as well as in a mixture of gases (N_2 + 0.4% O_2 and H_2 + 3% O_2). In Fig. 2 are shown the curves which characterize the relationship between the amount of acetone formed in 2 hours and the temperature. As indicated by a comparison of curves 1 and 2, the presence of 0.4% of oxygen lowers the reaction rate at a temperature of 300° C more than two-fold. The curves showing the temperature dependence of the electrical conductivity of zinc oxide measured in these experiments are presented in Fig. 3. As is clear from Fig. 3, the electrical conductivity of zinc oxide in the presence of oxygen decreases 2-5-fold, depending on the temperature. Similar results were ob-

tained in runs made in a hydrogen atmosphere, as well as in a mixture of $H_2 + 3\% O_2$.

The existence of a general dependence of the reactivity, electrical conductivity, and catalytic activity of zinc oxide on the gaseous phase composition indicates that the same cause underlies the activation of these processes. Myasnikov and Pshezhetskii believe that the change in the properties of zinc oxide consists in a change in the concentration of electrons in the conduction zone or in the concentration of the interstitial zinc ions. According to modern concepts (1, 2), a disturbance of the ratio of zinc-to-oxygen atoms in the solid oxide occurs with the alteration of the partial pressure of oxygen in the atmosphere, as a result of which the interatomic bond energy changes and, accordingly, so do the properties of zinc oxide. The problem of the chemical bond (short-range order) is basic in the chemistry of semiconductors (15).

Chromium Oxide. The reaction $MgO + Cr_2O_3 = MgCr_2O_4$ at 950° C proceeds to the extent of 35% in hydrogen, 53.6% in argon, and 67% in air (Table 3). The amount of the resulting chrome spinelide, therefore, increases with increase in oxygen concentration in the gaseous phase. As is evident from Fig. 4, a similar relationship is observed between the electrical conductivity of Cr_2O_3 and oxygen pressure (16). The reactivity and electrical conductivity of Cr_2O_3 change in direct relationship.

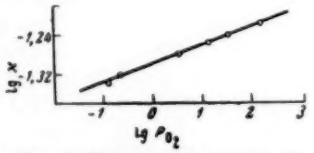

Fig. 4. Relation between the electrical conductivity of chromium oxide and oxygen pressure at 800°C (κ, $ohm^{-1} cm.^{-1}$, and P_{O_2}, mm. Hg). According to Hauffe and Block.

At still higher temperatures an inverse relationship is observed: reactivity (Table 3), sintering (Table 4) and agglomerative recrystallization of chromium oxide are enhanced by a lowering of the partial pressure of oxygen in the gaseous phase. There are no experimental data on the electrical conductivity of Cr_2O_3 at high temperatures (1,350-1,750° C). One may presume that the electrical conductivity of Cr_2O_3 has the same complex temperature dependence relative to oxygen concentration as is found in the reactivity of chromium oxide.

Titanium Dioxide. We ran some experiments on heating samples of titanium dioxide to temperatures of 1,350° C and 1,550° C with a two-hour hold. The annealing was done in air and in argon. At 1,350° C the linear shrinkage of the samples was equal to 18.2% in air and 20.7% in argon. The collective recrystallization of titanium dioxide occurred more intensively in argon than in air. The dimensions of the crystals after heating to 1,550° C in argon attained 180 μ, while in air the size was up to 60 μ. In samples annealed in argon the formation of an oxygen-poor phase was observed on the periphery and along the grain boundaries. The samples had a deep blue color.

The paper by White (2) states that a sample of titanium dioxide acquired a deep blue color and became a semiconductor on having been heated in air to somewhat above 1,500° C. It is evident from Fig. 5 that the electrical conductivity of titanium dioxide rises with a decrease in oxygen pressure (17). The sintering processes and those of collective recrystallization are intensified and the electrical conductivity rises after a disturbance of the stoichiometric composition in titanium dioxide.

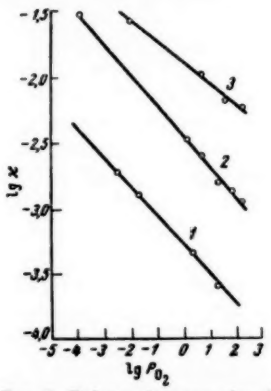

Fig. 5. Relation between the electrical conductivity of titanium dioxide and oxygen pressure: 1) 300°C; 2) 900°C; 3) 1000°C (κ, ohm^{-1} cm^{-1}, and P_{O_2}, mm. Hg).* According to Hauffe, Tränckler-Greese and Grunewald.

*Translator's Note: "$\kappa ohm^{-1} cm^{-1} \kappa = P_{O_2}$ mm. Hg" in the original.

SUMMARY

1. The effect of oxygen pressure on the kinetics of the reactions $ZnO + Al_2O_3 = ZnAl_2O_4$ and $MgO + Cr_2O_3 = MgCr_2O_4$ was studied.

2. The general nature of the influence of the gaseous medium on the progress of some physicochemical processes was confirmed experimentally: for zinc oxide - the comparison of the reactivity, the catalytic activity, and electrical conductivity; for chromium oxide - the comparison of reactivity and electrical conductivity; for titanium dioxide -

the comparison of agglomerative recrystallization, sintering, and electrical conductivity.

3. The kinetics of these physicochemical processes is controlled by the deviation of the composition of the semiconductor oxides from the stoichiometric ratios as a result of the dissociation of the oxides or the adsorption of oxygen by them.

LITERATURE CITED

1. Hedvall, J. A., *J. Glass Technol.* 40, 405 (1956).
2. White, I., *Trans. Brit. Ceram. Soc.* 56, 553 (1957).
3. Kramers, W. I., and Smith, J. R., *Ibid.*, 56, 590 (1957).
4. Williams, J., Barnes, E., Thacray, R. W., and Murray, P., *Ibid.*, 56, 608 (1957).
5. Hauffe, K., Reaktionen in und an festen Stoffen, 597, Berlin (1955).
6. Přibil [Prshibil], R., "Kompleksony v khimicheskom analize" [*Complexons in Chemical Analysis*] [Translator's Note: presumably a translation from Czech] IL [Foreign Literature Publishing House], Moscow (1955).
7. Budnikov, P. P., and Berezhnoi, A. S., *Reaktsii v tverdykh fazakh*, p. 48, Promstroiizdat [State Publishing House of Literature on Building Materials], (1949). Materials], 1949.
8. Mellor, J. W., "Treatise on Inorganic and Theoretical Chemistry," Vol. 11, p. 206 (1943).
9. Weller, S. W., and Voltz, S. E., *J. Am. Chem. Soc.* 76, 4695 (1954).
10. Vol'kenshtein, F. F., *Uspekhi Fiz. Nauk* 60, 249 (1956).
11. Hedvall, J. A., "Einführung in die Festkörperchemie" [*Introduction to the Chemistry of Solids*], p. 86-102, Braunschweig (1952).
12. Rees, A., *Chemistry of Defect Crystals*, [Translator's Note: a Russian translation, possibly of "Chemistry of the Defect Solid State"] IL [Foreign Literature Publishing House], Moscow (1956).
13. Shalyt, S. S., Elektroprovodnost poluprovodnikov, Izdat. Leningrad. doma nauch.-tekh. propagandy [Leningrad Publ. House of Scientific and Technical Propaganda], Institut Poluprovodnikov Akad. Nauk SSSR [Semiconductor Institute, Academy of Sciences of the USSR] No. 1-2, Leningrad, (1956).
14. Myasnikov, I. A., and Pshezhetskii, S. Ya., *Doklady Akad. Nauk SSSR* 99, 277 (1954).
15. Luzhnaya, N. P., and Goryunova, I. A., *Vestnik Akad. Nauk. SSSR*, No. 11, 17 (1958).
16. Hauffe, K., and Block, J., *Z. Physik. Chem.* 198, 232 (1951).
17. Hauffe, H., Grunewald, H., and Tränckler-Greese, R., *Z. Elektrochem.* 56, 937 (1952).

V. A. Kargin
V. A. Kabanov
V. P. Zubov
I. M. Papisov

USSR

Polymerization of Acetone

It is shown that, by using the principle of preliminary ordering of monomeric molecules in the reaction system, it is possible to polymerize substances which are incapable of polymerization under normal conditions. In the case described, this ordering was achieved by crystallization of the monomer.

THE transition of a liquid monomer to a polymer is known to involve a decrease in the entropy of the system. Therefore, from the most general thermodynamic considerations it follows that homogeneous liquid-phase polymerization can occur only with a positive heat effect (Q). In actual fact,

$$\Delta Z = \Delta H - T\Delta S,$$

where ΔZ is the change in the isobaric isothermal potential during the transition of the monomer to the polymer, $\Delta H = -Q$ is the change in heat content, ΔS is the change in the entropy of the system, and T is the absolute temperature. The inequality $\Delta Z < 0$ must hold for the process to occur spontaneously and when $\Delta S < 0$, this is possible only if $\Delta H < 0$ and $|\Delta H| > |T\Delta S|$, i.e., $Q > 0$. The heat effect of the reaction may be determined as the algebraic sum of the energies of the bonds ruptured as a result of the reaction and the bonds formed, with the former considered as negative values and the latter as positive.

If we estimate the heat effect of the polymerization of carbonyl compounds, for example, acetaldehyde or acetone, then by taking the energy of the

This article first published in *Doklady Akad. Nauk. SSSR* 134, No. 5, 1098-1099 (1960). The authors are associated with the M. V. Lomonosov Moscow State University.

C-O bond in the polymer as equal to the mean energy of the C-O bond in ethers, we find that the heat effect of the polymerization of acetone equals −6 kcal./mole and of acetaldehyde, zero (the energy of the C = O bond in acetone equals 156 kcal./mole and in acetaldehyde, 150 kcal./mole and the mean energy of the C-O bond in ethers is 75 kcal./mole). Thus, from this estimate it may be concluded that the polymerization of acetaldehyde and acetone in a homogeneous liquid phase is impossible. However, if the monomeric liquid is changed to a system of ordered monomer molecules in the initial state, i.e., the entropy of the initial system is decreased, the picture may be changed substantially. One method of ordering the molecules of the monomer is to freeze the latter. The change from liquid to crystalline monomer decreases the entropy of the system by the entropy of fusion. For organic liquids, the entropy of fusion normally lies within the range of 13 ± 3 cal./(deg.) (mole) (1), which is obviously commensurate with the entropy change during the transition of a liquid monomer to an amorphous polymer. A decrease in the entropy of the starting system leads to a decrease in the negative entropy of polymerization. At sufficiently low temperatures, the latter may even change sign. In this case, polymerization involving a negative heat effect becomes possible. Thus, in some cases the phase state of the monomer in the system may have a decisive effect on the capacity of this monomer to polymerize, which is determined by the thermodynamic parameters of the initial and final systems. For example, it is well known that acetaldehyde, which is incapable of polymerization at normal pressures in the liquid phase, is readily polymerized in the solid state close to the melting point (2-4).

In view of these considerations, we attempted to polymerize acetone through the C = O double bond by using the method we developed for low-temperature polymerization in systems obtained by simultaneous condensation of molecular beams of monomer and initiator on a strongly cooled wall (5-7).

The experiments were carried out in an instrument and by a procedure analogous to those described in (5, 6). The initiator used was metallic magnesium, whose vapor was slowly condensed in vacuum together with the vapor of carefully dried acetone on a surface cooled with liquid nitrogen. The ratio of acetone to magnesium in the condensation was approximately 200 : 1. The condensate deposited on the cooled wall consisted of a vitreous molecular mixture of acetone and magnesium. As the layer thickened, the distance between its constantly renewed surface, and the cooled wall increased. As a result of this, the temperature of the outer surface of the vitreous condensate increased continuously and finally reached a value at which spontaneous coordinated rearrangements of the monomer molecules began in the surface layer. In the absence of initiation centers in the system, this process should have led to crystallization of the monomeric glass. However, in the given case, the mobility of the particles arising during the disorder-order phase transition resulted in their instantaneous polymerization. The same phenomenon could be observed by gradually raising the temperature of the wall on which the condensation was carried out. In other words, at the moment at which the transition to the solid phase occurred, conditions were created which kinetically favored combination of the ordered monomer molecules into polymeric chains.* A polymer of acetone was formed and this consisted of a white elastic mass. The polymer was soluble in its own monomer. The polyacetone was extremely unstable at room temperature and decomposed to form acetone. When rubbed in the hands, a sample of polyacetone rapidly changed to a drop of monomer. The most stable samples of the polymer existed for not more than 10-12 hrs. in the presence of oxygen and moisture. A polymer obtained by condensation of acetone together with traces of vinyl acetate was found to be somewhat more stable. Evidently, it should be possible to stabilize polyacetone by blocking the active ends of the polymeric chains.

The instrument for condensation of molecular beams was connected to a viscometer. The design of the instrument made it possible to prepare solutions of the polymer obtained and to measure the viscosity of these solutions directly in vacuum without the admission of atmospheric moisture and oxygen. The specific viscosity of a solution of polyacetone in acetone, measured by this method in one experiment, equaled 0.6 (with a solution concentration of 0.5 g./100 ml.).

On the example of acetone it was shown that by using the principle of preliminary ordering of monomeric molecules in the reaction system, it is possible to polymerize substances which are incapable of polymerization under normal conditions. In the given case, this ordering was achieved by crystallization of the monomer. Conditions favorable to the formation of polymeric chains from ordered monomer molecules arose at the moment when a phase transition of the disorder-order type occurred in the vitreous monomer.

*Quantitative considerations on the mechanism of the formation of a polymeric chain in an ordered system of monomeric molecules were recently put forward by Semenov.[8]

LITERATURE CITED

1. Karapet'yants, M. Kh., *Khimicheskaya termodinamika*, Moscow (1953).
2. Letort, M., *Compt. rend.* 202, 767 (1936).
3. Letort, M., and Duval, X., *Ibid.*, 216, 58, 608 (1943).
4. Letort, M., Duval, X., and Pollin, J., *Ibid.*, 224, 50, (1947).
5. Kargin, V. A., Kabanov, V. A., and Zubov, V. P., *Vysokomolekulyarnye Soedineniya* 1, 265 (1959).
6. Kargin, V. A., and Kabanov, V. A., *International Symposium on Macromolecular Chemistry, reports and Authors' Abstracts, Section II*, p. 453, Moscow (1960).
7. Kabanov, V. A., Sergeev, G. B., Zubov, V. P., and Kargin, V. A., *Vysokomolekulyarnye Soedineniya* 1, 1859 (1959).
8. Semenov, N. N., *Chemistry and Technology of Polymers, No. 7-8, Proceedings of the International Symposium on Macromolecular Chemistry*, p. 196, Moscow (1960).

Yu. A. Shlyapnikov
V. B. Miller
M. B. Neiman
E. S. Torsueva
B. A. Gromov

USSR

Thermo-Oxidative Degradation of Polypropylene – a Study of the Comparative Effectiveness of Some Antioxidants

Description of a technique for studying the effectiveness of several different stabilizers simultaneously, together with experimental data on the comparative effectiveness of thirteen different stabilizers in the oxidation of propylene.

As already mentioned in our previous publications (1, 2), polypropylene is oxidized relatively readily by oxygen at elevated temperatures. Therefore, it has become necessary to select the most effective inhibitors of the thermo-oxidative degradation of polypropylene.

We studied the stabilizing effect of various substances, mainly aromatic amines and phenols. Many of these substances had been suggested previously as stabilizers of rubber (3) as well as food fats (4, 5).

To characterize the effectiveness of a stabilizer, we used the duration of the induction period of oxidation of polypropylene under standard conditions: at a temperature of 140° C, oxygen pressure of 300 mm. Hg, and a concentration of 0.01 mole/kg. (at times, 0.003 mole/kg. in addition) of the inhibitor additive.

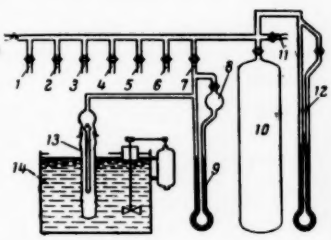

Fig. 1. Diagram of the apparatus set-up: 1-7) outlets to separate sections of apparatus; 9) differential manometer with bulb 8; 10) oxygen cylinder; 11) take-off for gas sampling; 12) manometer; 13) reaction vessel; 14) thermostat.

The duration of the induction period under such conditions may reach several tens of hours. Therefore, to speed up the work, we constructed a special set-up (Fig. 1) which allowed us to study the oxidation of seven different polypropylene samples simultaneously. Seven identical sections 1-7 of the apparatus, each of which consisted of a differential manometer 9 and a reaction vessel 13 connected to it, were sealed to the glass tube manifold of the

This article first published in *Vysokomolekulyarnye Soedineniya* 2, No. 9, 1409-1412 (1960). The authors are associated with the Institute of Chemical Physics of the Academy of Sciences of the USSR.

apparatus. A glass tube sealed at both ends was inserted into the upper part of the reaction vessel for reduction of its volume. The average volume of a section was 10.5 ml. Half of this volume (5.2 ml.) was at the experimental temperature while the remainder was at room temperature. The vessels were immersed in thermostat 14 filled with a silicone oil. The thermostat was equipped with a special lifting device for this purpose. The work was facilitated by the fact that during a study of oxidation of various samples under identical conditions the induction periods ended, as a rule, at different times in the various reaction vessels.

The most important part of the work was the mixing of the polypropylene with the stabilizer. We developed the following technique of mixing: the powdered polypropylene was mixed with a weighed sample of the substance being tested by grinding in a mortar; a solvent which dissolves the stabilizer but does not dissolve the polypropylene (such as alcohol) was added into the mortar. The mixture was dried and ground once more in the mortar, after which films about 0.1 mm. thick were pressed from it (more accurately, 0.010 g./cm.^{2}). The pressing was done in a special press form under an inert gas atmosphere at 120-130°C and a pressure of about 120 kg./cm^2.

Our experiments on the oxidation of polypropylene films that did not contain a stabilizer showed that in the oxidation of films up to 0.2 mm. thick the rate of oxygen absorption in the initial stage of the reaction was independent of film thickness.

The kinetic curves of the oxidation of the films are shown in Fig. 2: 1-3) films of equal surface area but different masses, and 4-6) those with equal mass but different surface areas (i.e., of different thickness). Curves 1-3 differ from each other considerably while the initial parts of curves 4-6 are almost coincident with each other. Therefore, the oxidation reaction takes place within the volume of the film and not on its surface.

Some preliminary experiments showed that the

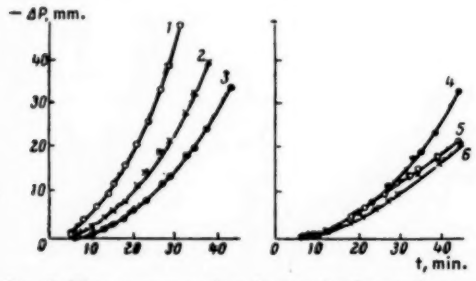

Fig. 2. Kinetic curves of oxidation of polypropylene films: 1-3) films with the same surface area (S = 8 cm.^{2}) 4-6) films of the same mass (0.050 g.). Film thickness: 3, 4) 0.0061; 2, 5) 0.0102; 1, 6) 0.0190 g./cm^2.

stabilizers, especially those with a low molecular weight, are readily volatilized from the polymer film on being heated in a vacuum. For this reason the technique of studying the oxidation of our films containing a stabilizer was changed in comparison with that described previously (2). Heating of polypropylene in a vacuum was done prior to the mixing with the stabilizer; the stabilizer-containing film was placed in the reaction vessel, the latter was evacuated at room temperature, filled with oxygen and heated only then. For the same reason as much as possible the least volatile substances should be used for stabilizing polypropylene.

Several kinetic curves of polypropylene oxidation at 140°C and 300 mm. Hg oxygen pressure are shown in Fig. 3, curve 1 showing the results without a stabilizer, the others showing the effects of the addition of 0.003 mole/kg. of benzidine, diphenylamine, and Neozone D.

Fig. 3. Kinetic curves of polypropylene oxidation; 1) without additive; 2) with addition of benzidine; 3) with diphenylamine; and 4) Neozone D; T = 140°C; P_{O_2} = 300 mm. Hg; additive concentration 0.003 mole/kg.

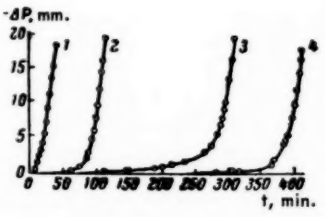

It is evident from this figure that, while the action of some stabilizers (benzidine, Neozone D) amounts to but an increase of the induction period duration, others (diphenylamine) retard the oxidation even after the termination of the induction period.

Table 1 shows the values of induction period durations τ of the oxidation of polypropylene under standard conditions with addition of various stabilizers (0.01 mole/kg.).

Values of induction period duration in polypropylene oxidation in the presence of lower concentrations of some stabilizers are shown in Table 2.

As is evident in a comparison of these tables, the most effective stabilizer among those studied by us was diphenyl-p-phenylenediamine, followed by Neozone D (phenyl-β-naphthylamine), propyl gallate, and Ionol. All these substances are effective stabilizers of rubbers (3) and food fats (4, 5) not only at elevated temperatures but also at temperatures close to room temperature. Therefore, the assertion made by Bresler and co-workers (6) that for the stabilization of polymers one must use substances which are poor stabilizers at room temperature, not only fails to indicate the routes to a search for new stabilizers, but actually contradicts the results of our experiments. It should be added that the experimental data cited in the paper by these authors fail to provide any basis for such

Table 1.
Comparative effectiveness of some stabilizers in propylene oxidation

($T = 140°C$; $P_{O_2} = 300$ mm. Hg; stabilizer concentration 0.01 mole/kg.)

Stabilizer	Chemical formula	r, min.
Without additives		18
Cyclohexylbenzene	$C_6H_5 \cdot CH(CH_3)_2$	25
Thiourea	$(NH_2)_2CS$	80
2, 4-Dinitrophenylhydrazine	$H_2N-NHC_6H_3(NO_2)_2$	137
2, 5-Di-tert-butylhydroquinone	$C_6H_2(OH)_2(C_4H_9)_2$	200
Diphenylamine	$(C_6H_5)_2NH$	400
Benzidine	$H_2N-C_6H_4-C_6H_4-NH_2$	700
Polygard	$P(O-C_6H_4-C_9H_{19})_3$	850
2, 4, 6-Tri-tert-butylphenol	$HO-C_6H_2(C_4H_9)_3$	920
Hydroquinone monobenzyl ether	$C_6H_5CH_2-O-C_6H_4OH$	1200
Ionol (2, 6-di-tert-butyl-4-methylphenol)	$HO-C_6H_2(C_4H_9)_2CH_3$	1400
Propyl gallate	$C_3H_7OCO \cdot C_6H_2(OH)_3$	2300
Neozone D (phenyl-β-naphthylamine)	$C_6H_5-NH-C_{10}H_7$	> 4000
Diphenyl-p-phenylenediamine	$C_6H_5-NH-C_6H_4-NH-C_6H_5$	> 4000

conclusions. We failed to observe even a single instance of acceleration of the oxidation process under the influence of easily oxidizable phenols or amines.

SUMMARY

1. A technique was suggested for a study of the effectiveness of stabilizers of the thermo-oxidative degradation of polymers which allows for a study of oxidation of several different samples simultaneously.

2. The effect of some antioxidants on the stability of polypropylene relative to thermo-oxidative degradation was studied.

Table 2.
Relative effectiveness of some stabilizers of polypropylene oxidation at concentrations of 0.001 and 0.003 mole/kg.

($T = 140°C$; $P_{O_2} = 300$ mm. Hg)

Stabilizer	Concentration, mole/kg.	
	0.001	0.003
Diphenylamine	80	250
Neozone D	100	380
Propyl gallate	-	800
Diphenyl-p-phenylenediamine	-	> 3000

LITERATURE CITED

1. Miller, V. B., Neiman, M. B., Pudov, V. S., and Lafer, L. I., *Vysokomolekulyarnye Soedineniya* 1, 1696 (1959).

2. Miller, V. B., Neiman, M. B., and Shlyapnikov, Yu. A., *Ibid.*, 1, 1703 (1959).

3. Angert, L. G., and Kuz'minskii, A. S., *Rol i primenenie antioksidantov v kauchukakh i rezinakh*, p. 20, Goskhimizdat [State Scientific and Technical Publishing House of Chemical Literature], Moscow (1957).

4. Emanuel, N. M., Knorre, D. G., Lyaskovskaya, Yu. N., and Piul'skaya, V. I., *Myasnaya Ind. SSSR*, No. 2, 52 (1958).

5. Knorre, D. G., Lyaskovskaya, Yu. N., Piul'skaya, V. I., and Emanuel, N. M., *Zhur. Priklad. Khim.* 32, 1359 (1959).

6. Bresler, S. E., Os'minskaya, A. T., and Popov, A. G., *Vysokomolekulyarnye Soedineniya* 2, 130 (1960).

G. D. Efremova
R. O. Koroleva

USSR

The Equilibrium Solid-Liquid-Gas in the System Melamine-Ammonia-CO_2

Basic, experimentally obtained equilibrium data in a field of direct industrial application.

A study of the three-phase equilibrium solid-liquid-gas in the system melamine-ammonia at temperatures above the critical temperature of NH_3 showed that, because of solution of NH_3 in liquid melamine, the melting point of the latter (354° C) depends significantly on the pressure of NH_3 (1). At a pressure of about 700 kg./cm.^{2}, melamine melts at about 250° C. The curve of the three-phase equilibrium under these conditions intersects the critical curve of the two-phase equilibrium, critical phenomena are observed between the liquid and gaseous phases in the presence of solid melamine, and the three-phase equilibrium solid-liquid-gas changes to a two-phase equilibrium solid-gas.

In the present work, we studied the three-phase equilibria solid-liquid-gas in the systems melamine-CO_2 and melamine-NH_3-CO_2.

EXPERIMENTAL

A weighed portion of melamine was charged into a steel column and NH_3 was measured in. The column was then placed in a furnace and the apparatus was heated to 200-250° C. After this, CO_2 was measured into the column by means of a calibrated hydraulic press. It is impossible to measure out the CO_2 entering the apparatus at room temperature, since solid ammonium carbamate immediately forms in the column and, on heating the ammonium carbamate, a urea synthesis reaction begins (2). Therefore, in measuring, we took care that the pressure in the apparatus did not exceed the saturated vapor pressure of ammonium carbamate (3). In this case, NH_3 and CO_2 remain completely in the gas phase, and the synthesis of urea does not take place in the gas phase (2). After feeding CO_2 into the apparatus, the furnace was set in motion, the contents of the column were stirred, and the temperature and pressure were observed. The furnace was then heated 10-20° C and, again after stirring and equalizing the temperature, the pressure and temperature were noted. At the end of the experiment, the column was removed from the furnace and, in order to avoid the possibility of urea formation, was cooled rapidly with a water-ice mixture (at temperatures below 100° C, the reaction velocity is very low (2)).

The column was then cooled to −20° C. At this temperature, the ammonium carbamate formed from NH_3 and CO_2 on cooling the column has a vapor pressure of 1 mm. Hg (3). The valve was opened further, and the gas leaving the column (NH_3 or CO_2) was absorbed by titration with alkali or acid solution. After this, the column was opened and washed several times with ice water. The solution was transferred to a measuring flask, NH_3 and CO_2 were determined, and an analysis for urea was performed. For this, the solution was evaporated on a water bath, the precipitate was weighed, again dissolved in water, and melamine was determined in the solution as melamine cyanurate (4). The equality of the weights of the initial precipitate and of melamine indicates that no urea is formed during the experiment.

The three-phase equilibrium in the systems melamine-CO_2 and melamine-NH_3-CO_2 was studied by the method involving a break in the pressure-temperature curve (the experimental set-up was described in Ref. (1)).

Fig. 1 shows the p-t curves obtained by us in a study of the three-phase equilibrium in the system melamine-CO_2 at various ratios of melamine and CO_2 in the starting mixture. The absence of a break in the p-t curves indicates that CO_2 is practically insoluble in liquid melamine. Hence it follows that the melting point of melamine should increase with increasing pressure according to the thermodynamic equation (5):

This article first published in *Zhur. Fiz. Khim.*, Vol. 35, No. 4 (1961). The authors are associated with the Government Institute for the Nitrogen Industry.

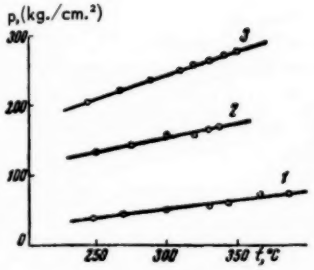

Fig. 1. p-t relationships in the system melamine-CO_2.

$$\frac{dp}{dT} = \frac{1}{T}\frac{\Delta H}{\Delta V},$$

where ΔH and ΔV are the changes in the enthalpy and volume of melamine on melting.

Fig. 2 shows the curve forming the boundary of the three-phase equilibrium in the system melamine-NH_3 (1). The broken curve represents the assumed course of the melting curve of melamine under a pressure of CO_2.

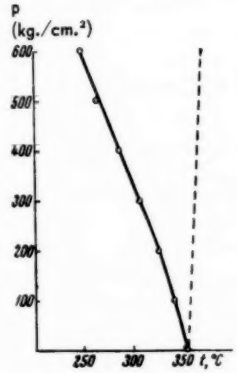

Fig. 2. Three-phase curve in the system melamine-NH_3.

It could be assumed that the three-phase curves in the system melamine-NH_3-CO_2 would be located between the melting curve of melamine and the three-phase curve of the system melamine-NH_3. The experiments, however, did not confirm this assumption.

Fig. 3 shows the p-t curves obtained in three different experiments. Analogous curves were also obtained in all the other experiments.

In Fig. 3, the part a-b of the broken curve expresses the p-t relationship in the region of the two-phase equilibrium solid melamine-gaseous solution. An increase in pressure with increase in temperature is observed until melting of melamine begins. Melting of melamine begins at point b, and the system changes from the region of two-phase solid-gas equilibrium to the region of three-phase solid-liquid-gas equilibrium. There is, therefore, a break in the curve at point b. On further increase in temperature, the pressure no longer increases, but decreases, since the gas

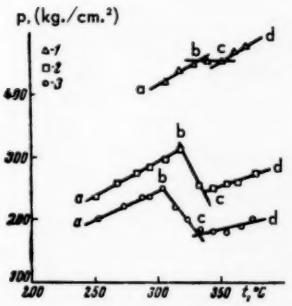

Fig. 3. p-t relationships in the system melamine-NH_3-CO_2. 1-84.4, 2-35.4, 3-35.7 mole percent CO_2.

mixture dissolves in liquid melamine. As soon as all the melamine melts, the system changes from a region of three-phase equilibrium to a region of two-phase liquid-gas equilibrium, and a second break (point c) appears on the p-t curve. The section b-c expresses the p-t relationship in a certain part of the curve of three-phase equilibrium. The composition of the gas mixture in equilibrium with the liquid solution is not constant on the three-phase curve because of the different solubilities in liquid melamine of the components of the gas mixture (NH_3 and CO_2). Therefore, in computing p and t of the three-phase curve for the system melamine-NH_3-CO_2 (for a constant ratio of NH_3 to CO_2 in the gas mixture) we considered only the first point of the three-phase curve, i.e., the break point b.

If the CO_2 content in the starting gas mixture does not exceed about 27 mole percent, the three-phase curves are located at lower temperatures (Fig. 4) than the three-phase curve in the system melamine-NH_3. This is possible only in the case where, at a given temperature and pressure, the total concentration of NH_3 and CO_2 in liquid melamine on solution from the mixture is greater than the solubility of pure NH_3. Since CO_2 is insoluble

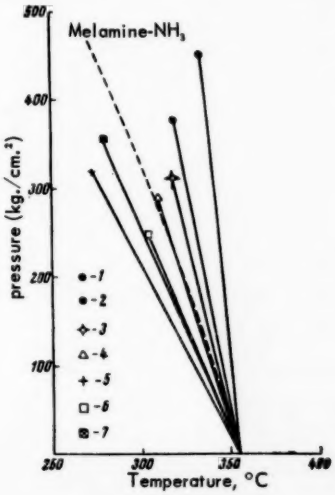

Fig. 4. Curves of three-phase equilibrium in the system melamine-NH_3-CO_2: 1-84.4, 2-42.9, 3-35.4, 4-27.5, 5-13, 6-3.6, 7-2.7 mole percent CO_2.

in liquid melamine, it may be assumed that the NH_3 dissolved in the latter carries CO_2 along into the solution.

SUMMARY

The solubility of melamine in liquid and gaseous CO_2 was studied at temperatures from room temperature to 250° C and pressures of up to 400 kg./cm^2. The data showed that melamine is practically insoluble in both liquid and gaseous CO_2. It was shown that CO_2 is practically insoluble in liquid melamine.

*The authors express their gratitude to I. R. Krichevskii for advice and attention in the course of the work.

The region of three-phase equilibrium solid-liquid-gas in the system melamine-NH_3-CO_2, existing at temperatures above the critical temperature of NH_3, was studied.

LITERATURE CITED

1. Krichevskii, I. R., Efremova, G. D., *Zhur. Fiz. Khim.* 33, 1328 (1959).
2. Frejaques, M., *Chim. & Ind.* (Paris) 60, 22 (1948).
3. Stull, D. R., *Tables of Vapor Pressures of Individual Substances* (Russian edition), Moscow, 1949.
4. Kazarnovskii, S. N., Lebedev, O. P., *Trudy Gor'k. Politekh. Inst.* 11, 54 (1955).
5. Lewis, G. N. and Randall, M., *Chemical Thermodynamics* (Russian edition), 1936.

G. D. Efremova
G. G. Leont'eva

USSR

The Solubility of Melamine in Solutions of Dicyandiamide in Liquid Ammonia

In preparing a solution of dicyandiamide in liquid ammonia for synthesis of melamine from dicyandiamide, it is necessary to allow for the solubility of melamine in liquid ammonia in the presence of dicyandiamide. If the melamine dissolves incompletely, its crystals can block equipment lines.

THE first stage in the continuous method for synthesizing melamine from dicyandiamide (1) is the preparation of a solution of dicyandiamide in liquid ammonia; the solution then enters the reactor where the formation of melamine takes place.

The starting technical dicyandiamide always contains a certain amount (3-5%) of melamine, whose solubility in liquid ammonia is low (2). If, on dissolving technical dicyandiamide in liquid ammonia, the melamine dissolves incompletely, then its crystals can block communications. Therefore, in preparing the solution, it is necessary to allow for the solubility of melamine in liquid ammonia in the presence of dicyandiamide. This information is not found in the literature.

We investigated the solubility of melamine in solutions of dicyandiamide in liquid ammonia in sealed glass ampoules, by a method described previously (2).

In the experiments we used doubly recrystallized dicyandiamide, containing no melamine (the absence of melamine was checked by reaction with cyanuric acid (3). The concentration of the main product in recrystallized melamine was 99.5%. Ammonia (from a cylinder) was dried by passing it through a column filled with caustic potash.

The data obtained (Figs. 1 and 2) show that the solubility of melamine depends on the concentration of dicyandiamide in liquid ammonia. Thus, for example, at a dicyandiamide concentration of 4.6 g. per 100 g. NH_3 in the solution, the solubility of melamine decreases with increasing temperature, and the solubility curve is analogous to the solubility curve of melamine in pure ammonia. At a

This article first published in *Khim. Prom.* (1960/8).

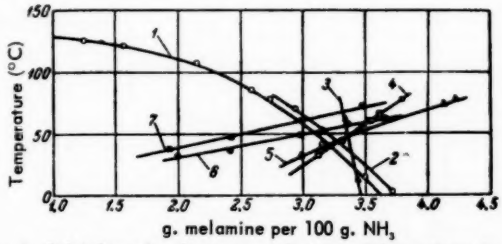

Fig. 1. Solubility of melamine in solutions of dicyandiamide in liquid ammonia.

dicyandiamide content of 9.2 g. per 100 g. NH_3, the solubility of melamine depends little on temperature. A further increase in concentration of dicyandiamide in the solution leads to a change in the character of the solubility curve: on increasing the temperature, the concentration of melamine in the solution does not decrease, but increases. It is clearly seen from Fig. 2 that, at a dicyandiamide concentration of about 14 g. per 100 g. NH_3, the solubility of melamine is generally independent of temperature.

Since, in the synthesis of melamine from dicyandiamide by a continuous method, the concentration of dicyandiamide in the liquid ammonia solution is 50 weight per cent, and the solvent temperature is about 70° C, the content of melamine in this solution should not exceed 4%. For larger amounts of melamine in the starting dicyandiamide, the melamine will partly remain as a residue in the preparation of the solution, and this inevitably leads to blockage of the communications and the liquid pump.

In a saturated solution, when the solid phase is in equilibrium with the liquid solution, we have

$$\mu_2 = \mu_2' \quad \text{and} \quad d\mu_2 = d\mu_2'$$

where μ_2 and μ_2' are the chemical potential of the component in solution and in the solid state, respectively.

In a ternary solution, if the concentrations of components 1 (ammonia) and 3 (dicyandiamide) are constant, then at constant pressure, the chemical potential of component 2 (melamine) will depend only on its concentration in the solution and on temperature. Hence,

$$\left(\frac{\partial \mu_2}{\partial n_2}\right)_{P,\,T,\,n_1,\,n_3} dn_2 + \left(\frac{\partial \mu_2}{\partial T}\right)_{P,\,n_1,\,n_2,\,n_3} dT = \left(\frac{\partial \mu_2'}{\partial T}\right)_P dT \qquad (1)$$

$$\left(\frac{\partial \mu_2}{\partial n_2}\right)_{P,\,T,\,n_1,\,n_3} dn_2 - S_2 dT = -S' dT \qquad (2)$$

where $\overline{S}$ and S_2' are the partial molar entropy of melamine in solution and in the solid state, respectively.

From (2), it follows that:

$$\left(\frac{\partial \mu_2}{\partial n_2}\right)_{P,\,T,\,n_1,\,n_3} dn_2 = (\overline{S}_2 - S_2')\, dT = -\frac{\overline{H}_2 - H_2'}{T}\, dT \qquad (3)$$

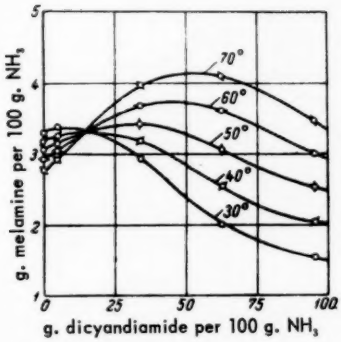

Fig. 2. Isotherms of the solubility of melamine in solutions of dicyandiamide in liquid ammonia.

where $\overline{H}_2$ and H_2' are the partial molar heat content of melamine in solution and in the solid state, respectively.

From (3) we have:

$$\left(\frac{\partial T}{\partial n_2}\right)_{\text{coexistence}} = T\frac{\left(\frac{\partial \mu_2}{\partial n_2}\right)_{P,\,T,\,n_1,\,n_3}}{\overline{H}_2 - H_2'} \qquad (4)$$

The derivative $(\partial \mu_2/\partial n_2)_{P,\,T,\,n_i\,(i \neq 2)}$ is always zero or greater than zero. Therefore, the sign of $(\partial n_2/\partial T)_{\text{coexistence}}$ or, in other words, the character of the dependence of the solubility of melamine on temperature, is determined by the sign of the difference $\overline{H}_2 - H_2'$, i.e., by the sign of the heat of solution of melamine in a solution of dicyandiamide in liquid ammonia.

The fact that the solubility of melamine in solutions of dicyandiamide in liquid ammonia can increase or decrease with increasing temperature, depending on the concentration of dicyandiamide in the solution, indicates that the heat of solution changes sign as the concentration of dicyandiamide in the solution increases.

If the heat of solution is zero $(\overline{H}_2 - H_2' = 0)$, then $(\partial n_2/\partial T)_{\text{coexistence}} = 0$, i.e. the solubility will not depend on temperature. This is precisely what we observe in the case where the concentration of dicyandiamide in the solution is about 14 g. per 100 g. NH_3.

LITERATURE CITED

1. Gol'dberg, N. A., Zagranichnyi, V. I., *Doklady Akad. Nauk SSSR* 124, 635 (1959).

2. Krichevskii, I. R., Efremova, G. D., *Zhur. Fiz. Khim.* 33, 1328 (1959).

3. Kazamovskii, S. N., Lebedev, O. L., *Trudy Gor'k. Politekh. Inst. im. A. A. Zhdanova* 11, 54 (1955).

G. P. Korneichuk
V. A. Roiter
V. Ya. Vol'fson
Ya. V. Zhigailo
A. Z. Lyubiteleva*

UKRAINE, USSR

Peculiarities of the Catalytic Oxidation of Naphthalene. Part 2

Data obtained in an industrial reactor show that a combination charge of vanadia catalysts is superior to a conventional vanadium pentoxide catalyst.

It was shown earlier (1, 2) that the low selectivity (about 70%) of fused vanadium pentoxide in the vapor-phase oxidation of naphthalene to phthalic anhydride is due to a large extent to internal diffusion retardation in the pores of the catalysts. In (2) were shown methods of increasing the productivity** and selectivity of vanadia catalysts by the use of a combination charge composed of a partially reduced vanadia catalyst and coarse crystalline vanadium pentoxide. It is known that a partially reduced catalyst has a higher melting point than vanadium pentoxide, and this counteracts fusion-plugging of the tubes of the reactor when overheating occurs in the catalyst mass. Coarse crystalline vanadium pentoxide exhibits increased selectivity.

The aim of the present investigation was to compare the operation of the proposed combination charge with that of catalysts used in the industry: fused vanadium pentoxide and a complex vanadia-potassia-sulfate-silica gel catalyst in catalyst columns corresponding in size to those used in the industry. It was also of interest to investigate changes in productivity and selectivity with respect to the products of the oxidation of naphthalene and to study the temperature conditions along the bed.

The investigation of the vanadia catalysts was carried out in a single tube of an industrial reactor, used in the actual size (length 2.5 m., diameter 1.9 cm.). For convenience, it was cut into five equal sections and each of these was bent into a cell in the form of a U. The reactor was placed in a lead bath. Each cell of the reactor was equipped with an exit tube terminating in a valve for sampling. The length (depth) of the catalyst beds studied was 45 cm. in each cell. The first cell along the flow of the gas had two additional exit tubes for withdrawing samples at 15 cm. intervals. At six points along the column, temperature was measured with iron-constantan thermocouples. The heating of the bath was done with the aid of an electrical heater, a relay, and a contact thermometer.

The construction of the reaction apparatus is pictured in Fig. 1, which shows how the tubes of the reactor are made tight with the aid of conical fittings with slip nuts, and the disposition of the thermocouple wells (1-6) and the tubes for sampling (I-VII).

A diagram of the entire apparatus is shown in Fig. 2.

Air was passed from the compressor through valve 11, flowmeter 2, the preheater furnace coil 3, into the shelf-type naphthalene vaporizer made of sheet steel, where it was saturated with naphthalene (3). The naphthalene-air mixture, heated to 280°C in furnace 5, passed into the reaction apparatus 6 (Fig. 1). The reaction gases then passed into the glass condenser 7, and the uncondensed products of oxidation into the scrubber 8 packed with porcelain rings sprayed with water.

To determine the yield of the products from their weight, the glass condenser 7 (Fig. 2), which permitted visual observations of the color of the products, was disconnected, and a system of metal condensers was connected.

The mercury manometer 1 served to measure the pressure when the air flow rate was regulated and varied.

*The experimental work was done with the cooperation of A. T. Beskrovnaya, L. S. Fal'kovich, and T. A. Sidorovich.

**Translator's Note: A Soviet term denoting a variation of the "activity" concept and usually expressed in wt. units of a given product or consumed feed per unit volume of catalyst. In the present case "productivity" is expressed in moles/min.

This article first published in *Ukrain. Khim. Zhur.* 26, No. 4, 432-439 (1960). The authors are associated with the L. V. Pisarzhevskii Institute of Physical Chemistry of the Academy of Sciences of the Ukrainian SSR, Rubezhnoe Chemical Combine.

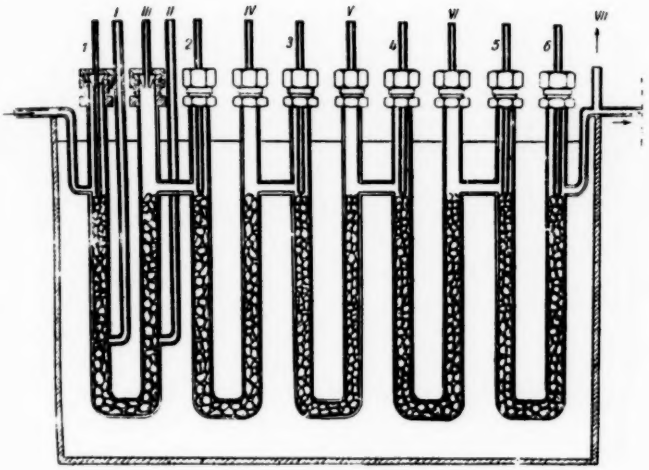

Fig. 1. Converter

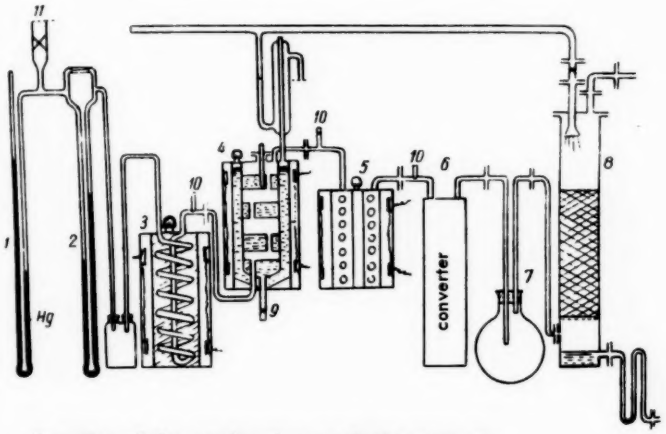

Fig. 2. Diagram of apparatus

Samples of the condensing products were removed for analysis with the aid of glass traps placed in Dewar flasks with ice. The amount of gas passed through the traps was measured with a Mariotte vessel. The acid products were determined by titration with alkali, maleic anhydride was determined iodometrically, 1,4-naphthoquinone was determined photocolorimetrically, and carbon monoxide, carbon dioxide, and oxygen with a gas analyzer.

To determine the composition of the catalyst along the column with respect to the amount of vanadium (lower and higher valence states), use was made of a method described in Ref. (4).

In industrial reactors, the catalyst bed has no breaks and large free spaces. In the reactor used in the present work (Fig. 1), rather large spaces not filled by the catalyst were present above the catalyst beds in the cells and in the connecting tubes. According to the heterogeneous-homogeneous theory of chain processes (5), chains initiated on the active surface of a catalyst in the presence of free spaces are propagated in the space. It was thus necessary to estimate the possibility of the occurrence of heterogeneous-homogeneous oxidation of naphthalene and the products of its mild oxidation in the free spaces of our reactor. To this end, the following experiments were carried out.

1. The first cell along the gas flow was charged with an industrial vanadia catalyst (Fig. 1), and the remaining four cells were left empty. The catalytic reaction was then carried out at a bath temperature of 430°C (100% conversion). The composition and concentration of the reaction products at the end of the catalyst column and after passing through the empty cells were the same.

2. The first four cells were left empty and the fifth cell was charged with the catalyst. In this case, no reaction was found to take place ahead of the catalyst column. These experiments thus led to the conclusion that, under the conditions used by us, free spaces in the reactor had no noticeable effect on the course of the catalytic process.

Table 1

Comparative data on the productivity and selectivity of vanadia catalysts with respect to phthalic and maleic anhydride and testing conditions*

Catalysts	Phthalic anhydride		Maleic anhydride	
	W, moles/min.×10³	S, %	W, moles/min.×10⁴	S, %
Industrial t = 410°C, V = 40 liters/min. h = 600 mm. Hg m = 674 g. $C_N = 67\times10^{-3}$ g./liter d = 10 × 10 × 5 mm.	15.7	73.0	18.1	8.67
Combination charge t = 390°C, V = 46 liters/min. h = 680 mm. Hg m = 631 g. $C_N = 66\times10^{-3}$ g./liter d = 10 × 10 × 5 mm.	18.3	77.0	12.7	5.35
Complex vanadia catalyst t = 370°C, V = 10 liters/min. h = 75 mm. Hg m = 210 g. $C_N = 43\times10^{-3}$ g./liter d = 5 × 5 mm.	2.58	77.0	0.25	7.5
Industrial, fine grain t = 410°C, V = 60 liters/min. h = 820 mm. Hg m = 343 g. $C_N = 63\times10^{-3}$ g./liter d = 3 × 3 mm.	23.5	77.0	26.3	8.8

*W = productivity relative to the volume of the catalyst charge; S = selectivity in percent of naphthalene oxidized to the product in question; V = flow rate of naphthalene-air mixture; m = weight of catalyst; C_N = concentration of naphthalene in gas mixture; d = grain size.

COMPARISON OF THE PRODUCTIVITY AND SELECTIVITY OF VANADIA CATALYSTS

The method described above was used in studying the catalytic process on an industrial and a combination charge of vanadia catalysts, as well as on a charge of a complex vanadia catalyst, under conditions of complete conversion of naphthalene. At a given temperature and concentration of the naphthalene-air mixture, the highest flow rates of the gas mixture at which no breakthrough of naphthalene is yet observed at the end of the catalyst column were determined by the indicator method (6).* The use of the indicator method made it possible to compare rapidly and reliably the productivities and selectivities of vanadia catalysts differing in composition, grain size, and structure, under conditions of complete conversion of naphthalene.

*The principle of the indicator method is as follows. To a small amount of the oxidation products condensed in a tube on a cotton plug are added a few drops of chloroform and 0.2-0.3 g. of aluminum chloride. In the presence of even traces of napthalene in the products the cotton plug turns blue-green.

In Table 1 are listed the characteristics of the catalyst charge, the conditions under which the catalysts were tested, and their productivity and selectivity with respect to phthalic and maleic anhydride. In Table 2 are listed the data on the operation of the combination charge over an ex-

Table 2

Productivity and selectivity with respect to phthalic anhydride of a combination charge of vanadia catalysts and conditions under which it was tested

Bath temp., °C	V, liters/min.	h, mm. Hg	C_N, g./liter×10³	Naphthalene consumed, kg.	Experiment time, hrs.	Phthalic anhydride obtained, kg.	% phthalic anhydride in condensation products	S for phthalic anhydride
380	38	420	73	2.500	12	2.380	97.5	78.0
390	46	580	68	2.894	12	2.647	97.6	77.0
380	48	600	68	2.808	12	2.860	97.5	85.0
375	50	640	66	3.460	14	3.100	97.8	76.2
370	50	670	58	3.170	14	2.850	97.8	76.2
375	50	640	65	2.000	13	1.800	97.7	77.0

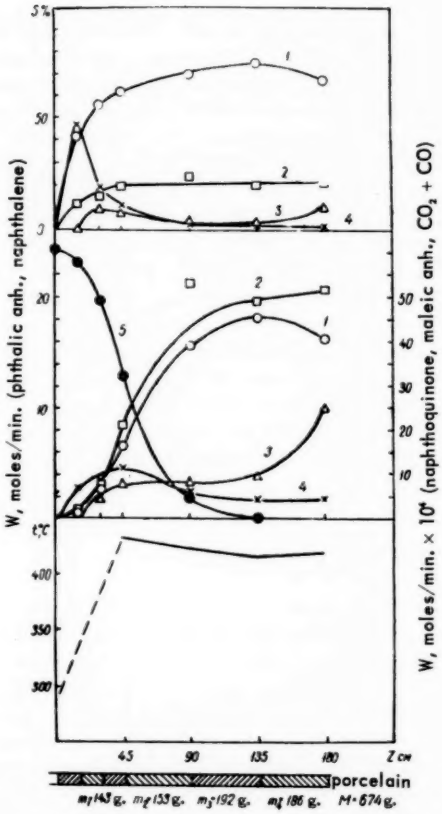

Fig. 3. Changes in productivity and selectivity with respect to the products of oxidation of naphthalene, productivity with respect to consumption of naphthalene, and the temperature of an industrial catalyst along the bed at a converter bath temperature of 410°C under non-optimal process conditions. 1) Phthalic anhydride; 2) $CO_2 + CO$; 3) maleic anhydride; 4) naphthoquinone; 5) naphthalene (the scale for productivities with respect to phthalic anhydride and naphthalene is 10 times that for the other products.

tended period of time, with a determination of the yield of phthalic anhydride from the weight of the product.

As may be seen from the data given, a consistent yield of phthalic anhydride on the industrial catalyst does not exceed 72-73%, while on a combination charge, at a high productivity, it is as high as 76-85%. This points to a considerable advantage of the combination charge as compared with an industrial catalyst from fused vanadium pentoxide.

As can be seen from the data of Table 1, fine granules of the industrial catalyst also have a high productivity, and their selectivity with respect to phthalic anhydride is as high as 77%. This effect was obtained as a result of a decrease in diffusion retardation by decreasing the grain size. However, a defect of the fine grained catalyst, which prevents its industrial use, is the ease with which it sinters together and its high resistance to gas flow.

For purposes of comparison, Table 1 lists data on the productivity and selectivity of a complex vanadia catalyst (vanadium sulfate on silica gel with potassium sulfate as promoter) at 370°C. The selectivity of this catalyst is 77%, but its productivity is seven times lower than that of the combination charge. When the process temperature is lowered to 345°C, the yield of phthalic anhydride rises to 85-90%, but productivity is lowered to less than one-half that obtained with the same catalyst at 370°C.

LAYER-BY-LAYER ANALYSIS OF THE OPERATION OF THE VANADIA CATALYST

The method of investigation used made it possible to follow changes in the concentration of naphthalene and its reaction products along the catalyst column. Typical results of an investigation of the operation of an industrial vanadia catalyst by this method are shown in Fig. 3. Worthy of note is the high selectivity with respect to 1,4-naphthoquinone (45%) at a low conversion of naphthalene. When conversion is increased, selectivity drops to 1-2%.

In the experiment under discussion, the flow rate was selected so that complete conversion of naphthalene would take place at the end of the third cell. Then, as can be seen from Fig. 3, undesirable oxidation of the desired product takes place in the last fourth of the bed, apparently chiefly to maleic anhydride. This leads to a decrease in selectivity with respect to phthalic anhydride by 6-7%. It is seen from the experimental data given that the maximum yield of phthalic anhydride is found at the point in the catalyst bed where the concentration of naphthalene becomes zero.

To achieve the optimum selectivity with respect to phthalic anhydride at the exit from the entire catalyst bed, it is thus necessary to establish the maximum flow rate at which there is still no breakthrough of naphthalene. The selectivity maximum then shifts to the end of the bed.

Exceeding the flow rate above that given is likewise not admissible. This is largely because in the oxidation of naphthalene in fixed beds of vanadia catalysts their chemical composition along the bed varies and depends on the flow rate of the gas mixture. Under optimum process conditions, there is automatically established a composition of the catalyst charge which corresponds to the maximum yield of phthalic anhydride. This composition corresponds to the presence of lower oxides of vana-

dium at the beginning of the bed, which are formed by the reduction of vanadium pentoxide by naphthalene, and at the end, chemically unchanged vanadium pentoxide, since the products of the oxidation of naphthalene do not possess reducing properties under these conditions. At flow rates exceeding the optimum rate, i.e., during operation with naphthalene breakthrough, vanadium pentoxide is reduced to the lower oxides over the entire column. It is known (7) that phthalic anhydride is unstable on the lower oxides in the absence of naphthalene. Consequently, upon returning to optimum operating conditions, the yield of phthalic anhydride is decreased until the catalyst is oxidized in the tail portion of the reactor. The optimum flow rate of the gas mixture is limited both on the high and low ends of same.

The results that have been obtained have also been used by us to determine the kinetics and the mechanism of the process (8). In studying the kinetics of the processes by the flow method in short catalyst beds, such as are used in laboratories, one must take into account longitudinal mixing which affects the concentration drop in the bed compared with that calculated from the kinetic equation. This defect is eliminated when kinetics is studied in a long bed, since in this case the distortion of the concentrations along the bed by longitudinal mixing will be very slight. Moreover, the values of concentrations in the bed are not obtained by calculation but are determined experimentally.

Layer-by-layer analysis of catalyst operation is of interest from three points of view: first, it offers a picture of the concentration drops and the temperature variations along the bed, which is of great importance in planning an industrial installation; secondly, it makes it possible to determine rapidly the optimum conditions for the process; and thirdly, it makes it possible to obtain kinetic data on the process under conditions under which longitudinal mixing is practically absent.

TESTING THE OPERATION OF THE COMBINATION CHARGE IN AN INDUSTRIAL REACTOR

The data on the advantage of the combination charge obtained in a model reactor were verified under industrial conditions. The catalyst prepared for industrial tests was given preliminary tests during three days in a model apparatus, and gave an 80-85% yield of phthalic anhydride. During the preparation of a larger amount of the catalyst, the method of preparing coarse crystalline vanadium pentoxide was improved over that described in the literature (2). In place of a crucible for fusing and crystallizing vanadium pentoxide, we used pans (60 × 50 cm.) made from stainless steel and stacked four-high on a metal carriage and placed in a high-inertia electric furnace. The monocrystal plates formed during slow cooling of the melt were as much as 20-30 cm. in size.

The combination charge was used for 22 months in an industrial reactor. Even under conditions of poor heat removal and insufficient isothermicity, a consistent yield of phthalic anhydride of 76-78% was obtained. This reduced by 25% the nonproductive consumption of naphthalene. It should be noted that the productivity of the combination charge remained high and equaled 0.295 kg. of naphthalene per hour per kg. of catalyst. On an industrial catalyst used for the same length of time, the yield of phthalic anhydride did not exceed 70% and productivity was 0.275 kg. of naphthalene per hour per kg. of catalyst.

SUMMARY

1. Using a scaled-up apparatus and an industrial reactor, data were obtained which show that a combination charge of vanadia catalysts is superior to an industrial vanadium pentoxide catalyst. The yield of phthalic anhydride in the scaled-up apparatus on a combination catalyst charge was as high as 80-85%. In industrial reactors, under less favorable conditions of heat removal and equalization of temperature, the selectivity of the combination charge is 76-78% (69-70% on an industrial charge), which reduces by 25% the nonproductive consumption of naphthalene. The productivity of the catalyst was not diminished.

2. Data have been obtained on the changes in the concentration of naphthalene and its oxidation products, and on the temperature along the bed of vanadia catalysts. It has been found that at a given temperature and concentration of naphthalene in the gas mixture, an optimum flow rate exists which ensures a maximum yield of phthalic anhydride; this corresponds to the highest flow rate at which breakthrough of naphthalene is not yet taking place.

3. The method used, in combination with the indicator method of detecting unreacted naphthalene, may be recommended for a rapid and reliable estimate of the productivity and selectivity of catalysts for the oxidation of naphthalene and for obtaining kinetic relationships under conditions under which distortion of the data by longitudinal mixing in the bed is impossible.

*We wish to express our sincere thanks to the Scientific Director of the Central Plant Laboratory of the Rubezhnoe Chemical Combine, S. T. Rashevskaya, for her continued interest and assistance.

LITERATURE CITED

1. Korneichuk, G. P., Zhigailo, Ya. V., Roiter, V. A., and Garkavenko, I. P., *Zhur. Fiz. Khim.*, 29, No. 6, 1073 (1955).
2. Korneichuk, G. P., Roiter, V. A., and Zhigailo, Ya. V., *Khim. Prom.*, 1958, No. 7, 22.
3. Zhigailo, Ya. V., *Zavodskaya Lab.*, 10, 1255 (1956).
4. Makhovka, P. P., *Ibid.*, 5, 533 (1957).
5. Polyakov, M. V., *Voprosy khimicheskoi kinetiki, kataliza i reaktsionnoi sposobnosti* (Problems of Chemical Kinetics, Catalysts, and Reactivity), p. 368, Izdat. AN SSSR (Publ. Acad. Sci. USSR), Moscow, 1955.
6. Korneichuk, G. P., *Zavodskaya Lab.*, 8, 920 (1956).
7. Ushakova, V. P., Korneichuk, G. P., and Roiter, V. A., *Ukrain. Khim. Zhur.*, 23, No. 2, 191 (1957).
8. Vol'fson, V. Ya., Korneichuk, G. P., Roiter, V. A., and Zhigailo, Ya. V., *Ibid.*, (in press).

V. Ya. Vol'fson
G. P. Korneichuk
V. A. Roiter
Ya. V. Zhigailo

UKRAINE, USSR

Peculiarities of the Catalytic Oxidation of Naphthalene. Part 3

An investigation of the mechanism of naphthalene oxidation over vanadia catalysts by a kinetic method, using the procedure developed in the preceeding article. Conditions simulated those found in industrial applications.

VAPOR-PHASE catalytic conversion of various substances over fixed catalyst beds is widely used in industry. However, very few studies are found in the literature which deal with processes taking place in deep beds of fixed catalysts (2).

The present investigation was undertaken to obtain data on the mechanism of naphthalene oxidation over vanadia catalysts by the kinetic method, under conditions simulating those used in industry, using a previously developed procedure (2).

The investigation was carried out on an industrial fused vanadium pentoxide catalyst, using a catalyst charge proposed by us earlier ("combination charge") (3), as well as on pellets of industrial vanadia-potassia-sulfate-silica gel catalyst ("complex vanadia catalyst"). In studying the oxidation of naphthalene on the industrial vanadia catalyst, use was made of a charge similar in composition and make-up to the industrial charge. The first fourth of the bed (first cell) was packed with coarse granular fused vanadium pentoxide (size 7 × 10 mm.)* and the remainder with fine granules (5 × 7 mm.). The combination charge, to the extent of one-fourth of the depth of the bed, consisted of partially reduced catalyst (7 × 10 mm.), followed by coarse crystalline catalyst (5 × 7 mm.). Each experiment was run without interruption for 12-14 hours, taking samples along the length of the bed every 2-3 hours up to the completion of the experiment. Information was obtained on the change in the concentrations of naphthalene, naphthoquinone, phthalic anhydride, maleic anhydride, carbon dioxide, and carbon monoxide along the catalyst bed.

Figs. 1, 2, and 3 show typical experimental data for fused vanadium pentoxide, for the combination charge, and for the complex vanadia catalyst. Along the abscissa is plotted the length of the catalyst bed in cm., and along the ordinates, respectively, temperature in °C, productivity**(W), and selectivity

This article first published in *Ukrain. Khim. Zhur.* 26, No. 5, 588-593 (1960). The authors are associated with the L. V. Pisarzhevskii Institute of Physical Chemistry of the Academy of Sciences of the Ukrainian SSR, Rubezhnoe Chemical Combine.

*Translator's Note: literally (diameter 7 × 10 mm.)

**Translator's Note: a Soviet term denoting a variation of the "activity" concept and usually expressed in wt. units of a given product or consumed feed per unit volume of catalyst. In the present case "productivity" is expressed in moles/min.

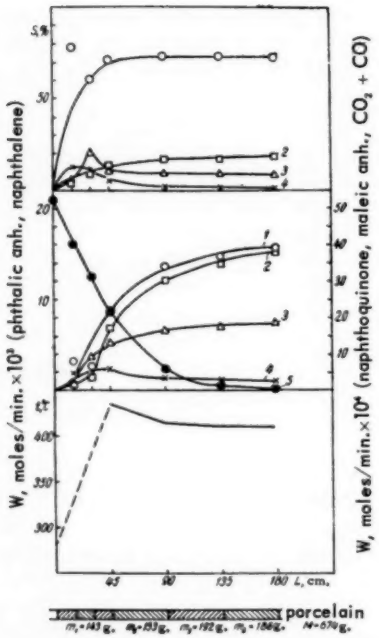

Fig. 1. Changes in productivity, selectivity with respect to the products of oxidation of naphthalene, productivity with respect to consumption of naphthalene, and temperature of an industrial vanadia catalyst along the catalyst bed at a converter bath temperature of 410°C. 1) phthalic anhydride; 2) CO_2 + CO; 3) maleic anhydride; 4) naphthoquinone; 5) naphthalene.

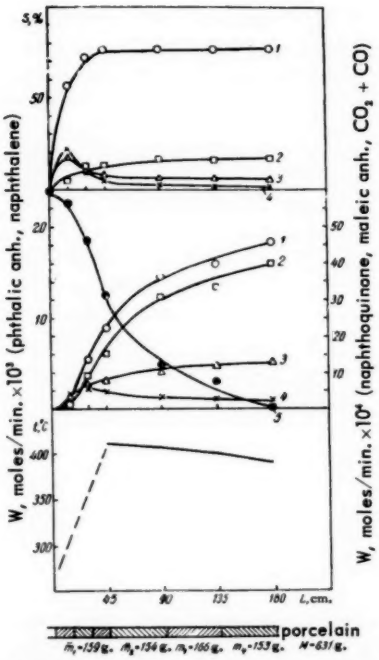

Fig. 2. Changes in productivity and selectivity with respect to the products of oxidation of naphthalene, productivity with respect to consumption of naphthalene, and the temperature of a combination charge of vanadia catalyst along the catalyst bed at a converter bath temperature of 390°C. 1) phthalic anhydride; 2) CO_2 + CO; 3) maleic anhydride; 4) naphthoquinone; 5) naphthalene.

(S) for each of the oxidation products and productivity based on the consumption of naphthalene; also given are the weight of the catalyst, in grams, charged to the individual cells ($m_{1,2,3,4}$) and the total weight of the catalyst (M).

Examination of the experimental data makes it possible to determine some general relationships governing the catalytic oxidation of naphthalene under conditions simulating those found in industry, as well as the characteristics of the process on different types of vanadia catalysts.

First of all, while in long (deep) beds of vanadia catalysts overheating in the front part of the reactor reaches 50-60°C, the temperature drop in the working space on the complex catalyst does not exceed 15°C. This temperature regime is the result of the relatively low productivity of the complex catalyst (the maximum allowable charge of naphthalene is 4 to 5 times less than with the vanadia catalyst), and leads to the result that naphthalene is oxidized practically uniformly along the bed of the complex catalyst, about 25-30% of the naphthalene in each cell. When vanadia catalysts are used, up to 50% of the naphthalene entering the reactor is oxidized in the first cell. This is largely responsible for the lower selectivity with respect to phthalic anhydride for vanadia catalysts as compared with the complex catalyst.

While with vanadia catalysts a clear temperature maximum is always found precisely at the end of the first cell, in the case of the complex catalyst the maximum is less distinct and is displaced towards the middle of the reactor tube with increasing flow velocity. This difference in the temperature regimes on the catalysts studied is to a certain degree responsible for the observation that the maxima of selectivity with respect to naphthoquinone and maleic anhydride are stretched more in the complex catalyst and the selectivity with respect to phthalic anhydride reaches an optimum value only towards the end of the bed.

The continuous increase in productivity with respect to phthalic and maleic anhydride and the products of severe oxidation along the bed with vanadia catalysts and the productivity with respect to phthalic anhydride and naphthoquinone on the complex catalyst justify the assumption of a pre-

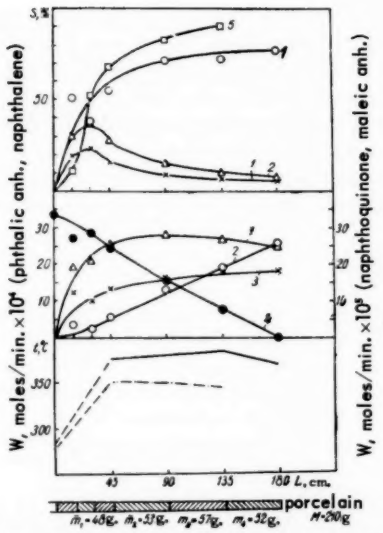

Fig. 3. Changes in productivity and selectivity with respect to the products of oxidation of naphthalene, productivity with respect to consumption of naphthalene, and the temperature of a complex vanadia catalyst along the catalyst bed at a converter bath temperature of 370°C. 1) phthalic anhydride; 2) maleic anhydride; 3) naphthoquinone; 4) naphthalene. The graph also shows changes in selectivity with respect to phthalic anhydride (5) and the temperature along the catalyst bed (–·–·–) at a converter bath temperature of 345°C.

dominantly parallel mechanism for their formation from naphthalene. At the same time, examination of the curves for the change in the productivity with respect to maleic anhydride and naphthoquinone shows that the stability of these side products of the mild oxidation of naphthalene is different on the catalysts studied: maleic anhydride is stable on vanadia catalysts but is partially oxidized on the complex catalyst (maximum on the productivity curve), whereas naphthoquinone is stable on the complex catalyst and is partially oxidized on vanadia catalysts. The latter fact, in conjunction with the first-order kinetics of the formation of naphthoquinone on the complex catalyst, as shown below, is probably the reason why on the complex catalyst the curve for the change in selectivity with respect to naphthoquinone falls more slowly along the catalyst column.

The fact, mentioned above, that the individual products of mild oxidation of naphthalene partially react further during the reaction justifies the assumption that the oxidation of naphthalene occurs (under conditions simulating industrial conditions) according to a consecutive-parallel mechanism, with a parallel mechanism predominating.

Our conclusion that the oxidation of naphthalene takes place by a consecutive-parallel mechanism

Table 1*

Comparison of rate constants of individual reactions (vanadia catalysts)

Form of Catalyst	Temp., °C	Phthalic anhydride	Maleic anhydride	Naphthoquinone		Profound oxidation
		$k_1 \times 10^3$	$k_2 \times 10^5$	$k_3 \times 10$	$k_4 \times 10^3$	$k_5 \times 10^3$
Industrial catalyst (our data)	410	4.6	0.0835	5.4	2.55	1.5
Coarse crystalline cat. (Ushakova's data)	410	15.9	0.152	1.06	–	7.64
Combined charge (our data)	390	4.5	0.0665	4.75	2.47	1.10
Coarse crystalline cat. (Ushakova's data)	392	8.8	0.0762	0.51	–	3.6

*The slight disagreement in the values of the constants of the individual reactions may be due to a difference in the specific surface areas of the catalysts in the studies being compared.

is in agreement with results obtained previously (4, 5).

The kinetic relationships of a chemical reaction determined under conditions excluding diffusion control are usually altered quite markedly when the process is conducted on an industrial scale. It was of interest to determine whether the kinetic relationships of the oxidation of naphthalene determined previously (4, 5, 6) could be applied under industrial conditions.

The method of graphical differentiation* of the curves for the change in productivities was used to calculate the rates of the individual reactions. It was assumed in these calculations that the results of graphical differentiation of the continuously rising curves for productivity (with respect to phthalic anhydride, maleic anhydride, and the products of complete oxidation for vanadia catalysts, and with respect to phthalic anhydride and naphthoquinone on the complex catalyst) give the rate of the oxidation of naphthalene to the corresponding products, whose further oxidation could be neglected. On the other hand, in differentiating curves with a maximum (productivity with respect to naphthoquinone on vanadia catalysts and with respect to maleic anhydride on the complex catalyst) the results obtained should be regarded as a difference between the rates of formation and further oxidation of the corresponding products.

*Graphical differentiation was carried out starting from the last third of the first cell to the end of the bed.

Table 2

Rate constants of individual reactions at 370°C (complex vanadia catalysts)

	Phthalic anhydride		Maleic anhydride				Naphtho-quinone	
	$k_7 \times 10^4$	order	$k_7 \times 10^3$	order	$k_7 \times 10^3$	order	$k_7 \times 10^3$	order
Our data	22.7	0	0.144	1.0	0.72	1.0	0.1	1.0
Ioffe's data (5, 6)		1.0				1.0		1.0

The kinetic relationships found have the following form.*

On vanadia catalysts

Rate of formation of phthalic anhydride	$v_1 = k_1 C_N$
" " " " maleic anhydride	$v_2 = k_2 C_N^{0.5}$
" " " " naphthoquinone	$v_3 = k_3 C_N^{2.0}$
" " oxidation of naphthoquinone	$v_4 = k_4 C_{NQ}$
" " severe oxidation of naphthalene	$v_5 = k_5 C_N$

On complex vanadia catalysts

Rate of formation of phthalic anhydride	$v_6 = k_6$
" " " " maleic anhydride	$v_7 = k_7 C_N$
" " oxidation of maleic anhydride	$v_8 = k_8 C_{MA}$
" " formation of naphthoquinone	$v_9 = k_9 C_N$

Here the k's are the reaction rate constants, C_N is the concentration of naphthalene, C_{MA} is the concentration of maleic anhydride, and C_{NQ} is the concentration of naphthoquinone.

The reaction rate constants are listed in Tables 1 and 2, which also show the values of the constants obtained in Ref. (4). The reaction orders found by us are in agreement with those obtained under conditions excluding diffusion control and in the studies by Ioffe (5, 6).** This enables us to state that under optimum conditions the oxidation of naphthalene in long beds of vanadia catalysts takes place according to a regime close to external kinetic, and the slight lack of isothermal conditions and the variable composition of the catalyst charge along the bed in this case did not seriously alter the kinetic relationships. The conclusion that has been drawn confirms the results obtained earlier in studying this process by the diaphragm method (7).

*The rates of the processes are expressed in moles/sec².

**It should be noted that a variable order of the reactions leading to the formation of phthalic anhydride was demonstrated in (5): zero-order at low temperatures and first-order at high temperatures.

The rate constant for the formation of phthalic anhydride on a combination catalyst charge at 390°C is practically the same as the rate constant for this process on the industrial vanadia catalyst at 410°C, while the rate constant for the reaction of severe oxidation of naphthalene is somewhat lower, which ensures a higher selectivity with respect to phthalic anhydride on the combination catalyst charge.

SUMMARY

1. The kinetics of the oxidation of naphthalene on three types of vanadia catalysts has been studied in a reactor simulating an industrial reactor. The method used made possible a study of the change in the concentrations of naphthalene and its oxidation products and to measure temperature changes along the length of the catalyst bed.

2. The individual reactions taking place in the oxidation of naphthalene on vanadia catalysts obey the following kinetic equations. Rate of formation of phthalic anhydride $v_1 = k_1 C_N$, rate of formation of maleic anhydride $v_2 = k_2 C_N^{0.5}$, rate of formation of naphthoquinone $v_3 = k_3 C_N^2$, rate of formation of the products of severe oxidation $v_5 = k_5 C_N$, and the rate of oxidation of naphthoquinone $v_4 = k_4 C_{NQ}$.

3. The following kinetic relationships governing the individual reactions apply in the oxidation of naphthalene on a complex vanadia catalyst. Rate of formation of phthalic anhydride $v_6 = k_6$, rate of formation of maleic anhydride $v_7 = k_7 C_N$, rate of formation of naphthoquinone $v_9 = k_9 C_N$, and the rate of oxidation of maleic anhydride $v_8 = k_8 C_{MA}$. Evidence has been presented for a consecutive-parallel mechanism of the oxidation of naphthalene.

4. Under optimum conditions the oxidation of naphthalene in industrial systems follows a regime close to external kinetic.

LITERATURE CITED

1. Darby, P. W., and Kemball, C., *Trans. Faraday Soc.*, 53, No. 6, 832 (1957).

2. Korneichuk, G. P., Roiter, V. A., Zhigailo, Ya. V., Vol'fson, V. Ya., and Lyubiteleva, A. Z., *Ukrain. Khim. Zhur.*, 26, No. 4, (1960).

3. Korneichuk, G. P. Roiter, V. A., and Zhigailo, Ya. V., *Khim. Prom.* 1958, No. 7, 22.

4. Ushakova, V. P., Korneichuk, G. P., and Roiter, V. A., *Ukrain. Khim. Zhur.*, 23, 310 (1957).

5. Ioffe, I. I., and Sherman, Yu. G., *Zhur. Fiz. Khim.*, 28, 2095 (1954).

6. Ioffe, I. I., and Sherman, Yu. G., *Ibid.*, 29, 692 (1955).

7. Korneichuk, G. B., Zhigailo, Ya. V., Roiter, V. A., and Garkavenko, I. P., *Ibid.*, 29, 1073 (1955).

S. G. Lyubetskii
B. A. Dolgoplosk
B. L. Erusalimskii

USSR

Polymerization of Ethylene under the Influence of Free Radicals. Kinetics of Ethylene Polymerization in Benzene and Heptane Solution

A study of the kinetics of ethylene polymerization in solution in benzene and in heptane under the influence of azoisobutyronitrile, under pressures up to 100 atmospheres.

MOST of the studies dealing with the mechanism and kinetics of radical polymerization of ethylene have been run in the gas phase (1-6). An attempt at a kinetic analysis of experimental data on ethylene polymerization in the pressure range of 100 to 1,500 atm. under the influence of azoisobutyronitrile in the presence of water was made by Kodama and coworkers (7), but the insolubility of the initiator and the polymer in water made a rigid interpretation of the experimental results impossible. The only study of the kinetics of the liquid-phase polymerization of ethylene was that made by Laita (8), in which the photochemical decomposition of azoisopropane was used for the initiation.

The kinetics of ethylene polymerization in solution in benzene and in heptane under the influence of azoisobutyronitrile (diniz) under pressures up to 100 atm. was the subject of the present research.

Apparatus and Technique for Running the Experiments. A diagram of the set-up for running the polymerization is shown in Figure 1. The apparatus consists of dilatometer 1 adapted for work under pressure, a thermostat jacket 2, provided with observation windows, an ultrathermostat and magnetic stirrer 3. The dilatometer is a stainless steel tank connected to a thick-walled glass tube 4, the upper end of which is closed with a metal cap. The latter is connected to a needle valve and a pressure gauge. The inside diameter of the tube 4 is 2.5 mm. The total volume of the dilatometer is about 23 cc. The position of the meniscus in tube 4 is determined by means of a filar microscope with an accuracy of ±0.06 mm. which corresponds to 0.1-0.3% contraction. The temperature within the jacket was maintained with an accuracy of ±0.05°C.

A weighed sample of the azoisobutyronitrile solution in the appropriate solvent was weighed into the dilatometer reservoir with an accuracy of ±0.001 g. The reservoir was connected to tube 4, to the vacuum system, and to the ethylene cylinder. Removal of the air from the dilatometer was accomplished by repeated, alternating evacuation of the previously frozen (at −70°C) solution and filling of the reactor with ethylene. After the disconnection of the vacuum line, the dilatometer was filled with ethylene and weighed, and the excess ethylene was released, the weight of the ethylene in the dilatometer being adjusted to the necessary value with an accuracy of 10 mg. Then, the dilato-

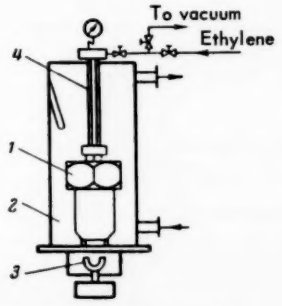

Fig. 1. Diagram of the set-up for ethylene polymerization.

This article first published in *Vysokomolekulyarnye Soedineniya*, 3, No. 5, 734-739 (1961). The authors are associated with the Institute of High Polymers of the Academy of Sciences of the USSR, Scientific Research Institute of Polymerization Plastics.

meter was placed into the jacket 2, preheated to the reaction temperature. The period of thermostating was 10 to 20 min. The instant of the stabilization of the meniscus at the uppermost position was taken as the initial moment. Cold water was fed into the jacket and the ethylene pressure was relieved in order to stop the reaction. The reaction mixture was treated with hot alcohol, the polymer was washed thoroughly and dried in vacuum at 50-55°C. The molecular weight of the polymer was determined by the viscosimetric method (in a decalin solution at 135°C) and calculated by the equation (11):

$$[\eta] = 3.873 \cdot 10^{-4} \cdot \overline{M}_n^{0.738},$$

where $\overline{M}_n$ is the number average molecular weight, (η) is the intrinsic viscosity, with the concentration being expressed in g./100 ml. of solution.

Starting Materials. Benzene and heptane were purified with sulfuric acid, treated with sodium bicarbonate, dried with anhydrous copper sulfate, and distilled from metallic sodium. The hydrocarbons used by us had the following constants: benzene – b.p. 80.10°C and n_D^{20} 1.5010 (according to the literature data, b.p. 80.09°C and n_D^{20} 1.5011 (13); and heptane – b.p. 98.50°C and (n_D^{20}) 1.3877 (according to the literature data, b.p. 98.427°C and n_D^{20} 1.38764 (13)). Azoisobutyronitrile was purified by recrystallization from ethyl alcohol and had a m.p. of 103.2°C (according to the literature data, the m.p. is 103-104°C (14). Commercial ethylene was purified by successive passage through columns with calcined aluminum oxide, potassium hydroxide, activated carbon and phosphoric anhydride. A partial polymerization of ethylene was run in an autoclave in the presence of azoisobutyronitrile and benzene in order to remove the impurities that inhibit the polymerization process. The process was run up to 5-7% conversion, after which the solvent was frozen out and the ethylene was collected in a special cylinder. The ethane content of ethylene purified in this manner was not over 1.5% by volume. We studied the effect of monomer and initiator concentrations and of the nature of the solvent on the kinetics of ethylene polymerization and on the molecular weight of the polymer. All experiments were run at 70°C.

RESULTS OF EXPERIMENTS WITH POLYMERIZATION AND DISCUSSION

Polymerization in Benzene. The ethylene pressure during the polymerization in benzene was varied from 40 to 85 atm. which corresponds to a monomer concentration in solution of 3.65 to 7.66 moles/liter. The initiator concentration in the liquid phase was varied within the range of 0.0005-0.006 mole/liter. Fig. 2 shows change in the solution volume as a function of the degree of conversion during the polymerization of ethylene in benzene. Similar data were obtained for the polymerization of ethylene in heptane.

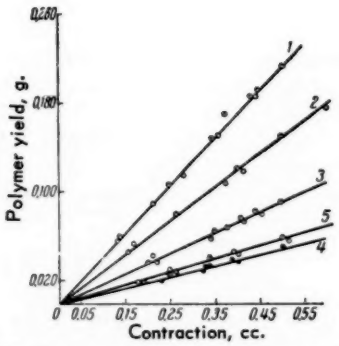

Fig. 2. Contraction of the solution as a function of the conversion during the polymerization of ethylene in benzene at 70°C. Initiator concentration: 0.514 × 10^{-3} mole./liter. Ethylene concentration, moles/liter: 1) 3.65; 2) 4.75; 3) 6.32; 4) 7.06; 5) 7.66.

The dependence of the polymer yield on the duration of the polymerization at various levels of initiator concentration and with a constant monomer concentration is shown in Fig. 3.

It is evident from Fig. 3 that the polymerization rate remains almost constant with conversions not over 5%.

The data obtained by us on the relation of the polymerization rate and molecular weight of the polymers to the initiator concentration are shown in Table 1.

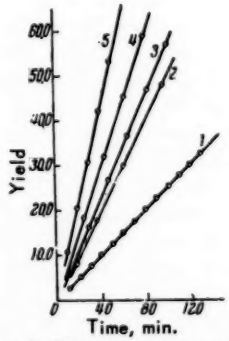

Fig. 3. Rate of ethylene polymerization in benzene at 70°C. Ethylene concentration: 6.32 moles/liter. Initiator concentration, moles/liter: 1) 0.514 × 10^{-3}; 2) 1.485 × 10^{-3}; 3) 1.830 × 10^{-3}; 4) 3.090 × 10^{-3}; 5) 6.25 × 10^{-3}.

Table 1

Dependence of the ethylene polymerization rate in benzene and of the molecular weight of the polymer on the initiator concentration at 70°C
Ethylene concentration: 6.32 moles/liter

Azoisobutyronitrile concn. (I)×10³ moles/liter	Polymerization rate ω, g./(liter)(min.)	Polymerization rate $V_P \times 10^5$ moles/(liter)(sec.)	Number average mol. wt., $\bar{M}_n \times 10^{-3}$	$\frac{1}{\bar{P}_n} \times 10^2$
0.514	0.0143	0.85	8.0	0.339
	0.0145	0.86	8.2	0.341
1.485	0.0250	1.49	6.0	0.468
	0.0247	1.47	5.9	0.470
1.830	0.0272	1.62	5.6	0.505
	0.0274	1.63	5.5	0.508
3.090	0.0355	2.12	4.7	0.615
	0.0366	2.12	4.5	0.620
6.250	0.0504	3.00	3.2	0.830
	0.0507	3.02	3.4	0.825

The logarithmic dependence of the ethylene polymerization rate on the initiator concentration (Fig. 4a) has a rectilinear character. The order of the reaction relative to initiator concentration is 0.51, indicating a bimolecular mechanism of chain termination.

The dependence of the initial rate of ethylene polymerization V_p on the monomer concentration (M) is characterized by values shown in Table 2.

The logarithmic relationship between the rate of ethylene polymerization and monomer concentration

Table 2

Dependence of the initial rate of ethylene polymerization in benzene on the monomer concentration* at 70°C
Initiator concentration: 0.514×10^{-3} mole/liter

Pressure, atm.	(M), moles/liter	$V_P \times 10^5$, moles/(liter)(sec)	$\bar{M}_n \times 10^{-3}$	$\frac{1}{\bar{P}_n} \times 10^2$
40.0	3.85	0.405	5.2	0.539
		0.407	5.2	0.539
50	4.75	0.608	6.5	0.434
		0.605	6.4	0.437
65.0	6.32	0.867	8.0	0.347
		0.865	8.1	0.345
80.0	7.66	1.093	11.3	0.247
		1.090	11.2	0.250
85.0	7.06	0.962	11.4	0.244
		0.964	11.3	0.247

*The ethylene concentration was determined experimentally. The process of ethylene polymerization was not studied beyond the monomer concentration of 7.66 moles/liter, since beyond this pressure the system was in a state beyond the critical.

Table 3

Dependence of the rate of ethylene polymerization in benzene in the presence of azoisobutyronitrile and of the degree of polymerization on temperature

Temp., °C	Pressure, atm.	(M), moles/liter	(I)×10³, moles/liter	$V_P \times 10^5$ moles/(liter) (sec.)	$\bar{P}_n$
70	65.0	6.32	1.830	1.68	195
				1.63	197
60	74.0	8.17	1.861	0.85	345
				0.88	340
50	62.5	8.25	2.042	0.37	452
				0.38	452

is shown in Fig. 4b. The order of the reaction with respect to the ethylene concentration in the solution is equal to 1.25 and is practically constant over the concentration range studied.

Experiments on the polymerization of ethylene in benzene were also run at 50°C and 60°C in order to determine the activation energy of ethylene polymerization. The results obtained are shown in Table 3 and Fig. 5.

It follows from these data that the activation energy of the process of ethylene polymerization under the influence of azoisobutyronitrile is equal to 20 ±1 kcal./mole. The experimental results on the polymerization of ethylene run at various monomer and initiator concentrations allowed us to secure the data needed for the calculation of the chain transfer constants. It follows from the dependence of the degree of polymerization on the reaction rate and the monomer: solvent ratio that the constants of chain transfer through the monomer and through the benzene are equal to 5×10^{-4} and 1.8×10^{-3}, respectively (see Fig. 6a and b).

Polymerization in Heptane. The polymerization of ethylene in heptane was run at 70°C with an azoisobutyronitrile concentration of 1.52×10^{-3} moles/liter. The main results are shown in Table 4.

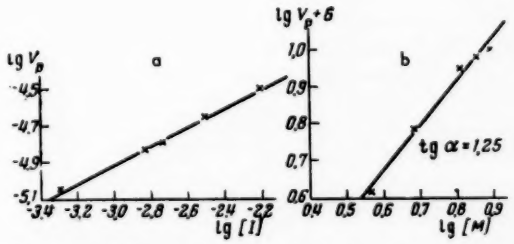

Fig. 4. Dependence of the rate of ethylene polymerization in benzene at 70°C: a) on initiator concentration; (M) = 6.32 moles/liter; b) on monomer concentration; (I) = 0.514×10^{-3} mole/liter.

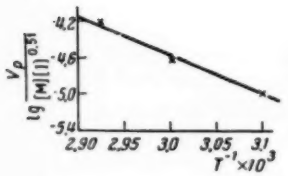

Fig. 5. Dependence of the rate constant of ethylene polymerization in benzene on temperature.

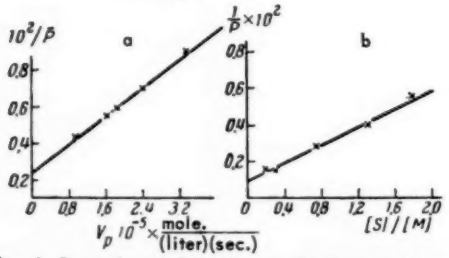

Fig. 6. Dependence of the degree of polymerization of ethylene at 70°C on: a) rate of reaction; solvent – benzene; (M) = 6.32 moles/liter; b) on the benzene : monomer ratio; (I) = 0.514 × 10^{-3} mole/liter.

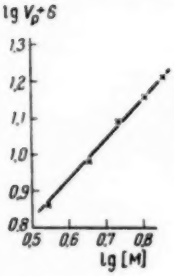

Fig. 7. Dependence of the rate of ethylene polymerization in heptane on the monomer concentration at 70°C; (I) = 1.52 × 10^{-3} mole/liter.

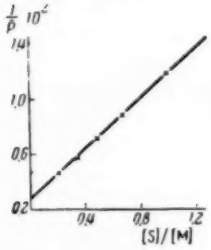

Fig. 8. Dependence of the degree of ethylene polymerization on the heptane : monomer ratio at 70°C; (I) = 1.52 × 10^{-3} mole/liter.

It follows from Fig. 7, in which the logarithmic dependence of the ethylene polymerization rate on its concentration in heptane is shown, that the reaction rate is proportional to the first power of the monomer concentration.

It was found from the dependence of the degree of polymerization of ethylene on the ethylene: heptane ratio (Fig. 8) that the chain transfer constant through heptane is equal to 9 × 10^{-3}.

The calculation of the composition of the reaction mixtures was made on the basis of data secured by us on the densities of the benzene-ethylene mixtures (Fig. 9) and from the data provided by Kay (9) on the densities of heptane-ethylene mixtures.

Table 4

Polymerization of ethylene in heptane in the presence of asoisobutyronitrile

Pressure, atm.	(M), moles/liter	Rate of polymerization		(S)/(M)	$\bar{M}_n \times 10^{-3}$
		g./(liter)(min.)×10^3	moles/(liter)(sec.)× 10^5		
40.5	3.45	1.36	0.81	1.380	1.8
51.0	4.36	1.72	1.02	0.986	2.4
60.0	5.41	2.13	1.27	0.670	3.2
70.5	6.28	2.48	1.48	0.477	4.0
81.5	7.17	2.83	1.68	0.342	4.9
90.0	7.73	3.06	1.82	0.205	6.0

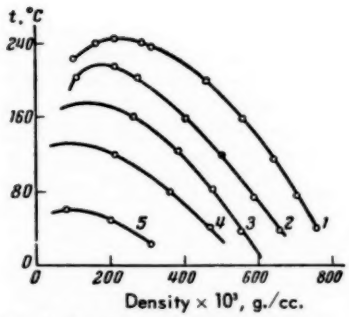

Fig. 9. Dependence of density on the temperature in the system ethylene-benzene. Mixture compositions, mole %: 1) 24.4; 2) 46.6; 3) 65.2; 4) 76.0; 5) 94.0.

SUMMARY

1. The kinetics of ethylene polymerization in benzene and heptane solution, initiated by azoisobutyronitrile, was studied under pressures up to 100 atm. The equation for the polymerization rate $V_p = K(M)^{1-1.25} \times (I)^{0.51}$ was derived on the basis of the experimental data.

2. The total activation energy of ethylene polymerization and the constants of chain transfer by the monomer, benzene, and heptane were determined.

LITERATURE CITED

1. Stanley, A., *J. Chem. Ind.* 49, 349 (1930).

2. Steacie, E., *Atomic and Free Radical Reactions*, p. 175, New York, 1954.

3. Muthana, M., and Mark, H., *J. Polymer Sci.*, 4, 527 (1949).

4. Thomasson, K., *Petrol. Refiner*, 35, 191 (1950).

5. Henes, R., Bryant, W., Larchar, A., and Pease, D., *Ind. Eng. Chem.*, 49, 1071 (1957).

6. Laird, R., Morell, A., and Seed, L., *Transactions Faraday Soc.*, 22, 126 (1956).

7. Kodama, S., Matshushima, Y., Uneyoshi, A., and Shimidzu, T., *J. Polymer Sci.*, 41, 89 (1959).

8. Laita, Z., *Ibid.*, 38, 247, 459 (1959).

9. Kay, W., *Ind. Eng. Chem.*, 40, 1459 (1948).

10. Uberreiter, A., *Makromol. Chem.*, 8, 21 (1952).

11. Hodgman, C., *Handbook of Chemistry and Physics*, pp. 760, 956, New York, 1955.

12. Overberger, R., et al., *J. Am. Chem. Soc.*, 71, 2661 (1949).

M. S. Nemtsov USSR

Kinetic Relationships in the Reaction of Olefins with Sulfuric Acid

Reactions with sulfuric acid form the basis for a considerable number of commercial processes: production of ethyl, isopropyl, and isobutyl alcohols, preparation of pure isobutylene for production of butyl rubber, alkylation of isoparaffin and aromatic hydrocarbons. This article is an attempt at construction of a unified mathemetical theory for this type of process.

It would be difficult to find an area of chemistry in which more contradictory observations and conclusions have been accumulated than in the study of reactions of unsaturated hydrocarbons with concentrated sulfuric acid. However, despite the many papers on this subject that have been published in the scientific literature since the period of the classical studies by Butlerov, there is no unified theory about these processes at this time, and many of the observed phenomena have not even been rationally explained in general. This gap in chemical science is all the less justifiable since the reactions of olefins with sulfuric acid form the basis for a considerable number of commercial processes: production of ethyl, isopropyl and isobutyl alcohols, preparation of pure isobutylene for the production of butyl rubber, alkylation of isoparaffin and aromatic hydrocarbons, etc.

The present paper represents an attempt to answer some of the general questions connected with the peculiarities of these reactions.

The problem was simplified by the fact that the author had at his disposal the considerable volume of materials from experimental work performed in a study of the process of adsorption of propylene by sulfuric acid in grid plate column reactors.*

The process was first run in a hollow vertical apparatus which consisted of a pipe 170 mm. in diameter and 2.2 m. long, in the lower part of which a disperser with 20 openings of 3 mm. diameter each had been mounted. Later, the height of the reactors was increased and two interchangeable dispersers were used: one with 110 openings of 1 mm. diameter and a second one with one nipple of 20 mm. diameter.

*The work was done by T. V. Prokof'ev, P. I. Markosov, G. I. Gol'dshtein, and L. F. Guzhanskaya according to the plan recommended in its main part by the author of the present publication.

This article first published in *Khim. Prom.*, 1960, No. 8, pp. 15-23.

The propylene fraction, containing on the average 80% propylene, was fed under predetermined pressure through a preheater and entered the reactor in the gaseous state with a predetermined velocity through the disperser. The propylene content at the intake and at the exit was controlled by gas analysis during the entire run. The amount of the absorbed propylene was determined by the analysis of periodically taken samples of the reaction liquid; the analysis was run by hydrolysis of isopropyl hydrogen sulfate with distillation of the resulting alcohol and the determination of the latter in the distillate by specific gravity measurements.

DERIVATION OF EQUATIONS FOR COMPUTATION

The first dependable kinetic data, suitable for a quantitative description of the reaction between olefins and sulfuric acid, were the results of measurements made by Davis and co-workers (1-3). They made the measurements in reactors which insured a sufficiently reliable determination of the interfacial area between the liquid and the gas. These data allowed the conclusion to be drawn that the rate of absorption of the olefin is directly proportional to the area of the interface between the liquid and the gas, to the partial pressure of the olefin in the gas, and to its physical solubility in the liquid. It was shown at the same time that the reaction rate is practically independent of the intensity of agitation of the sulfuric acid in cases in which its surface layer is not destroyed.

These observations led Davis and co-workers to the conclusion that the reaction takes place in a thin surface layer of the acid in which an equilibrium concentration gradient of the reactants is established, which predetermines the rate of olefin absorption. Starting with these premises, the process taking place in the stagnant reaction film may be described satisfactorily after a simultaneous solution of the diffusion and the kinetic (rate) equations.

However, in contrast to these experiments by Davis, who ran the reaction with a practically immobile boundary layer between the liquid and the gas, stagnation of the reaction film is not realized in the case of the operation of a grid-plate reactor with gas bubbles which rise rapidly to the top of the liquid. Thus, with motion of one of the phases relative to the other, one cannot speak of a stagnant film in the sense of the concepts of Nernst (4) or Langmuir (5), since in this case the material transfer in the reaction film is determined chiefly by convectional, rather than molecular, diffusion.

Unfortunately, despite the considerable advances recently achieved in the hydrodynamics of heterogeneous chemical processes, the problem of a quantitative description of mass transfer in absorption systems still remains unsolved (6). Nevertheless, as a first approximation, it seems possible to analyze the experimental data by using a simplified solution for the process model in a stagnant film so that the necessary correction could be introduced after a comparison with the experimental data.

Using the general method of simultaneous solution of diffusion and kinetic equations (7-9), we start with the following simplified assumptions.

1. The reaction takes place almost entirely within the reaction film.

2. Owing to the use of highly concentrated propylene and the relatively small degree of its conversion, one can neglect the resistance of the gas film.

3. The rate of diffusion of the reaction products from the reaction film into the bulk of the sulfuric acid is sufficiently great so that their accumulation in the reaction film has practically no effect on the rate of binding of the propylene.*

The rate of propylene diffusion into an elementary layer of the reaction film ΔS, located at distance S from the inner boundary of the reaction film, may be described according to Fick's second law by the equation:

$$\left(\frac{\partial C}{\partial \tau}\right)_S = D\left(\frac{\partial^2 C}{\partial S^2}\right)_\tau \qquad (1)$$

where C is the concentration of dissolved propylene; τ is time; and D is the coefficient of the rate of diffusion of propylene in sulfuric acid.

In accordance with the consecutive reactions which take place reversibly during the process:

$$C_3H_6 + H_2SO_4 \underset{k_3}{\overset{k_1}{\rightleftharpoons}} C_3H_7OSO_3OH$$

$$C_3H_6 + C_3H_7OSO_3OH \underset{k_4}{\overset{k_2}{\rightleftharpoons}} C_3H_7OSO_3OC_3H_7$$

the rate of chemical absorption of propylene in the elementary layer ΔS is described, generally speaking, by the kinetic equation:

$$\left(\frac{\partial C}{\partial \tau}\right)_S = k_1 C C_a + k_2 C C_{ips} - k_3 C_{ips} - k_4 C_{dis} \qquad (2)$$

where C_a is the concentration of free sulfuric acid; C_{ips} is the concentration of isopropyl hydrogen sulfate; and C_{dis} is the concentration of diisopropyl sulfate.

However, an approximate calculation made from the experimental data provided by Nazarov and Khain (10) and using the equations for consecutive reactions showed that the magnitude of the rate constant of the secondary reaction k_2 is about 6 times smaller than that of the constant of the primary reaction k_1. The values of the constants of both reverse reactions are still smaller, since the reaction equilibrium of propylene absorption is shifted quite far to the right.

Thus, it is possible to drop all of the last three terms in the kinetic Eq. (2) as a first approximation. In addition, as will be shown later, the reaction rate is almost independent of the concentration of free sulfuric acid in the reaction liquor in the region of medium degrees of saturation of sulfuric acid, a fact that allows us to introduce the quantity C_a into the rate constant in this case, thus obtaining a simple kinetic equation of the first order for an irreversible reaction:

$$\left(\frac{\partial C}{\partial \tau}\right)_S = kC \qquad (2a)$$

In an equilibrated process in which the rate of diffusion of propylene into the elementary layer ΔS and the rate of its consumption in the reaction with the acid are equal, Eqs. (1) and (2a) give:

$$D\left(\frac{\partial^2 C}{\partial S^2}\right)_\tau = kC \qquad (3)$$

and after integration one has:

$$C = Ae^{S\sqrt{\frac{k}{D}}} - Be^{-S\sqrt{\frac{k}{D}}} \qquad (4)$$

The integration constants A and B are determined from the boundary conditions, which follow from the assumption made above that the reaction occurs almost entirely within the reaction layer of thickness h and that the boundary layer of sulfuric acid is saturated with respect to the propylene dissolved in it, i.e., $C = C_0$ at $S = h$ and $C = 0$ at $S = 0$.

*The assumption that the concentration of reaction products is the same in the reaction film as in the bulk of the liquid (9) is not quite valid as, in this case, the exit of these substances from the film was impossible. This conditional assumption is based on the experimental fact that the reaction rate depends but little on the degree of saturation of the sulfuric acid over a fairly wide interval (see below).

Accordingly, after eliminating the integration constants from Eq. (4), we obtain the expression

$$C = C_0 \frac{e^{S\sqrt{\frac{k}{D}}} - e^{-S\sqrt{\frac{k}{D}}}}{e^{h\sqrt{\frac{k}{D}}} - e^{-h\sqrt{\frac{k}{D}}}} \qquad (5)$$

which describes the change in the concentration of the dissolved propylene in the reaction film through its entire thickness.

The rate of absorption of propylene from the gaseous phase is determined, according to the above, by the rate of its diffusion through the outer surface of the stagnant film described according to Fick's first law by the following equation:

$$\frac{dx}{d\tau} = D\sigma\left(\frac{\partial C}{\partial S}\right)_{S=h} \qquad (6)$$

where x is the amount of propylene absorbed in time τ; σ is the surface area of the interface between the liquid and the gas; and $(\partial C/\partial S)_{S=h}$ is the concentration gradient of dissolved propylene at the outer surface of the reaction film.

The value of $(\partial C/\partial S)_{S=h}$ is found by differentiation of Eq. (5) with respect to S and a subsequent substitution of h for S. As a result of substituting the resulting expression into (6) we derive the following kinetic equation:

$$\frac{dx}{d\tau} = C_0\sigma\sqrt{kD}\,\frac{e^{h\sqrt{\frac{k}{D}}} + e^{-h\sqrt{\frac{k}{D}}}}{e^{h\sqrt{\frac{k}{D}}} - e^{-h\sqrt{\frac{k}{D}}}} \qquad (7)$$

in which the exponential term is the inverse hyperbolic tangent of the argument $h\sqrt{k/D}$.*

The value of the saturation concentration C_0, from Henry's law, can be described by the expression:

$$C_0 = \beta P_{pr}$$

where β is the solubility coefficient of propylene in the reaction fluid and P_{pr} is the partial pressure of propylene in the gas.

Accordingly we obtain from Eq. (7) the final form of the expression below:

$$\frac{dx}{d\tau} = \frac{\sqrt{kD}}{th\left(h\sqrt{\frac{k}{D}}\right)}\beta\sigma P_{pr} = k'\sigma P_{pr} \qquad (8)$$

The following remarks must be made after the consideration of Eq. (8).

1. β in this case is not constant since the solubility of propylene can vary considerably with the degree of saturation of sulfuric acid by it, and this relationship has not been examined experimentally by anyone as yet.

2. A quantitative description of σ is no less difficult in a process involving bubbling. The total surface area of the interface depends in this case both on the number and the size of the gas bubbles. The latter is determined by two oppositely directed processes: break-up and coalescence of the bubbles. Break-up depends on the size of the disperser perforations and on the velocity of the gas stream, as well as on the interaction of the radial component streams of the liquid in the reactor. The coalescence of the bubbles is determined first of all by the probability of bubble collisions, i.e., is a function of their concentration in the liquid. The probability of dispersion and coalescence also depends on the surface tension in the boundary layer of the liquid, i.e., specifically on the radius of curvature of the bubble. Finally, their number in a unit volume of the liquid is a function of the velocity of their ascent, which in turn is determined by the dimensions and shape (11), as well as by their concentration in space.

3. Under the conditions of a bubbling process, D and h cannot, as has been mentioned, be considered as constant, since they have the physical meaning of constants only under the conditions when the reaction takes place in a stagnant film.

With a sufficiently rapid sliding of a gas bubble along the layers of the liquid flowing past it, a quite considerable renewal of the reaction film undoubtedly occurs, leading to a large increase in the effectiveness of the mass transfer process.

An experimental confirmation of this fact is provided by the work done by Adeney and Becker (12). These workers, in studying the absorption of air during its passage through a water-filled tube in the form of large cylindrical gas bubbles of various lengths, had shown that the rate of absorption through a unit surface of the upper hemisphere of a rising bubble is seven times greater than that through the side or tail surfaces.

The dependence of the rate of diffusion of a gas through the interface between a liquid and a gas bubble on the rate at which the latter rises can be evaluated by a comparison of the results of the cited paper by Adeney and Becker with the observations made by Ledig and Weaver (13), who measured the rate of solution of carbon dioxide in water, the former being fed in the form of spherical bubbles whose volume was 0.036 cc. A recalculation by us (14), using the data provided by the above workers, showed that the relative rate of mass transfer through a unit area of the interface of a large spherical bubble was 2.5 times greater in the work done by Adeney and Becker than for the small bubbles

*A similar expression had been first derived by Hatta (7) in the description of the rate of chemisorption of a gas by a liquid, using a modified Lewis and Whitman equation.

used in the work done by Ledig and Weaver. This result is a natural consequence of the increase of the rate at which spherical bubbles rise with increase of their dimensions (15). Thus, the great acceleration of mass transfer occurring during the sliding of a gas bubble in a liquid, which is favorable from the point of view of the effect desired, introduces additional difficulties into the problem of a quantitative description of the bubbling type of chemisorption process.

For the experimental confirmation and evaluation of the effect of these phenomena on the process of absorption of propylene by sulfuric acid, it was possible, as indicated above, to start with simplified relationships, subsequently corrected directly on the basis of experimental data. Accordingly, we combined the quantities β, D, h and k, as shown in Eq. (8), into a provisional constant k^I and for the calculation of σ we started with the provisional assumption that within the bubble column there is established for each type of disperser a certain constant average geometric size of a spherical bubble that is independent of the pressure, the feed rate of the gas and the level of the reaction liquid (sulfuric acid), i.e., that the average diameter of such bubbles d = constant.

Then, the number of bubbles suspended in 1 m.^{3} of the liquid volume will be equal to:

$$n = \frac{V}{P\omega v} = \frac{6V}{P\omega\pi d^3} \tag{9}$$

Where V is the volume of gas (m.^{3}) adjusted to atmospheric pressure and fed during one hour through a column cross-sectional area equal to 1 m.^{2}; P is pressure (atm. abs.); ω is the velocity of ascent of gas bubbles (m./hr.); and v is the volume of a single bubble (m.^{3}).

From this we find the variable interfacial area per cubic meter of reaction liquid volume to be:

$$s = n\Delta\sigma = \frac{6V\pi d^2}{P\omega\pi d^3} = \frac{6V}{P\omega d} \tag{10}$$

where $\Delta\sigma$ is the surface area of a single gas bubble.

For changing the differential Eq. (8) into the integral form we introduce the notation as follows:

V_0 is the volume of original gas fed through a 1 m.^{2} cross section of the column at P = 1 atm. abs. (m.^{3}/hr.);

x is the variable amount of absorbed propylene in the column with a cross-sectional area of 1 m.^{2} for elevation of the gas to the height of bubbling layer l, (m.^{3}/hr.);

a is the content of propylene in the original gas (parts by volume).

Considering that during the residence of the gas bubble in the reaction zone $\tau = 1/\omega$, from which $d\tau = dl/\omega$, and that the variable partial pressure of propylene $P_{pr.} = P(V_0a - x)/(V_0 - x)$, we have the following equation as a result of appropriate subsitutions in Eq. (8).

$$\frac{dx}{dl} = \frac{6k^I}{\omega^3 d}(V_0a - x) = k^{II}(V_0a - x) \tag{11}$$

which after having been integrated between the limits from $l = 0$ and $x = 0$ to $l = L$ and $x = x_1$ (where L is the total height of the bubbled layer and x_1 is the final amount of absorbed propylene) gives the following expression:

$$k^{II} = \frac{2{,}3}{L} \log \frac{V_0a}{V_0a - x_1} \tag{12}$$

or

$$k^{III} = \frac{1}{L} \log \frac{1}{1 - y}$$

where $y = x_1/V_0a$ = the converted fraction of propylene.

In the experiments described below, the actual height of the bubbling layer of sulfuric acid L was not measured directly, but could be computed from the data on the elevation of the acid level obtained experimentally in a glass model of the reactor. It was shown by direct experiments that the increase in the height of the bubbling layer followed a linear empirical equation shown below, in the case of a change in the feed of an inert gas (within limits of its linear velocity in the empty section from 0 to 0.06 m./sec.):

$$L = L_0(1 + 5w)$$

where L is the height of the sulfuric acid layer with gas bubbling through it; L_0 is the same in the absence of bubbling; and w is the linear velocity of the gas in the free column section in m./sec.

For the calculation of the latter value under the conditions of propylene absorption, we calculated the arithmetic mean of w between the entry and the exit to and from the column, which led to the computational formula below:

$$L = L_0\left[1 + 5w_0\left(1 - \frac{ay}{2}\right)\right] \tag{13}$$

where w_0 is the linear velocity of the compressed gas at entry into the column.

Using Eqs. (12) and (13), we calculated the values of the provisional constants k^{III} for experiments, the conditions of which are given in Table 1.

RELATIONSHIP BETWEEN REACTION RATE AND DEGREE OF SATURATION OF THE ACID

Examination of the data in Table 1 shows first of all that at low degrees of saturation of sulfuric acid with propylene, as well as at rather considerable

degree of saturation, the reaction rate constants are smaller than with intermediate degrees of saturation.

The lowered reaction rate evidently depends at first on the previously mentioned relatively low solubility of propylene in fresh acid in comparison with the acid that has been enriched with the reaction products. The retardation in the region of high degrees of saturation must be explained by the approach to the state of equilibrium in the reaction, which takes place at smaller and smaller degrees of saturation of the acid, the lower is the propylene partial pressure. However, the fact that in the region of intermediate degrees of saturation of the acid, the values of k^{III} remain constant for each individual experiment within the experimental accuracy explains the acceptability of the provisional assumptions made above.

Only the data for the degrees of saturation of sulfuric acid which assure a sufficient constancy of the values of reaction rate constants are shown in the Tables which follow in connection with these observations.

RELATION OF REACTION RATE AND PRESSURE

Examination of the data in Table 1 also shows that values of k^{III} calculated from Equation (12) rise greatly with increased pressure. This growth indicates the insufficient justification of some of the simplifying assumptions which provided the basis for the derivation of the computational equations for this process. First, this is related to the tentative assumption about the rapid removal of reaction products from the reaction film and to the elimination from rate Eq. (2) of terms describing the effects of the reverse reactions. With consideration of the latter, the description of the effect of the propylene partial pressure on the state of chemical equilibria in the film would obviously lead to introduction of an additional parameter P_{pr}^{n} into Eq. (12). The existing experimental material, however, is insufficient for a single-valued clarification of the detected inconsistency or for a derivation of a theoretically sound and more precise equation. Therefore, we are limiting ourselves for the present to the introduction of only an empirical correction

Table 1

Dependence of reaction rate on degree of saturation of the acid and on pressure (temperature: 60-70°C; H_2SO_4 concentration: 80%; diameter of disperser perforations: 3 mm.)

Average linear velocity of the compressed gas, m./sec.	Pressure, atm. abs.		Height of bubbling layer L, m.	Absorbed part of propylene, y	Molar saturation of the acid $\frac{C_3H_6}{H_2SO_4}$	$k^{III}\times10^2$ from Eq. (12)	$k^{IV}\times10^2$ from Eq. (14)
	Operating P	Partial $P_{C_3H_6}$					
0.064	2.5	1.90	1.04	0.019	0.025	0.8	0.4
0.064	2.4	1.95	1.06	0.040	0.083	1.7	0.9
0.064	2.4	1.95	1.08	0.045	0.152	1.9	1.0
0.064	2.3	1.85	1.11	1.058	0.243	2.3	1.3
0.064	2.3	1.85	1.12	0.060	0.344	2.4	1.4
0.064	2.3	1.80	1.16	0.060	0.439	2.4	1.4
0.064	2.4	1.85	1.19	0.061	0.534	2.3	1.3
0.064	2.4	1.80	1.21	0.048	–	1.8	1.1
0.064	2.4	1.80	1.21	0.014	0.775	0.6	0.3
0.023	6.2	3.35	0.89	0.077	0.069	3.9	1.3
0.023	6.2	3.45	0.96	0.083	0.278	4.0	1.3
0.023	5.7	3.45	1.03	0.090	0.454	4.0	1.3
0.023	5.5	3.50	1.06	0.097	0.593	4.2	1.3
0.023	5.5	3.70	1.12	0.103	0.755	4.8	1.3
0.023	5.5	3.75	1.18	0.108	0.990	4.2	1.3
0.023	5.3	3.90	1.25	0.113	1.110	4.2	1.2
0.020	8.8	6.5	1.02	0.134	0.434	6.1	1.1
0.020	9.3	6.7	1.25	0.191	0.766	7.4	1.3
0.020	9.1	6.7	1.37	0.199	1.150	7.0	1.3
0.015	15.2	10.5	0.86	0.204	0.500	11.7	1.4
0.015	13.1	11.3	1.24	0.298	1.410	12.4	1.4
0.015	14.1	11.3	1.57	0.053	1.830	1.6	0.2

into Eq. (12), which now takes the following form:

$$k^{IV} = \frac{k^{III}}{P_{pr}^{0.9}} = \frac{1}{LP_{pr}^{0.9}} \log \frac{1}{1-y} \qquad (14)$$

where P_{pr} is the mean value of propylene partial pressure in the column.

In the calculation of the value of P_{pr} we estimated the hydrostatic pressure drop from the column height, which gave considerable corrections for experiments with a high acid level.

As is shown by the values of k^{IV} calculated from Eq. (14) (for intermediate degrees of saturation of the acid) and shown in Tables 1, 2 and 3, these maintain a satisfactory constancy over a wide interval of changes in operating pressure (with various degrees of saturation of the acid and for various diameters of the plate perforations).

RELATION BETWEEN REACTION RATE AND RATE OF PROPYLENE FEED AND HEIGHT OF THE BUBBLING LAYER

As indicated above, during the derivation of the kinetic Eqs. (12) and (14) we postulated tentatively that the size of the gas bubbles is independent of the rate of gas feed into the column.

This presumption, which is valid for low degrees of saturation of the liquid with the gas bubbles, is, generally speaking, invalid during intense bubbling, since the probability of collision of the bubbles is proportional to the square of the concentration of bubbles suspended in the liquid. On the other hand, as indicated earlier, more favorable conditions may be created for the primary dispersion of the gas on leaving the disperser with increased rate of flow of the gas stream in the plate perforations.

In order to check the overall effect of these factors on the process, we ran some experiments, the results of which are summarized in Table 3, showing that the values of k^{IV} calculated by means of Equation (14) decline regularly with increasing rate of propylene feed (see the runs made at 3 atm. abs. and at 9 atm. abs. with the height of the bubbling layer equal to approximately 1.5 m.). The graphically shown dependence of variations of k^{IV} on the rate of gas flow shown in Figure 1 (the run series made at 3 atm. abs.) is nonlinear, as should have been expected, and is described satisfactorily by the following equation:

$$k^{V} = k^{IV} + 0.55\,w^{2} \qquad (15)$$

in which the second power dependence is in agreement with the above-cited phenomenon of coalescence of the gas bubbles. In case of increased height of the bubbling layer, the values of k^{V} decline regularly (experiments with disperser No. 1) which agrees with the increased probability of coalescence of small gas bubbles into larger ones with increased height and, accordingly, increased time of their rise in the column.

RELATION BETWEEN REACTION RATE AND DIMENSIONS OF DISPERSER PERFORATIONS

Materially different results were secured from experiments run with a disperser consisting of a nipple with an internal diameter of 20 mm. As indicated by the data in Table 3, the change in the height of the bubbling layer from 1.4 to 4.5 m., i.e., more than 3-fold, failed to alter, within the accuracy of the determinations, the values of the rate constants calculated with Eq. (14) or Eq. (15).

The regularity of these results follows from the indicated picture of dispersion and coalescence in the gas stream. The probability of the development of these opposed processes, under otherwise similar conditions, should be largely governed by the size of the gas bubbles. Actually, the probability

Table 2

Dependence of reaction rate on pressure (H_2SO_4 concentration: 80%)

Temp. of absorption, °C	Diameter of plate perforations, mm.	Experimental conditions		Average values of the rate constant	
		Calculated mean partial pressure of propylene	Molar saturation of acid C_3H_6 / H_2SO_4	$k^{III}\times10^2$ from Eq. (12)	$k^{IV}\times10^2$ from Eq. (14)
60-70	3	1.8	0.25-0.70	2.3	1.4
60-70	3	3.5	0.10-1.00	4.1	1.3
60-70	3	6.6	0.75-1.60	7.2	1.3
60-70	3	10.9	0.50-1.40	12.0	1.4
70 ±5	1	2.1	0.36	2.8	1.35
70 ±5	1	5.6	1.29	7.6	1.35
70 ±5	20	2.2	0.20	1.9	0.90
70 ±5	20	5.2	0.56	4.9	0.95

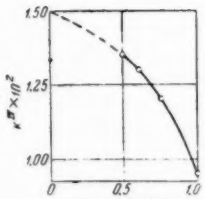

Fig. 1. Relation between reaction rate and linear velocity of the gas.

of deformation and break-up of the bubble increases with increase in the dimensions, i.e., with increased radius of curvature, leading to decreased strength of the sphere.

Evidently, there must be some average size of the gas bubble that makes equal the probabilities of break-up and coalescence under the given set of conditions. The size of such a bubble may be characterized by the value of the critical diameter which determines, under the given conditions, the statistical impossibility of change in the mean size of the surface area of the interface and the change in the intensity of mass transfer by the process of coalescence of gas bubbles.

The reality of these ideas is confirmed by the relationship observed by us in the above-cited experiments between the reaction rate and the dimensions of the perforations in the dispersers, graphically shown in Fig. 2. In plotting this curve, the relative rates of the reaction run with the disperser having 1 mm. perforations were calculated by means of Eq. (15), while those for experiments made with the other dispersers, which showed a practical independence of the reaction rate on the linear velocity of the gas feed, were calculated by means of Eq. (14). The shape of this curve shows that the considerable change in the rate of absorption of propylene with decreased diameter of the perforations is observed only for the dispersers with fine perforations. Increase of the hole diameters beyond 10 mm. resulted in substantially constant effectiveness of the process. Consequently, for a given system, the "critical" size of the gas bubbles is reached when the hole diameter in the disperser

Table 3

Dependence of reaction rate on rate of gas feed, diameter of disperser perforations, and height of bubbling layer (H_2SO_4 concentration: 80%; temperature: 70 ±5°C)

Average linear velocity of the compressed gas, m./sec.	Pressure, atm. abs.		Height of bubbling layer, m		Absorbed fraction of propylene, y	Molar saturation of the acid $\frac{C_3H_6}{H_2SO_4}$	$k^{IV}\times10^2$ from Eq. (14)	$k^{V}\times10^2$ from Eq. (15)
	Operating P	Partial P_{pr}	Without bubbling L_o	With bubbling L				
Disperser No. 1 (100 holes, d = 1 mm.)								
0.050	3.1	2.1	1.08	1.35	0.083	0.36	1.35	1.50
0.061	2.9	2.0	1.11	1.44	0.080	0.39	1.30	1.50
0.076	3.6	2.6	1.14	1.57	0.088	0.45	1.20	1.50
1.100	3.0	2.0	1.05	1.58	0.066	0.27	0.95	1.50
0.070	2.8	1.8	2.19	2.96	0.132	0.27	1.15	1.40
0.078	2.8	1.9	2.29	3.19	0.148	0.37	1.20	1.55
0.067	3.0	2.1	3.28	4.40	0.205	0.34	1.10	1.35
0.035	9.2	5.5	1.29	1.51	0.238	0.85	1.45	1.50
0.045	9.0	5.6	1.53	1.87	0.279	1.29	1.35	1.45
0.056	9.3	5.6	1.41	1.80	0.240	1.16	1.20	1.35
0.037	10.3	5.7	2.94	3.47	0.415	1.19	1.20	1.30
0.037	9.5	5.6	2.99	3.56	0.419	1.21	1.20	1.30
0.044	9.4	5.2	4.05	4.94	0.431	0.99	0.95	1.05
0.045	10.0	5.2	4.41	5.38	0.502	1.22	1.10	1.20
Disperser No. 2 (1 hole, d = 20 mm.)								
0.053	3.5	2.2	1.07	1.36	0.057	0.20	0.90	1.15
0.075	3.0	2.1	3.45	4.76	0.196	0.36	0.95	1.25
0.043	9.1	5.2	1.13	1.38	0.144	0.56	0.95	1.05
0.035	9.4	5.7	1.27	1.50	0.164	0.76	0.90	1.00
0.041	8.3	5.4	1.41	1.71	0.170	1.16	0.90	0.95
0.038	9.7	5.3	3.74	4.45	0.372	0.68	0.90	0.95

is but 10 mm. The reaction rate's independence of any further increase in the perforation diameters is the result of the fact that the larger bubbles are broken up, at the very instant of exit from the disperser, into bubbles of "critical" size, and thereafter their geometric surface remains practically constant on the average.

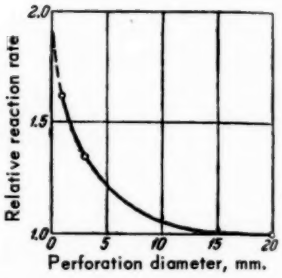

Fig. 2. Dependence of reaction rate on diameter of perforations in the disperser.

DEPENDENCE OF REACTION RATE ON SULFURIC ACID CONCENTRATION AND TEMPERATURE

The appropriate measurements, the results of which are given in Table 4, are unfortunately insufficiently accurate for a quantitative treatment. Nevertheless, even approximate comparisons of these data with those obtained by other workers would be of considerable interest and would lead to some important generalizations.

For this purpose we collected in Table 5 the average values of the constants k^{IV} from Tables 1 and 4 for various temperatures and sulfuric acid concentrations, while the approximate values of the reaction acceleration coefficients with increased acid concentration for the various temperatures are also shown there. Experimental data obtained by other workers on the effect of sulfuric acid concentration on the rate of propylene absorption under the conditions of virtual stagnation of the reaction film of the acid at the phase boundary are shown in Table 6 for comparison. The comparison shows that while in the latter instance a change of acid concentration from 70 to 85% led to a 20- to 30-fold acceleration of the reaction, this acceleration in a

Table 4

Dependence of reaction rate on sulfuric acid concentration and temperature (disperser with a hole diameter of 3 mm.)

H_2SO_4 concentration, %	Temp., °C	Absorbed pressure of propylene atm. abs.	Average linear velocity of the compressed gas, m./sec.	Height of bubbling layer L, m.	Absorbed fraction of propylene, y	Molar saturation of the acid $\frac{C_3H_6}{H_2SO_4}$	$k^{IV}\times10^2$ from Eq. (14)
70	60-70	9.9	0.0160	0.78	0.089	0.260	0.65
70	60-70	10.7	0.0160	0.83	0.091	0.540	0.60
70	60-70	10.9	0.0160	0.89	0.109	0.905	0.65
70	60-70	11.1	0.0160	0.99	0.121	1.240	0.65
70	90-95	10.7	0.0185	0.78	0.069	0.160	0.50
70	90-95	10.8	0.0185	0.89	0.210	0.560	0.75
70	90-95	10.9	0.0185	1.04	0.210	1.120	1.15
70	90-95	10.6	0.0185	1.20	0.172	1.585	0.80
75	60-70	10.3	0.0125	0.79	0.074	0.310	0.55
75	60-70	11.0	0.0125	0.89	0.084	0.700	0.50
75	60-70	11.3	0.0125	1.03	0.197	1.230	1.05
75	90-95	10.6	0.0145	0.80	0.123	0.420	0.85
75	90-95	10.9	0.0145	0.89	0.076	0.625	0.45
75	90-95	10.5	0.0145	1.03	0.214	1.210	1.20
75	90-95	10.6	0.0145	1.21	0.184	1.640	0.85
80	35-40	10.4	0.0155	0.81	0.139	0.355	1.00
80	35-40	10.8	0.0155	0.95	0.131	0.740	0.80
80	35-40	10.3	0.0155	1.15	0.163	1.250	0.80
80	90-95	9.8	0.0150	0.80	0.170	0.320	1.30
80	90-95	11.8	0.0150	0.97	0.147	0.665	0.75
80	90-95	10.9	0.0150	1.21	0.204	1.210	0.95
85	60-70	10.6	0.0185	1.04	0.348	1.070	2.10
85	60-70	10.4	0.0185	1.48	0.157	1.480	0.65
85	90-95	10.8	0.0185	0.98	0.229	0.590	1.50
85	90-95	10.7	0.0185	1.32	0.218	1.180	0.95

Table 5

Effect of acid concentration and temperature on rate of propylene absorption in a grid plate reactor

Concentration of original sulfuric acid wt. %	Average values of kIV×10² for intermediate saturation of acid, at			Relative reaction rates at	
	35-40°C	60-70°C	90-95°C	60-70°C	90-95°C
70	–	0.7	0.8	1.0	1.0
75	–	0.7	0.8	1.0	1.0
80	0.9	1.3	1.0	1.9	1.3
85	–	1.4	1.2	2.0	1.5

Table 6

Effect of sulfuric acid concentration on rate of propylene absorption in a "stagnant film"

Concentration of original sulfuric acid, wt. %	Reaction rate constants w×10⁴	
	According to Davis at 25°C (2)	According to Temkin at 15°C (17)
70	0.53	1.1
75	1.26	1.7
80	4.0	4.5
85	16.6	22.6
87	38.2	44.6

grid plate reactor did not exceed 1.5 to 2-fold.

A contradiction that is no smaller than this is detected also in the comparison of the data secured by various workers on the effect of the temperature on the reaction rate. In Table 7 are shown all the data found in the literature on this matter; these data indicate that the experimentally observed values of activation energy may vary within a wide range of limits depending on the conditions under which the process is carried out.

Thus the most reliable measurements made by Gel'bshtein and Temkin (17) for the immobile layer of the acid, i.e., under conditions of actual stagnation of the reaction film gave, both for propylene and for ethylene, rather high values of E. Data obtained by Pigulevskii for a slowly rotating absorption vessel agree with this, although the method used for these measurements in this study was imperfect and the error in the determination of E could have been considerable.

However, under the conditions of intensive renewal of the interfacial surface during gas bubbling in a column reactor, only a small change of reaction rate was detected with a change in the temperature (E = 1,000 cal.). The magnitude of the activation energy calculated approximately by us from the experimental data obtained by Plant and Sidgwick (19) for absorption of ethylene in a grid plate laboratory reaction (E = 4,000 cal.) was also considerably below the value obtained by Gel'bshtein and Temkin (17) for the same reaction under the conditions of a stagnant layer (E = 6,000 cal.).

An explanation of the apparent contradiction in these data may be found by an analysis of Eq. (8) cited above, which is transformed for demonstrative purposes into the following form:

Table 7

Dependence of reaction rate of absorption of olefins by sulfuric acid on the temperature (according to the data obtained by various workers)

Olefin	Process conditions	H_2SO_4 concentration, %	Temp., °C	Activation energy E cal./mole	Literature reference
Propylene	Slowly rotating reactor	88	20-30	9500	(16)
	Stagnant acid layer	68	15-40	6000*	(17)
		86	10-20	4500	
	Kinetic region	67	42-75	7500	(18)
	Bubbling in empty column	70-75	65-93	1000	Present work
Ethylene	Stagnant acid layer	85	60-80	6650*	(17)
		93.5	40-70	6000	
		97	15-30	5900	
	Bubbling in a laboratory reactor	93	50-100	4000	(19)
n-Butylenes	Kinetic region	70	65-95	0	(20)
Isobutylene	Mechanical stirring in liquid-liquid system	65	14-35	10500	(21)

*The values of E cited in the paper by Gel'bshtein and Temkin (17) were calculated by the authors starting with values of the kinetic constants k; however, the reaction rate in a stagnant diffusion layer is proportional to $\sqrt{k}$. In all other cases cited in this Table the calculation of E was done by a direct comparison of reaction rates, which yields values of E that are half as great. Therefore, to insure the comparability of the results obtained by various workers the data of paper (17) were recalculated accordingly.

$$\frac{dx}{d\tau} = \frac{\beta P_{pr}{}^{a} D\left(h\sqrt{\frac{k}{D}}\right)}{h\,\mathrm{th}\left(h\sqrt{\frac{k}{D}}\right)} = \frac{\beta P_{pr}{}^{a} D}{h} \cdot \frac{\gamma}{\mathrm{th}\,\gamma} \qquad (8a)$$

where $\gamma = h\sqrt{k/D}$ is the argument of the hyperbolic tangent.

It follows from Eq. (8a) that for values of $\gamma < 0.3$, the rate of propylene absorption should be virtually independent of the value of the rate constant of the chemical reaction k, since the values of the hyperbolic tangent within these are almost equal to its argument (deviation of not over 3%), i.e., th $\gamma \approx \gamma$.

Accordingly, Eq. (8a) assumes the following form:

$$\frac{dx}{d\tau} = \frac{D}{h}\beta P_{pr}{}^{a} \qquad (16)$$

If $\gamma > 2.0$, the value of th γ practically reaches its limiting value of unity and Eq. (8a) is transformed into:

$$\frac{dx}{d\tau} = \sqrt{D}\beta P_{pr}{}^{a}\sqrt{k} \qquad (17)$$

Thus, the character of the reaction may change qualitatively after alteration of the value of γ by less than a factor of 7 from the practical independence of the reaction rate relative to sulfuric acid concentration and temperature (Eq. (16), which does not contain the rate constant of the chemical reaction proper) to the usual dependence with the sole difference that these relationships are weakened by the location of the k constant under the square root sign (Eq. (17)).

The physical meaning of these transformations of Eq. (8a) which agree completely with the indicated deviations among the experimental data of various workers consists in the fact that in accomplishing the process without a renewal of the stagnant reaction film (1, 2, 3, 17) the thickness of the latter reaches its normal value determined by the properties of the liquid and, therefore, under otherwise similar conditions this uniquely determines the parameter γ and its sufficiently large value. However, in the case of continuous renewal of the surface of the interface, for example, during the rapid rise of rather large gas bubbles through an empty grid plate column, a sharp reduction of the mean thickness of the reaction film should occur.

In agreement with this, the value of γ in Eq. (8a) decreases, which is reflected in a reduced influence of acid concentration and temperature on the rate of olefin absorption.

The fact that in an empty grid plate column both of these parameters change the process rate but very little, according to the data shown in Table 5, indicates the realization under these conditions of a rather effective renewal of the surface of the interface, i.e., in this case the value of γ approaches 0.3.

In the light of these considerations, Rustamov (18), who claimed to have run the absorption of olefins in sulfuric acid in a thin layer which assured the progress of the reaction in the "kinetic region," should have obtained activation energy values twice as great as those obtained under the conditions of a "stagnant film." Accordingly, for propylene, E should have been equal to 12,000 cal./mole from Temkin's data (17). However, the value of E = 7,500 cal. obtained by him does not completely agree with this value, which may be considered to be a fact that does not agree with the theory. However, according to the other data obtained by Rustamov (20) for absorption of normal butylenes, a value of E was obtained that was close to zero, which cannot in any manner correspond to the "kinetic region" but agrees completely with the data for the process run in a grid plate column with intense renewal of the surface. Unfortunately, the cited papers by Rustamov were written so briefly that the problem of the reality of attainment of the "kinetic region" remains unclear to the reader.

SOME PRACTICAL CONSEQUENCES

A logical conclusion from the consideration of Eqs. (8), (16) and (17) is that the selectivity of the process is higher during its performance under conditions which insure the maintenance of a stagnant reaction film since, in this case according to Eq. (17), the reaction rate is determined to the greatest degree by the value of the rate constant of the chemical reaction proper k. During the intensive renewal of the surface of the interface the rate of absorption of various olefins would be practically the same according to Eq. (16), since the diffusion coefficients depend rather little on the structure of the molecules. Unfortunately, the direct experimental data are lacking for a confirmation of this point.

From the point of view of these situations, considerable interest attaches to the industrial data for the process of selective extraction of isobutylene from its industrial mixtures with normal butylenes, as described in the literature with sufficient detail (21). In this process the liquid butane-butylene fraction is agitated with sulfuric acid by means of high-capacity circulating pumps that evidently insure a sufficiently intense dispersion of the liquid, which should expectedly lead to a sharp disturbance of the process conditions in the "stagnant film," i.e., to deterioration of its selectivity.

However, this latter supposition is confuted not only by the industrial production data on the rela-

tively low degree of absorption of normal butylenes but also by the large value of E = 10,500 cal. shown in Table 7, which is characteristic for the process in a "stagnant film."

Actually, the intense renewal of the surface of the phase boundary that is observed during gas bubbling through empty columns is a natural result of the rapid rise of the rather large gas bubbles along the immobile liquid phase or one that moves in the opposite direction. During the mechanical agitation of two immiscible liquids the flows produced by the propeller stirrers move both the dispersed and the dispersing phases in the same direction and to the same degree, i.e., the rates of their motion relative to each other remain quite small, and the smaller is the diameter of the particles of the dispersed fluid, the smaller would be the velocity of relative motion and the probability of breakup of the droplets.

Finally, the preservation of the "stagnent film" should be aided by the selection of sulfuric acid as the dispersing phase, the small drops of the acid thus preserving the "stagnant film" on their inner surfaces at practically any rate of motion of the dispersed phase. This condition is evidently observed also in the industrial process shown above.

SUMMARY

1. Kinetic equations were derived which satisfactorily describe, for dispersers with openings of various diameters, the dependence of the rate of propylene absorption in a grid plate reactor on the pressure, the degree of olefin conversion and the rate of its feed.

2. On the basis of experimental data we introduced the concept of a "critical" size of a gas bubble that excludes the influence of the rate of feed and the height of the bubbling layer on the rate of olefin absorption, i.e., parameters which aid the coalescence of small bubbles.

3. An explanation of the apparent contradiction among the experimental data obtained by various workers concerning the dependence of the process rate on temperature and sulfuric acid concentration was suggested on the basis of an analysis of a model of the reaction in the film.

4. Hypotheses were made on the basis of this analysis about the possibility of increasing the selectivity of isobutylene absorption from its industrial mixtures by using equipment and conditions that insure the progress of the reaction in a "stagnant" film, which is not subject to an intensive renewal.

LITERATURE CITED

1. Davis, H. S., *J. Am. Chem. Soc.*, 50, 2780 (1928).
2. Davis, H. S., and Schuler, R., *Ibid.*, 52, 721 (1930).
3. Davis, H. S., and Crandall, G. S., *Ibid.*, 52, 3757, 3769 (1930).
4. Nernst, W., *Z. Physik. Chem.* 47, 55 (1904).
5. Langmuir, J., *Phys. Rev.*, 34, 321 (1912).
6. Levich, V. G., *Fiziko-khimicheskaya gidrodinamika* (Physicochemical Hydrodynamics), p. 464, 1959.
7. Hatta, T., *Technol. Rep. Tôhoku Imp. Univ.*, 10, 119, 136, 613 (1932).
8. Abkin, A., Medvedev, M., and Temkin, M., *Zhur. Fiz. Khim.*, 13, 713 (1939).
9. Belopol'skii, A. P., *Zhur. Priklad. Khim.*, 19, No. 1181 (1946).
10. Nazarov, N. A., and Khain, S. S., *Materialy po krekingu* (Materials for Cracking) Vol. III, *Trudy Zavoda "Khimgaz"* ("Khimgaz" Plant Reports), p. 455, 1936.
11. Levich, V. G., reference (6), p. 392.
12. Adeney, W. E., and Becker, H. G., *Phil. Mag.*, 38, 317 (1919).
13. Ledig, P. G., and Weaver, E. R., *J. Am. Chem. Soc.*, 46, 650 (1924).
14. Nemtsov, M. S., *Zhur. Priklad. Khim.*, 33, 1075 (1960).
15. Binder, R. C., *Chem. Met. Eng.*, 51, No. 8, 104 (1944).
16. Pigulevskii, V. V., *Trudy VI Mendeleevskogo S'ezda*, 2, No. 1, 713 (1935).
17. Gel'bshtein, A. M., and Temkin, M. I., *Zhur. Fiz. Khim.*, 31, 2703 (1957).
18. Rustamov, Kh. R., Dissertation, Inst. Chem. Phys. Acad. Sci. USSR (1955); referred to in *Doklady Akad. Nauk SSSR*, 114, 848 (1957).
19. Plant, S. G. P., and Sidgwick, N. V., *J. Chem. Ind.*, 40, 14T (1921).
20. Rustamov, Kh. R., and Chirkov, N. M., *Zhur. Fiz. Khim.*, 30, 266 (1956).
21. Bauman, G. P., and Smith, M. R., *Petrol. Refiner* 33, No. 5, 156 (1954).

A. G. Kasatkin
S. Z. Kagan
V. G. Trukhanov

USSR

Empirical Equilibrium Distribution Equations for Liquid-Liquid Systems

Possibilities for maximum recovery of extracted material are established independently of the type of process (batch, or continuous extraction, or extraction with a different relative flow direction of the phases, with or without removal of the mixture).

RELATIONSHIPS pertaining to the equilibrium distribution of material in liquid-liquid systems have important significance for the analysis of liquid extraction processes and the selection of a rational design of equipment for their exploitation. On the basis of equilibrium distribution data the possibilities for maximum recovery of the extracted material are established independent of the organization of the process (batch or continuous extraction, and also extraction with a different relative flow direction of the phases, with or without removal of the mixture). The conditions for carrying out the extraction have an effect only on the location of the operating line (concentration line).

Despite the fact that the statics of extraction processes have been treated to a significantly greater extent than their dynamics, up to the present time there are not available sufficiently reliable generalized relations for the equilibrium distribution in two immiscible liquid phases. Empirical equations, with the aid of which it is possible to calculate the entire equilibrium distribution curve from two points characterizing the composition of coexisting equilibrium phases, have been presented by different authors. Best known (1, 2) are the equations of Hand, Bachman and Othmer.

According to Hand (3) the relation between mole fractions of distributed material y in the extract and mole fractions of distributed material x in the original solvent is expressed for the majority of systems by the equation

$$\frac{y}{y_e} = k_1\left(\frac{x}{x_r}\right)^n \qquad (1)$$

where y_e is the mole fraction of the extracting solvent in the extract; x_r is the mole fraction of the original solvent in the raffinate; k_1 and n are empirical constants.

The equation presented by Bachman (4, 5) and used by him as the basis for analyzing the results of the studies of Brancker et al. (6) has the form

$$y_e = a + b\frac{y_e}{x_r} \qquad (2)$$

where a and b are experimentally determined constants.

Othmer and Tobias (7), in analyzing equilibrium data, obtained the following relation for liquid-liquid systems with limited mutual solubility of components

$$\log\frac{1-y_e}{y_e} = k' \cdot \log\frac{1-x_r}{x_r} + k'' \qquad (3)$$

where k′ and k″ are constants.

The advantage of the equation presented by Hand in comparison with Eqs. (2) and (3) consists in the fact that the concentration of distributed material in both phases is considered in it. In the Othmer and Tobias equation this concentration enters in implicit form. Thus, for mutually insoluble liquids $1 - y_e = y$, so that in this case Eq. (3) reduces to Eq. (1).

In agreement with Eqs. (1) and (3) plots of equilibrium distribution in logarithmic coordinates represent identical straight lines.

The Bachman equation does not reflect an equilibrium distribution coefficient in explicit form. In addition, the empirical coefficients a and b in this equation do not reflect the physicochemical phenomena arising in the distribution of material between phases and connected with the dissociation and association of molecules of the dissolved material.

In the more general form the relation between equilibrium compositions of raffinate and extract may be presented in the form

$$y = Ax^n + Bx^{n-1} \ldots Fx \qquad (4)$$

where n = 1, 2, 3 . . . depending on how many molecules of the distributed material combine into one;

This article first published in *Khim. Prom.* No. 6, 50-54 (1960).

A, B . . . F are coefficients dependent on the degree of association of molecules of the distributed material and the distribution coefficient.

Eq. (4) is based on the assumption that molecules of distributed material are present in the extract in monomer form.

Association of molecules of distributed material in the primary solvent may be presented in the form

$$2x_1 \rightleftharpoons x_2 \qquad (5')$$

$$3x_1 \rightleftharpoons x_3 \qquad (5'')$$

. . . . . .

$$nx_1 \rightleftharpoons x_n \qquad (5^n)$$

where the subscripts 1, 2, 3 . . . n designate monomeric, dimeric and polymeric molecules of the distributed material in the primary solvent.

From Eqs. (5′) - (5^n) in conformity with the law of mass action

$$\frac{x_2}{x_1^2} = C_2 \qquad (6')$$

$$\frac{x_3}{x_1^3} = C_3 \qquad (6'')$$

. . . . .

$$\frac{x_n}{x_1^n} = C_n \qquad (6^n)$$

where C_2, C_3 . . . C_n are constants dependent on the temperature.

The total concentration of distributed material in moles of monomer in the primary solvent is expressed by the equality

$$x = x_1 + 2x_2 + 3x_3 + \ldots + nx_n \qquad (7)$$

Replacing in Eq. (7) the concentrations of dimers and polymers by the concentrations of monomers expressed in Eqs. (6′) - (6^n) we obtain

$$x = x_1 + 2C_2x_1^2 + 3C_3x_1^3 + \ldots + nC_nx_1^n \qquad (8)$$

The concentration of distributed material in the extract as a function of the concentration of the monomer in the raffinate may be expressed by the overall distribution expression

$$y = Kx \qquad (9)$$

where K is the distribution coefficient.

On the basis of Eqs. (8) and (9) we obtain the final equation

$$y = Kx_1 + 2KC_2x_1^2 + 3KC_3x_1^3 + \ldots + nKC_nx_1^n \qquad (10)$$

This equation confirms the validity of Eq. (4), whereby

$$nKC_n = A$$

$$(n-1)KC_{n-1} = B$$

. . . . . .

$$K = F$$

Numerical values of the quantities A, B . . . F may be found from experimental data by the power reduction method in Eq. (10).

Let us assume that the equilibrium relation for some liquid-liquid system is represented by curve 1 (Fig. 1). This curve in the general case may be expressed by Eq. (4). Let us represent this equation in the form of the function $y/x = f(x)$. Then, the new curve 2 (equation of curve 2: $y/x = Ax^{n-1} + Bx^{n-2} + \ldots + F$) may be constructed in Fig. 1 with coordinates y/x vs. x, which after its extrapolation to the ordinate, intercepts the segment F; for a given liquid-liquid system this segment corresponds to the distribution coefficient according to Eq. (9).

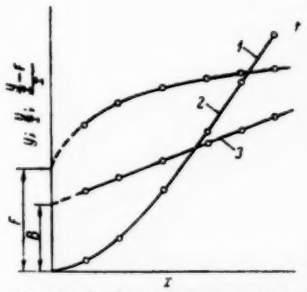

Fig. 1. Analytical development of the relation between equilibrium phase concentrations for liquid-liquid systems.

For simplification of the following transformations, we assume that in the raffinate associated molecules of the polymer contain not more than three original molecules of the distributed material (n = 3). Then in coordinates corresponding to the new functional relation $\frac{y}{x} - F/x = f(x)$, we obtain the straight line 3 (equation of the straight line 3: $\frac{y}{x} - F/x = Ax^{n-2} + B = Ax + B$), intercepting the segment B on the ordinate, equal in the present case to $2KC_2$. Tangent of the angle of inclination of this straight line gives the value of A equal to $3KC_3$. Thus, an analytical expression of the equilibrium curve for the examined liquid-liquid systems may be found.

In the case of the presence in the raffinate of polymer molecules consisting of n initial molecules, it is necessary to carry out (n - 1) transformations, similar to the ones described above. However, as the results of application of the equilibrium

data by this method show, for the overwhelming majority of liquid-liquid systems (for the concentration range of industrial interest) the magnitude of $n \neq 3$ for systems in which the distributed material is an inorganic compound and, apparently, $n \leq 4$ for systems in which the distributed material is an inorganic compound. One may assume that the proposed method may be extended to vapor-liquid and gas-liquid systems because of the analogy between the principles of intermolecular interaction in the liquid phase for these systems and liquid-liquid systems.

Eq. (10) was verified on different liquid-liquid systems accounting for the three possible types of equilibrium lines (Fig. 2). For systems having maximum points on the equilibrium distribution curve (Figs. 2b and 2c)*, it is apparently impossible to obtain a single equation in the concentration range from 0 to the critical point K. In these cases the final straight line obtained by successive reduction of degree in Eq. (10) must have breaks and consequently specific equations for the straight line segments of the broken line must be obtained.

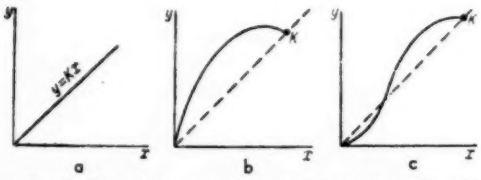

Fig. 2. Possible types of equilibrium lines for liquid-liquid systems.

Hand's attempt to describe the equilibrium distribution curve by a single Eq. (1) can hardly be justified. Thus, for example, a check of this equation on water-acetone-1, 1,2-trichloroethane system (8) showed that the Hand equation is applicable only in the region of low concentrations of distributed material (acetone) - up to 0.14 weight fraction in the water layer.

Eq. (10) was used for working up the experimental equilibrium data obtained by the authors and other investigators. As a result, empirical equilibrium curve equations were found for 30 different liquid-liquid systems (see Table).

Presented below are typical examples of the treatment of experimental data for some systems. For these systems the following sequence was used to describe components: initial solvent - distributed material - extracting solvent.

Example 1. Systems water-isopropyl alcohol-diisopropyl ether (9) (Fig. 3a); water-pyrocatechol-diisopropyl ether* (Fig. 3b).

*Fig. 2c is for "azeotropic" liquid-liquid systems; in the foreign literature these systems are known as "Soluttrop" systems; in the Soviet literature a corresponding term does not exist.

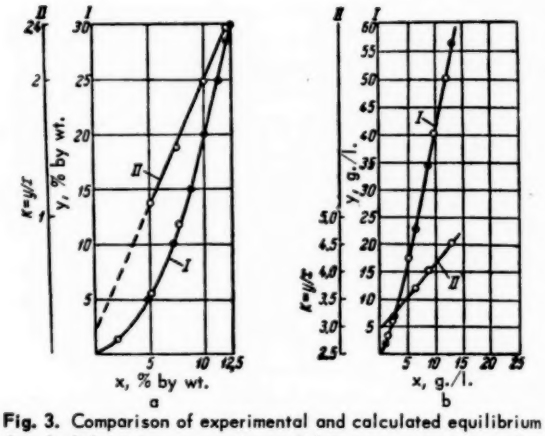

Fig. 3. Comparison of experimental and calculated equilibrium data (solid points are experimental data; open points are calculated): a) system water-isopropyl alcohol-diisopropyl ether; $y = 0.18x^2 + 0.2x$; b) system water-pyrocatechol-diisopropyl ether; $y = 0.1x^2 + 3x$.

In Figs. 3, 4, and 5, besides the equilibrium curves I, the auxiliary lines II, III and IV, constructed in accordance with the proposed method (see Fig. 2), are presented. The numbers on the vertical lines in these Figures correspond to numbers on the equilibrium curve and the auxiliary lines.

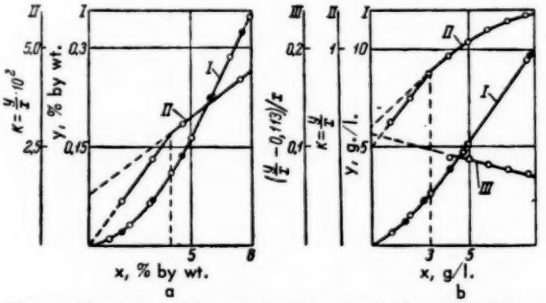

Fig. 4. Comparison of experimental and calculated equilibrium data (solid points are experimental data; open points are calculated): a) system water-acetic acid-benzene; $y_1 = 0.00715x^2$, $y_2 = 0.0039x^2 + 0.013x$; b) system glycerine-ethylamine-acetone; $y_1 = 0.127x^2 + 0.5x$; $y_2 = -0.005x^3 + 0.6x$.

From Fig. 3 it is seen that the equilibrium relations for these systems satisfy an equation of the type

$$y = Ax^2 + Bx$$

Example 2. Systems: water-acetic acid-benzene (10) (Fig. 4a); glycerine-ethylamine-acetone (11) (Fig. 4b).

*From the data of I. V. Filippov (All-Union Scientific Research Institute of the Petroleum Industry).

Table 1.

Empirical equilibrium curve equations for liquid-liquid systems

System (solvent-distributed material-extracting solvent)	Units	Concn. range of distributed material in initial solvent	Empirical equation	Literature source
1. Water-ethylamine-chloroform	mmole/liter	0-20.0	$y = 0.006x^2 + 0.4x$	(11)
2. Water-phenylacetic acid-xylene	"	0-4.5	$y = 0.122x^2 + 0.28x$	(11a)
3. Water-phenylacetic acid-nitrobenzene	g.-mole/liter	0-0.1	$y = 224x^2 + 4x$	(11a)
4. Water-phenylacetic acid-toluene	"	0-0.065	$y = 17.2x^2$	
	"	0.065-0.12	$y = 65.5x^2 + 6.8x$	(11a)
5. Water-phenylacetic acid-isoamyl alcohol	"	0-0.08	$y = 27.3x$	(11a)
6. Water-phenylacetic acid-chloroform	"	0-0.01	$y = 914x^2 + 2x$	(11a)
7. Water-phenylacetic acid-benzene	"	0-0.016	$y = 25x^2 + 0.7x$	(11a)
8. Water-benzylmethylamine-ethyl ether	mmole/liter	0-1.2	$y = 5.5x$	(11b)
9. Water-benzylmethylamine-xylene	"	0-1.2	$y = 2.92x^2 + 4.5x$	(11b)
10. Water-acetylsalicylic acid (aspirin)-ethyl ether	"	0-0.55	$y = 3.28x^2 + 4x$	
	"	0.55-1.25	$y = 1.18x^2 + 5.3x$	(11c)
11. Water-acetylsalicylic acid-xylene	mole/liter	0-17	$y = 0.015x^2 + 0.17x$	(11c)
12. Water-acetylsalicylic acid-chloroform	g.-mole/liter	0-0.02	$y = 420x^2 + 0.7x$	(11c)
13. Water-acetylsalicylic acid-toluene	"	0-0.016	$y = 26x^2 + 0.22x$	(11c)
14. Alcohol-water hydrochloric acid solution (61.5% water, 14% ethyl alcohol, 24.5% hydrochloric acid)-vanillin-dichloroethane	wt. %	0-3	$y = 0.5x^2 + 0.75x$	
15. Water-phenylethyl alcohol-carbon tetrachloride	"	3-6	$y = -0.0783x^2 + 0.95x^2$	(12)
	"	0-0.3	$y = 2.2x$	
	"	0.3-0.535	$y = 2.98x^2 + 1.35x$	(12)
	"	0.535-1.05	$y = 6.75x^2 - 0.8x$	
16. Alcohol-water hydrochloric acid solution-vanillin-benzene	"	0-1.85	$y = 0.4x^2 + 0.6x$	
	"	1.85-7	$y = 0.0272x^3 + 0.39x^2 + 0.7x$	(12)
17. Tar water-phenol-diisopropyl ether	g./liter	0-1.8	$y = 15.45x^2 - 4x$	(*)
18. 15% hydrochloric acid-acetic acid-chlorobenzene	wt. %	0-0.15	$y = 4x^2 + 2x$	
	"	0.15-0.72	$y = 0.388x^2 + 2.5x$	(10)
	"	0.72-1.5	$y = 2.98x^2 + 0.75x$	
19. 15% hydrochloric acid-phenol benzene	"	0-0.12	$y = 10.8x^2 + 2.7x$	
	"	0.12-0.64	$y = 1.18x^2 + 3.8x$	(10)
	"	0.64-1.34	$y = 5x^2 + 1.3x$	
	"	1.34-2.6	$y = 9.14x^2 - 4.2x$	
20. 0.05 N HNO_3-uranyl nitrate-20% solution of DAMPA in kerosine	g./liter	0-75	$y = -0.0292x^2 + 3x$	
	"	75-84	$y = -0.0176x^2 + 2.4x$	(13)
	"	84-90	$y = 0.00866x^2 + 1.74x$	
21. Water-acetic acid-benzene	wt. %	0-3.9	$y = 0.00715x^2$	(10)
	"	3.9-8	$y = 0.0039x^2 + 0.013x$	
22. Glycerine-ethylamine-acetone	mmole/liter	0-3	$y = 0.127x^2 + 0.5x$	
	"	3-8	$y = -0.0005x^3 + 0.113x^2 + 0.6x$	(11)
23. 4 N HNO_3-zirconium nitrate-10% solution of DAMPA in kerosine	wt. %	0-7.5	$y = 0.0037x^4 + 0.0045x^3 + 0.053x^2 + 0.5x$	(**)
24. Water-isopropyl alcohol-diisopropyl ether	"	0-12.5	$y = 0.18x^2 + 0.2x$	(9)
25. Water-pyrocatechol-diisopropyl ether	"	0-13	$y = 0.1x^2 + 3x$	(*)
26. 24.2% ammonium sulfate solution-caprolactam-azeotropic mixture (benzene + cyclohexane)	g./liter	0-50	$y = 0.0143x^2$	(***)
27. 40% ammonium sulfate solution-caprolactam-benzene	"	0-7	$y = 3.48x^2 + 1.2x$	(***)
28. Trichloroethylene-caprolactam-water	"	0-36.7	$y = -0.03x^2 + 4.45x$	(***)
	"	36.7-52	$y = 3.35x$	
29. Azeotropic mixture (benzene + cyclohexane)-caprolactam-water	"	0-10	$y = 21x$	(***)
30. 40% ammonium sulfate solution-caprolactam-azeotropic mixture (benzene + cyclohexane)	"	0-10	$y = x^2$	(***)

*See previous footnote.
**See subsequent footnote.
***From data of A. G. Kasatkin, S. Z. Kagan and V. G. Trukhanov (The D. I. Mendeleev Moscow Chemical Engineering Institute).

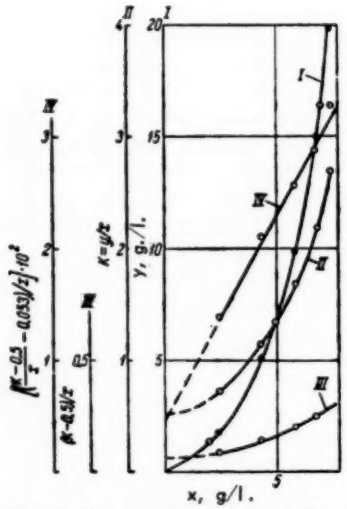

Fig. 5. Comparison of experimental and calculated equilibrium data for the system: 4N HNO_3-zirconium nitrate-10% solution of diisoamyl ether of methylphosphinic acid (DAMPA) in kerosine. $y = 0.0037x^4 + 0.0045x^3 + 0.053x^2 - 0.5x$.

For the system water-acetic acid-benzene the break of the line in y/x vs. x coordinates is characteristic. As a result, for the lower portion of the curve the equilibrium equation has the form

$$y = Ax^2$$

and for the upper portion

$$y = A_1x^2 + B_1x$$

In Fig. 4b (system glycerine-ethylamine-acetone) a case is shown where the auxiliary line in y/x vs. x coordinates has a straight and a curved portion.

For the part of the equilibrium curve corresponding to the straight part of the auxiliary line

$$y = Ax^2 + Bx$$

for the part of the equilibrium curve corresponding to the curved part of the auxiliary line

$$y = A_1x^3 + B_1x^2 + C_1x$$

Apparently, the presence of two equations for two parts of the equilibrium curve in a given case is connected with a change in the intermolecular interaction at some critical concentration corresponding to the break point in the auxiliary line.

Example 3. System 4 N HNO_3-zirconium nitrate-10% solution of diisoamyl ether of methylphosphinic acid (DAMPA) in kerosine* (Fig. 5).

This system illustrates the complexity of empirical equations for some compounds, reflecting the complex processes that occur with the interaction of components. For this case an empirical equation of the following form is obtained:

$$y = Ax^4 + Bx^3 + Cx^2 + Dx$$

Calculation according to the formulas presented in the Table shows good agreement between the calculated and the experimental data, which fact points out the broad applicability of the proposed method of treating experimental equilibrium data in liquid-liquid systems.

LITERATURE CITED

1. Treybal, R. E., *Liquid Extraction*, McGraw-Hill Book Company, New York, 1951.

2. Kortüm, G., and Buchholz-Meisenheimer, H., Die Theorie der Destillation und Extraktion von Flussigkeiten *(The Theory of Distillation and Extraction of Liquids)*, Springer Verlag, Berlin, 1952.

3. Hand, D. B., *J. Phys. Chem.* 34, 1961 (1930).

4. Bachman, I., *Ibid.*, 44, 446 (1940).

5. Bachman, I., *Ind. Eng. Chem.*, Anal. Ed. 12, 38 (1940)

6. Brancker, A. V., Hunter, T. G., and Nash, A. W., *Ibid.*, 12, 35 (1940).

7. Othmer, D. F., and Tobias, P. E., *Ind. Eng. Chem.* 34, 693 (1942).

8. Treybal, R. E., Weber, L. D., and Daly, J. F., *Ibid.*, 38, 8, 817 (1946).

9. Frere, F. J., *Ibid.*, 41, No. 10, 2365 (1949).

10. Planovskaya, M. A., Candidate's Dissertation MKhTI im. D. I. Mendeleeva (The D. I. Mendeleev Moscow Chemical Engineering Institute), 1950.

11. Seidel, A., *Solubilities of Organic Compounds*, D. Van Nostrand Company, Inc., New York, p. 161, 1941.

11a. *Ibid.*, 583.

11b. *Ibid.*, 616.

11c. *Ibid.*, 631.

12. Kiseleva, E. N., Candidate's Dissertation, VNIISNDV (All-Union Scientific Research Institute of Synthetic and Natural Aromatic Substances), 1956.

13. Shevchenko, V. B., Slepchenko, I. G. Shmidt, V. S., and Nenarokomov, E. A., *Atomnaya Energiya* 7, 3 (1959).

*From data of V. V. Tarasov (The D. I. Mendeleev Moscow Chemical Engineering Institute).

G. M. Panchenkov
Yu. M. Zhorov
Yu. Yui-lin

USSR

Kinetic Aspects of the Catalytic Cracking of Heavy Distillate Stocks

It is shown that the heavy stock cracking reaction occurs in the transition region between internal and external diffusion, which permits use of low-index catalysts with poorly developed surface.

A study of the kinetics of cracking heavy stock is of great industrial interest, since, as a result of the deficiency of light gas oil fractions, catalytic cracking installations in a series of plants have converted to the processing of heavy gas oils with an end point exceeding 500°C (1).

Important investigations on heavy stock kinetics have been conducted in our country and abroad (2-5). They have shown the industrial advantage of cracking heavy stocks and have made it possible to recommend effective conditions for the process. However, in these studies peculiarities in the kinetics were not shown, reaction kinetic constants were not determined and, in particular, researches devoted to defining the region in which the cracking reaction proceeds are absent. Furthermore, investigations conducted on large installations give a significant spread of results, which is explained by a change in the thermal regime of the reactors, by nonuniformity in the feed stock feed rate and by other factors. Fig. 1, on which the relations are given between the conventional overall severity of cracking and the yield of liquid cracked products and the volumetric rate of stock feed for different temperatures, constructed by us from the data of A. V. Agafonov (2), is presented as an example. From Fig. 1 it is seen that it is difficult to judge the change in the yield of liquid cracked products with a change in temperature.

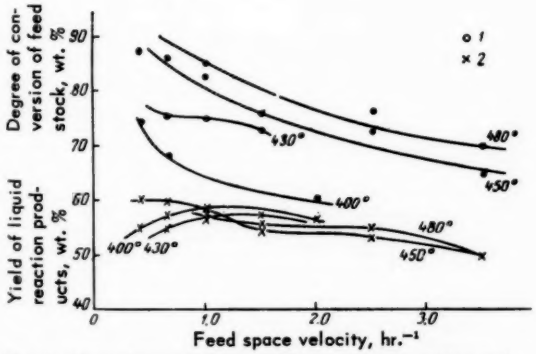

Fig. 1. Dependence of the overall severity of cracking and yield of liquid products of catalytic cracking reaction of heavy gas oil on stock feed rate from data of A. V. Agafonov (2). 1) Overall severity of cracking; 2) yield of fraction boiling up to the initial boiling point of the feed stock (IBP 320°C).

This article first published in *Khim. i Tekhnol. Topliv. i Masel*, 5, No. 11, 4-8 (1960). The authors are associated with the I. M. Gubkin Moscow Institute of Petrochemical and Gas Industry.

In this connection a study was undertaken of the kinetics of cracking heavy gas oil from the Romashkino crude with the following characteristics.

Specific gravity d_4^{20}	0.9006
Fractional distillation, °C:	
IBP	260
10%	322
50%	390
EP	496
Sulfur content, %	1.92
Viscosity ν_{50}, centistokes	22.73
Pour point, °C	−32

Tests were conducted in a standard flow reactor of MINKh and GP (the I. M. Gubkin Moscow Institute of Petrochemical and Gas Industry) (6). The feed rate was controlled by the change in the rate of motion of clockwork connected with the piston of a medical syringe. Ordinary experimental and analytical techniques were used.

For the cracking, four samples of synthetic aluminosilicate (silica-alumina) catalyst were used whose characteristics are presented in Table 1.

The results of the experiments are presented in Figs. 2-4, which make it possible to understand some of the peculiarities of the kinetics of heavy stock cracking.

From Fig. 2 it is seen that the liquid cracked products (by liquid cracked products we mean the fraction of catalyzate boiling under 260°C) go through a maximum, which falls with an increase in temperature and corresponds to a feed space

Table 1.
Characteristics of aluminosilicate catalyst samples used in the cracking of heavy gas oil

Inspections	Catalyst Samples			
	No. 1	No. 2	No. 3	No. 4
BET specific surface area, m.²/g.	305	400	480	305
Pore volume, cm.³/g.	0.526	1.0	1.5	0.526
Mean pore radius, Å	27	55	80	27
Bulk weight, g./cm.³	0.63	0.45	0.27	0.54
Particle size, cm.	0.45	0.42	0.40	0.037
Al_2O_3 content of catalyst, %	12.8	10.0	10.0	12.8

velocity of 0.6–0.7 hr^{-1}. Consequently, for the formation of liquid products the reaction appears to be a consecutive one. We found the same dependence also in the cracking of light gas oil (7). Since gas and coke are final products of the cracking reaction, Scheme I may be used for describing the kinetics of the reaction.

$$A \rightarrow \nu_1 B + \nu_2 C + \nu_3 D$$
$$\rightarrow \nu_4 C + \nu_5 D$$

where A is feed; B is liquid cracked products; C is gas; D is coke; and the ν's are stoichiometric coefficients.

In studying the kinetics of complex reactions it is convenient to evaluate kinetic constants, not set by the kinetic equations for each stage, as is ordinarily done, but determining the rate of reaction according to experimental curves. In reference (8) we have shown that the rate of reaction realized in stream W may be expressed by the equation:

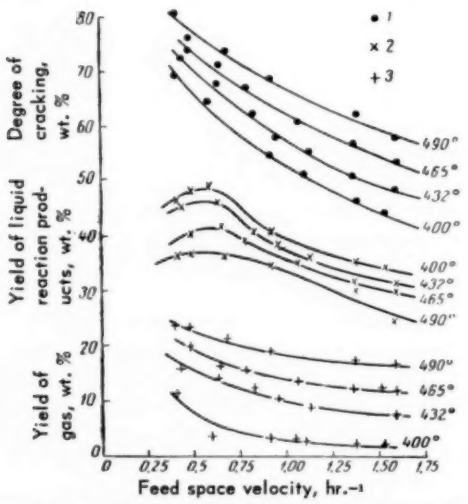

Fig. 2. Dependence of the overall severity of conversion and yield of liquid products of the catalytic cracking reaction of heavy gas oil on catalyst No. 1 on stock feed rate. 1) Overall degree of conversion; 2) yield of liquid reaction products; 3) yield of gas.

$$W = -\frac{n_0^2}{s_0 l}\frac{dx}{dn_0},$$

where n_0 is the reactant feed rate; x is the degree of conversion; $s_0 l$ is the entire catalyst surface in the reactor.

This equation permits the finding of the reaction rate from experimental curves $x = f(n_0)$, and from the change in the reaction rate at identical degrees of conversion with change in temperature - the apparent activation energy.

The analysis of the curves of Figs. 1 and 2 according to this formula was conducted by us for the determination of the activation energy of the first stage of the process according to Scheme I. Calculations are presented in Table 2.

From the data in Table 2, the magnitudes of the apparent activation energies, presented below, were calculated.

Temperature interval, °C	Magnitude of activation energy, kcal./mole
From authors' data	
400-432	10.3
432-465	8.4
465-490	7.6
From data of A. V. Agafonov	
400-450	29.0
450-480	14.4

The low magnitude of the apparent activation energy, not associated with the occurrence of a reaction in the kinetic region, is of interest. Furthermore, with a rise in the temperature, the activation energy falls, which also is not characteristic

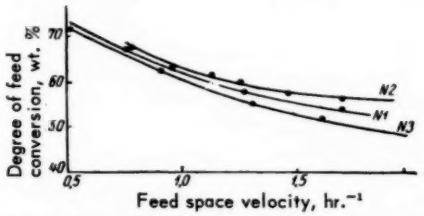

Fig. 3. Dependence of the overall degree of conversion in catalytic cracking of heavy gas oil on feed rate for catalysts No. 1, 2, and 3.

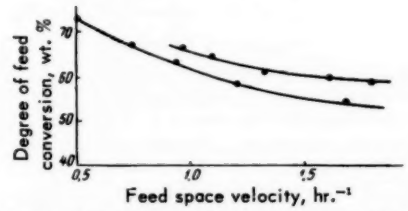

Fig. 4. Dependence of the overall degree of conversion in catalytic cracking of heavy gas oil on stock feed rate for catalysts No. 1 and 4.

Table 2.

Calculation of the apparent heavy stock cracking reaction rate from experimental curves of $x = f(n_0)$ (Figs. 1 and 2)

Temperature of test, °C	Weight fraction, x	n_0, hr.$^{-1}$	const* $\frac{dx}{dn_0}$	const* w
Obtained by analysis of curves, Fig. 2				
400	0.65	0.544	0.470	0.139
432	0.65	0.697	0.408	0.198
465	0.65	0.856	0.346	0.254
490	0.65	1.110	0.253	0.312
Obtained by analysis of curves, Fig. 3				
400	0.75	0.375	2.356	0.332
450	0.75	1.725	0.355	0.995
480	0.75	2.350	0.268	1.478

*The constant coefficient "const" appears because of the arbitrary choice of scale. It may be calculated precisely, but for determination of the activation energy its magnitude is not needed.

of the kinetic region. All this presupposes the presence of a diffusion resistance; judging by the low magnitude of the activation energy, the reaction may be occurring close to the external diffusion region.

In order to show the role of internal and external surface, experiments were conducted on catalyst No. 2, possessing pores of larger size and smaller bulk density than catalyst No. 1, but roughly with the same internal surface per unit volume. On catalyst No. 3, possessing still wider pores with a lower total surface per unit volume; and on catalyst No. 4, representing catalyst No. 1 ground to a particle size of 0.25–0.5 mm. (Figs. 3 and 4). The external surface per unit volume of catalysts No. 2 and 3 is a little greater, and of catalyst No. 4 approximately 15 times greater than that of catalyst No. 1.

Upon comparison of the results of experiments on catalysts No. 1, 2 and 3 (Fig. 3) the similarity of the degrees of conversion at identical space velocities is noted. Along with this is noted the minor effect of the catalyst activity and its internal surface. This result definitely attests to the minor role of the catalyst internal surface in the breakup of heavy molecules of the feed stock.

From comparison of the results of experiments on catalysts No. 1 and 4, it is evident that an increase in the external surface area leads to a noticeable increase in the observed reaction rate; the difference is especially noticeable at intermediate degrees of conversion.

The obtained data indicate that the observed heavy stock cracking reaction rate depends but little on the internal and significantly on external transport. However, occurrence of reaction in the purely external diffusion region is unlikely, since the internal surface of the catalyst exerts some effect, and the activation energy of the external diffusion reactions ordinarily does not exceed 2 to 5 kcal./mole, which is significantly lower than the activation energy of the catalytic cracking of heavy stock (10 to 15 kcal./mole).

Experiments were conducted by us on the thermal cracking of the investigated stock at 465°C, showing that purely thermal cracking under these conditions affects not more than 3% of the feed stock and should not distort the catalytic cracking results, i.e., that the observed activation energy is not exaggerated.

Consequently, the heavy stock catalytic cracking reaction at temperatures above 460°C occurs in the transition region between the external and internal diffusion regions close to the external diffusion region.

This justifies the use of low index catalysts with little developed surface for cracking heavy stocks, since the rate of breakup of the heavy molecules is determined not by the activity of the catalyst and its structure, but by the rate of arrival of these molecules to the catalyst surface. This leads to the fact that the major portion of the coke is laid down close to the external surface of the catalyst and uniform coking during cracking is not observed. The latter explains the accumulation of coke at the external catalyst surface observed by D. P. Dobychin (9).

It should be pointed out that the quality of the cracked products is determined by the secondary reaction, which probably occurs in the kinetic region, and therefore the liquid products obtained on catalysts of different activity will differ in quality at the same overall degrees of conversion.

Consideration of the relations shown makes it possible to visualize ways for intensifying heavy stock cracking processes. An increase in the cracking rate will be promoted by all factors increasing the supply of material to the external surface of the catalyst, the more effective of which appear to be the use of high stock feed rates and small-sized catalyst.

SUMMARY

1. The kinetics of the catalytic cracking of heavy gas oil from Ramashkino crude oil was studied. A kinetic scheme for the process was shown.

2. It was shown that the heavy stock cracking reaction occurs in the transition region between internal and external diffusion, which permits the use for cracking of low index catalysts with poorly developed surface.

3. The developed relations make it possible to devise means for the intensification of heavy stock cracking processes.

LITERATURE CITED

1. Smirnov, N. P., and Galinich, E. G., *Novosti Neftyanoi Tekhniki*, No. 2, 3 (1957).
2. Agafonov, A. V., and Krasivichev, V. V., *Khim. i Tekhnol. Topliv i Masel*, No. 10 (1956).
3. Amerik, B. K., *Trudy vtoroi nauchnotekhnicheskoi konferentsii po voprosam bureniya, dobychi i pererabotki* (Transactions of the Second Scientific and Engineering Conference on Drilling, Production and Refining Problems), Groznyi, 1957.
4. Agafonov, A. V., *Khim. i Tekhnol. Topliv i Masel*, No. 9 (1959).
5. Dart, *Khim. i Khim. Tekhnol.*, No. 2 (1955).
6. Panchenkov, G. M., and Baranov, V. Ya., *Izvest. Vysshikh Ucheb. Zaved. Ministerstva Vysshego Obrazovaniya SSSR, Ser. Neft i Gaz*, No. 6 (1958).
7. Panchenkov, G. M., and Zhorov, Yu. M., *Doklady Akad. Nauk SSSR*, 130, No. 6 (1960).
8. Panchenkov, G. M., and Tret'yakova, V. S., *Ibid.*, 87, No. 2 (1952).
9. Dobychin, D. P., and Klibanova, Ts. M., *Zhur. Fiz. Khim.*, 33, 869 (1959).

G. M. Panchenkov
Yu. M. Zhorov

USSR

A Method for the Determination of the Rates and Kinetic Constants of Complex Chemical Reactions in a Flowing System

Based on the magnitude of the activation energy of a heterogeneously catalyzed process and its temperature dependence, an idea can be obtained concerning the region in which the process is taking place.

As shown by us previously (1), the experimentally determined relationship for the conversion of a starting material as a function of the feed rate can be readily used to find the rate of chemical reaction without the knowledge of the kinetic equation of the process. The dependence of the reaction rate on temperature at a given constant conversion of the starting material makes possible the determination of the activation energy of the process. On the basis of the magnitude of the activation energy of a heterogeneously catalyzed process and its temperature dependence, an idea can be obtained concerning the region in which the process is taking place.

The proposed method, discussed in the case of simple reactions (1), is easily seen to be correct only when the reaction rate is a function of the conversion of the starting material the amount of which, in relative units, is equal to x, i.e., $W = f(x)$, and independent of the number of moles of this substance, n_0, passed into the reactor in unit time.

This article first published in *Doklady Akad. Nauk* 135, No. 5, 1172-1175 (1960). The authors are associated with the I. M. Gubkin Institute of the Petrochemical and Gas Industry, Moscow. The paper was presented by Academician A. V. Topchiev on June 21, 1960.

Since the reaction rate is a function of the partial pressures of the reacting substances P_{Ai}, the dependence of W on n_0 will be determined by the dependence of P_{Ai} upon n_0. The latter, as has already been shown (2), may be expressed in terms of the conversion of one of the reacting substances by the relationship

$$P_{A_i} = \frac{\frac{n_{0A_i}}{n_{0A_1}} - \frac{\nu_i}{\nu_1} x_{A_1}}{\frac{\sum n_{0A_i}}{n_{0A_1}} - \frac{\sum \nu_i}{\nu_1} x_{A_i}} P_0, \qquad (1)$$

where ν_i are stoichiometric coefficients, and P_0 is the total pressure in the reactor.

It is seen from the expression (1) that the quantity P_{Ai} is independent of n_0 in two cases: 1) when only one substance reacts; and 2) when several substances react, but the composition of the reaction mixture remains the same in all the experiments, only the rate at which the reaction mixture of a given composition is fed into the reactor being varied.

In a more general case, when several substances react and the composition of the reaction mixture is different in each case, the reaction rate will be a function not only of the amount of substance reacted

x, but also of the feed rate of the starting substance, n_0. Consequently, applying to the expression for heterogeneously catalyzed reactions obtained previously (1),

$$-\frac{S_0 l}{n_0^2} = \frac{d}{dn_0}\int_0^x \frac{dx}{W} \tag{2}$$

the theorem of the differentiation of a definite integral with respect to a parameter, there is obtained

$$-\frac{S_0 l}{n_0^2} = \int_0^x \frac{\partial}{\partial n_0}\left(\frac{1}{W}\right)dx + \frac{1}{W}\frac{dx}{dn_0} \tag{3}$$

where S_0 is the surface area of the catalyst per unit length of its depth (bed) in the reactor, and l is the length of the reaction zone.

When the quantity W is independent of n_0, expression (3) converts into the previously derived (1) relationship

$$W = -\frac{n_0^2}{S_0 l}\frac{dx}{dn_0} = \frac{1}{S_0 l}\frac{dx}{d(1/n_0)} \tag{4}$$

We have used this expression to determine the kinetic quantities (constants) in the case of simple reactions. The method developed herein can be used successfully also for the kinetic description of complex reactions.

A number of industrially important reactions (cracking of individual hydrocarbons and petroleum fractions, dehydrogenation of hydrocarbons, dehydration of alcohols, and others) take place via stable intermediates. For example, catalytic cracking takes place according to the scheme

$$\begin{array}{l} A \xrightarrow{W_1} \nu_1 B + \nu_2 D + \nu_3 C \\ \quad\quad \big| \xrightarrow{W_2} \nu_4 D + \nu_5 C \end{array}$$

where A is the starting substance, B is the intermediate, and C and D are the final products. The reactions rates W_1 and W_2 are measured on the basis of the conversions of substances A and B.

The analysis of the kinetics of the first stage of a consecutive reaction presents no difficulties. To obtain the relationships for the kinetic analysis of the second stage of the reaction, let y represent the relative conversion of substance B, u its relative yield, and z the relative yield of the reaction product C (in each case as a fraction of the amount of the substance A passed in unit time). The rate of the second stage of the reaction then may be expressed in the form

$$W_2 = \frac{n_0 dy}{S_0 dl} \tag{5}$$

Remembering that

$$W_2 = k_2 \sigma_B \tag{6}$$

where σ_B is the fraction of the surface covered by substance B, and that σ_B is independent of n_0, i.e.,

$$\sigma_B = \varphi_1(x, y) = \varphi_2(x, u) \tag{7}$$

making use of the device applied above (integration of (5) and differentiation of the resulting expression with respect to n_0), there is obtained:

$$W_2 = -\frac{n_0^2}{S_0 l}\frac{dy}{dn_0} \tag{8}$$

However, experiment does not give the quantity y but the quantity u, the relative yield of the intermediate B. For the case under consideration, $u = \nu_1 x - y$. To pass from the variable y to the variable u, we look for the difference $\nu_1 W_1 - W_2$. On the basis of the formulas (4) and (8),

$$\nu_1 W_1 - W_2 = -\frac{n_0^2}{S_0 l}\frac{\nu_1 dx - dy}{dn_0} = -\frac{n_0^2}{S_0 l}\frac{du}{dn_0} \tag{9}$$

hence

$$W_2 = -\frac{n_0^2}{S_0 l}\left(\frac{\nu_1 dx}{dn_0} - \frac{du}{dn_0}\right) = \frac{1}{S_0 l}\left[\frac{\nu_1 dx}{d(1/n_0)} - \frac{du}{d(1/n_0)}\right] \tag{10}$$

The value of du/dn_0 can be found from the experimental dependence of the yield of intermediate B on the feed rate of the starting material A. In the special case when the yield of the intermediate passes through a maximum, $du/dn_0 = 0$, and consequently

$$W_2 = \nu_1 W_1 \tag{11}$$

Knowing the reaction rate at different temperatures and concentrations of the product, it is not difficult to find other kinetic quantities as well. For example, the activation energy of the second stage may be found from the change in reaction rate with temperature at a constant σ_B. However, since σ_B is determined by the variables x and y, or, which is the same, x and u, it is necessary to choose for the calculation a conversion x at which the same values of u are obtained for all the temperatures (see Fig. 1). When such a conversion has been found, activation energy is readily calculated after the reaction rates have been determined for the

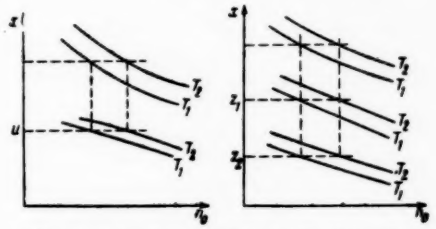

Fig. 1. Selection of points for the determination of the activation energy of the second stage of a consecutive reaction (left) and a complex parallel reaction (right).

points found. The error of such a determination will be somewhat higher than in the analysis of the first stage of the reaction because of cumulation of the errors in the determination of the quantities x and u.

When one of the reaction products is formed only in the second stage (for example, product C, $\nu_3 = 0$), the rate of the second stage may be expressed in terms of the relative yield of this product. Since in this case $y = \frac{\nu_1}{\nu_3} z$, applying this relationship to (8), there is found

$$W_2 = -\frac{(\nu_1/\nu_3)\, n_0^a}{S_0 l} \frac{dz}{dn_0} = \frac{\nu_1/\nu_3}{S_0 l} \frac{dz}{d(1/n_0)} \qquad (12)$$

By way of example, let us also examine a parallel reaction of the type

The rate of each stage of such a reaction with respect to any one substance (e.g., A_1) can be expressed in terms of the relative yield of the product of the stage under discussion (e.g., B_1^i). Representing the relative yield of this product by z_i, we may write

$$W_i = -\frac{(\nu'/\nu_1^i)\, n_{0A_1} dz_i}{S_0 dl} \qquad (13)$$

When the composition of the reaction mixture in the entire series of experiments with different feed rates remains constant, then, using the method described above, there is obtained

$$W_i = -\frac{(\nu'/\nu_1^i)\, n_{0A_1}^2}{S_0 l} \frac{dz_i}{dn_{0A_1}} = \frac{\nu'/\nu_1^i}{S_0 l} \frac{dz_i}{d(1/n_{0A_1})} \qquad (14)$$

Consequently, studying the changes in the relative yield of the products of such a reaction which result from changes in the feed rate of the starting mixture, it is possible to determine the kinetic characteristics of any stage of a reaction. Assuming that $W_i = k\Pi\sigma A_i$, the activation energy of any stage of a complex parallel reaction can be determined only at conversions of the substance A_1 to which correspond constant yields of each of the reaction products (Fig. 1).

The methods of determining the reaction rate from the yields of the final product may be used not only with complex but also with simple reactions. In the latter case they may be used also to test the correctness of an experiment, for example, by comparison of the activation energy calculated from the curves for the total conversions and from curves for the relative yields of the product, or by verification, for a given temperature, of the constancy of the ratio of the reaction rates calculated for constant feed rate of the reactant from the curve shown.

All the relationships that have been derived remain valid also for homogeneous reactions. In this case the quantity ρ, the cross section of the reactor, replaces the quantity S_0 in all the expressions obtained.

LITERATURE CITED

1. Panchenkov, G. M., and Zhorov, Yu. M., *Doklady Akad. Nauk SSSR*, 130, No. 6 (1960).

2. Panchenkov, G. M., and Zhorov, Yu. M., *Sbornik Zhur. Fiz. Khim., Kinetika i Kataliz*, p. 3, Izd. AN SSSR (Publ. Acad. Sci. USSR), (1960).

G. M. Panchenkov
V. A. Skoblo
Yu. M. Zhorov

USSR

Determination of Effective Diffusion Coefficients in Porous Sorbents

A mathematical treatment of external-diffusional, internal-diffusional, and mixed sorption rates.

THE process of the sorption of vapors and gases by porous adsorbents consists of three consecutive stages: 1) the approach of the substance being sorbed to the external surface - external diffusion; 2) the transport of the sorbed substance within the pores of the adsorbent - internal diffusion; and 3) the sorption step itself.

The rate of the slowest of the stages must be controlling with respect to the rate of the process of sorption as a whole. It is well known that the sorption step itself takes place virtually instantaneously; consequently, this stage of the process is almost never controlling for the rate of the adsorption process as a whole.

Because of this, we encounter in practice sorption rates which are external-diffusional, internal-diffusional, or mixed.

For many porous sorbents, it is well known that the rate of penetration of the molecules of the sorbate within the pores is the limiting (or controlling) stage of the sorption process. However, sorption kinetics in the internal-diffusional region have been studied but slightly up to the present time. The presently available solution to this problem is obtained on the basis of Fick's second law, but extremely complicated equations are obtained for even the simplest cases (1-3); this makes it difficult to analyze the experimental data.

Let us consider a sorption process taking place on a spherical grain of sorbent having radius R_b. It will be assumed that the concentration of the sorbate at the external surface of the grain remains constant and equal to C_0 during the entire sorption process. This assumption corresponds to the physical conditions usually present in sorption processes where sorption of the substance by the sorbent changes but slightly its concentration in the bulk (of the system) and where the concentration at the external surface of the sorbent grain does not vary up to the time of its complete saturation because of convection, mixing, or a sufficiently high rate of external diffusion in the gaseous phase.

Let us use a so-called quasi-homogeneous grain model for describing the sorption process; this was developed in detail by Pshezhetskii (4), and describes the transport process taking place within the porous sorbent grain by means of the Fick equation. However, the diffusion coefficient loses its usual meaning here and becomes an "effective" quantity D_{ef}, which depends but slightly on the concentration of the sorbate.

Moreover, we will assume that the decrease in sorbate concentration along a grain radius is linear at any instant. This assumption is somewhat arbitrary, but it enables one to obtain solutions in closed form for the rate equations, which can be solved readily. This assumption is widely used in the diffusional kinetics of chemical reactions (5, 6) and sorption processes (3); furthermore, the results of such approximate and rigorous approaches - both qualitatively as well as quantitatively - are very similar. Timofeev (3) showed, from a study of the diffusional rates of sorption, that the major decrease in sorbate concentration within the sorbent occurred linearly, and that deviations from linearity began to occur only at relative concentrations of less than 0.2.

In view of the fact that sorption is a more rapid process than diffusion, an equilibrium, which depends on the shape of the sorption isotherm, is established at each point within the grain between the sorbate in the gaseous phase and at the surface.

Let us assume that time τ has elapsed from the start of sorption, and that the sorption front has reached the layer r during this time (Fig. 1). In accordance with the foregoing statements, the sorbate concentration falls from C_0 at the external surface to zero in the sphere of radius r. Then, for any layer s located between R_b and r, the concentration C_s and the pressure p_s of the sorbate are determined by the equations:

This article first published in *Izvest. Vysshikh Ucheb. Zaved., Neft i Gaz* 4, No. 1, 73-77 (1961). The authors are associated with the I. M. Gubkin Institute for Petrochemical and Gas Industry.

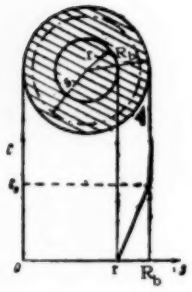

Fig. 1. Schematic illustration of the filling of a porous sorbent grain by sorbate vapors.

$$C_s = \frac{s-r}{R_b-r} C_0 \tag{1}$$

$$p_s = \frac{s-r}{R_b-r} p_0 \tag{2}$$

During the time interval $d\tau$, elapsed after the state described, a quantity of the substance da_τ enters into the grain; this is determined from Fick's first law as follows:

$$da_\tau = 4\pi R_b^2 D_{ef} \left(\frac{\partial C}{\partial s}\right)_{s=R_b} \cdot d\tau, \tag{3}$$

and, since according to (1):

$$\left(\frac{\partial C}{\partial s}\right)_{s=R_b} = \frac{C_0}{R_b-r} \tag{4}$$

then

$$da_\tau = 4\pi R_b^2 D_{ef} \frac{C_0}{R_b-r} \partial\tau \tag{5}$$

and

$$a_\tau = 4\pi R_b^2 D_{ef} C_0 \int_0^\tau \frac{d\tau}{R_b-r} \tag{6}$$

Since $r = \psi(\tau)$, where the shape of the function $\psi(\tau)$ is not known to us, it is not possible to find the magnitude of the integral in Eq. (6) from the available data.

The sorbate within the grain in the layer $R_b - r$ is present to the extent of a_{ads} on the surface of the sorbent and to the extent of a_{vol} in the free volume, consequently:

$$a_\tau = a_{ads} + a_{vol} \tag{7}$$

The quantity of substance sorbed in a layer located within the limits of radii s and s + ds is equal to:

$$da_{ads} = 4\pi s^2 \sigma_s \frac{a_\infty}{\sigma_0} ds, \tag{8}$$

where a_∞ is the quantity of substance per unit volume of sorbent at complete saturation corresponding to the pressure p_0 of the sorbate in the gaseous phase; σ_s is the fraction of the surface that is occupied - this is determined from the sorption isotherm at the sorbate pressure p_s; σ_0 is the fraction of the surface that is occupied at a sorbate pressure of p_0.

From Eq. (8) we find the total quantity of sorbed substance to be:

$$a_{ads} = 4\pi \frac{a_\infty}{\sigma_0} \int_r^{R_b} \sigma_s s^2 ds \tag{9}$$

The amount of substance present in the free volume within a layer lying in the range of radii s and s + ds is:

$$da_{vol} = \alpha \frac{p_s}{RT} 4\pi s^2 ds \tag{10}$$

where α is the fraction of free volume within the grain; and R is the universal gas constant.

From Eq. (10) we find the total quantity of sorbate present in the gaseous phase within the grain; this is:

$$a_{vol} = \frac{4\pi\alpha}{RT} \int_r^{R_b} p_s s^2 ds \tag{11}$$

Substituting Eqs. (6), (9), and (11) into (7) and dividing through by 4π, we obtain:

$$R_b^2 D_{ef} C_0 \int_0^\tau \frac{d\tau}{R_b-r} = \int_r^{R_b} \left(\frac{a_\infty}{\sigma_0}\sigma_s + \frac{\alpha}{RT} p_s\right) s^2 ds \tag{12}$$

In order to go from Eq. (12), which cannot be used directly, to the final equations, we differentiate it with respect to τ, using $d/d\tau = (d/dr)\cdot(dr/d\tau)$ for the right-hand member. Thus:

$$R_b^2 \cdot D_{ef} \cdot C_0 \frac{d\left[\int_0^\tau \frac{d\tau}{R_b-r}\right]}{d\tau} = \frac{d\left[\int_r^{R_b} \left(\frac{a_\infty}{\sigma_0}\sigma_s + \frac{\alpha}{RT} p_s\right) s^2 ds\right]}{dr} \cdot \frac{dr}{d\tau} \tag{13}$$

In the left member we have the usual derivative of a definite integral with respect to its lower limit: this is equal to the function under the integral sign. In the right member, the variable with respect to which the differentiation is being performed, is present in the function under the integral sign and the differentiation must be performed by means of the formula for differentiation using a parameter. Considering also the fact that the function under the integral sign reverts to zero at s = r, we find:

$$R_b^2 D_{ef} \frac{C_0}{R_b - r} = \left[\int_r^{R_b} \frac{\partial \left(\frac{a_\infty}{a_0} a_s + \frac{\alpha}{RT} p_s \right) s^3}{\partial r} \, ds \right] \frac{dr}{d\tau} \quad (14)$$

Solving Eq. (14), we obtain finally:

$$R_b^2 D_{ef} C_0 \tau = \int_r^{R_b} \left(R_b - r \right) \int_r^{R_b} \frac{\partial \left(\frac{a_\infty}{a_0} a_s + \frac{\alpha}{RT} p_s \right) s^2}{\partial r} \, ds \cdot dr \quad (15)$$

Eq. (15) relates the sorption time to the depth to which the sorption wave front penetrates for any isotherm shape.

It should be noted that for sorbents which sorb a large quantity of sorbate, the amount of the substance sorbed on the surface is significantly greater than the quantity of substance present in the free space (voidage) within the grain. Consequently, for sorbents of this type, Eq. (15) can be simplified to:

$$R_b^2 D_{ef} C_0 \tau = \int_r^{R_b} \left(R_b - r \right) \int_r^{R_b} \frac{\partial \left(\frac{a_\infty}{a_0} a_s \right)}{\partial r} s^3 \, ds \, dr \quad (16)$$

The relationship found may be used for determining the effective diffusional coefficient D_{ef}, whose magnitude is determined in the following manner.

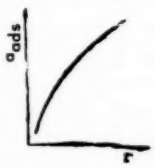

Fig. 2. Relationship between a_{ads} and τ determined from Eq. (9).

1. Construct a plot of $a_{ads} = f(\tau)$ from the experimental data (Fig. 2).

2. Knowing the shape of the sorption isotherm $a = f(p)$ and the dependence of p on s given by Eq. (2), we remove the integrals in Eqs. (9) and (16), and plot the curve $a_{ads} = \varphi(r)$ using Eq. (9) (Fig. 3).

3. Assigning a series of values for a_{ads}, we find from the curves (see Figs. 2 and 3), r and τ corresponding to a single value of a_{ads}. The relationship between these values of r and τ is described by Eq. (16). We can find the magnitude of D_{ef} by substituting the values found into Eq. (16).

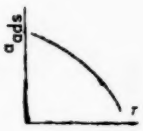

Fig. 3. Experimental dependence of a_{ads} on r.

It should be noted that in determining the value of D_{ef} we can use rate (kinetic) data for the initial stage of saturation, since Eqs. (15) and (16) do not describe the entire sorption process but refer only to that stage in which the sorption wave front is moving toward the center of the grain. The subsequent saturation of the granule to the equilibrium state is not described by the equations derived, although rate relationships for this second stage may be obtained by using the same considerations. Moreover, this second stage is automatically excluded from consideration in determining the value of D_{ef}, since according to the above paragraphs 2 and 3 the sorption values up to the start of the second stage are utilized.

LITERATURE CITED

1. Wicke, E., *Kolloid. Zhur.*, 86, 295 (1939).

2. Berrer, P., *Diffuziya v tverdykh telakh* (Diffusion in Solid Bodies), (a Russian translation), Foreign Literature Publishing House, 1948.

3. Timofeev, D. P., *Zhur. Fiz. Khim.* 29, No. 4, 723-729 (1955) and 32, No. 9, 2005 (1958).

4. Pshezhetskii, Dissertation, *Macrokinetika i dinamika lkataliticheskiky protssessov* (Macrokinetics and Dynamics of Catalytic Processes), the Karpov Institute of Physical Chemistry, Moscow, 1951.

5. Weeller, A., *Advances in Catalysis* 3, 249 (1951).

6. Panchenkov, G. M., and Zhorov, Yu. M., *Trudy Moskovskogo instituta neftekhimicheskoi i gazovoi promyshlennosti im. akad. I. M. Gubkina* (Transactions of the I. M. Gubkin Moscow Institute for Petrochemistry and the Natural Gas Industry), No. 28, 3-9 (1960).

L. Yu. Artyukh
L. A. Vulis
V. P. Kashkarov

KAZAKHSTAN, USSR

Combustion of Gas Flowing at the Surface of a Plate

Analysis of surface conditions and corresponding velocity, temperature, and concentrations in the boundary layer. New critical conditions for ignition and extinction associated with bodies moving at high velocities in the atmosphere.

A theoretical analysis of problems combining both the theory of the boundary layer of a compressible gas and the physics of combustion presents considerable interest at present. Many works, in particular references (1, 2) and others, have been devoted to the study of heterogenous combustion of gas flowing at the surface of a body when the rate of reaction is infinitely high (diffusion combustion). References (3-5) consider certain aspects of the same problem when the finite rate of combustion is taken into account.

By using the example of a homogenous stream of compressible gas flowing about a burning plate, the present article gives a complete exposition of the results of such studies and, at the same time, generalizes, and adds considerably to the previously published data. In the approximation obtained, the change of the velocity, temperature, and concentration profiles along the length of the plate have been taken into account (using "quasi-auto-analogue" quasistationary solutions). The study was limited to laminar flow in the boundary layer along the plate.

Although combustion is essentially a non-steady state process, the relatively low linear velocity of burning of the solid phase permits one to regard the processes in the boundary layer of the gas as quasistationary, i.e., the displacement of the reaction surface can be neglected.

The system of differential equations describing the given phenomenon consists of the continuity equation,

$$\frac{\partial}{\partial x}(\rho u) + \frac{\partial}{\partial y}(\rho v) = 0, \qquad (1)$$

the equation of motion (steady state plane flow),

$$\rho u\frac{\partial u}{\partial x} + \rho v\frac{\partial u}{\partial y} = \frac{\partial}{\partial y}\left(\mu\frac{\partial u}{\partial y}\right), \qquad (2)$$

the energy equation, written in the form of the total enthalpy balance (summation of the physical and chemical enthalpies and of the kinetic energy),

$$\rho u\frac{\partial H}{\partial x} + \rho v\frac{\partial H}{\partial y} = \frac{\partial}{\partial y}\left(\lambda\frac{\partial T}{\partial y} + \mu u\frac{\partial u}{\partial y} + \rho D\frac{\partial h}{\partial y}\right), \qquad (3)$$

the diffusion equation for the reacting gas,

$$\rho u\frac{\partial h}{\partial x} + \rho v\frac{\partial h}{\partial y} = \frac{\partial}{\partial y}\left(\rho D\frac{\partial h}{\partial y}\right), \qquad (4)$$

the equation of state for an ideal gas,

$$P = \rho RT, \qquad (5)$$

as well as equations giving viscosity, thermal conductivity, and diffusion coefficients as a function of temperature,

$$\frac{\mu}{\mu_\infty} = \frac{T}{T_\infty}, \quad \frac{\nu}{\nu_\infty} = \frac{a}{a_\infty} = \frac{D}{D_\infty} = \frac{T^2}{T_\infty^2} \quad c_p = \text{const}. \qquad (6)$$

where, u and v are vector components of the velocity along the x and y axes of the plate, respectively; P, ρ, and T are the pressure, density and temperature, respectively; R is the gas constant; μ, λ, and D are the viscosity, thermal conductivity, and diffusion coefficients, respectively; $\nu = \mu/\rho$ and $a = \lambda/\rho c_p$ are the kinetic viscosity and thermal diffusivity, respectively; c_p is the specific heat at constant pressure; $h = qc$ is the chemical enthalpy (q and c are the thermal effects of the reaction and the concentration, respectively, and it is assumed that $q \approx \text{const}$); and $H = c_pT + h + v^2/2$ is the total enthalpy.

The boundary conditions are:

a) at the surface of a plate ($y = 0$):

This article first published in *Inzhener.-Fiz. Zhur.*, 4, No. 3 (1961). The authors are associated with the Kazakh State University, Alma-Ata.

$$u = v = 0,$$

$$-\lambda_w \left.\frac{\partial T}{\partial y}\right|_w = \rho_w k_0 \exp\left(-\frac{1}{\Theta_w}\right) h_w + Q_w = \rho_w D_w \left.\frac{\partial h}{\partial y}\right|_w + Q_w; \quad (7.a)$$

b) at a great distance from the plate ($y \to \infty$):

$$u = u_\infty, \quad T = T_\infty, \quad h = h_\infty \quad (7.b)$$

The subscripts w and ∞ refer to the quantities at the wall and at a large distance from it. The symbol $\theta = RT/E$ in the Arrhenius equation (E is the activation energy and k_0 is a constant) represents a dimensionless temperature. The quantity Q_w denotes the heat flux (by radiation, conduction through the wall, etc.). For simplicity we shall assume that $Q_w = \alpha(T_w - T_{0\infty})$, where α is the heat transfer coefficient, and $T_{0\infty} = T_{0\infty} + u_\infty/2c_p$ is the value of the inhibiting temperature outside the boundary layer.

It should be noted that in writing the equation for the boundary conditions, we have neglected thermal diffusion, thermal conductivity by diffusion, and the molar flow* of mass resulting from the change of the number of molecules in the reaction (it is assumed that the reaction takes place with an excess of inert gas, such as nitrogen, in the case of combustion in air).

With boundary condition (7.a), which includes the finite rate of reaction (of the first-order), the given problem does not have an auto-analogue solution. Without resorting to the artificial method of reducing the problem to an auto-analogue problem (4), we shall retain the same forms of solution in terms of the Dorodnitsyn variables as in the auto-analogue problem, assuming the constants resulting from integration of equations (3) and (4) to be functions of the coordinate x.

Without entering into the details of the solution, which are considered in reference (4), it should be noted that the solution of the dynamic problem in terms of Dorodnitsyn variables remains in the same form as in the ordinary Blasius problem. By contrast, the integrals of the energy equation and the diffusion equation will have a local significance, i.e., they will have different values for different magnitudes of the independent variable x in the plane of Dorodnitsyn variables. In the physical flow plane (x, y), the profiles of all variables (velocity, temperature, and concentration) will change along the plate.

In this method of obtaining an approximate solution to the problem, which we have arbitrarily denoted as a "quasi-auto-analogue" solution, it is assumed that the spatial fields of the velocity, temperature, and concentration consist, in a sense, of an infinite number of auto-analogue profiles u, T and c, which are close to one another. Without being exact, this solution makes it possible to obtain a qualitatively correct picture of the phenomenon and one which is close to the true picture in quantitative terms. An exact solution of the problem can be obtained by numerical integration of equations (1) to (7).

To find the "quasi-auto-analogue" profiles of u, P and c (in Dorodnitsyn variables), solutions of the transcendental equations from the theory of the thermal regimes of combustion are used, where the boundary conditions at the reaction surface can be applied.

For this purpose, let us transform equations (7a) to the form used in problems dealing with the thermal regimes of combustion (6). We introduced the following dimensionless variables: the temperature, $\theta = RT/E$ and the completeness of combustion $\Phi = 1 - h/h_\infty$, and the following dimensionless parameters: calorific value $\vartheta = (qRc_\infty\sigma_D/Ec_p)(K/I)$, the characteristic (relative) time of diffusion $\tau = (k_0\Theta_\infty/D_\infty)\, K\sqrt{(x\nu_\infty/u_\infty)}$, and the heat transfer coefficient $\beta = (\alpha D_\infty/\lambda_\infty k_0\Theta_\infty)(1/1K)$ (here $I = F''^{\sigma}_w/\int_0^\infty F''^{\sigma}d\varphi$, $K = F''^{\sigma}_w D/\int_0^\infty F''^{\sigma} D d\varphi$). The values of Θ_w and $\tilde{h}_w = h_w/h_\infty = 1 - \Phi$, which play the role of constants of integration in the corresponding equations of the boundary layer, are found from the following equation*

$$\Phi = \frac{\tau}{\tau + \exp\frac{1}{\Theta_w}} = \frac{1}{\vartheta}\left[\Theta_w - \chi\Theta_\infty + \beta\tau(\Theta_w - \Theta_{0\infty})\right], \quad (8)$$

where

$$\chi = 1 + \sigma(\gamma - 1)M_\infty^2 \int_0^\infty F''^{\sigma}\left(\int_0^\varphi F''^{2-\sigma}d\varphi\right)d\varphi;$$

$$\Theta_{0\infty} = \left(1 + \frac{\gamma - 1}{2}M_\infty^2\right)\Theta_\infty;$$

M_∞ is the Mach number of the incident stream; and $\gamma = c_p/c_v$.

The transcendental equation (8) was solved graphically in the plane $\Phi - \Theta_w$. Typical results of the solution are given in Figs. 1 and 2.

As in other cases of studying the thermal conditions of combustion, equation (8) shows the possibility that two types of processes can exist - a hysteresis process (instability - translator's note) with the critical conditions for ignition and extinc-

*Translator's note: In Russian usage, the term "molar flow" usually refers to macroscopic flow, as opposed to molecular flow.

*In the denominator of the first fraction in equation (8), the factor θ_w in front of the exponent is neglected for simplification. This produces no appreciable distortions (6).

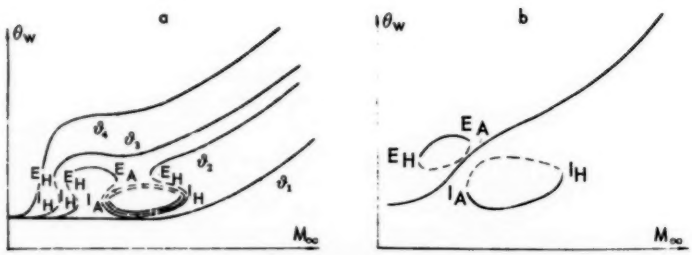

Fig. 1. Dependence of the surface temperature on the velocity of the incident flow for given parameters of heat transfer, β, and distance x, and at different values of the calorific value $\vartheta_4 > \vartheta_3 > \vartheta_2 > \vartheta_1 = 0$. I - point of ignition, E - point of extinction (the subscripts A and H denote adiabatic and heat-exchange values respectively).
a - instability regime; b - stable regime (with isolated segments of θ_w).

tion, and a normal (stable) process with a continuous change of surface temperature when one of the parameters is varied. In the given problem, the changes in the gas temperature at a large distance from the surface $\Theta_{0\infty}$, and in the calorific value ϑ, as well as in the heat transfer coefficient β, will not add anything new to the previously known results (6), and we shall therefore confine ourselves to a detailed analysis of the effect of the parameter τ (and of the flow velocity M_∞ and the coordinate x entering into it).

From the physical point of view, the given problem is distinguished by the fact that it takes into account the heat of friction generated in the boundary layer. This effect increases as the M_∞ number increases. It is therefore natural to assume that, and this is confirmed by computation, in the region of large values of M_∞ (of the order of several units), and in spite of the existence of additional convective heat transfer (Q_W), the heat generated through friction exceeds the amount of heat removed. In this case, the process will again reach a high temperature level.

For better understanding of this phenomenon, let us recall the usual dependence of the steady state temperature on the flow velocity for heterogenous combustion. The region of stable combustion (at large values of Φ and Θ_W) is limited on two sides - at low values of the velocity (i.e., large values of τ) because of the influence of heat transfer, and at large values of the velocity (low values of τ) because of the finite rate of the chemical reaction. Thus, a smooth or a step-like (ignition and extinction) rise and fall of the temperature curve takes place in the region of small and large values of the velocity, respectively. According to Ya. B. Zel'dovich (7), whose results are generalized for the case of heterogenous combustion in (6), the accepted terms for the critical phenomena are "heat-exchange" phenomena at small velocities and "adiabatic" phenomena at large velocities.

In the given problem, as we have already noted, as the velocity increases a repeated rise of the temperature curve should be observed. This will take place smoothly or in steps - with a new, third set of critical conditions for ignition and extinction appearing in the same sequence as in the "heat-exchange" conditions. Here, an increase of M_∞ will lead to ignition, and a decrease to extinction. On the contrary, for "adiabatic" critical conditions, an increase in the velocity will lead to extinction, and a decrease to ignition.

As in the region of low values of the velocity ($M_\infty < 1$), where heat transfer plays an important role, at large values of the velocity and with the effect of heat generation, the temperature curve can have various forms. In addition to a smooth rise in the temperature of the surface or a step-like change (ignition and extinction), equation (8) permits the existence of closed portions of the curve, confined on both sides by ignition. On these curves, only the lower branches (the "depression" - the solid lines in Figure 1) have a real significance. The upper branches (dotted lines) correspond to unstable and, consequently, unattainable equilibrium states. We recall that in the region of low values

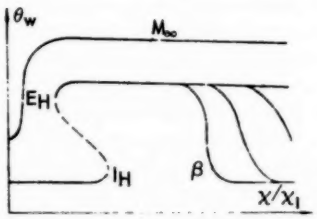

Fig. 2. The change in the temperature along the burning plate (for the scale of the x-coordinate, the length of the plate up to the point of ignition x_1 is taken) with a given calorific value ϑ for two values of the velocity of the incident flow.

of the velocity, closed temperature curves confined on both sides by extinction are encountered. On these curves, only the states of the upper branch are stable. For a portion of a curve confined by two uniform critical conditions (two ignitions or two extinctions), which play the role of single-ended "escapes" from these states, a transition of the system to this region is quite feasible physically, although this is not apparent from Figure 1. The point here is that this transition can be accomplished as a result of a change in even one of the parameters ($\Theta_{0\infty}$, ϑ, etc.) which is taken to be constant in constructing the diagram. These parameters represent in essence plane sections of a multidimensional surface $\Phi = \Phi(\Theta_W, \vartheta, \tau, \beta)$, and it is therefore not surprising that the "entrance" to the closed portion is not evident in the plane $\Phi - \Theta_W$.

The graphs given in Figure 1 are sketches of the graphical solutions of equations (8). They show clearly the above-noted peculiarities of the phenomenon, the effect of the change in the parameters, etc.

What we have said refers to the effect of the flow velocity. With regard to the other characteristic quantity entering into the parameter τ - the x-coordinate - an example of the dependence of Θ_W on x is shown in Figure 2.

It can be seen from this drawing that ignition (if it does take place) occurs at a certain distance from the front edge of the plate. If there is a large increase in the x-coordinate because of the growing role of heat exchange, as well as the growing role of consumption of the reacting gas near the plate and the resulting increase in diffusion resistance, there will be a decrease (smooth or step-like) in the temperature curve. Thus, in a developed and an unstable process, an increase of the x-coordinate leads to ignition in the region of small values of x and to extinction in the region of large values of x.

The values of the temperature Θ_W and the concentration c_W obtained by a graphical solution of equation (8) as a function of the x-coordinate with known values of all the other parameters make it possible to complete the problem and to construct the profiles of u, T and c in the cross-section of the flow. An example of this is shown for two cross-sections (before and after ignition) in Figure 3. From the physical point of view, the "distention" of the boundary layer after ignition is of interest here.

We note that, in terms of the nature of the process, the state before ignition is practically one of kinetic combustion (there is no decrease in the concentration in the boundary layer), while after ignition the state is one of diffusion combustion

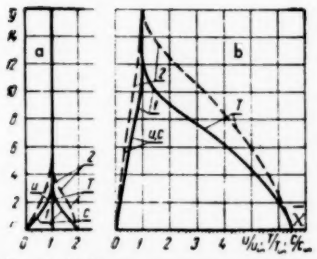

Fig. 3. Velocity, temperature, and concentration profiles in the boundary layer at a burning plate for $\sigma = \sigma_0 = 1$, $M_\infty = 2$, $\theta_\infty = 0.02$, $\vartheta = 0.1$.
a - before ignition ($1 - \bar{x} = 0.5$; $2 - \bar{x} = 0.99$); b - after ignition ($1 - \bar{x} = 1$; $2 - \bar{x} = 2$.

(concentration at the wall $c_W = 0$). This result is typical of the hysteresis process with an exothermic heterogenous reaction, when the combustion takes place only in the neighborhood of the diffusion region. From this point of view there is considerable interest in computing the critical conditions for ignition and extinction on the one hand, and in computing the steady-state diffusion combustion on the other. This last computation can of course be made, as in article (1), with a simple boundary condition $c_W = 0$ (an infinitely high rate of reaction). However, such a formulation of the problem would make it impossible to determine the condition for stability of the process, the region of stable combustion, the effect of different parameters on ignition and interruption of the combustion (extinction), etc.

The solution given above contains implicitly the effect of the ratio of the transfer coefficients, because the Prandtl numbers σ and σ_D appear in the expressions for the dimensionless variables. However, we shall not dwell upon this question, because the quantitative effect of these numbers is unknown.

In order to generalize this solution to the case of combustion of a plate with a turbulent boundary layer, the formulation of the problem and the same method of solution can be applied from the theoretical point of view. Omitting all details, let us note only that the parameter $\tau \sim \chi^{1/2}$ in the laminar boundary layer will depend to an extremely small extent on the x-coordinate in the turbulent layer ($\tau \sim \chi^{1/2}$). This makes the use of the "quasi-auto-analogue" solution more grounded in this case, which has a practical significance.

In conclusion, let us point to the practical significance of the problem we have considered: it can be regarded as one of the limiting schemes of ignition and combustion of a body moving with a large velocity in the atmosphere.

LITERATURE CITED

1. Baulin, E. P., *Doklady AN SSSR*, 113, 1235 (1957).
2. Eckert, E. R. G., and Hartnett, J. P., *Z. angew. Math. Phys.*, IXb, 18, 259 (1958).
3. Vulis, L. A., and V. P. Kashkarov, Annotatsiya dokladov Vsesoyuznogo s'ezda po teoreticheskoi i prikladnoi mekhanike *(Proceedings of the All-Union Conference on Theoretical and Applied Mechanics)*, p. 56, Moscow (1960).
4. *Ibid.*, Doklady na 3-m Vsesoyoznom Soveshchanii po teorii goreniya *(Proceedings of the 3rd All-Union Conference on the Theory of Combustion)*, Power Engineering Institute, Academy of Sciences of the USSR, (1960).
5. *Ibid.*, Sb. "Issledovanie protsessov perenosa. Voprosy teorii otnositel'nosti" *(Investigation of Transfer Processes. Problems in the Theory of Relativity - Symposium)*, Ed. by Prof. L. A. Vulis, No. 2, A, (1960).
6. Vulis, L. A., Teplovoi rezhim goreniya *(Thermal Regime of Combustion)*, State Power Institute, Moscow-Leningrad, (1954).
7. Zel'dovich, Ya. B. and Yu. Z. Zysin, Zh. T. F., *(Journal of Technical Physics)* 11, No. 6, 501, (1941).

N. I. Gel'perin
V. B. Kvasha

USSR

Maintaining Optimum Temperature Conditions in Chemical Reactors*

Rectification and distillation heat-exchange procedures used to maintain the desired temperature distribution in reactors.

In calculating and designing chemical reactors for processes with high thermal effects, the major problem is to determine and maintain an optimum heat field in the working zone of the reactor.

Let us assume that each unit volume of catalyst performs at maximum efficiency. Let us further assume that the catalyst does not become deactivated and that there are no side reactions.

Analysis of kinetic relationships which govern homogeneous as well as heterogeneous catalytic processes shows that even when the above assumptions hold, uniform conversion of reactants (y) along the length of the working zone of reactor (l) can be achieved only when the temperature field changes in accordance with certain mathematical laws (Gel'perin and Kvasha), (1).

These authors have shown, among other things, that in the synthesis of hydrocarbons from CO and H_2, taking dy/dl = const., the temperature field can be described by equation (1) if the process is run without recirculating the reactants (Fig. 1, A).

$$T = \frac{E}{R} \cdot \frac{1}{\ln K_1 + \ln \frac{22.4(1-V)\cdot P}{W_{sv}\cdot N'_{H_2}} + \ln \frac{1 - y_k \cdot \frac{l}{L}}{\frac{1}{N'_{H_2}} - B_1 \cdot y_k \cdot \frac{l}{L}} - \ln y_k} \qquad (1)$$

*I. B. Rapoport, V. Ya. Krugilikov and V. G. Einstein participated in various phases of this study.

This article first published in *Khim. Prom.*, No. 1, 51-56 (1961).

Equation (2) holds when the reactants are recirculated:

$$T_c = \frac{E}{R} \cdot \frac{1}{\ln K_2 + \ln \frac{22.4(1-V)P}{W_{sv}\left(N'_{H_2} + r\cdot N''_{H_2}\right)} + \ln \frac{1 - y_c \cdot \frac{l}{L}}{\frac{1}{N'_{H_2\,mixt.}} - B_2 \cdot y_c \cdot \frac{l}{L}} - \ln y_c} \qquad (2)$$

where
- T – temperature, °K;
- E – apparent activation energy, cal./mole;
- R – gas constant (1.9869 cal./(degree) · (g.-mole);
- K_1, K_2 – constants;
- V – relative volume of catalyst;
- N''_{H_2} – molar hydrogen fraction of the initial gas;
- W_{sv} – space velocity of reactants, $nm.^3/(m.^3)$ (hour);
- P – total pressure in the system, atm.;
- y_k – total extent of conversion of the starting material, fraction of a unit;
- B_1, B_2 – stoichiometric coefficients;
- r – recirculation factor, equal to the volume ratio of recirculated to initial gas;
- N''_{H_2} – molar hydrogen fraction in the waste gas;
- $N'_{H_2\,mixt.}$ – molar hydrogen fraction in the initial gas mixture;

y_c — extent of conversion of the initial gas mixture during one cycle, fraction of a unit;

L — total length of the working zone of reactor.

If the temperature gradient along the length of the working zone of the reactor is given, then the temperature distribution in the heat carrier zone is also known, provided conversion (hence heat evolution) is uniform and, further, that a boiling liquid is used as the heat carrier.

In recent studies (1-4), new methods, known as rectification and distillation heat exchange procedures, were used to maintain a given temperature distribution.

RECTIFICATION HEAT EXCHANGE PROCEDURE

In this method a specially selected mixture of two or more components, brought to boiling, is introduced into the heat carrier zone, filled with packing. As the mixture evaporates, it undergoes rectification, with the result that the boiling point of the heat carrier rises along its downward course. Obviously the temperature gradient across the heat carrier zone depends on the liquids selected for the mixture, on the type of packing used, and on the working pressure in the system.

O. Dorschner (2) was the first to investigate the reactification heat exchange method, but his work suffers from serious methodological defects. Moreover, a number of important points have not been properly clarified, such as the selection of mixtures, effect of reaction parameters on temperature gradient along the length of the system, installation controls, etc.

Our experimental study was undertaken with a view to clearing up some of these questions.

The laboratory installation (Fig. 2) was described in an earlier report (4).

To check the stability of the system, in particular the effect of local heat evolution (simulating overheating of this zone), three heaters 8 were installed near the fractionating column: on the lower lid of the column, and at a distance of 867 mm. and 1,570 mm. from the lid. Each heater consisted of a coil made of red copper tubing, diameter 8 × 1 mm. (height of coil 37 mm., inner diameter 62 mm.). A Nichrome wire coil, diameter 0.3 mm., insulated with Raschig packing rings 4 × 4 × 0.7 mm., was inserted into the tubing. The thermal load of these heaters was regulated by an automatic transformer and was rated by an astatic wattmeter.

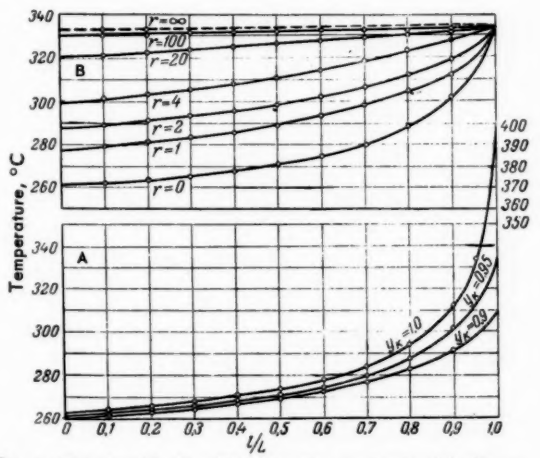

Fig. 1. Relationship T = f(l/L) for the synthesis of hydrocarbons from CO and H on iron catalysts. Conversion of reactants is uniform. (A - no recirculation; B - recirculation; total extent of conversion equals 0.95).

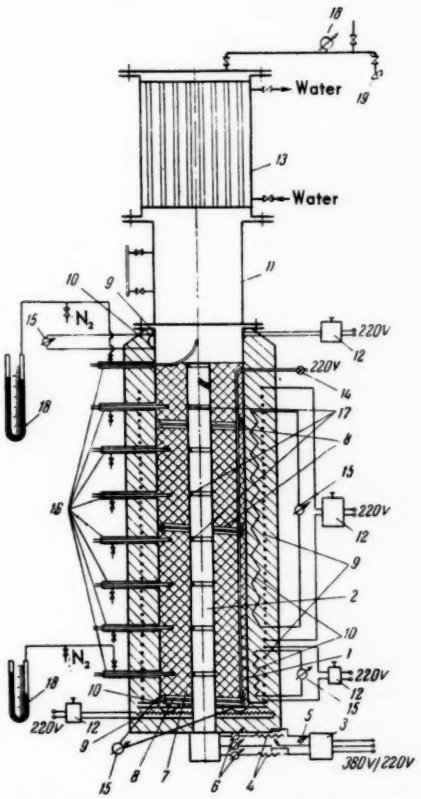

Fig. 2. 1 - reactor; 2 - central heating element; 3 - transformer; 4 - rheostats; 5 - voltmeter; 6 - ammeters; 7 - packing; 8 - heaters; 9 - oven for compensating electric heating; 10 - differential thermocouples; 11 - bridging coil; 12 - laboratory automatic transformers; 13 - condenser; 14 - two-way switch, wattmeter and autotransformer; 15 - zero galvanometer; 16 - tube connections; 17 - thermocouples on the heater wall; 18 - manometer; 19 - safety valve.

Wall temperature of the central heater was measured at the level of thermocouple junctions within the zone. Thermocouples 17 used in these measurements were cushioned by a layer of insulating material and fitted into grooves milled in the heater walls. The thermocouples were shielded by stainless foil plates 0.2 mm. thick. (The lead-out of the thermocouples from the installation is not shown in the schematic diagram). The thermocouple junctions were sealed to prevent the outflow of heat from the bead, i.e., a lowering of the measured temperatures.

Temperature difference between the installation wall and the heat carrier zone was measured with the aid of a portable potentiometer and an electronic amplifier, built under the supervision of V. Demidovski in the workship of the VNII NP (All-Union Scientific Research Institute for Processing of Petroleum and Gas and for the Production of Synthetic Liquid Fuel).

The following experimental procedure was used: With the caloric power of the heater at a maximum, the system was charged with a sufficient quantity of the heat carrier so that the entire packing was covered with a vapor-liquid mixture. The dynamic level of the liquid was regulated by means of a gage glass mounted on the upper tube connection of the column. This level was kept constant for all heater loads. (Whenever the caloric power decreased, the necessary amount of liquid was added). Pressure rise was achieved by feeding an inert gas to the system. Full-scale showering was used in these experiments.

Narrow-boiling fractions of normal hydrocarbons were used as the heat carrier components. These were obtained by rectification of products synthesized from CO and H_2. The boiling ranges for these fractions are tabulated below. Characteristics of the packing were reported earlier (4).

Preliminary experiments led to the following conclusions:

Fraction	Beginning of boiling, °C	End of boiling, °C
Initial synthetic oil	100	293
1st	68	101
2nd	109	128
3rd	136	149
4th	155	173
5th	169	192
8th	203	258
9th	257	267
10th	269	289
11th	290	330
12th	270	380
Paraffin	306	377

1) The amount of heat carrier charge required by the system is determined by the specific caloric power of the heater (SCH) and by the free volume of the packing.

2) If the heat carrier charge is insufficient, there is a danger of overheating the upper portion of the reactor tube, since the latter is washed only by vapor.

3) An excessive heat carrier charge causes a higher temperature differential along the height of the column, due largely to temperature rise in the bottom sector.

Two methods are available for compounding the heat carrier (Fig. 3):

a) changing the percent content of components in the mixture;

b) selecting components which differ to a greater or lesser extent in their boiling point.

An illustrative instance of temperature distribution along the height of the column is shown in Fig. 4, as obtained for certain fractions. The temperature gradient depends on the SCH, since an increase of this value causes a rise of temperature differential along the length of the heat carrier zone (Fig. 5). (This is due largely to temperature rise in the lower portion of the column). The effect of SCH on temperature distribution increases with the decrease in the geometrical dimensions of the packing elements.

The efficiency of separation, hence temperature differential along the height of the system, is

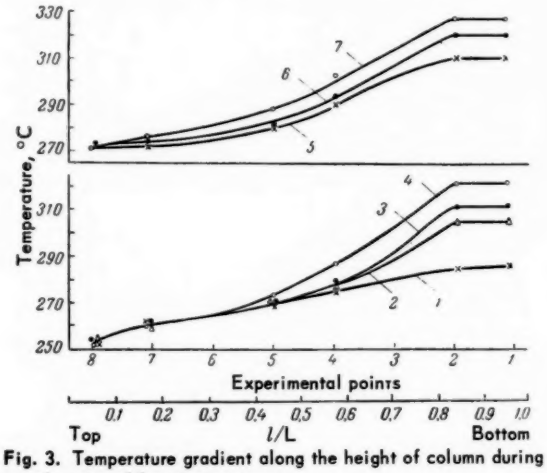

Fig. 3. Temperature gradient along the height of column during rectification of fraction mixtures.

Curve	Fraction, vol. %		
	257–267°	269–289°	306–377°
1	90	—	10
2	80	—	20
3	70	—	30
4	60	—	40
5	—	90	10
6	—	80	20
7	—	70	30

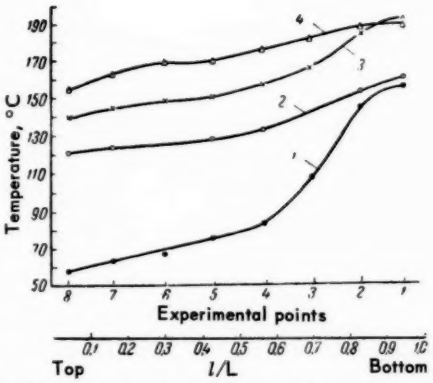

Fig. 4. Temperature gradient along the height of column during rectification of fraction mixtures (vol. %).

Fractions	Curves			
	1	2	3	4
68—101°	80	—	—	—
109—128°	—	75	—	—
136—149°	—	—	68	—
155—173°	—	—	—	83
203—258°	—	—	—	17
257—267°	—	25	—	—
269—289°	—	—	32	—
306—377°	20	—	—	—

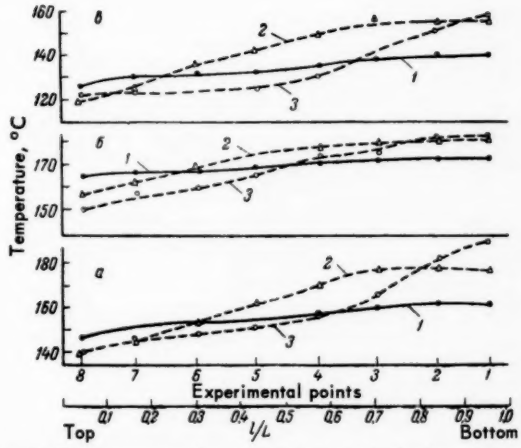

Fig. 6. Temperature gradient along the height of column in relation to geometric dimensions of the packing element, in rectification of various mixtures. (a - 68% fr. 136-149°C + 32% fr. 269-289°C; b - 83% fr. 155-173°C + 17% fr. 203-258°C; c - 75% fr. 109-128°C + 25% fr. 257-267°C).
1 - 4.7 × 4.9 × 0.7 mm.; 2 - 8.6 × 8.7 × 1.0 mm.; 3 - 12.7 × 12.3 × 1.1 mm.)

greatly influenced by the geometric dimensions of the packing element (Fig. 6). Other conditions being equal, the temperature differential increases as these decrease (see above).

The system was regulated while in operation by either one of two methods: a) pressure was changed with the aid of an inert gas (N_2, CO_2) (Fig. 7); b) the reflux was fed to various points along the height of the column. For the same heat carrier, temperature rise is effected by changing the packing. As the reflux is fed to points lying at different levels of the columns, the temperatures at points above the inlet become equalized.

Local evolutions of heat in the mid- and upper portions of the column, effected to simulate overheating of the working zone of the reactor, produced a marked temperature rise and some changes in the shape of the temperature distribution curve. This happened, however, only when the SCH value was high (over kcal./(m.^{2})(hour). In cases where the lower portion of the column was overheated, a considerable change in the temperature gradient was observed also when the SCH value was small (Fig. 8). On the other hand, with high SCH values, intense overheating of the bottom of the column (8–10% of the total amount of heat supplied by the heater) resulted in rapid expulsion of liquid from the system.

To calculate temperature distribution along the

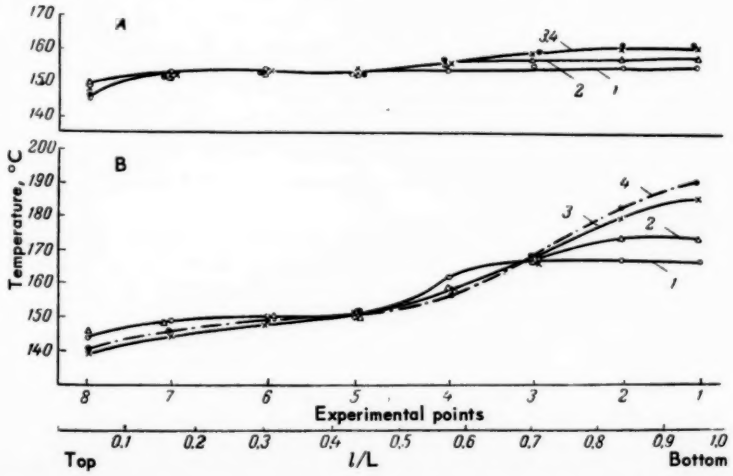

Fig. 5. Temperature gradient along the height of column as a function of specific caloric power of heater (SCH-kcal./(m.^{2}) (hr.), for rectification of a mixture containing 68% of a fraction 136-149°C, and 32% of a fraction 269-289°C away from the operating heat production capacity of the heater.
1.- SCH = 2,200; 2.- SCH = 4,200; 3.- SCH = 5,500; 4.- SCH = 5,900.

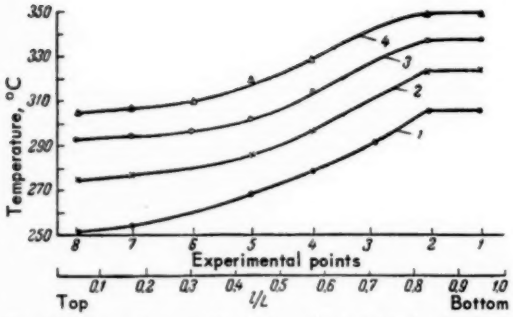

Fig. 7. Temperature gradient along the height of column in rectification of a mixture containing fraction 257-267°C, 80% and fraction 306-377°C, 20%.
1 - normal pressure; 2 - 0.47 gage atmosphere; 3 - 1.13 gage atm.; 4 - 1.8 gage atm.

height of the column, it is necessary to establish the mathematical law governing heat transfer from the reactor tube to the boiling mixture, under conditions of the heat carrier zone being filled with the packing.

As shown by preliminary analysis of experimental data, the heat transfer factor increases sharply along the length of the tube, in the upward direction. Fig. 9 demonstrates the relationship between the heat transfer coefficient and linear vapor velocity. An analogous, but less marked, rise was observed by N. K. Elukhin and I. P. Vishnev (5) in a study of heat transfer during the boiling of oxygen in vertical pipes.

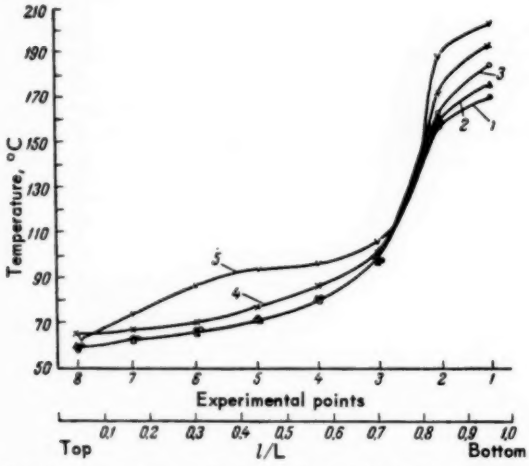

Fig. 8. Temperature gradient long the height of column, with local heat supply ($q_{lb.}$)* to the bottom of column, and SCH = 7,300 kcal./(m.²) (hour). (Mixture: fraction 68-101°C, 80% + fraction 206-377°C, 20%).
1 - $q_{lb.}$ = 0; 2 - $q_{lb.}$ = 2% of the caloric power of central heater; 3 - $q_{lb.}$ = 4%; 4 - $q_{lb.}$ = 6%; 5 - $q_{lb.}$ = 8%.
*$q_{lb.}$ is local heat at bottom of column.

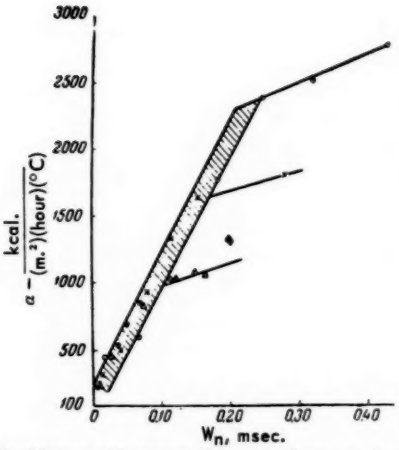

Fig. 9. Coefficient of heat transfer α in relation to linear vapor velocity W_n through the free cross-section of column. in rectification heat-exchange procedure.
o - SCH = 7,600 kcal./(m.²) (hr.); x - SCH = 4,650; Δ - SCH = 2,920; • - SCH = 1,400.

DISTILLATION HEAT EXCHANGE PROCEDURE

This method offers wider possibilities than the rectification procedure, as regards regulating temperature distribution along a column while in operation (3). In this method, a specially selected binary or multi-component mixture is brought to boiling and pumped through the space around the working zone of the reactor. The mixture, caused to flow directly through the system, merges with the reactants entering the reaction vessel. The heat of reaction supplied to the flowing mixtures causes its continuous evaporation. The low-boiling components evaporate predominantly. As a result, temperatures along the height of the packing layer (i.e., along the working zone of the reactor) become distributed in accordance with local composition of the boiling liquid mixture. The concentration of high-boiling components in the packing layer will of course increase in the same direction in which the heat carrier is pumped into the system, and so will the boiling point. To investigate these manifestations, an installation was built which included a circulation reactor model, shown in Fig. 2, and the necessary regulating and measuring devices (Fig. 10).

The reactor model consisted of column 1, bridging coil 2, and condenser 3. A vapor tube with a reflector cap was inserted into the coil.

The circulation system comprised refrigerator 4, circulation pump 7, heater 8, graduated vessel 5, and pressure tank 6.

Mixtures of narrow-boiling fractions of aliphatic and aromatic hydrocarbons were used in the experiments. The Raschig glass rings, 4.7 × 4.9 × 0.7

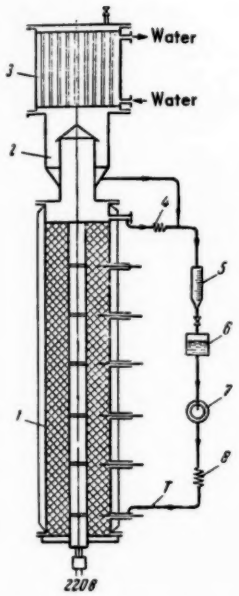

Fig. 10. Experimental installation for the distillation cooling procedure.
1 - column; 2 - bridging coil; 3 - condenser; 4 - refrigerator; 5 - graduated vessel; 6 - pressure tank; 7 - circulation pump; 8 - heater.

mm., served as packing. The mixture was pumped in upward.

Preliminary experiments conducted in a glass model, 40 mm. in diameter, demonstrated that the packing interferes with the stirring of the mixture along the height of the system, aimed at temperature equalization. It was further shown that in this method, as in rectification heat exchange procedure, the temperature differential increases with decreasing geometrical dimensions of the packing element, other conditions being equal.

Temperature distribution along the height of the column depends on the SCH of the central heater. When the SCH rises, the temperature differential increases (Fig. 11).

A change in the rate of pumping in the heat carrier leads to a change in the shape of the curve for temperature distribution along the height of the column (Fig. 12). Hence, varying the pumping rate is a convenient method of regulating the system

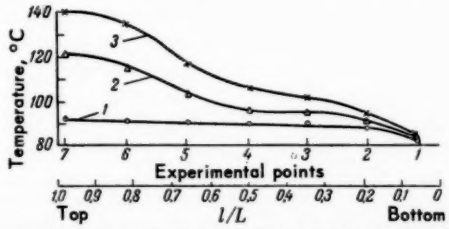

Fig. 11. Temperature gradient along the height of column in relation to SCH, in the distillation cooling method. (Mixture: 70% fr. 62-115°C + 30% fr. 203-258°C).
1 - SCH = 2,650 kcal./(m.²) (hour); pumping rate W_{pump} = 7.15 m.³/m.² through free cross-section, per hour; 2 - SCH = 4,650, W_{pump} = 7.150; 3 - SCH = 8,800, W_{pump} = 7.550.

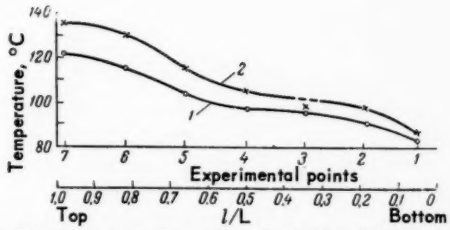

Fig. 12. Temperature gradient along the height of column in relation to pumping rate W_{pump}, in the distillation cooling method. (Mixture: 70% fr. 62-115°C + 30% fr. 203-258°C).
1 - W_{pump} = 7.15 m.³/m.² through free cross-section, per hour; 2 - W_{pump} = 5.35.

while in operation.

Another way of regulating the system is to feed the heat carrier to different points along the height of the column.

From our experiments it can be concluded that a desired temperature gradient in a heat exchange system will be achieved by proper selection of heat carrier, packing, and pumping rate.

In the distillation method, the same peculiarities of heat transfer from the wall to the boiling liquid are observed as noted in the rectification cooling method.

Coming back to Fig. 9, it should be stressed that special attention must be paid to the following facts. The heat transfer factor was seen to rise along the height of the pipe in the course of the boiling process. Even more important is its additional rise due to the presence of a packing. Under the conditions of our experiments as described, with the same liquid boiling in the pipe, the heat transfer factor was at least 2.5 times higher when the packing was present. This is perfectly understandable, considering the tendency of the vapor current to occupy the central portion of the packing, forcing the liquid out toward the periphery of the tube. It should be said, parenthetically, that filling the heater pipes with packings of a specific shape, made of specified materials and having specified dimensions, may prove the right way to intensify the performance of heating chambers in evaporating, distilling, rectifying and other equipment.

With this objective in mind we have undertaken a special study, and shall report the results in the near future.

LITERATURE CITED

1. N. I. Gel'perin, and V. B. Kvasha, *Khim. i Tekh. Topliv i Masel* (Chemistry and Technology of Fuels and Oils) (in press).
2. O. Dorschner, *Chem. Ing. Techn.* 25, No. 5, 277 (1953).
3. V. B. Kvasha and A. V. Velynsk, Russian Author's Certificate 116463 (1958).
4. N. I. Gel'perin and V. B. Kvasha, *Khim. Prom.* (Chemical Industry), No. 5, 406 (1960).
5. N. K. Elukhin and I. P. Vishnev, *Kislorod* (Oxygen), No. 4, 5 (1959).

Yu. G. Zelinski
V. V. Kafarov

USSR

Hydrodynamic Conditions on Open-Grid (Turbogrid) Trays

An attempt to define more closely the hydrodynamic processes occurring on grid plates, and to determine optimum operating conditions.

OPEN-GRID and perforated trays are featured extensively in absorption and distillation columns of recent design (1-20). However, the specific hydrodynamic conditions which develop on such trays have not been fully analyzed, nor have the optimum service conditions been ascertained to date.

In the present work, an attempt was made to define more closely hydrodynamic processes occurring on grid plates. Our experiments were carried out in columns 57, 114, and 400 mm. in diameter, with bar-type stainless steel plates stamped from sheets 1.5-2.5 mm. thick (parallel slots milled in the flat sheet: see Table below). The 114 mm. column and a water-air contacting system were used in most test runs.

The 114 mm. diameter column (Fig. 1) consists of three cylindrical glass sections 1, each 500 mm. high, mounted on a metal receiver 2, which is provided with a glass (water) level gauge. The sections are separated by distributing tray 3 and working tray 4. An alcohol manometer 5, which can be set at any angle to the horizontal plane, serves for measuring working-tray (bubble plate) resistance. A high-pressure blower 6 drives air into the installation with a baffle 7 controlling the air supply. A standard variable diaphragm with a water manometer 8 are provided to measure the quantity of air entering the system. Air pressure in front of the diaphragm is measured by water manometer 9; the temperature at the inlet to the installation, by a mercury thermometer 10. Water consumption is measured by rotameter 11 (and regulated by valve 12). Thermometer 13 measures the water temperature. Water flows into the installation from pressure tank 14, in which the liquid level is kept constant. Water is removed from the installation through stopcock 15 and drainage tank 16. Droplets of water entrained by the air current are trapped by cap 17 mounted on the top section and are returned to the column.

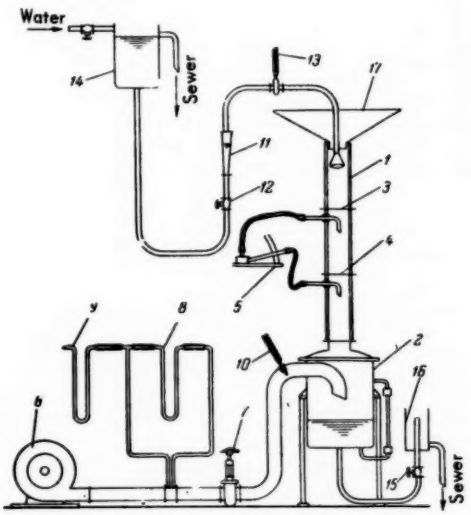

Fig. 1. Installation for hydrodynamic test-runs of grid trays in a 114 mm diameter column: 1–column sections; 2–receiver; 3–distributing plate; 4–bubble-cap plate; 5–manometer; 6–blower; 7–baffle; 8 and 9–manometers; 10 and 13–thermometers; 11–rotameter; 12–control valve; 14–pressure tank; 15–stopcock; 16–drainage tank; 17–cap.

Grid tray characteristics*

Trays	Diameter, mm.	Free area of cross-section, %	Average width of slot, mm.
1st	57	20.5	3.19
2nd	57	27.9	3.19
3rd	57	24.3	3.23
4th	57	21.9	2.23
5th	114	24.7	3.32
6th	400	24.1	3.24
7th	114	20.7	3.16
8th	114	18.3	2.18
9th	114	18.1	3.17
10th	114	16.2	3.15
11th	400	17.4	2.21

*The slot width was measured every 5 mm. with the aid of inside calipers and micrometer.

This article first published in *Khim. Prom.*, No. 2, p. 122 (1961).

EXPERIMENTAL PROCEDURE

First, the required water and air consumption were determined. After stabilizing the tray performance, the temperatures of water and air as well as the pressure gradient were measured. The bed of froth on the working plate and the water level in the receiver were also measured (the latter with the level gauge). Next, valves 12 and 15 were closed rapidly and simultaneously, and the feeding of water to the installation was discontinued. After both plates had been drained, the water level in the receiver was again measured. The overall liquid holdup on both plates was calculated on the basis of the difference in the water level of the receiver before and after the draining of the trays. Test runs with the working plate removed showed the holdup to be equal on the distributing and the working tray, provided the showering rate and air consumption were the same for each plate. Consequently, the holdup on the working tray was considered equal to one-half of the total amount of liquid drained from both plates.

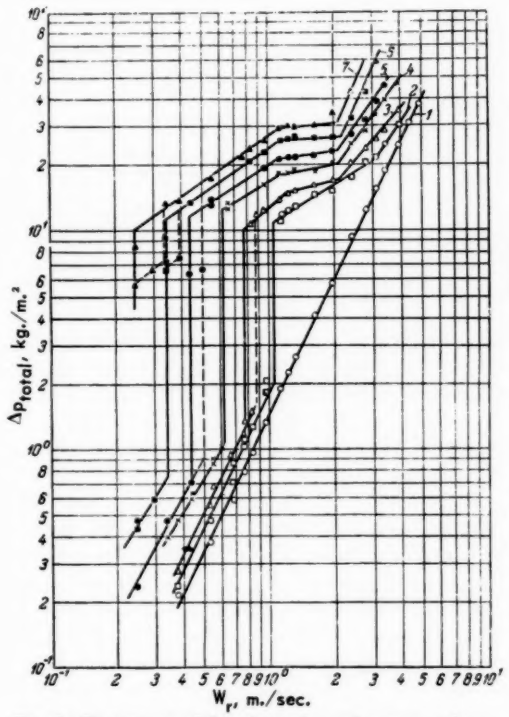

Fig. 2. Resistance of 7th plate, dry and wet, as a function of gas throughput over the entire cross-sectional area of column:
1–dry plate; 2–L = 1650 kg./(m.²)(hour); 3–L = 3,780 kg./(m.²)(hour); 4–L = 8,060 kg./(m.²)(hour); 5–L = 11,200 kg./(m.²)(hour); 6–L = 16,000 kg./(m.²)(hour); 7–L = 21,000 kg./(m.²)(hour).

Several series of test runs were performed, with the showering rate kept constant in each series, while the air supply rate was varied. Under these conditions, curves $\Delta p_{total} = f_1(W_g)$, $h_n = f_2(W_g)$, $P = f_3(W_g)$ were obtained for each plate at different showering rates.

A relationship between the working-plate resistance and gas throughput over the entire cross-sectional area of the column, without showering and with showering of variable intensity, is plotted for the 7th plate in logarithmic coordinates (Fig. 2). In Fig. 3 the same relationship is given for resistances of the 5th, 7th, 8th, 9th and 10th plates, the showering rate amounting to L = 8,060 kg./(m.²)(hr.).

The graphs in Fig. 4 and 5 are plotted for the same plates and showering rate. Functional relationships are shown between the head of aerated liquid as well as liquid holdup on the working plate and gas throughput, starting with the rates at which the initial liquid buildup is observed on the plate.

HYDRODYNAMIC CONDITIONS

As shown by these graphs, the hydrodynamic conditions that develop on grid plates vary, depend-

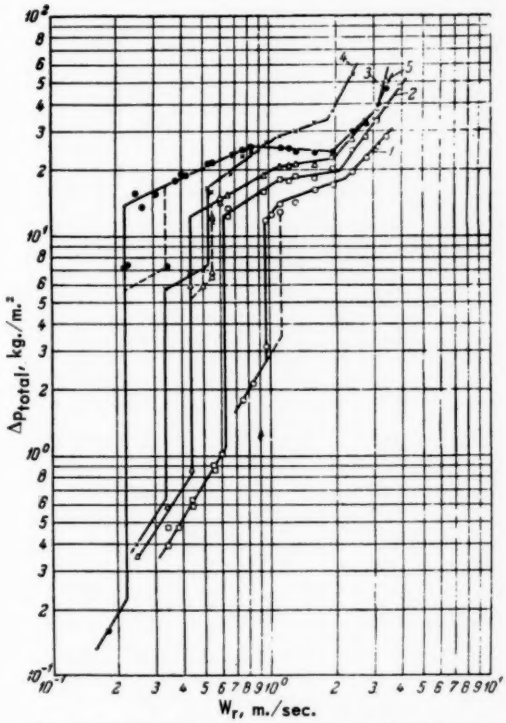

Fig. 3. Resistances of various plates as functions of gas throughput over the entire cross-sectional area of column: L = 8,060 kg./(m.²)(hour).
1–5th plate; 2–7th plate; 3–9th plate; 4–10th plate; 5–8th plate.

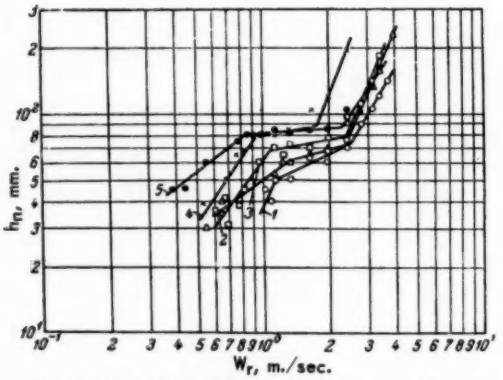

Fig. 4. Aerated liquid buildup as a function of gas throughput over the entire cross-sectional area of column. Graph plotted for different plates. L = 8,060 kg./(m.²)(hour). (Curves numbered as in Fig. 3.)

ing on liquid flow and gas current velocities. A characteristic feature is the non-uniform variation of plate resistance as well as of liquid buildup and holdup, caused by changes in the speed of the gas current.

The first condition can be defined as a wet plate condition. It develops when the gas passes freely at a low velocity through a portion of the cross-sectional area of the slots. The liquid draining through the remaining sector of the same area contacts the gas only along the surface of the film (7, 17, 18, 19). Under these conditions, the plate resistance varies roughly as the square of the gas velocity, at constant showering rate (Figs. 2 and 3). When this rate varies, the wet plate resistance, plotted in logarithmic coordinates, appears as a series of straight lines running parallel to dry plate resistance. They are arranged in ascending order, the higher the resistance the greater the showering intensity. The shape and order of curves suggest that, within the limits of the "wet conditions", the portion of free area taken up by liquid will remain constant for a given showering rate. It will increase with rising intensity and decrease with diminishing intensity (at L = 0 the entire plate area will be occupied by gas). Under "wet conditions", the liquid holdup is negligible and, in fact, cannot be measured.

As the speed of gas flowing through the slots increases, the friction between the gas and the draining liquid also increases. At a certain point the friction forces cause a liquid buildup on the plate (a liquid mist being first "suspended", as it were). This takes place at all showering rates, since the speed of gas throughput over slot area free from liquid remains constant. As the showering rate is varied, however, the portion of slot area taken up by liquid will change accordingly. Therefore, the rate of suspension, when evaluated for the entire cross-sectional area of the column, will depend on the shape of the plate and on the intensity of showering. Points corresponding to gas velocities at which suspension of liquid occurs may be termed "suspension points".

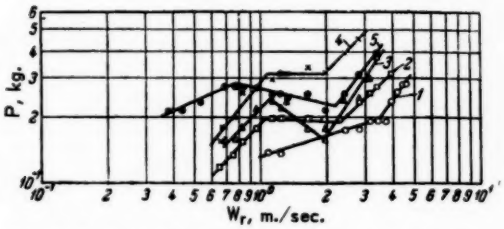

Fig. 5. Liquid buildup on different plates as a function of gas throughput over the entire cross-sectional area of column. L= 8,060 kg./(m.²)(hour). (Curves numbered as in Fig. 3.)

PLATE RESISTANCE

Suspension of the liquid is accompanied by sharp increase of plate resistance, followed by the development of bubbling action on the grid plate. As gas begins to bubble through the layer of liquid, the lower zone remains comparatively clear, with but a few bubbles passing through it, in contrast to the upper zone, which turns to foam. With increasing speed of gas and constant showering rate, the lower zone will gradually shrink, until all of the liquid has changed to turbulent foam. The regions of gas throughput and liquid drainage constantly shift along the slots, but their distribution on the plate remains fairly uniform.

As seen from Figs. 2-5, plate resistance, aerated liquid buildup and the quantity of liquid increase with increasing speed of gas, under conditions of bubbling action, at constant rate of showering, and will increase further with showering of greater intensity. As the gas throughput increases the portion of slot area taken up by the draining liquid will be reduced (as evidenced by the increase of liquid buildup on the plate). At the same time gas bubbles will form at a higher rate, until all of the liquid on the plate has turned to froth.

As the bubbling action is initiated (causing the "suspension" of liquid), a "hysterisis" phenomenon is observed. With rising speed of gas and constant showering rate, the relative increase in the rate of gas throughput over the entire cross-sectional area of the column, necessary to effect a liquid buildup, is greater than the corresponding decrease of the gas velocity eliminating the buildup. The latter apparently absorbs more energy from the gas current than is needed for a liquid holdup

on the plate. It follows that if some liquid is fed to the plate at a time when the speed of gas is slightly below the rate of suspension, a liquid buildup will occur even under these conditions. Therefore, in measuring suspension velocity, care must be taken that liquid is fed to the plate at a uniform rate. This precaution cannot be achieved, however, if the distributing tray is of the same size as the working tray. For this reason the distributing plate used in our experiments, up to the point where the speed of gas became high enough to cause suspension, had a free cross-sectional area greater than that of the bubbler plate. In this case, the suspension of liquid occurred as a rule at higher gas velocities than with distributing and working plates of equal size. The gas velocity was calculated with respect to the entire cross-sectional area of the column (see dotted lines in Figs. 2 and 3).

EFFECT OF BUBBLING

The bubbling process is completed when all of the liquid on the plate changes over to a state of turbulent foam. The point corresponding to gas velocity reached at that moment may be termed the "aeration point", and the plate performance which follows is the "aeration operation", or "emulsification". Within the limits of this operation, at constant rate of showering, plate resistance and liquid buildup increase very slightly. The amount of liquid on the plate may, in fact, decrease in some instances. Apparently, under these conditions the portion of slot area taken up by liquid remains roughly constant. Hence, the increase in the amount of gas passing through the liquid is due to further increase of bubble formation, or else the bubbles increase in size, while the area over which they form remains constant. Inasmuch as by the end of the bubbling action (at the aeration point) all of the liquid on the plate is found to be in a state of froth, it can be assumed that no further increase in the rate of bubble formation is possible. It follows that, under the conditions of aeration, the bubbles increase in volume with increasing gas velocity. This phenomenon was reported earlier (22). It occurs as the gas bubbles through a single round aperture. At a certain gas velocity, which was determined experimentally, the bubbles begin to increase in volume. The same (corresponding to the jet stage of bubbling action) is reached also in cases where gas is bubbled through a large number of openings in a sieve plate, as described in an earlier report (23). In our study, gas velocities corresponding to the aeration point were much higher than those observed before. This is probably due to the fact that the regions along the slot area through which the gas passes as it leaves the grid plate keep on shifting; this interferes with the formation of gas jets and, furthermore, delays the next stage in the bubbler plate performance.

As the aeration phase is completed, the velocity of the gas flowing through the slots increases to the point where individual bubbles begin to coalesce, forming a stream. The gas streams flowing through different areas of the plate cause the aerated liquid to oscillate. Therefore the point corresponding to the gas velocity at which stream formation is noted, can be referred to as the "oscillation point" and the next phase of the plate performance may be termed the "oscillation stage". During this phase, the flow of liquid through the slots changes sharply. At lower gas velocities, the liquid drains at a uniform rate ("rains") through all the slots. As oscillation sets in, the liquid is seen to flow in small quantities through those plate areas which correspond to the shifting trough of the oscillation wave. This stage is further characterized by intense entrainment of liquid splashes.

OSCILLATION PHASE

The passing over to the oscillation phase is accompanied by marked increase in the buildup of the aerated liquid as well as in the liquid holdup (Figs. 4 and 5). As a consequence, the total plate resistance increases (Figs. 2 and 3).

The aerated liquid is seen to oscillate conspicuously only where the showering rate is low and friction between gas and liquid particles is high enough to overcome the inertia of liquid held by the plate. At higher showering rates the liquid holdup increases and oscillation becomes less marked.

As the oscillation phase is terminated, flooding of the column sets in. The liquid stops draining through the slots, with the result that plate resistance, liquid holdup, and the head of froth increase at the same time. Finally, the liquid begins to splash from the column.

Examination of the various phases in grid plate performance leads to the conclusion that stream velocities corresponding to the aeration point should be regarded as optimum, with respect to mass transfer, since at this point the area of interphase contact reaches a maximum. The interval of stream velocities between suspension and oscillation points can be defined as the working interval, inasmuch as it comprises both bubbling action and aeration.

It should be pointed out that these phases are not always clearly defined. As indicated by the above data, suspension velocities depend in a large measure on the plate showering rate. With low-intensity showering, suspension velocities may exceed stream velocities corresponding to the aeration point, which are not much affected by the showering rate. In such

cases, the liquid buildup developed during the suspension phase assumes at once the character of highly turbulent foam, and the bubbling action is eliminated. Furthermore, with increasing gas speed at a constant showering rate, the plate resistance increases more sharply than it does in the course of normal aeration. This increase, when plotted in log coordinates, appears as a series of straight lines for all velocities below that corresponding to the flooding point of the column (Fig. 2, curve 2 for L = 1,650 kg./(m.^{2})(hour).

COLUMN DIAMETER

To check the effect of column diameter on the hydrodynamics of grid plates, several experiments were carried out using columns 57 and 400 mm. in diameter. The 400 mm. diameter column consisted of steel sections, with observation windows. Plate separation amounted to 300 mm. in the 57 mm. column and to 475 mm. in the 400 mm. column. The installations were similar to the one described above, except that no device was provided for measuring the liquid holdup on the plate. The working procedure was basically the same as above.

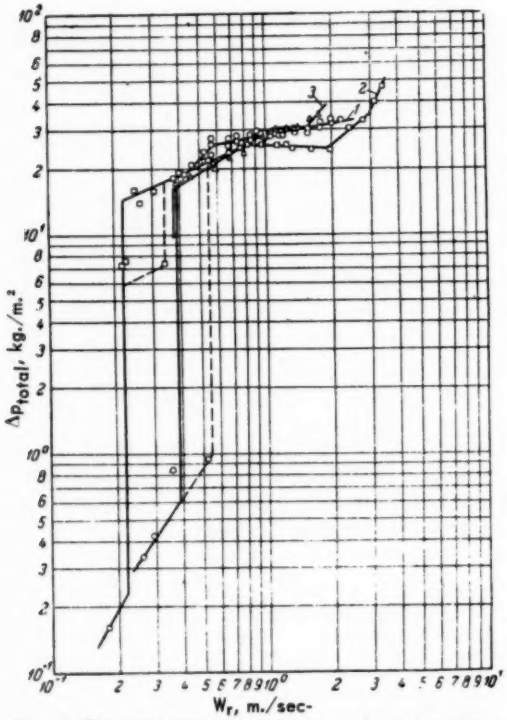

Fig. 6. Plate resistance as a function of gas throughput velocity over the entire cross-sectional area of column. Graph plotted for plates of different diameters. 1–4th plate, L = 7,840 kg./(m.^{2})(hour); 2–8th plate, L = 8,060 kg./(m.^{2})(hour); 3–11th plate, L = 7,960 kg./m.^{2})(hour).

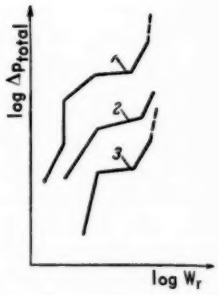

Fig. 7. Resistance of curves for plates of different types: 1–turbogrid plates (the authors' data); 2–perforated ripple plates; 3–sieve plates.

A functional relationship between plate resistance and gas throughput over the entire cross-sectional area of the column is shown in Fig. 6 for three plates of different diameters. The geometrical shapes of the plates are pretty much alike, and the showering intensity values are fairly close and remain constant. A similar relationship between plate resistance and gas velocity is shown for plates 11 and 8, while the data for plate 4 differ from both. This deviation is due to the distorting wall effect when a narrow column is used. The distortion becomes pronounced if the showering rate is high, and is particularly marked in the oscillation phase. In the latter case, the oscillating motion of liquid on the plate changes to pulsations in the vertical direction, followed by violent fluctuations of plate resistance.

From the above it can be concluded that, below a certain value of plate diameter, the column wall effect becomes apparent to the point where experimental results obtained with narrow columns cannot be applied to wider columns without introducing a correction.

The relationship between plate resistance and gas velocity, at a constant showering rate, shown for turbogrid trays, is quite similar to data recently obtained for perforated ripple plates (24) as well as sieve plates (21, 25). Variation of resistance is plotted in Fig. 7 for the three types of plates. The graph is based on the authors' data as well as on the reports of other investigators. A close similarity of performance is demonstrated for grid, ripple, and sieve plates.

NOTATION:

Δp_{total} – total wet plate resistance, kg./m.^{2};
P – liquid holdup on plate, kg.;
h_n – aerated liquid buildup on plate (height), mm.;
W_r – linear velocity of gas throughput over the entire cross-sectional area of column, m./sec.;
L – weight velocity of liquid per unit of cross-sectional area of column showering rate), kg./m.^{2})(hour).

LITERATURE CITED

1. *Chem. Eng. News*, 30, No. 40, p. 4164 (1952).
2. *Ind. Eng. Chem.*, 44, No. 9, p. 13A (1952).
3. *Petr. Eng.*, 26, No. 5, C-17 (1954).
4. *Chem. Eng. Progr.*, 50, No. 2, p. 57 (1954).
5. *Petr. Proc.*, 7, No. 10, p. 1447 (1952).
6. *Erdöl u. Kohle*, 8, No. 5, p. 9 (1955).
7. Van den Berg, G. J., *J. Inst. Petr.*, 41, No. 374, p. 45 (1955).
8. Kafarov, V. V., *Khim. Nauka i Prom.*, No. 1, p. 81 (1957).
9. Kuzminykh, I. N. and Babushkina, M. D., *Bumazh. Prom.*, No. 12, p. 5 (1955).
10. Kuzminykh, I. N., *New Techniques in the Production of Sulfite Cellulose*, Goslebumizdat (State Publ. House for the Wood Pulp Paper Ind.), (1956).
11. Aerov, M. E., Darovskikh, E. P., *Khim. Prom.*, No. 2, 92 (1957).
12. Dilman, V. V., Darovskikh, E. P., Aerov, M. E., Akselrod, L. S., *Khim. Prom.*, No. 3, p. 156 (1956).
13. Aerov, M. E., *Khim. Nauka i Prom.*, No. 1, p. 97 (1957).
14. Kuzminykh, I. N., *Khim. Prom.*, No. 4, p. 234 (1956).
15. Aerov, M. E., Motina, G. L., Golovanova, L. P., *Zhur. Priklad. Khim.*, No. 4, p. 567 (1957l.
16. Aerov, M. E., Motina, G. L., Potarin, M. M., *Zhur. Priklad. Khim.*, No. 7, p. 1100 (1957).
17. Dalninsk Polytech. Inst., *Transactions*, No. 1, p. 65 (1959).
18. Gervinka, M. Gerny, O., *Chem. Průmysl*, No. 6, p. 232 (1955).
19. Kasatkin, A. G., Dytnerski, Yu. I., Umarov, S. U., *Khim. Prom.*, No. 3, 166 (1958).
20. Eduljee, H. E., *Brit. Chem. Eng.*, No. 1, p. 24 (1959).
21. Arnold, D. S., Plank, C. A., Schoenborn, E. M., *Chem. Eng. Progr.*, 48, No. 11, p. 633 (1952).
22. Van Klevelen, D. W., Hoftijzer, P. J., *Chem. Eng. Progr.*, 46, No. 1, p. 29 (1950).
23. Akselrod, L. S., Dilman, V. V., *Khim. Prom.*, No. 1, p. 28 (1954).
24. Hutchinson, M. H., Baddour, R. F., *Chem. Eng. Progr.*, 52, No. 12, p. 503 (1956).
25. McAllister, R. A., McGinnis, P. H., Plank, C. A., *Chem. Eng. Sci.*, No. 1, p. 25 (1958).

M. S. Furman
A. D. Shestakova
I. L. Arest-Yakubovich
N. A. Lyubitsina

USSR

Oxidation of n-Butane in the Liquid Phase under Pressure

Optimum conditions determined for oxidation of n-butane by air to acetic acid, under pressure and in the presence of a solvent - a process with important economic implications.

THE oxidation of n-butane in liquid phase, among other hydrocarbons, is a significant reaction, rich in possibilities. The products formed are of major economic importance, while the use of butane, which is inexpensive, will widen the raw-material base and will reduce the cost of production.

Oxidation of hydrocarbons in the liquid phase develops at lower temperatures (100-200°C) than in the gaseous phase (350-400°C). This is quite essential for preserving the valuable oxidation products. Moreover, oxidation in the liquid phase is a more selective process. It yields primarily three useful products (acetic acid, methylethylketone, ethyl acetate) (1-4), while oxidation in the gaseous phase produces formaldehyde, acetaldehyde, methyl and ethyl alcohols, acetone, formic and acetic acids (5, 6).

This article first published in *Khim. Prom.* No. 1, 6-11, (1961).

An industrial-scale oxidation, by air, of n-butane in the liquid phase, in the presence of a solvent, was performed at a large plant in the United States. The steady growth of the plant's output capacity confirms the efficiency of this process and its excellent prospects for the future (7).

The oxidation of n-butane can be carried out either at temperatures below 152°C (the critical temperature) or in a solvent at temperatures above 152°C (1-4, 8-13).

At low temperatures, the oxidation rate is relatively low. This suggested that it might prove a more promising procedure to oxidize n-butane in the liquid phase, in the presence of a solvent, at higher temperatures. Acetic acid was used as the

solvent. It does not become oxidized under the conditions of this process. It is, furthermore, a basic product of the same reaction; hence, separation – a subsequent step – is greatly facilitated.

EQUIPMENT

The oxidation of n-butane in the liquid phase in the presence of a solvent was carried out in an installation, shown schematically in Fig. 1. The basic piece of equipment in this layout is the reactor, a vessel with 700 ml. capacity, placed inside an autoclave made of stainless steel (Fig. 2). The reactor is made of glass or titanium to prevent corrosion of the vessel as well as the catalytic effect of metal salts formed as a result of corrosion. The apparatus, working under bilateral pressure, is equipped with a bubbler through which the air required for oxidation is passed. A housing for a thermocouple is also provided. Another such housing is built into the autoclave, where the thermocouple measures the wall temperature. The difference between this temperature and that of the reaction zone does not exceed 1°C when the process is well in progress.

The air fed to the reactor passes through the reaction mixture and enters a reflux condenser, together with butane vapor and other reaction gases. The vapor of n-butane, liquefied in the condenser, passes into the reactor. The gas leaving the condenser contains 8–10% butane. To keep the butane concentration constant in the reaction zone, the air fed to the reactor is previously passed through a measuring tank, where it is saturated with butane. The concentration of butane in this air is regulated by the temperature of the tank.

As the reaction is completed, the gas sampled for analysis is first passed through absorbers which contain water. There it is freed from small amounts of water-soluble reaction products which escape from the reactor. The gas is then passed through driers filled with calcium chloride and phosphorus pentoxide. Finally it enters the condensers, where it is freed from n-butane. The condensers are cooled with a solution of CO_2 in acetone. The amount of waste gas obtained is measured with a dry-gas meter. The gas sampled on completion of the reaction is analyzed for CO_2, O_2, CO, C_4H_{10}, N_2 and their contents are determined. In the liquid reaction products the analysis establishes the content of acetic acid, ethyl acetate, methylethylketone, ethyl alcohol, and water.

Acetic acid was determined by titration with alkali; the content of other acids (formic and propionic), by chromatography (14). The total content of these acids amounted to a small quantity.

Ester was determined by saponification with alkali after a preliminary determination of acetic acid (titration). Alcohol was determined by the esterification method (15); carbonyl compounds, by the hydroxylamine method, with titration performed by measuring the pH. Water was determined by the Fischer method.

The substances used in these experiments included: n-butane (which was chromatographically freed from homologues, then treated with sulfuric acid to remove the unsaturated hydrocarbons, whereupon it was found to contain 99–100% n-C_4H_{10}); glacial acetic acid (chemically pure) and a catalyst, cobalt stearate, prepared by a standard procedure (16).

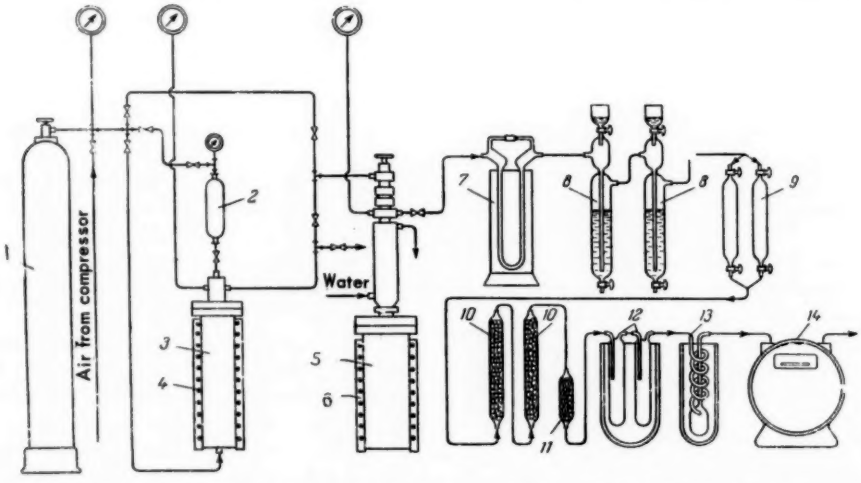

Fig. 1. Flowsheet of laboratory installation for oxidizing n-butane in the liquid phase: 1. cylinder filled with compressed air; 2. vessel filled with n-butane; 3. measuring tank; 4, 6. electric furnaces; 5. reactor; 7 rheometer; 8. absorbers filled with water; 9. pipettes for taking gas samples; 10. driers filled with $CaCl_2$; 11. drier filled with P_2O_5; 12, 13. condensers; 14. gas meters.

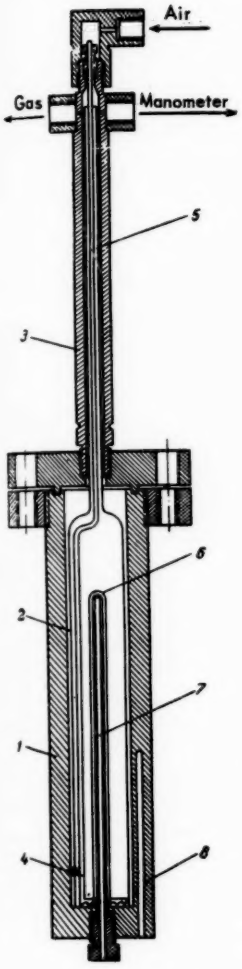

Fig. 2. Reactor:
1. autoclave; 2. reactor;
3. head of the autoclave;
4. bubbler; 5. reflux condenser; 6. housing for the reactor thermocouple;
7. jacket for autoclave thermocouple; 8. housing for the thermocouple.

The oxidation of n-butane in liquid phase at temperatures above the critical is based on the mutual solubility of n-butane and acetic acid taken in any ratio, under the above conditions. In the course of the reaction, water is formed along with other products. It is only partially miscible with n-butane, therefore the phase state of the system can be expected to change. As shown by I. R. Krichevski and G. D. Efremova, the system n-butane - acetic acid - water belongs in a rare group of tri-component systems which can form two liquid phases at temperatures above the critical temperature of the most volatile component. In this case, stratification is confined to a limited concentration region, which narrows down as the temperature increases. However, even when two liquid phases are formed, n-butane remains in solution and oxidation takes place only in the liquid phase. Conditions in each phase are different from those governing the oxidation in a homogeneous solution. The ability of the studied system to stratify facilitates the separation of reaction products.

The quantitative relation between the amounts of the solvent (acetic acid) and of the dissolved hydrocarbon (n-butane) affects the course of the reaction substantially. Experimental results indicating the effect of the ratio n-butane: acetic acid are shown in a graph (Fig. 3).

The gross weight of n-butane and acid charges remained the same(340 g.) in all experiments. The only variable was the ratio of the initial components (n-butane: acetic acid).

On the left ordinate is plotted the overall yield of useful reaction products, in g., recalculated per 100 g. of reacted n-butane (this total included ethyl alcohol). On the right ordinate is plotted the ratio reacted n-butane: total n-butane present in the reactor. (The latter value is given by the sum: initial charge of n-butane plus the quantity introduced from the measuring tank in the course of the experiment).

From the graph it is seen that an increase of the weight fraction of n-butane in the liquid phase leads to a decrease in n-butane conversion. At the same time the yield of useful products is increased; in other words, the utilization of n-butane is more efficient. When the ratio n-butane: acetic acid = 0.5 - 1.0, the conversion of n-butane is good and is associated with a high yield of the desired product: acetic acid.

The part played by the solvent is not limited to promoting the oxidation of n-butane in liquid phase at temperatures above the critical. The solvent actually participates in the process. For instance,

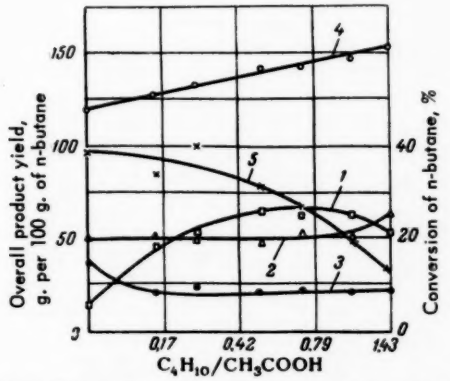

Fig. 3. Oxidation of n-butane as a function of the weight ratio n-butane: acetic acid (P = 60 atm., t = 165°C, w(rate of air supply) = 120 nl./hr.,* (duration of reaction) = 3 hrs., q (quantity of catalyst) = 0.03 g.). 1. acetic acid; 2. ethyl acetate; 3. methylethylketone; 4. overall yield of useful products; 5. conversion of n-butane.

* Tr. note: 120 liters per hour, under standard ('normal') conditions.

it aids in the destruction of peroxides formed in the course of the reaction, accelerating the latter. Our experiments have demonstrated, in effect, that peroxides are invariably formed, as byproducts of reaction, on oxidation of pure n-butane in a glass vessel at temperatures below its critical temperature. No peroxides are found, however, when n-butane is oxidized under the same conditions but in the presence of a solvent.

It is interesting to note that when a titanium reactor was used, no peroxides were found even in the absence of a solvent. It follows that the material of which the reactor walls are made affects the oxidation process.

The optimum residence time for liquid phase in the reaction zone was determined experimentally, with n-butane: acetic acid = 1:1 (170 g. of each). The results are given in Fig. 4.

During the first 3 hours, the conversion of n-butane and the yield of acetic acid increased linearly with the duration of experiment. Beyond this time interval, the reaction was inhibited. For practical purposes, therefore, the 3-hour interval was taken as the optimum residence time for liquid phase in the reaction zone.

EFFECT OF TEMPERATURE AND PRESSURE

The major factors controlling oxidation are temperature and pressure. The effect of pressure is demonstrated in Table 1. Variation of pressure from 50 to 80 atm. does not affect the composition of reaction products. The rate of the process, on the other hand, increases with rising pressure, which results in higher conversion of reactants:

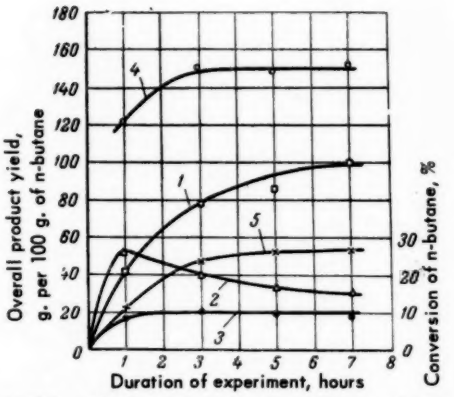

Fig. 4. Effect of the duration of experiment on oxidation (P = 60 atm., t = 165°C, w = 120 nl./hr., q = 0.03 g.): 1. acetic acid; 2. ethyl acetate; 3. methylethylketone; 4. overall yield of useful products; 5. conversion of n-butane.

n-butane and oxygen. The rise of pressure cannot change appreciably the concentration of the reacting hydrocarbon. Therefore, the observed acceleration of the process is probably due to a rise in oxygen concentration taking place as pressure increases in the reaction zone.

The effect of temperature on oxidation was studied in the interval 140-180°C (Table 2).

Raising the reaction temperature results in increased n-butane conversion. At 140°C the oxidation is not complete; quite a few intermediate compounds are found among the reaction products. As the temperature rises to 150°C, the yields of alcohol and methylethylketone are considerably lowered, but the yield of acetic acid is increased. Furthur increase of temperature has little effect on the yields.

Table 1

Effect of pressure on the oxidation process (t = 165°C, w = 120 nl./hour, q = 0.03 g.*, r = 6 hours)

Pressure, atm.	Conversion of butane, %	Composition of waste gases, vol. %					Yield of useful products, g.**				
		CO_2	O_2	CO	C_4H_{10}	N_2	CH_3COOH	C_4H_8O	C_2H_5OH	$C_4H_8O_2$	Total
50	20,7	1,8	8,7	0,5	9,6	79,4	96	22	1	34	153
60	30,0	2,4	6,2	0,7	9,2	81,5	104	18	2	31	155
80	43,5	3,1	3,8	0,6	5,8	86,7	94	23	6	30	153

*Corresponding to 0.018% of cobalt stearate dissolved in acetic acid introduced into reactor.
**Per 100 g. of reacted n-butane.

Table 2

Effect of temperature on the oxidation process (P = 60 atm., w = 120 nl./hour, q = 0.03g., r = 6 hours)

Temperature, °C	Conversion of butane, %	Composition of waste gases, vol. %					Yield of useful products,* g.				
		CO_2	O_2	CO	C_4H_{10}	N_2	CH_3COOH	C_4H_8O	C_2H_5OH	$C_4H_8O_2$	Total
140	3.7	0.2	18.5	0.4	7.0	73.9	48	31	16	29	124
150	18.2	1.5	9.6	0.3	8.6	80.0	92	17	4	40	153
165	30.0	2.4	6.2	0.7	9.2	81.5	104	18	2	31	155
180	39.4	3.4	3.8	0.9	8.7	83.2	99	22	3	28	152

*Per 100 g. of reacted n-butane.

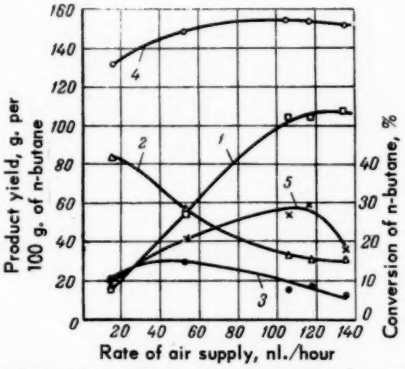

Fig. 5. Effect of air supply on the oxidation process (P = 60 atm., t = 165°C, τ = 6 hours, q = 0.03 g.): 1. acetic acid; 2. ethyl acetate; 3. methylethylketone; 4. overall yield of useful products; 5. conversion of n-butane.

From the cited data it is seen that at temperatures ranging 165-180°C, high conversion of n-butane (30-39%) is combined with a good yield of acetic acid. Data on the effect of air supply are shown in Fig. 5. At low airflow rates, conditions are created which favor the stabilization of ketone and ester (if there is a shortage of oxygen, the compounds formed in the reaction mixture are largely low-oxidation products). Increasing the air supply leads to a higher yield of the end product of oxidation, acetic acid. The conversion of n-butane is likewise intensified. In our experiments a maximum was reached when air was supplied at the rate of 110-120 nl./hour.

The oxidation of hydrocarbons in liquid phase can be carried out without the use of catalysts. The addition of a catalyst, on the other hand, affects both the triggering of the reaction and its subsequent stages.

The effect of the catalyst on the oxidation of n-butane can be seen from experimental data shown in Table 3.

EFFECT OF INTERMEDIATE PRODUCTS

When the catalyst charge amounts to 0.03 g. the conversion of n-butane is good and is combined with a maximum yield of acetic acid.

Table 3

Effect of the amount of catalyst on oxidation of n-butane (P = 60 atm., t = 165°C., w = 120 nl./hour, τ = 6 hours)

Catalyst charge, %	Conversion of n-butane, %	Yield of useful products, g.*				
		CH_3COOH	C_4H_8O	C_2H_5OH	$C_4H_8O_2$	Total
0.00	19.5	62	25	14	39	140
0.01	30.0	79	25	8	39	151
0.03	30.0	104	18	2	31	155
0.06	34.8	90	22	3	34	149
0.09	28.0	86	22	5	36	149

*Per 100 g. of reacted butane.

From the theory of chain reactions with degenerated branching, it is known that intermediate products can exert a substantial effect on the course of the reaction (18). In oxidation of n-butane in the liquid phase, methylethylketone is one of such intermediate products. In this connection it seemed interesting to study the effect of methylethylketone additions. As shown experimentally, its concentration at the end of the reaction remains constant, irrespective of the amount added to the reaction mixture:

Beginning of experiment g./ml.	End of experiment g./ml.	Yield of acetic acid g.*
0.000	0.021	63
0.022	0.023	83
0.037	0.020	113

*Per 100 g. of reacted n-butane.

If the initial ketone dosage is small, its formation in the course of the reaction continues until a certain concentration limit is reached. If the amount of the added ketone exceeds this limit, the excess ketone is converted to acetic acid. In this case the yield of acetic acid will obviously rise, while the conversion of n-butane will not change. Analogous observations were made on addition of another reaction product, ethyl acetate. This shows that neither methylethylketone nor ethyl acetate inhibits the reaction.

In this connection it was interesting to check the effectiveness of using a solvent made up of a reaction product containing acetic acid, methylethylketone, ester, water, and small quantities of other substances. From the data obtained (Table 4) it is seen that the use of a reaction product as solvent lowers the conversion of n-butane and the efficient utilization of this substance. The overall yield of useful products also decreases in this case, while the yield of acetic acid rises. This last face is due to the complete oxidation of the intermediate products, whose yields decrease sharply. If the solvent is made up of the low-boiling fraction of the product (under 100°C), the oxidation will be completed and the ketone, as well as ester, will be converted to acetic acid, under the conditions controlling the process.

The lowering of the reaction rate is probably related to the variations of n-butane concentration in the solution, since the presence of water in the reaction product functioning as solvent leads to stratification of the reaction mixture.

In Table 5 are given data obtained by G. D. Efremova and P. M. Koroleva, of the GIAP (State Institute of the Nitrogen Industry), while studying the phase state of the system n-butane - acetic acid.

Table 4

Composition of solvent: effect on the oxidation process (P = 60 atm., t = 165°C, w = 120 nl./hour, q = 0.03 g., r = 3 hours)

Composition of solvent, g.				Composition of gas phase, vol. %					Yield of useful products, g.*				Conversion of n-butane, %	Utilization efficiency, %
CH_3COOH	C_4H_8O	$C_4H_8O_2$	H_2O	CO_2	O_2	CO	C_4H_{10}	N_2	CH_3COOH	C_4H_8O	$C_4H_8O_2$	Total		
170.0	—	—	—	2.9	5.0	1.3	11.4	79.4	55.0	24.0	57.0	136.0	22.1	83.8
125.0	8.5	20.6	17.2	3.1	8.5	1.0	11.5	75.9	97.0	11.0	—	108.0	11.6	65.8

*Per 100 g. of reacted n-butane.

Table 5

Phase composition of the reaction medium

Concn. of acetic acid %	Composition of initial mixture, g.			Weight of lower layer, g.	Weight of upper layer, g.	Composition of lower layer, g.			Composition of upper layer, g.			Ratio n-butane: acetic acid	
	CH_3COOH	H_2O	C_4H_{10}			CH_3COOH	H_2O	C_4H_{10}	CH_3COOH	H_2O	C_4H_{10}	Lower layer	Upper layer
100	170	—	173	Unstratified									1,00
90,0	153	17	170	114	226	71	8	35	82	9	135	0,49	1,65
85,0	145	25	170	128	212	94	20	14	51	5	156	0,15	3,06
80,0	119	29	175	115	208	84	26	5	35	3	170	0,06	4,86

From these data it is seen that the use of acetic acid as a solvent causes a separation of the reaction mixture into two layers whenever the concentration of acetic acid falls below 100%. The ratio: reacting n-butane : solvent is not the same in the two layers. From the previously cited data (Fig. 3) it follows that the optimum value for the ratio n-butane : acid lies in the range 0.5-1. This condition is satisfied only by those experiments (Table 5) where the concentration of acetic acid equaled or exceeded 90%. Under these conditions, the conversion of n-butane is sufficiently high, and so is the yield of useful products.

CONCLUSIONS

1. Optimum conditions were determined for the reaction in which n-butane was oxidized under pressure by air oxygen into acetic acid in the presence of a solvent.

2. It was shown that addition of methylethylketone or ethyl acetate will not exert any negative effect on the process, and will in fact improve its selectivity. The concentrations of methylethylketone and ethyl acetate additions were found to approach the limiting value.

3. Glacial acetic acid proved an effective solvent. A reaction product reinforced with acetic acid can also be used.

LITERATURE CITED

1. Thornton, D. P., *Petrol. Process*, 8, 7, 1041 (1953).
2. *Oil Gas J.*, 52, 174 (1954).
3. Powers, E. G., *IV International Petroleum Congress*, 5, 57 (1956).
4. Sherwood, A. W., *World Petrol.*, 27, 11; 27, 12, 42 (1956).
5. *Chem. Eng. News*, 34, 20 (1959).
6. Furman, M. S., Badrian, A. S., Gol'tyayeva, N. A., Savchuk, S. N., *Gaz. Prom.*, No. 10, 36 (1958).
7. Wiezewich, P. I., Frolich, P. K., *Ind. Eng. Chem.*, 26, 367 (1934).
8. Quon, D., Lana, I., Dalla, Govier, C. W., *Canad. J. Chem.* 32, 880 (1954).
9. *US Patent* 2265948, 1941.
10. *US Patent* 2653962, 1953.
11. *US Patent* 2287125, 1938.
12. Emanuel, N. M., *Doklady Akademii Nauk*, 110, 245 (1956).
13. Blumberg, E. A., Maizus, Z. K., Emanuel, N. M., *Oxidation of Hydrocarbons in the Liquid Phase*, Publ. Acad. Sci. USSR, 1959, p. 125.
14. Shkol'nik, F. Ya., *Commission on Analytical Chemistry, Transactions*, 6, 505 (1955).
15. Gulyayeva, A. I., Polikarpova, V. F., Remiz, Z. K., *Analysis of Products Obtained in Divinyl Production from Ethyl Alcohol, by the method of S. V. Lebedev*, Goskhimizdat, 1950.
16. Denisov, E. T., *Graduation Thesis*, Moscow State University, 1956.
17. Knorre, D. G., Maizus, Z. K., Obukhova, M. K., Emanuel, N. M., *Uspekhi Khimii*, 26, 416 (1957). (This reference is not cited in the text. Transl.)
18. Kruglyakova, K. E., Emanuel, N. M., *Izvestiya Academii Nauk SSSR, OKhN*, 3, 417 (1959).

N. B. Yanovskaya
K. K. Potapova

USSR

Investigations of Polyacrylonitrile Fibers Obtained at Various Drafts

Investigation of changes in fiber texture brought about by changes in draft and temperature, and quantitative data on the structure of acrylonitrile fibers.

THE physical and mechanical properties of man-made fibers are mainly determined by spinning conditions. Previously we have shown (1) that when acrylonitrile fibers are spun with the use of various plasticizing and precipitating baths, the structural elements of the acrylonitrile fibers - fibrils consisting of bundles of macromolecules - assume various shapes and sizes. The character of their arrangement along the fiber is determined at drawing and depends on the draft.

This paper describes results of an electron microscope and x-ray investigation of polyacrylonitrile fiber - nitron, produced at various drafts and which was then subjected to thermal treatment.

For plasticizing and precipitating baths, preparation OP-10 (polyethylene glycol alkyl phenyl ethers) was used. The starting material for the spinning of the fiber is the polymer of acrylonitrile.

We have obtained an electron microscope photograph and an x-ray diffraction diagram of this polymer. Acrylonitrile polymer (Fig. 1) consists of small spheres about 0.2 μ in diameter. The x-ray diffraction pattern of the polymer powder (Fig. 2) has two interference (diffraction) rings which are located near each other. The sizes of the chain link as determined from the x-ray diffraction diagram are 5.18 and 5.49 Å; this means that there are two types of links which differ slightly in size.

The molecular weight of acrylonitrile fiber varies from 100,000 to 300,000, the molecular weight of one link of the macromolecule is equal to 53, and the number of cells in one macromolecule is from 4,400 to 5,700. As was mentioned above, the size of one cell is equal to about 5.3 μ, and therefore the length of an extended macromolecule of polyacrylonitrile varies within the limits of 2.3 to 3 μ.

We had at our disposal fibers with five different drafts (1.55, 1.87, 2.22, 2.53 and 2.87). The arrangement of fibrils could be observed with an electron microscope. It should be noted that a fiber with a low draft splits very poorly and it is difficult to observe it with an electron microscope. This may be explained by the fact that the macromolecules in such a fiber are randomly distributed and because of this such a fiber is brittle and easily broken.

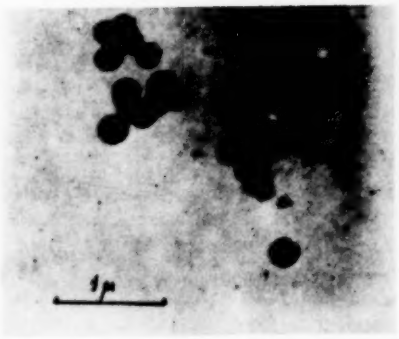

Fig. 1.

Fig. 3 shows an electron microscope photograph

Fig. 2.

This article first published in *Izvest. Vysshikh. Zaved., Tekhnol. Tekstil. Prom.*, No. 3 (16), 24-29 (1960). The authors are associated with the S. M. Kirov Leningrad Textile Institute.

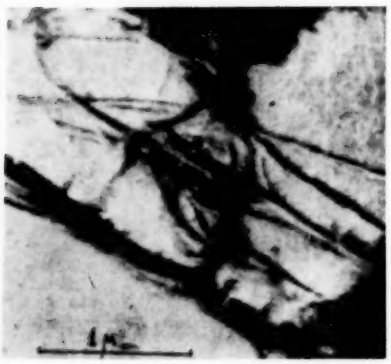

Fig. 3.

of a nitron fiber obtained with a high draft (2.87), magnified 13,000 times. As is evident from the figure, the fiber is split into separate fibrils and this permits determining their transverse size. The mean thickness of the fibrils obtained from 50 measurements made from different photographs, is about 250 Å, and their cross-sectional area is about 5×10^4 Å^2. The cross-sectional area of polyacrylonitrile fibers obtained with a draft of 1.25 is 200 μ^2 (2), and, therefore, with close packing the cross section contains about 5×10^5 fibrils.

With variation of the draft, the arrangement of the structural elements of the fibrils themselves, i.e., of the macromolecules, also changes. Since the separate fibrils do not split, it is impossible to observe the change of their structure with an electron microscope. These changes may be well observed using the x-ray diffraction method. Fig. 4 shows a series of x-ray photographs taken with

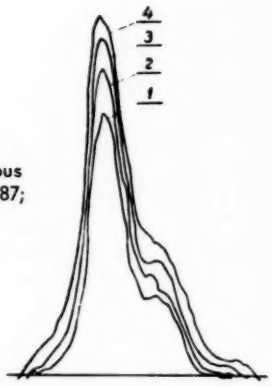

Fig. 5. Curves obtained for various drafts of the fiber: 1) 1.55; 2) 1.87; 3) 2.22; 4) 2.87.

fibers which were obtained with various drafts. All the x-ray photographs are characterized by two interference (diffraction) rings. However, in proportion to the increase of the draft, the x-ray photographs change - the interference arcs decrease in size with continuous increase of intensity on the equatorial parts. The change of this pattern is particularly evident in fibers with a high draft. A qualitative estimate of these changes may be made from the picture of the continuously changing texture of the fiber as a function of the draft.

The variation in intensity of the maxima was observed by using the instrument URS-50, which enabled us to investigate the maxima without making the x-ray photographs. The curves in Fig. 5 show the variation of the density of the interference rings along the equator of the diffraction pattern of the fibers. These curves show that the intensity of the maxima on the equator increases in proportion to the increase in the draft, and this indicates an in-

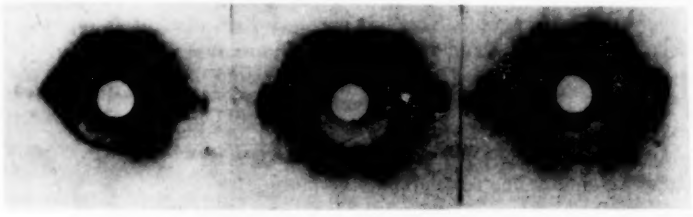

a b c

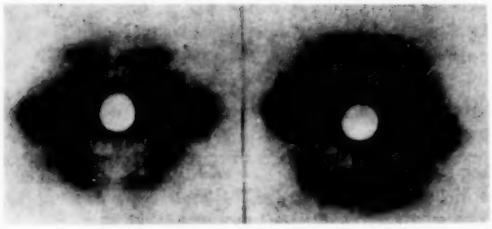

d e

Fig. 4. X-ray photographs of nitron fiber for various drafts. a) 1.55; b) 1.87; c) 2.20; d) 2.53; e) 2.87.

crease in the orientation of the macromolecules along the fiber.

The interference pattern produced on the x-ray photographs relates to the planes of reflection which are perpendicular to the axis of the fiber. The magnitude of the structural group along the fiber axis, which was obtained from these x-ray photographs, is 21 Å, i.e., the structural group contains 4 elementary links. This means that when a fiber is drawn (stretched), a rotation of the chain links of the macromolecules takes place which has a random thermal character. The structural group of the polyacrylonitrile may be represented as follows:

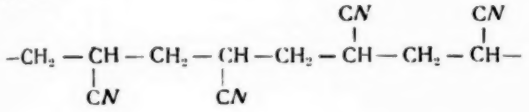

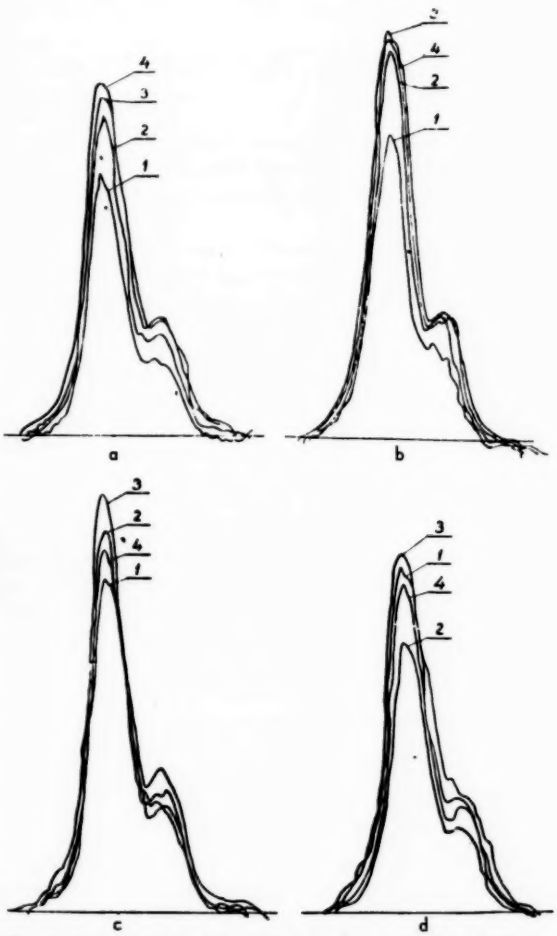

Fig. 6. Curves obtained for various drafts: a) 1.55; b) 1.87; c) 2.22; d) 2.87. 1) Unheated fiber; 2) heated to 80°C; 3) to 100°C; 4) to 110°C.

A fiber of acrylonitrile heated to temperatures of 80, 100, and 110° C was also investigated. This treatment shrank the fiber, and as a result of this the mechanical properties of the fiber were changed The dependence of the intensity of the interference maxima was determined along the equator of the x-ray patterns of the fibers heated to the various temperatures.

Fig. 6 (a, b, c, d) shows curves of the density variation of the maxima along the equator of the fibers heated to the various temperatures. It is evident from this Figure that, for heating to 100°C, the density of the maxima in the interference pattern increases for fibers with a draft from 1.55 to 2.53, and this indicates an improvement in their texture. With further heating of the fibers, the density of the maxima decreases, and this is apparently connected with rupture of the macromolecules, brought about by the heating, which results in worsening of the fiber texture.

Fibers with a draft of 2.87 show fluctuation in the density of the maxima with heating. Such changes in the interference pattern of the x-ray diagrams of the fibers are related to the change in their physical and mechanical properties with heating. Fig. 7 shows curves for the variation in the strength of fibers obtained with various drafts and heated to various temperatures; these curves show that the strength of the unheated fibers sharply increases with increase in the draft. After heating to 80°C the strength of the fibers increases much more slowly. Moreover, as compared with the unheated fibers, the fibers with a lower draft show greater strength and those with a higher draft show smaller strength. With heating of the fiber to 100°C,

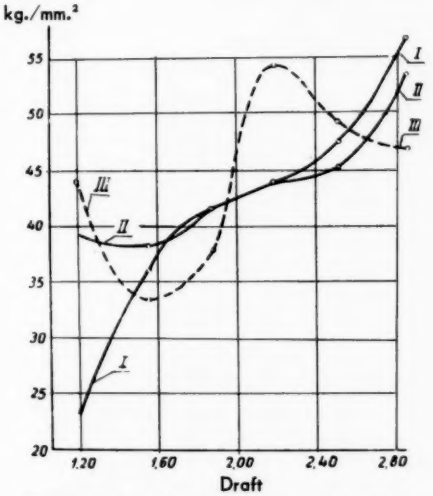

Fig. 7. Curves showing variation of the fiber strength with increase in draft. I) Unheated fiber; II) heated to 80°C; III) heated to 100°C.

fluctuation in its strength with variation of the draft is observed, and this is probably due to rupture of the macromolecules, as was mentioned earlier. From the above curves it is also evident that the fluctuation of the maxima in the interference pattern for fibers with a draft of 2.87 is associated with an increase of fiber strength with heating. The picture of the variation in fiber strength may serve as a kind of confirmation of the observed pattern of structural changes.

Therefore, the described investigation permits us to form a picture of the changes in fiber texture brought about by changes in draft and temperature, and also to obtain certain quantitative data concerning the structure of acrylonitrile fibers.

LITERATURE CITED

1. Yanovskaya, N. B., *Izvest. Vysshikh. Ucheb. Zaved., Tekhnol. Tekstil. Prom.* No. 4, 15 (1958).
2. Roskin, E. S., *Zhur. Priklad. Khim.* 30, No. 1 (1957).

P. V. Varentsov
M. S. Yufa

USSR

The Movement of a Bed of Solid Particles in Rotary Kilns

Dimensional analysis used to investigate role of various factors affecting a moving bed of solid particles in a rotary kiln, and a determination of scale-up conditions. Special attention is paid to the effect of particle size.

A number of investigators (1-11), studying the problem of the movement of a bed of solid particles in rotary kilns, have proposed empirical formulae for determining the rate with which the materials being treated in the kilns are moving. In the present work, an attempt was made to describe this phenomenon using dimensional analysis in order to explore the role of the different factors having an effect on the moving bed, and to determine the conditions for the scaling up of kilns.

An expression for the movement of a bed of solid particles in a rotary kiln (or rotating tubular furnace) may be expressed in the form of the following functional dependence:

$$w_s = f(w_g^a, \gamma_g^b, \gamma_s^c, \mu^e, d_s^h, D_f^i, w_f^j, \alpha_f^k, g^m, \beta_s^h, L_f^p, \varphi_f^q)$$

where w_s is the rate of movement of the solid particles, m./sec.; w_g is the gas velocity in the kiln, m./sec.; γ_g is the specific gravity (Translator's Note: sic; density is obviously meant) of the gas, kg./m.^{3}; γ_s is the specific gravity (Translator's Note: sic; density is obviously meant) of the solid particles, kg./m.^{3}; μ is the gas viscosity, kg./(sec.)(m.^{2}), d_s is the controlling size of the solid particles, m.; D_f is the kiln (furnace) diameter, m.; w_f is the peripheral (circumferential) velocity of kiln rotation, m./sec.; α_f is the kiln inclination angle, degrees; g is the acceleration due to gravity, m./sec.^{2}; β_s is the natural angle of repose of the solid particles; degrees; L_f is the kiln length, m.; and φ_f is the degree to which the kiln cross section is filled, m.^{2}.

The 13 variables listed are expressed in terms of four units of measurement. According to the π-theorem of dimensional analysis, the relationship between the listed variables must be determined by nine (13-4) similarity criteria and similarity simplexes. There are seven quantities which have different dimensional units ($w, \gamma, \mu, d, \alpha, g, \varphi$). The number of simplex criteria* is 13 − 7 = 6. The number of complex criteria* is 9 − 6 = 3.

Using the usual dimensional analysis procedure, we obtain the following expression involving three

This article first published in *Khim. Mashinostroenie*, No. 5, 22-26 (1959).

*Translator's Note: It would appear from the context (here and elsewhere) that a "simplex" group or criterion is a dimensionless group which contains a simple ratio of two variables; a "complex" group or criterion either involves more than two variables in a single dimensionless group, or it involves two variables in other than a linear ratio. Thus, (a/b) is a simplex, whereas (a/b^2) or (ac/b) are complexes.

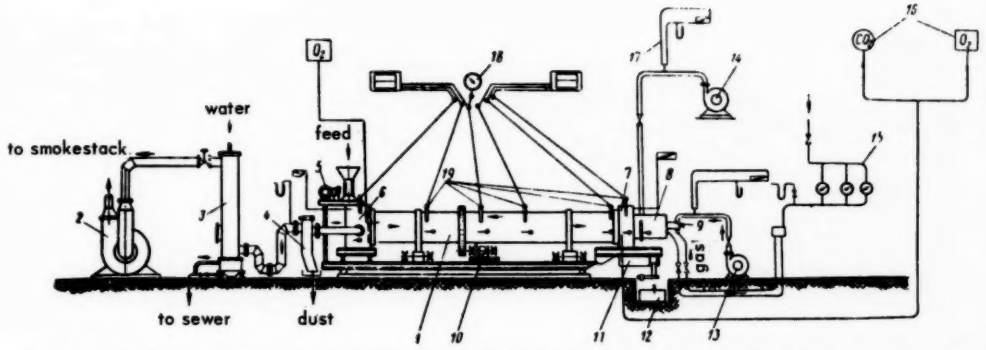

Fig. 1. Equipment arrangement of the experimental rotary kiln (furnace). 1) kiln; 2) exhaust fan; 3) scrubber; 4) multi-cyclone; 5) kiln feeder; 6) cold end of the kiln; 7) hot end; 8) furnace precombustion chamber; 9) gas burner; 10) kiln drive; 11) cooler (or condenser); 12) receiver for finished product; 13) primary air blower; 14) secondary air blower; 15) gas mains; 16) electrical gas analyzer for CO_2 and O_2; 17) Prandtl tube; 18) galvanometer and switch; 19) thermocouples.

criterial complexes and six simplexes:

$$\left(\frac{w_s}{w_g}\right) = f\left[\left(\frac{w_g\mu}{\gamma_g d_s^2}\right)^e \left(\frac{d_s g}{w_g^2}\right)^m \left(\frac{w_f}{w_g}\right)^j \left(\frac{\gamma_s}{\gamma_g}\right)^c \times \left(\frac{\varphi_f}{d_s^2}\right)^q \left(\frac{D_f}{d_s}\right)^i \left(\frac{\beta_s}{\alpha_f}\right)^n \left(\frac{L_f}{d_s}\right)^p\right] \quad (1)$$

The criterion (ratio, number) $d_s g/w^2 g$ corresponds to the Froude number (or group), while the criterion (ratio) $w_g\mu/\gamma_g d_s^2$ multiplied by the ratio $d_s g/w_g^2$ gives the Reynolds number.

As a result, Eq. (1) may be expressed in the following form:

$$\frac{w_s}{w_g} = f\left[Re^e Fr^m \left(\frac{w_f}{w_g}\right)^j \left(\frac{\gamma_s}{\gamma_g}\right)^c \left(\frac{\varphi_f}{d_s^2}\right)^q \left(\frac{D_f}{d_s}\right)^i \left(\frac{\beta_s}{\alpha_f}\right)^n \left(\frac{L_f}{d_s}\right)^p\right] \quad (2)$$

We replace the Froude number in Eq. (2) by the Gallileo criterion, $Ga = Re^2/Fr$, to simplify the modelling; then:

$$\frac{w_s}{w_g} = f\left[Re^e Ga^m \left(\frac{w_f}{w_g}\right)^j \left(\frac{\gamma_s}{\gamma_g}\right)^c \left(\frac{\varphi_f}{d_s^2}\right)^q \left(\frac{D_f}{d_s}\right)^i \left(\frac{\beta_s}{\alpha_f}\right)^n \left(\frac{L_f}{d_s}\right)^p\right] \quad (3)$$

The explicit form of the functional relationship between the similarity criteria (numbers) was determined experimentally.

The study of the movement of a bed (layer) of solid particles was conducted in a kiln 6 m. in length with an outside diameter of 714 mm. (Fig. 1). Its internal diameter was 300 mm. in certain tests and 550 mm. in others. The kiln was fitted with the necessary instruments; it was gas-fired and operated in a countercurrent manner.

Four materials (feed stocks) having different specific gravities (densities) were taken for the tests: run-of-mine pyrite, marble chips, sand, and coke. Each material was separated into four fractions by sieving. The average diameter of the particles of each fraction was determined using a FR-1 apparatus. The natural angle of repose of the material was determined by the Koler (Kohler?)* method (11) and was calculated using the formula:

$$\tan \alpha = \sqrt{\pi h^3/3v}$$

where h is the height of the cone of the material, cm., and v is the volume of the cone, cm^3.

The average velocity of the gas in the kiln was determined from the consumption of primary and secondary air and from the amount of gas burned. The time for charging the material into the kiln exceeded its residence time in the kiln by a factor of 2. A recording of the instrument readings was made every 30 minutes during the second half of the test. Average data for the steady state conditions were utilized in the calculations. After each test, the average residence time of the material in the kiln was determined by dividing the weight of the material discharged from the kiln by the average hourly change. The characteristics of the materials taken for investigating the movement of a bed of solid particles are given in the table (Table 1).

In studying the movement of a bed of solid particles in a kiln, we first established the dependence of w_s/w_g on each of the criteria (numbers, ratios) which appear in Eq. (3). This dependence was expressed by specific equations, which were then checked by comparing the results obtained with their use with the experimental data.

*Translator's Note: spelling uncertain because of backtransliteration from Russian.

Table 1

Material	Fraction I			Fraction II			Fraction III			Fraction IV		
	Particle size, mm.	Natural angle of repose, degrees	Density, kg./m.³	Particle size, mm.	Natural angle of repose, degrees	Density, kg./m.³	Particle size, mm.	Natural angle of repose, degrees	Density, kg./m.³	Particle size, mm.	Natural angle of repose, degrees	Density, kg./m.³
Marble chips	0.42	30.13	2739	1.70	27.0	2765	4.40	26.0	2793	7.28	25.87	2793
Sand	0.53	29.67	2650	1.54	27.33	2650	3.98	26.67	2656	7.38	26.50	2670
Run-of-mine pyrite	0.35	35.33	4422	1.55	27.38	4517	3.92	25.22	4452	7.17	23.27	4384
Coke	0.56	30.70	1789	1.51	27.60	1883	3.81	29.20	1939	7.07	29.00	1944

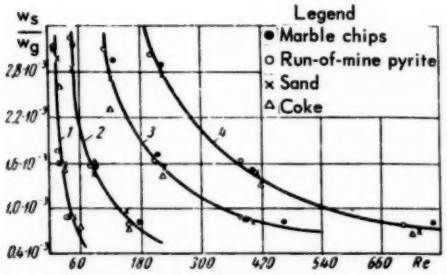

Fig. 2. w_s/w_g as a function of the Reynolds number. Ga varies over the following ranges: 1) 1.82 to 8.57; 2) 161 to 220; 3) 2,585 to 3,935; 4) 16,400 to 18,700.

The following specific equations were obtained:

$$\frac{w_s}{w_g} = \frac{0.0232}{Re}\,Ga^{0.33} \tag{4}$$

$$\frac{w_s}{w_s} = \frac{3.202}{Re}\left(\frac{\alpha_f}{\beta_s}\right)^{0.66} \tag{5}$$

$$\frac{w_s}{w_g} = 0.0572\,\frac{w_f}{w_g} \tag{6}$$

$$\frac{w_s}{w_g} = \frac{0.403}{Re}\left(\frac{\varphi_f}{d_s^2}\right)^{0.08} \tag{7}$$

The dependence of the ratio w_s/w_g on various numbers (ratios) are shown in Figs. 2-6.

It can be seen from Fig. 6 that a change in the gas temperature in the kiln does not affect the rate of motion of the bed of solid particles in it; in the general equation, this will be expressed by a constant coefficient which depends only on the specific gravity (density) of the material. The maximum difference in the values of w_s/w_g amounted to about 19% for the values for coke with a density of 1,944 kg./m.³ and for run-of-mine pyrite with a density of 4,384 kg./m.³. Consequently, if a single average coefficient is used for these materials, the maximum error will be about 9%. In this case, the

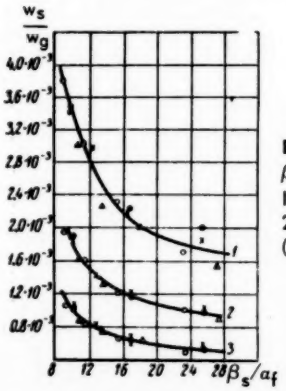

Fig. 3. w_s/w_g as a function of β_s/α_f. Re varies over the following ranges: 1) 195 to 235; 2) 372 to 435.3; 3) 695 to 770. (Symbols same as in Fig. 2.)

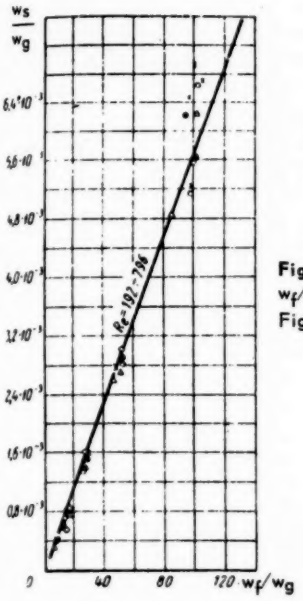

Fig. 4. w_s/w_g as a function of w_f/w_g. (Symbols same as in Fig. 2.)

ratio γ_s/γ_g can be eliminated from Eq. (3).

As can be seen from Fig. 7, the dependence of w_s/w_g on L_f/d_s for different materials is expressed by horizontal lines which lie close to one another. Consequently, the average rate of motion of the bed of solid particles in a rotary kiln is practically independent of the length of the kiln, and L_f/d_s can be eliminated from Eq. (3).

Setting the values of the ratios from Eqs. (4)-(7) into Eq. (3), and determining the overall coefficient and the exponent of Re by a method of successive approximations, we obtain the following criterial equation:

a) for a kiln 0.3 m. in diameter:

$$\frac{w_s}{w_g} = 0.000254\mathrm{Re}^{-0.01}\,\mathrm{Ga}^{0.33}\left(\frac{\alpha_f}{\beta_s}\right)^{0.66}\left(\frac{w_f}{w_g}\right)\left(\frac{\varphi_f}{d_s^2}\right)^{0.08}\left(\frac{D_f}{d_s}\right)^{0.93} \tag{8}$$

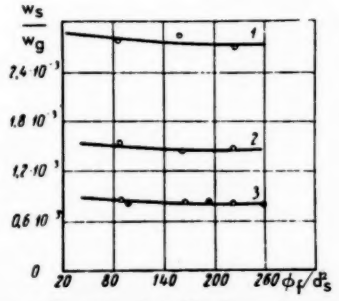

Fig. 5. w_s/w_g as a function of ϕ_f/d_s^3. Re varies over the following ranges: 1) 208 to 238; 2) 389 to 440; 3) 694 to 772. (Symbols same as in Fig. 2.)

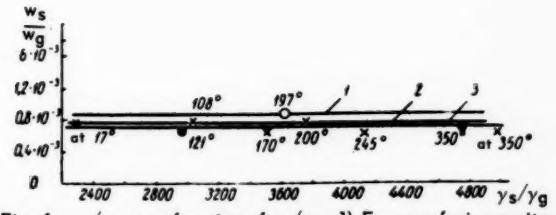

Fig. 6. w_s/w_g as a function of γ_s/γ_g. 1) For run-of-mine pyrite; 2) for sand; 3) for marble chips.

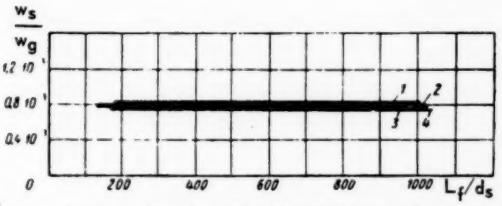

Fig. 7. w_s/w_g as a function of L_f/d_s. 1) For run-of-mine pyrite with Re ranging from 681 to 704; 2) for sand with Re ranging from 727 to 738; 3) for marble chips with Re ranging from 717 to 763; 4) for coke with Re ranging from 707 to 723.

b) for a kiln 0.55 m. in diameter:

$$\frac{w_s}{w_g} = 0.000167\mathrm{Re}^{-0.01}\,\mathrm{Ga}^{0.33}\left(\frac{\alpha_f}{\beta_s}\right)^{0.66}\left(\frac{w_f}{w_g}\right)\left(\frac{\varphi_f}{d_s^2}\right)^{0.08}\left(\frac{D_f}{d_s}\right)^{0.93} \tag{9}$$

The experimental data are compared in Fig. 8 with results calculated from Eq. (8).

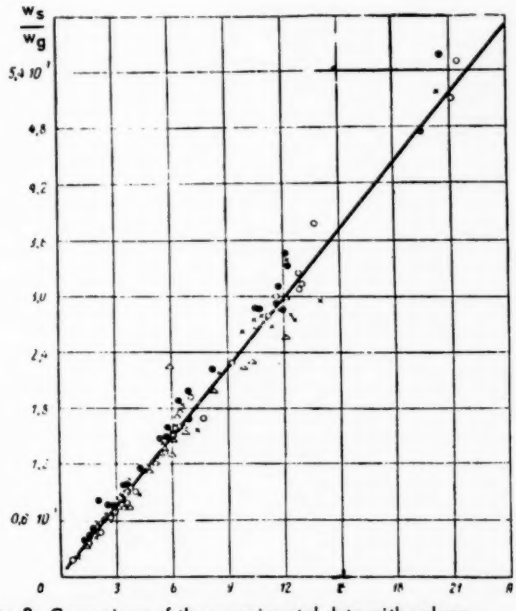

Fig. 8. Comparison of the experimental data with values calculated using Eq. (8). (Symbols are the same as those in Fig. 2.)

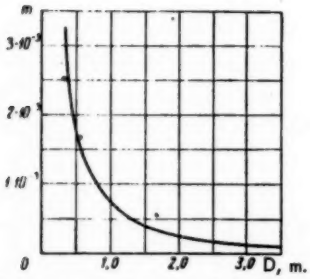

Fig. 9. Coefficient m as a function of the kiln diameter.

w_s/w_g and w_f/w_g appear in the first degree in Eqs. (8) and (9). They may be divided by one another, and then these equations are somewhat simplified and assume the following final form:

$$\frac{w_s}{w_f} = mRe^{-0.01}Ga^{0.33}\left(\frac{\alpha_f}{\beta_s}\right)^{0.66}\left(\frac{\varphi_f}{d_s^2}\right)^{0.08}\left(\frac{D_f}{d_s}\right)^{0.93}$$

where m is a coefficient depending on the kiln diameter.

In view of the impossibility of determining coefficient m experimentally for kilns of different diameters, it was found theoretically. For this purpose all of the necessary data were taken from the experiments, while the rates of movement of the material in kilns of different diameters were calculated using the Sullivan, Maier, and Ralston formula (1) which gives results sufficiently close to actuality:

$$\tau = \frac{\tau_0}{0.0963D\alpha} L$$

where τ is the residence time for the material in the kiln, hours; τ_0 is the time for one rotation of the kiln, hours; L is the kiln length, m.; D is the kiln diameter, m.; and α is the angle of inclination of the kiln, degrees.

The relationship obtained between the coefficient m and the kiln diameter is shown in Fig. 9. As can be seen, the experimental values of the coefficient for kilns 0.3 and 0.55 m. in diameter (points in the figure) lie sufficiently close to the curve calculated from the formula.

LITERATURE CITED

1. Sullivan, I. D., Maier, C. G., and Ralston, O. C., *Technical Paper of the U. S. Bureau of Mines*, No. 384 (1927).
2. Bayard, R. A., *Chem. Met. Eng.* 52, 100-102 (1945).
3. Voroshilov, A. P., *Sovremennye problemy sushil'noi tekhniki*, GONTI (State United Publishing House of Science and Technology), USSR (1938).
4. Khodorov, E. I., *Dvizhenie materiala vo vrashchayushchikhsya pechakh*, Promstroiizdat (State Publishing House of Literature on Building Materials) (1957).
5. Rutle, I., *Pit and Quarry*, 48, No. 1, 120-136 (1955).
6. Kramers, N., and Croockewit, P., *Chem. Eng. Sci.* 1, No. 6, (1952).
7. Vahl, L., and Kingma, W. C., *Ibid.*, 1, No. 6 (1952).
8. Anselm, W., *Zement-Kalk-Gips*, No. 11, 427-434 (1954).
9. Bigen, H., *Ibid.*, No. 11, 434-436 (1954).
10. Schwarz, V., and Bergkampf, E., *Ibid.*, No. 11, 424-427 (1954).
11. Andreev, A. F., Matveev, V. A., and Nikoforova, S. A., *Khim. Prom.*, No. 1-2, 14 (1946).

Somogyi, Ágnes
Géczy István
Dobó János

HUNGARY

Graft Copolymerization in the Presence of Benzoyl Peroxide-Dimethyl Aniline with the Aid of Irradiation

Experimental data on use of initiator-activators for graft copolymerization with irradiation, and determination of the optimum indicator-activator concentration at which grafting is relatively large and separation of homopolymers from the membrane is still possible.

HOMOPOLYMERIZATION initiated by high-energy irradiation usually progresses by the free-radical mechanism. All monomers that can be polymerized by the free-radical mechanism are suitable for polymerization. Several review papers have been published on this type of polymerization (1, 2, 3).

Experience shows that different monomers are not equally sensitive to irradiation, i.e. they do not utilize the absorbed energy to the same extent (4). The reactions of irradiation-insensitive compounds can be accelerated by the addition of irradiation-sensitive solvents (water, methanol). In such cases, the primary radicals are formed either in the solvent or on the partially formed polymer. The latter case is feasible because the polymer which does not contain a substantial number of double bonds is more sensitive to irradiation than the monomer (5).

Homopolymerization with irradiation has been extensively covered in the literature and has a well founded theory; however, only recently, reports dealing with irradiation-initiated graft copolymerization (1, 2, 5, 6, 7, 8) have been published. These reports often contain contradicting data.

The theory of irradiation-initiated graft polymerization is based on the premise that free radicals, acting as active centers, are formed in the polymer molecule upon irradiation.

EXPERIMENTS

There are no data on graft copolymerization or homopolymerization with irradiation in the presence of an initiator-activator system, although the theoretical as well as the practical significance of this type of experimentation is obvious. In our experiments we have investigated grafting with irradiation, of various monomers on polyvinyl chloride and polyethylene membranes in the presence of a benzoyl peroxide-dimethyl aniline initiator-activator system. Also, the amount of homopolymer formed from the monomers in the above system was determined.

EXPERIMENTAL METHOD

The monomers employed in our experiments were methyl methacrylate, vinyl acetate, and styrene. The monomers were purified by distillation and their purity was checked by refractometry. The polyethylene membrane was strongly oriented, its thickness was 0.034 mm., $\eta_{red.} = 0.73$, stretch 140%. The polyvinyl chloride membrane was made of PVC pearls, its thickness was 0.1 mm. and its "K" value was 88. The irradiation was carried out with a Stabili 250 X-ray machine, (made by Medicor X-Ray Works) with a 200 kv. and 15 ma. rating.

The monomers were prepared as solutions of fresh benzoyl peroxide-dimethyl aniline in various concentrations. The solutions were mixed before the experiments in a 1 : 1 mole ratio.

The membranes, of known weight and measuring 35 × 10 mm. were carefully cleaned with acetone. They were placed vertically in Jena-glass (Pyrex type-trans) test tubes, then 3 ml. of monomer was placed into each test tube containing various concentrations of the initiator-activator. Six test tubes were exposed to irradiation simultaneously. Two different concentrations (in batches of three test tubes each) of benzoyl peroxide-dimethyl aniline

This article first published in *Magyar Tud. Akad. Kemiai Oszt. Közl.*, 15, p. 18-28 (1961). The authors are associated with the Organic Chemical and Plastics Research Institute, Budapest, and the Chemical Plant Design Company, Budapest.

were used. The test tubes were cooled with acetone and dry ice, deaerated several times, and finally sealed. The irradiation was performed in several steps. In the case of methyl methacrylate, each experiment took 5 hours. During this time, 4 minutes out of each ½ hour period were devoted to irradiation, and 26 minutes to diffusion without irradiation.

When styrene was used, each experiment lasted 9 hours, during which time 20 minutes out of each ½ hour period were devoted to irradiation, and 10 minutes to diffusion without irradiation.

After the experiments, the test tubes were opened, the membranes removed and the adhered homopolymers removed by solvents. The amount of homopolymer in the monomers was determined by refractometry. The amount of grafting per unit weight of membrane was determined from the following, frequently cited, expressions:

$$y = \frac{P - P_0}{P_0}, \text{ that is } = \frac{P}{P_0} - 1,$$

where y is the weight increase per unit weight of starting polymer, P_0 is the weight of original membrane and P is the weight of the grafted membrane.

EXPERIMENTAL RESULTS

Grafting of Methyl Methacrylate on Polyethylene Membrane. First, the effect of the initiator-activator concentration on the amount of the graft copolymer formed was investigated.

Concentrations greater than 0.01 mole/liter of initiator-activator were not used because, due to fast homopolymerization, the starting monomer thickened in a few minutes while its temperature increased. For comparison, a sample not containing the initiator-activator was also tested, and samples containing benzoyl peroxide-dimethyl aniline in various concentrations were tested without irradiation. In the latter experiments, graft copolymerization did not take place to any considerable extent, while, obviously, substantial homopolymerization was experienced.

The weight increases of membranes at various X-ray intensities and initiator-activator concentrations are shown in Table 1 and Figures 1 and 2. The extent of homopolymerization is summarized in Table 2 and Figures 3 and 4.

The results show that the graft of monomer strongly increases in the presence of benzoyl peroxide-dimethyl aniline initiator-activator system.

The grafting of methylmethacrylate at 31,400 r./hr. radiation intensity and 0.005 mole/liter

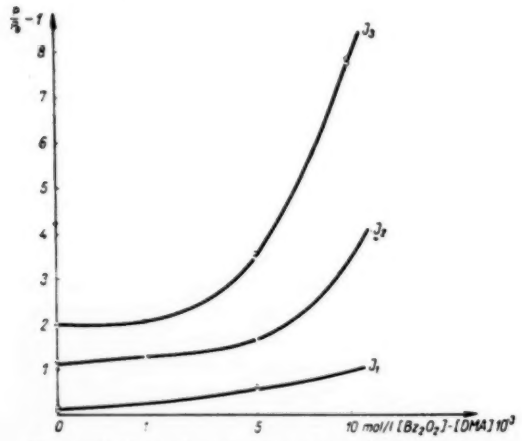

Fig. 1. Graft copolymerization of methyl methacrylate on polyethylene membrane as a function of initiator-activator concentration.
t: 25°C; abscissa scale: square root of concentration, mole/liter; J_1 = 9,600 r./hr.; J_2 = 16,000 r/hr.; J_3 = 31,400 r./hr.

Table 1
Graft copolymerization of methyl methacrylate on polyethylene membrane at various initiator-activator concentrations
t = 25°C; experimental time 5 hours

*Bz_2O_2-DMA mol/l	P_0	P	$\frac{P}{P_0} - 1$ g	$\frac{P}{P_0} - 1$ %
		I_0 = without irradiation		
0.00	0.0134	0.0134	—	—
	0.0129	0.0129	—	—
0.001	0.0161	0.0161	—	—
	0.0151	0.0151	—	—
0.005	0.0107	0.0110	0.029	2.9
	0.0145	0.0149	0.029	2.9
0.01	0.0114	0.0120	0.052	5.2
		I_1 = 9,600 r/h		
0.00	0.0129	0.0142	0.107	10.7
	0.0120	0.0132	0.108	10.8
0.001	0.0129	0.0183	0.436	43.6
	0.0116	0.0166	0.431	43.1
0.005	0.0123	0.0199	0.618	61.8
	0.0113	0.0176	0.600	60.0
0.01	0.0126	0.0230	0.825	82.5
	0.0128	0.0235	0.852	85.2
		I_2 = 16,000 r/h		
0.00	0.0110	0.0233	1.120	112.0
	0.0122	0.0271	1.220	122.0
0.001	0.0117	0.0273	1.333	133.3
	0.0122	0.0288	1.360	136.0
0.005	0.0128	0.0329	1.570	157.0
	0.0138	0.0364	1.640	164.0
0.01	0.0111	0.0461	3.153	315.3
	0.0133	0.0630	3.759	375.9
		I_3 31,400 r/h		
0.00	0.0122	0.0370	2.033	203.3
	0.0104	0.0317	2.048	204.8
0.001	0.0112	0.0352	2.157	215.7
	0.0126	0.0380	2.016	201.6
0.005	0.0131	0.0588	3.492	349.2
	0.0121	0.0550	3.550	355.0
0.01	0.0118	0.1044	7.847	784.7
	0.0133	0.1159	7.714	771.4

*Bz_2O_2 = Benzoyl peroxide
DMA = dimethyl aniline

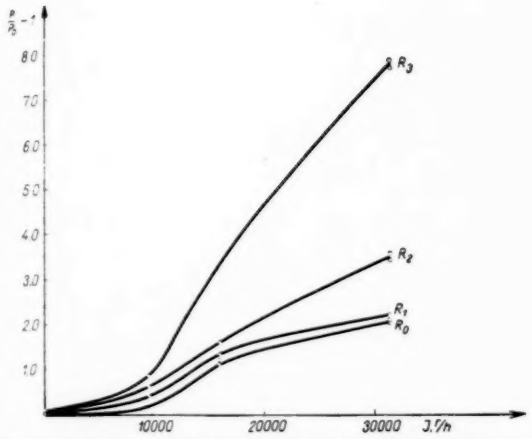

Fig. 2. Graft copolymerization of methyl methacrylate as a function of irradiation intensity.
t: 25°C; R_0: without initiator-activator; R_1 = 0.001 mole/liter Bz_2O_2 – DMA; R_2 = 0.005 mole/liter Bz_2O_2 – DMA; R_3 = 0.01 mole/liter Bz_2O_2 – DMA.

initiator-activator concentration was approximately 780%. This is relatively large as compared to 200% grafting under identical conditions without the initiator-activator. The influence of the increase of concentration of the initiator-activator in homopolymerization is much greater than that of increased irradiation intensity.

The Grafting of Vinyl Acetate and Styrene on Polyethylene Membrane. We have carried out experiments to graft pure and initiator-activator-containing vinyl acetate and styrene on polyethylene.

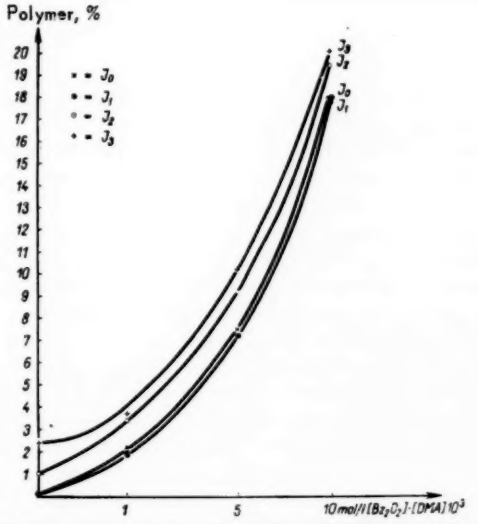

Fig. 3. Homopolymerization of methyl-methacrylate as a function of initiator-activator concentration at various irradiation intensities. t: 25°C; abscissa scale in square root of concentration.

Table 2
Homopolymerization of methyl-methacrylate at various initiator-activator concentrations

t = 25°C; experimental time 5 hours

Bz_2O_2-DMA mol/l	n_D^D	Homopolymer %	Bz_2O_2-DMA mol/l	n_D^D	Homopolymer %
I_0 = no irradiation			I_2 = 16,000 r/h		
0.00	1.4148	—	0.00	1.4154	1.0
0.001	1.4162	2.2	0.001	1.4168	3.4
0.005	1.4200	7.5	0.005	1.4212	9.2
0.01	1.4287	18.0	0.01	1.4288	19.5
I_1 = 9,600 r/h			I_3 = 31,400 r/h		
0.00	1.4148	—	0.00	1.4164	2.4
0.001	1.4158	1.9	0.001	1.4172	3.7
0.005	1.4198	7.2	0.005	1.4235	10.2
0.01	1.4278	17.8	0.01	1.4300	20.1

In the case of vinyl acetate grafting, copolymerization did not take place either with or without initiator-activator, but the measured refractive index indicated considerable homopolymer formation (see Table 3).

In the case of styrene, grafting takes place even without the initiator-activator, as has been known for a long time (1, 2, 5, 7). In this case, the extent of grafting was little influenced by the presence of the initiation-activator (see Table 4 and Figures 5 and 6). The homopolymerization was dependent only upon the concentration of the initiator-activator, while the intensity of irradiation had no significant effect.

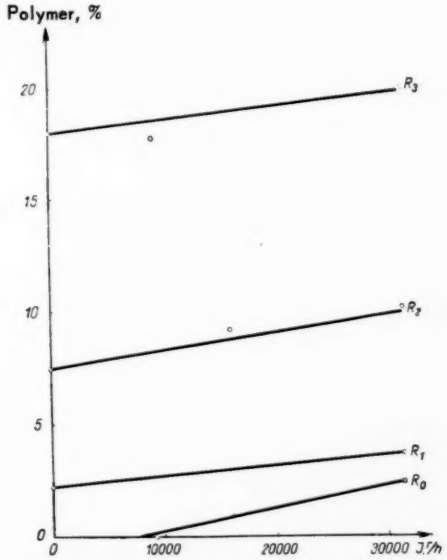

Fig. 4. Homopolymerization of methyl methacrylate as a function of irradiation intensity at various initiator-activator concentrations. t: 25°C; R_0: without initiator-activator; R_1 = 0.001 mole/liter Bz_2O_2 – DMA; R_2 = 0.005 mole/liter Bz_2O_2 – DMA; R_3 = 0.01 mole/liter Bz_2O_2 – DMA.

Table 3
Graft copolymerization of vinyl acetate on polyethylane membrane in the presence of initiator-activator

t = 25°C; experimental time 5 hours

Bz_2O_2-DMA mol/l	P_0	P	$\frac{P}{P_0}-1$	n_D^{20}	Homo-polymer %
		I_0 = without irradiation			
0.00	0.0103	0.0103	—	1.3960	0
	0.0103	0.0103	—	1.3962	0.1
0.001	0.0106	0.0106	—	1.3993	5.0
	0.0113	0.0113	—	1.3995	5.1
0.005	0.0114	0.0114	—	not measurable	—
	0.0110	0.0110	—	(thickened)	—
0.01	0.0105	0.0105	—	"	—
	0.0103	0.0103	—	"	—
		I_3 = 31,400 r/h			
0.00	0.0123	0.0124	—	1.3993	5.0
	0.0124	0.0124	—	1.3994	5.1
0.001	0.0106	0.0107	—	1.4810	6.5
	0.0122	0.0123	—	1.4011	6.5
0.005	0.0121	0.0121	—	not measurable	—
	0.0119	0.0119	—	(thickened)	—
0.01	0.0116	0.0117	—	"	—
	0.0118	0.0119	—	"	—

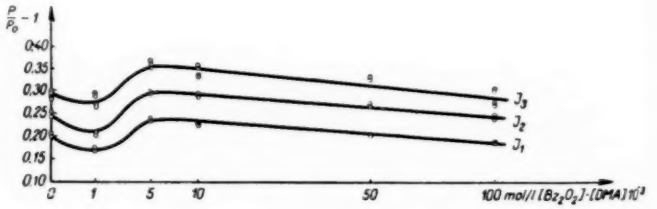

Fig. 5. Graft copolymerization of styrene as a function of initiator-activator concentration. t: 25°C; abscissa scale is square root of concentration; J_1 = 9,600 r./hr.; J_2 = 1,600 r./hr.; J_3 = 31,400 r./hr.

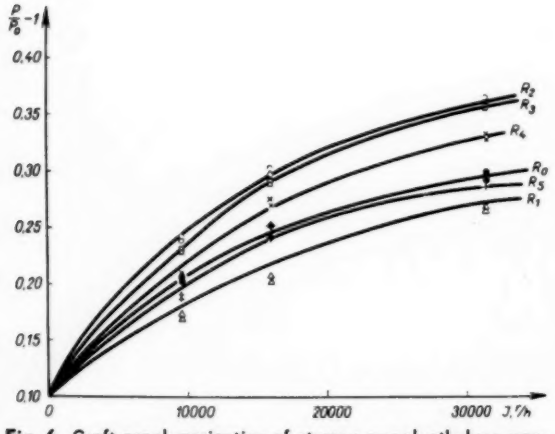

Fig. 6. Graft copolymerization of styrene on polyethylene membrane as a function of irradiation intensity. t: 25°C; R_0 = without initiator-activator; R_1 = 0.001 mole/liter Bz_2O_2 – DMA; R_2 = 0.001 mole/liter Bz_2O_2 – DMA; R_3 = 0.01 mole/liter Bz_2O_2 – DMA; R_4 = 0.05 mole/liter Bz_2O_2 – DMA; R_5 = 0.1 mole/liter Bz_2O_2 – DMA.

Grafting of vinyl acetate on polyvinyl chloride membrane, made of PVC pearl.

Based on the above, it seemed purposeful to use a membrane that swells in vinyl acetate. Polyvinyl chloride has such a property.

The initiator-activator concentration in this experiment was 0.001 mole/liter. At higher initiator-activator concentrations, the homopolymerization is so rapid that the separation of homopolymers from the membrane is impossible.

The results of the experiments with vinyl acetate are presented in Table 6. It can be seen that grafting does not take place without irradiation, but upon irradiation the grafting increases in the presence of the initiator-activator.

This last experiment was inconclusive, but it indicated that the grafting of vinyl acetate on polyvinyl chloride membrane could be increased by increasing the concentration of the benzoyl peroxide-dimethyl anyline initiator-activator system.

Table 4

Graft copolymerization of styrene on polyethylene membrane at various initiator-activator concentrations

t = 25°C; experimental time 9 hours

Bz_2O_2-DMA mol/l	P_0	P	$\frac{P}{P_0}-1$ g	$\frac{P}{P_0}-1$ %
	I_0= without irradiation			
0.00	0.0174	0.0174	—	—
	0.0138	0.0138	—	—
0.001	0.0178	0.0178	—	—
	0.0188	0.0188	—	—
0.005	0.0156	0.0158	0.013	1.3
	0.0180	0.0182	0.011	1.1
0.01	0.0198	0.0202	0.020	2.0
	0.0198	0.0202	0.020	2.0
0.05	0.0146	0.0153	0.048	4.8
	0.0204	0.0213	0.045	4.5
0.1	0.0158	0.0165	0.047	4.7
	0.0179	0.0187	0.044	4.4
	I_1 = 9,600 r/h			
0.00	0.0167	0.0201	0.203	20.3
	0.0171	0.0206	0.205	20.5
0.001	0.0147	0.0173	0.173	17.3
	0.0189	0.0222	0.171	17.1
0.005	0.0218	0.0271	0.243	24.3
	0.0213	0.0264	0.239	23.9
0.01	0.0204	0.0251	0.230	23.0
	0.0171	0.0210	0.228	22.8
0.05	0.0183	0.0221	0.208	20.8
	0.0185	0.0223	0.205	20.5
0.1	0.0187	0.0223	0.190	19.0
	0.0182	0.0216	0.187	18.7
	I_2 = 16,000 r/h			
0.00	0.0140	0.0174	0.243	24.3
	0.0155	0.0194	0.252	25.2
0.001	0.0157	0.0193	0.204	20.4
	0.0183	0.0221	0.208	20.8
0.005	0.0195	0.0253	0.297	29.7
	0.0202	0.0263	0.302	30.2
0.01	0.0216	0.0279	0.292	29.2
	0.0160	0.0206	0.288	28.8
0.05	0.0185	0.0236	0.276	27.6
	0.0174	0.0221	0.270	27.0
0.1	0.0189	0.0235	0.243	24.3
	0.0214	0.0268	0.252	25.2
	I_3 = 31,400 r/h			
0.00	0.0170	0.0221	0.300	30.0
	0.0174	0.0225	0.293	29.3
	0.0204	0.0269	0.284	28.4
	0.0186	0.0238	0.279	27.9
0.001	0.0167	0.0212	0.269	26.9
	0.0176	0.0223	0.267	26.7
	0.0208	0.0269	0.293	29.3
	0.0190	0.0246	0.295	29.5
0.005	0.0221	0.0302	0.367	36.7
	0.0205	0.0281	0.367	36.7
	0.0208	0.0284	0.360	36.0
	0.0198	0.0268	0.354	35.4
0.01	0.0198	0.0270	0.364	36.4
	0.0179	0.0243	0.358	35.8
0.05	0.0215	0.0287	0.337	33.7
	0.0160	0.0213	0.331	33.1
0.1	0.0202	0.0264	0.307	30.7
	0.0198	0.0259	0.308	30.8
	0.0205	0.0189	0.275	27.5
	0.0184	0.0199	0.274	27.4

Table 5

Homopolymerization of styrene under irradiation at various initiator-activator concentrations

t = 25°C; experimental time: 9 hours

Bz_2O_2-DMA mol/l	n_{25}^D	Homo-polymer %	Bz_2O_2-DMA mol/l	n_{25}^D	Homo-polymer %
I_0 = without irradiation			I_2 = 16,000 r/h		
0.00	1.5470	—	0.00	1.5471	0.2
0.001	1.5478	2.3	0.001	1.5473	1.5
0.005	1.5490	5.0	0.005	1.5487	4.3
0.01	1.5498	7.0	0.01	1.5496	6.3
0.05	1.5540	15.5	0.05	1.5535	14.8
0.1	1.5575	24.0	0.1	1.5572	23.8
I_1 = 9,600 r/h			I_3 = 31,400 r/h		
0.00	1.5471	0.1	0.00	1.5472	0.5
0.001	1.5473	1.5	0.001	1.5473	1.5
0.005	1.5486	4.0	0.005	1.5487	4.3
0.01	1.5496	6.3	0.01	1.5496	6.3
0.05	1.5535	14.8	0.05	1.5535	14.8
0.1	1.5572	23.8	0.1	1.5572	23.8

Table 6
Graft copolymerization of vinyl acetate on polyvinyl chloride membrane in the presence of initiator-activator

t = 25°C; experimental time: 5 hours

Bz_2O_2-DMA mol/l	P_0	P	$\frac{P}{P_0}-1$ / g	n_D^D	Homo-polymer %
		I_0 = without irradiation			
0.00	0,2632	0.2635	—	1.3962	0.05
	0,2629	0.2630	—	1.3965	1.50
0.001	0,2637	0.2637	—.	1.3998	5.25
	0,2377	0.2377	—	1.3998	5.25
		I_3 = 31,400 r/h			
0,00	0.2456	0.2615	0.0608	1.3995	5.15
	0.2172	0.2312	0.0644	1.3993	5.00
0.001	0.2591	0.2845	0.0980	not measurable (thickened)	—
	0.2637	0.2893	0.0975		—

CONCLUSIONS

From the experiments described above, it can be concluded that it is advantageous to use an initiator-activator for graft copolymerization with irradiation. For each monomer there exists an optimum initiator-activator concentration at which grafting is relatively large and the separation of homopolymers from the membrane is still possible.

The relatively large graft copolymerization in the case of methyl methacrylate can be explained by auto-acceleration, which takes place even in systems not containing the initiator-activator; this was recently determined (9). The irradiational grafting is an accelerating process in the presence of monomer, because free radicals are formed on the side-chains grafted as a result of irradiation. In all probability, the presence of an initiator-activator increases the auto-acceleration effect, and this could be the reason for the large amount of grafting observed in a relatively short time.

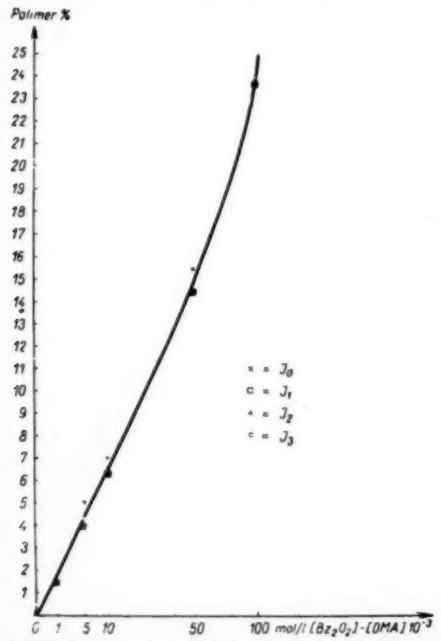

Fig. 7. Homopolymerization of styrene with irradiation as a function of initiator-activator at various X-ray intensities. Abscissa scale is square root of concentration.

The fact that grafting did not occur when vinyl acetate was used could be explained by the following. The polymerization of vinyl acetate proceeds rapidly, but vinyl acetate only swells polyethylene slowly and to a small extent. Thus, in the experimental time, homopolymerization rather than graft copolymerization takes place.

In the low X-ray intensity range that was used in the experiments, the homopolymerization was much more strongly influenced by the variation of the initiator-activator concentration than by the variation of the irradiation intensity. This is indicative of the fact that under the circumstances a much greater concentration of free radicals could be achieved by chemical methods than by irradiation.

As a final conclusion, it can be said that the extent of irradiation grafting could be increased by employing an initiator-activator.

SUMMARY

The extent of irradiation graft copolymerization can be increased, if the monomer contains an initiator-activator and is able to swell the polymer membrane. Such is the situation in the systems: polyethylene-methyl methacrylate, polyvinyl chloride-vinyl acetate in the presence of benzoyl peroxide-dimethyl aniline. Such copolymerization is dependent upon the intensity of irradiation and the concentration of the initiator-activator. Under

similar experimental circumstances, vinyl acetate could not be grafted on polyethylene, while the grafting of styrene on polyethylene is but little influenced by the presence of an initiator-activator.

The irradiation homopolymerization in the presence of benzoyl peroxide-dimethyl aniline is only dependent upon the initiator-activator concentration, while the intensity of X-ray irradiation has only a small effect.

LITERATURE CITED

1. Shapiro, A., *Ind. Plast. Mod.*, 8, No. 9, p. 67 (1956).
2. Shapiro, A., *Ind. Plast. Mod.*, 9, No. 1, p. 41 (1957).
3. Dobó, J., Telcs, I., *Műanyagipari Kutató Intézet Közleményei*, Budapest (1955).
4. Dobo, J., *Magy. Kém. Lapja*, 3, p. 76 (1958).
5. Nikitina, T. S. and Bagdasaryan, K. S., *Sbornik Akad. Nauk*, Moscow, 183 (1955).
6. Ballantine, D. S., *Mod. Pl.*, 35, p. 171 (1957).
7. Chen., W. K. W., Mesrobian, R. B., Ballantine, D. S., *J. Pol. Sci.*, 23, p. 903 (1957).
8. Henglein, A., Schnabel, W., Heine, K., *Angew. Chem.*, 70, p. 461 (1958).
9. Dobó, J., Somogyi, Á., *J. Chim. Phys.* 56, 863 (1959); *Magyar Kém. Folyóirat*, 65, p. 383 (1959).

V. T. Slavyanskii
E. N. Krestnikova
M. V. Proskuryakov

USSR

Study of Bubble Formation in Glass Melting under Vacuum

Most probable cause of bubble formation in molten glass under vacuum is supersaturation of the glass melt with gases. Variation of the pressure in industrial furnaces does not seem to influence bubble formation.

STUDIES of the formation of bubbles in glass have established that there are two main sources of bubble formation: gases which fill the pores of the ceramic shapes, which are liberated during the melting process as a result of the corrosion of the refractory by the molten components of the charge or by the liquid glass, and gases which are present in the glass melt itself and are physically dissolved therein or form chemical compounds.

It is comparatively easy to establish the origin of the "ceramic" bubbles by an analysis of the composition of the gas in the bubbles. They usually contain 80-90% nitrogen and 5-10% carbon dioxide gas and oxygen. The number of "ceramic" bubbles can be reduced by reducing the corrodibility and porosity of the refractory materials for pots or by lining them with platinum.

A second source of bubbles - gases present in the glass melt - is to a considerable extent conjectural because the composition of the gas bubbles of "nonceramic" origin usually differs sharply from the composition of the gas in the glass melt. The gases extracted from the glass melt consist chiefly of water vapors and carbon dioxide gas, while the "nonceramic" bubbles contain nitrogen, carbon dioxide gas, and a small amount of oxygen. (1)

The following explanation can be given for the difference of gas composition in the bubbles and in the glass melt. In bubbles which form during the initial stages of the melting, the gas composition corresponds to that contained in the glass melt. However, during the melting process, while the chemical composition of the vitreous melt and the temperature undergo changes, reactions can take place between the gases in the bubbles and the glass melt, which lead to a radical change in the gas composition in the bubbles.

When the temperature drops, such gases as oxygen and carbon dioxide are absorbed (2), while the nitrogen remains in the bubbles. If the bubbles which form during the melting of the charge and clarification of the glass melt consisted only of oxygen and carbon dioxide gas, then one could disregard these because they would appear at the start of the melting and disappear at the end. However,

This article first published in *Steklo i Keramika* 16, No. 9, 25-29 (1959).

in glass melting practice, it is necessary to deal with bubbles which contain nitrogen, even though the glass melting is conducted in nonporous vessels (nitrogen can come, for example, from the air which is included between the particles of the charge).

It is obvious that the glass melt is saturated with different gases, including nitrogen, which are capable of separating as bubbles. For this reason, during the melting process, the glass melt always conceals the potential danger of the formation of new bubbles and the completeness of the melting process, the completeness of clarification of the glass melt should, strictly speaking, be evaluated not only from the number of bubbles but also from the gas content of the glass melt.

The purpose of this study was to conduct at least a qualitative evaluation of the gas content in some borosilicate optical glasses. Such an investigation of various commercial glasses (window, dish, and apparatus) was conducted by Jebsen-Marwedel and Dinger. (3) However, these authors limited themselves only to a study of finished industrial glasses; moreover, their attempt to investigate optical glasses ended in failure.

In our work the problem was somewhat expanded - an investigation was made of the gas saturation of glasses as a function of the salt composition of the charge, nature of clarifying substances, mixing of the glass melt, and temperature of melting. Different types of optical glasses were used in the investigation: crown, flint, barium yellow, heavy crown. This made it possible to compare the action of the same clarifiers on glasses of fundamentally different chemical composition. Although the investigations were conducted with optical glasses, the results of the work are of significance in the melting of any type of silicate glasses.

In order to conduct the glass melting experiments under vacuum, use was made of an electric horizontal furnace with a flat temperature gradient from 1,200 to 700°C. The heater was a wire made of Kh25Yu5 alloy 2 mm. in diameter. Temperature variations in the fire space were within the limits of 5°. The gradient along the length amounted to about 18° per centimeter. The temperature in the furnace was controlled by an electronic automatic potentiometer EPD-17. The furnace arrangement is shown in Fig. 1.

In order to obtain the desired vacuum in the furnace, a quartz test tube about 50 cm. long and 28-30 mm. in diameter was inserted into the cold portion of the fire space in the furnace and positioned at a definite distance (usually up to the stop) in the furnace. The sealed end of the test tube was in the hottest portion of the furnace, while the other end protruded 10-15 cm. from the furnace. This end of the test tube was closed with a rubber plug provided

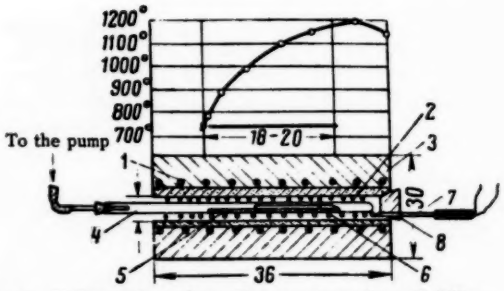

Fig. 1. 1) External winding; 2) internal winding; 3) filling; 4) quartz test tube; 5) platinum or graphite boat with glass sample; 6) protective quartz test tube; 7) thermocouple; 8) lightweight plug.

with a glass tube through which the air was exhausted. The vacuum was created by a forevacuum oil rotary pump RVN-20. The pressure in the system was measured with a U-shaped mercury manometer. A diagram of the apparatus is shown in Fig. 2.

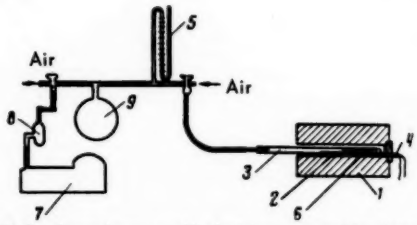

Fig. 2. 1) Gradient furnace; 2) platinum or graphite boat; 3) quartz test tube; 4) thermocouple; 5) manometer; 6) protective quartz test tube; 7) pump; 8) trap; 9) safety bulb.

In conducting the experiments under vacuum, the following boats were used: platinum - for glasses containing lead oxide* and carbon or graphite - for glasses which do not contain lead oxide. The advantage of graphite and carbon boats is that their surface is not wetted by the glass and after the experiment the glass sample is extracted easily.

Since the glass sometimes froths during the experiments, strikes the quartz test tube, and cracks during chilling of the test tube, use was made of a protective small quartz test tube 22-24 mm. in diameter and 15-18 cm. long in order to prevent this. The boat with the sample was placed in this test tube and then the small test tube, together with the boat, was placed in the larger one.

The glasses used for the experiments were melted in 3-liter quartz crucibles, in an atomizer-type furnace; twice during the course of melting, the glass melt was mixed with an iron rod. The

*These glasses blacken in a graphite or carbon boat: the lead oxide is reduced and droplets of lead appear on the glass-carbon interface.

specimens were processed in the form of rods 5-6 mm. in diameter and about 20 cm. long.

In the experiments for the determination of the influence of mixing on the gas content of the glass, glass cullet was melted in a crucible having a capacity of 45 ml. Melting was conducted in a laboratory Silit furnace; mixing was accomplished with a platinum stirrer at the rate of 100-120 rev./min. The conditions of these meltings depended on the mixing time and the temperature. The glass was poured into a heated metallic mold in the form of a boat and was annealed in a muffle heated to 500-550°C.

The results of preliminary experiments show that the pressure at which bubbles form in the glass melt varies for different glasses from 50 mm. Hg. and lower. Heating was continued for 30 minutes; during this time, the sample was completely heated and further holding in the furnace did not change the experimental results.

BUBBLE FORMATION

In order to investigate the process of bubble formation, the following experimental conditions were adopted. The test sample was heated in a preheated and thermostated furnace for 30 minutes; after the heating, the desired vacuum (5-50 mm. Hg., depending on the chemical composition and temperature history of the glass) was rapidly created, and the glass was held under these conditions in the furnace for 1 minute; then the test tube was removed from the furnace and chilled in the air. After this, the vacuum was broken and the sample was removed from the test tube.

The results of the experiments were evaluated from the temperature of the start of bubble formation and the frothing temperature of the glass. The temperature of bubble formation was established with an accuracy of up to 10-20°C. This temperature characterizes the gas saturation of the glass, or more correctly, the magnitude of gas loss during the melting under vacuum. The lower the temperature of the start of bubble formation, the greater the capability of the glass to liberate gases and to form bubbles and the greater its gas saturation.

In accordance with the above-described procedure, an investigation was made of bubble formation under vacuum in the following four optical glasses: TK-10, BK-10, K-8, and F-8 which have a different chemical composition. (4) Besides this, a study was made of the influence of the salt composition of the charge and of the nature of the clarifiers on the temperature of bubble formation during the glass melting under vacuum. Experimental glasses were melted from charges of different salt composition - nitrates, carbonates, mixtures of nitrates with carbonates and with different clarifiers. The results of the investigations are shown in Figs. 3-6.

In conducting the experiments, we strove to observe the same conditions for all the glasses under investigation. However, this was not always possible, because in some cases the pressure of 50 mm. was insufficient for bubble formation, while the vacuum of 20 mm. caused excessively strong frothing.

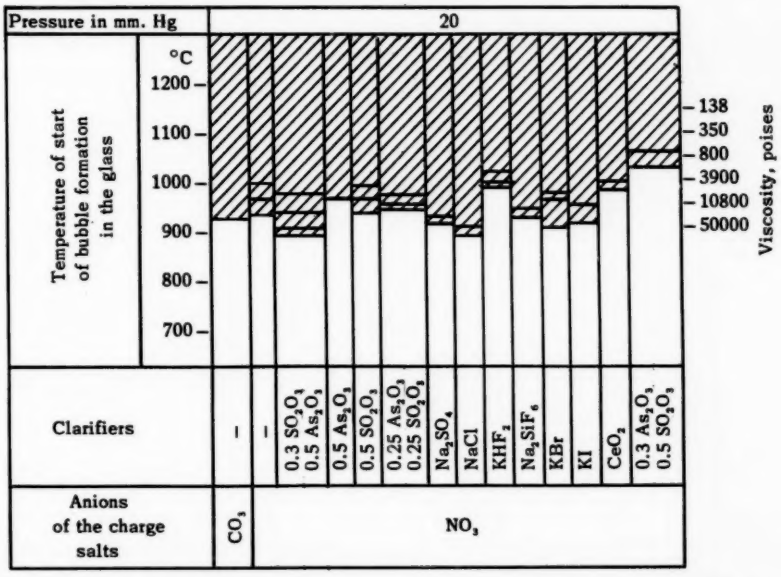

Fig. 3. Temperature of the start of bubble formation during the heating of glass TK-10.

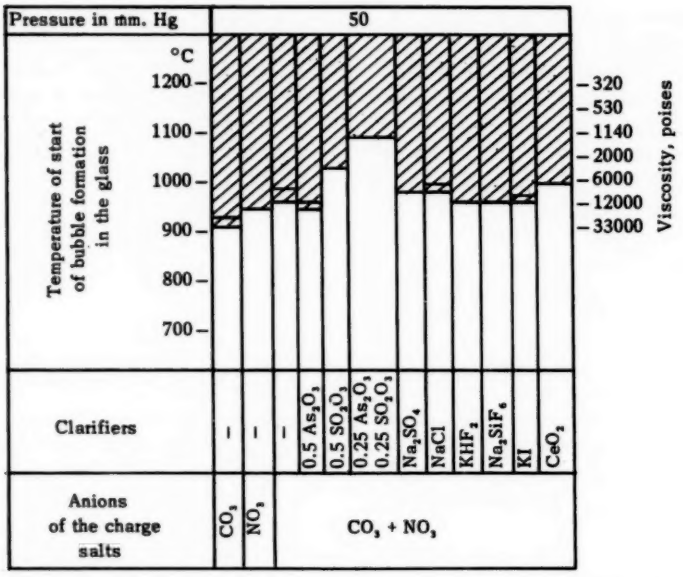

Fig. 4. Temperature of the start of bubble formation during the heating of glass BK-10.

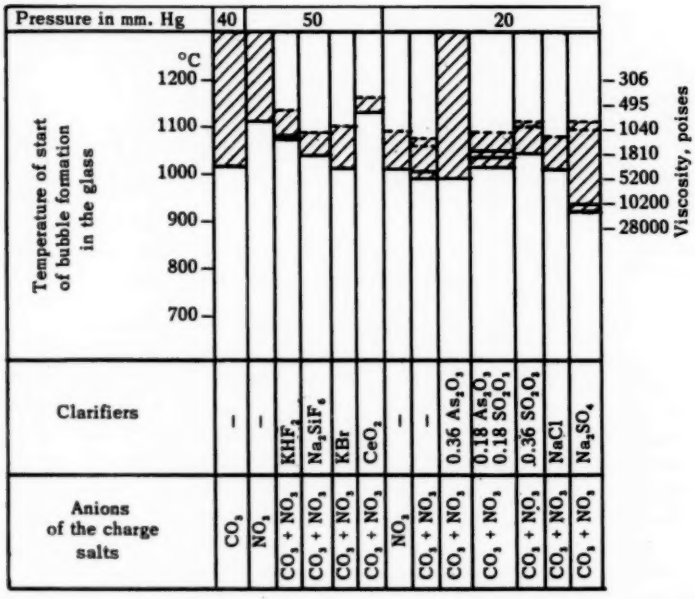

Fig. 5. Temperature of start of bubble formation during heating of glass K-8. The dotted lines indicate the end of bubble formation.

It is seen from Figs. 3-6 that in glasses K-8, TK-10, and BK-10 the temperature of the start of bubble formation depends but little on the nature of the clarifiers and lies approximately within the limits of 900-1,000°C. An exception is glass BK-10 with the clarifier 0.25 As_2O_3 + 0.25 Sb_2O_3 (Fig. 4); in this case, the temperature of the start of bubble formation is somewhat higher.

The viscosity of these glasses within the indicated interval varies within the limits of 10^3-10^4 poises and also does not exert a special influence on the temperature of the start of bubble formation.

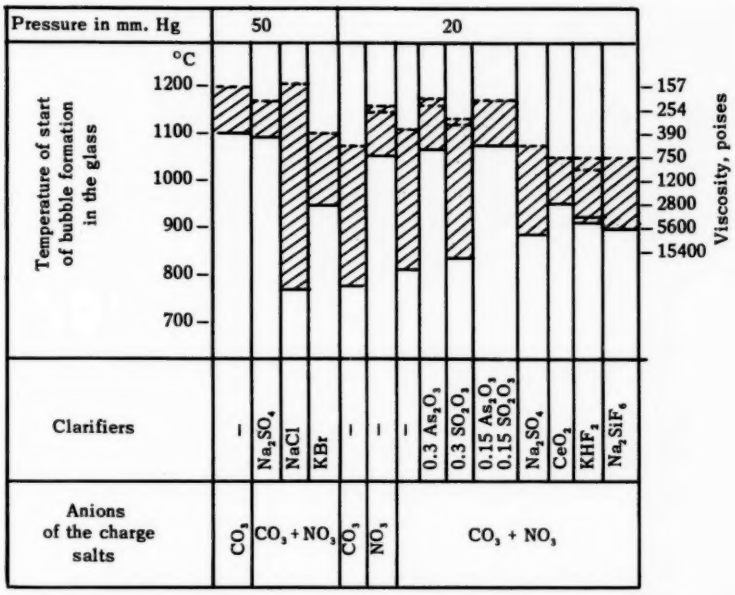

Fig. 6. Temperature of start of bubble formation during heating of the glass F-8. The dotted lines indicate the temperature of the end of bubble formation.

This also is not affected by sharp differences in the chemical composition of the glasses.

However, the behavior of the F-8 glass was different. In this glass, the action of the clarifying substances is more pronounced.

It is necessary to point out one more characteristic: in the glasses TK-10 and BK-10, the formation of bubbles takes place over the entire region of high temperatures (i.e., up to the end of the boat which is at a temperature of 1,200°C), while in the glasses K-8 and F-8, there is a temperature boundary above which no bubbles were observed under the conditions of our experiments. In Figs. 5-6, this is shown by a dotted line.

The existence of a field of high temperatures at which in the glasses K-8 and F-8, as distinct from BK-10 and TK-10, bubbles do not form (more correctly, form but succeed in leaving the melt) can obviously be explained by the peculiarity of their chemical composition, which determines another nature of sorption of the gases by the melted glasses.

A series of experiments was conducted to study the effect of mixing of the glasses at 1,400°C and 1,450°C in a platinum crucible. Since, as a result of mixing, there is vigorous outgassing, then, in order for the bubbles to form, it is necessary at times to lower the pressure to 5-2 mm. Hg. The reproducibility of the experiments was good. Their results are shown in Figs. 7 and 8.

As shown by the experiments, during mixing, glasses melted even without clarifiers and from a purely carbonate charge contain practically no gas. Hence, it follows that mixing of optical glasses during the melting is necessary not only to obtain a uniform glass melt, but, to a no lesser extent, to remove the gas from the glass.

As shown above, the formation of bubbles in a molten optical glass takes place only with a pressure decrease to 50-20 mm. Hg. At the same time, the opinion is generally widespread that even insignificant variations of the atmospheric pressure in the furnace influence the processes of bubble formation in the molten glass melt. The results of our experiments do not confirm this. The need of a high vacuum (up to 50 mm. Hg. and, after mixing, even up to 5 mm. Hg.) for the formation of bubbles in molten glass is shown without exception by all the experiments (over 200).

Similar results were obtained in the work by Jebsen-Marwedel and Dinger with the only difference that a vacuum of 200-300 mm. Hg. was required for bubble formation in the glasses which they investigated. This is, obviously, explained by the fact that the glasses were melted by them in tank furnaces of great capacity without mixing and were more saturated with gases.

How is one to explain the need of a considerable reduction in pressure in order to form bubbles in the molten glass? Let us examine possible causes of bubble formation in the glass during a drop in the pressure.

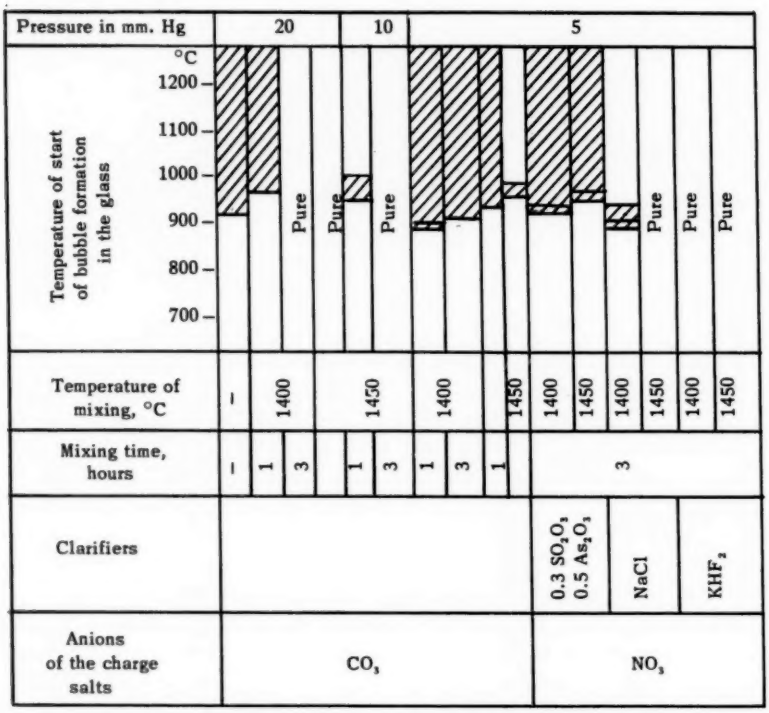

Fig. 7. Effect of mixing on the temperature of start of bubble formation during the heating of glass TK-10. The dotted lines indicate the temperature of the end of bubble formation.

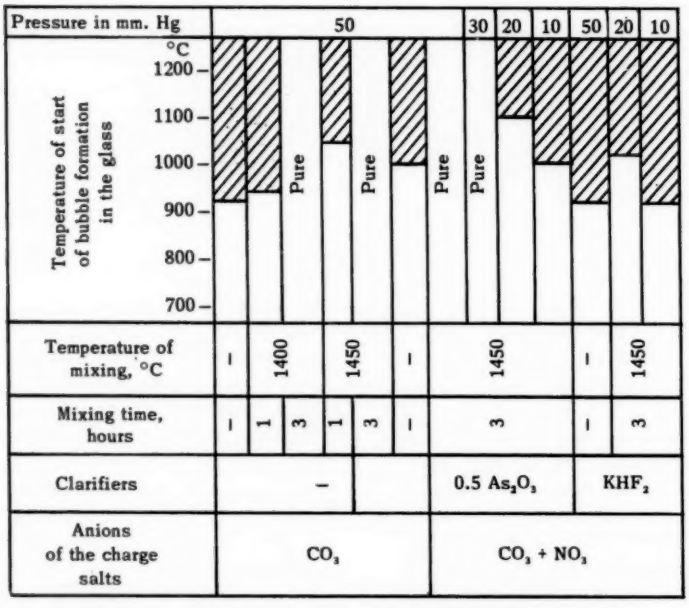

Fig. 8. Effect of mixing on the temperature of start of bubble formation during the heating of glass BK-10.

It could be assumed that a drop in pressure creates conditions for boiling when the vapor pressure of the melt is equal to the external pressure. However, the vapor pressure of the highly volatile components at 900-1,000°C (temperature of the start of bubble formation) amounts to a fraction of a millimeter of mercury; we, however, lower the pressure only to 20-50 mm. Hg. An experimental confirmation of boiling also was not obtained: during an examination of the samples with the unaided eye and under the microscope, no condensates were observed on the inside surface of the bubbles. Consequently, this assumption is hardly correct.

It is possible that a drop in pressure causes a shift of the chemical reactions toward the side of the formation of gaseous products. This could be seen from the composition of the gas in the bubbles. However, there is still no method available for the analysis of the gas separating from the glass melt. For this reason, the problem of a shift in the chemical reactions remains open.

One can think that the formation of bubbles under vacuum takes place as a result of the separation of the gases which are physically dissolved in the glass melt and which supersaturate it. The results of our experiments on the study of the influence of mixing serve as indirect proof of this. The gas content of the molten glass drops sharply after mixing. Since we accomplished the mixing at atmospheric pressure, only those gases could separate which are physically dissolved in the glass melt and supersaturate it.

From our point of view, the most probable cause of bubble formation in molten glass under vacuum is the supersaturation of the glass melt with gases. However, the need of a high vacuum is explained by the large expenditure of work for the formation of a new phase in a strongly viscous medium.

Thus, we proposed a procedure for the evaluation of the gas saturation of glasses from the temperature of the start of bubble formation during the melting of the glass under vacuum.

It has been established that, in order for bubbles to form during the melting of some optical glasses under vacuum, the pressure should be reduced at least to 50 mm. Hg.

Mixing of the molten glass frees it of gas to such an extent that a pressure reduction to 20-5 mm. Hg. is necessary for bubble formation. In some cases, however, even such a pressure drop is insufficient.

The assumption is advanced regarding the supersaturation of the glass melt with gases physically dissolved therein and which are capable of separating as bubbles during the melting of the glass under vacuum.

The results obtained in the experiments lead to the conclusion that variations of the pressure in industrial furnaces do not exert an influence on bubble formation in the glass. At the same time, all possible mechanical effects on the molten glass melt can cause the formation of a large number of bubbles.

LITERATURE CITED

1. Slavyanskii, V. T., *Gazy v Stekle*, Ororongiz (State Publishing House of the Defense Industry), Moscow (1957).
2. Vargin, V. V., *Stekol'naya promyshlennost*, No. 7 (1938). Pollyak, V. V., *Sbornik nauchnykh rabot po steklu*, Promstroiizdat (State Publishing House of Literature on Building Materials), 64 (1950).
3. *Verres et Refractaires*, p. 19, August (1947).
4. *Spravochnik po voennoi optike*, Gostekhizdat (State Publishing House of Theoretical and Technical Literature), pp. 200-201, Moscow-Leningrad (1945).

L. M. Mirzoeva

AZERBAIDZHAN, USSR

Determination of Solid Phase Concentration in a Two-Phase Medium in Upward Motion in a Vertical Tube

A mathematical treatment of relative motion between the components in two-phase flow, including the effect of slippage.

It is well known that when a two-phase system is in motion, whether it be liquid-gas, liquid-solid, or gas-solid, the average velocities of the phases are not equal to each other. The existence of relative motion between the components is one of the important properties of two-phase flow.

In the case of the motion of a two-phase system that we were considering, specifically, in the case of the motion of a mixture of gas and solid particles upward in a vertical tube, the phenomenon of "slippage" is more clearly expressed than in horizontal tubes; this cannot be ignored when performing an investigation. This phenomenon leads to the condition that the fraction of the cross section occupied by each of the components does not correspond to the value that would be obtained by a calculation based on the feed rates for the gaseous and solid substances.

In other words, the nominal concentration of the mixture does not correspond to the actual concentration in the vertical portion of the tube. The actual concentration of solid particles will always be greater than the flowing concentration, i.e., the fraction of the cross section occupied by solid particles is in fact greater than the fraction of the cross section for the case in which slippage is absent.

The magnitude of slippage σ is determined by the ratio of the difference in the absolute velocities of the carrier and the suspended phases to the velocity of the carrier phase, i.e.,

$$\sigma = \frac{C' - W}{C'} = \frac{U}{C'} \qquad (1)$$

where C' is the actual absolute velocity of the gas in the vertical portion of the tube, m./sec.: W is the absolute velocity of the solid particles, m./sec.; and U is the relative velocity of the solid particles, m./sec.

The motion of the particle and the gas in a vertical tube at absolute velocities C' and W is equivalent to the fall of the particle at a relative velocity $C' - W$ in a moving gaseous medium.

In this case, the relative motion of a particle takes place under the action of two forces: the force of gravity (without correcting for the Archimedean lifting force (buoyancy) and the force due to the resistance of the gaseous medium, which is directed opposite to the relative motion of the particle.

As the particle falls, its velocity increases and the resisting force of the medium also increases, while the force of gravity remains constant; as a result of this, a point is reached when the particle begins to move with zero acceleration, or, stated in other words, it acquires a certain final uniform velocity.

At this state, the force of gravity is equal to the resisting force of the gaseous medium.

The resisting force of the gaseous medium, which acts on the particle which is moving through it, is expressed by the formula:

$$P = C_0 F \rho_g U^2 \qquad (2)$$

in which C_0 is a coefficient related to the shape of the particle and is a function of the Reynolds number.

For spherical particles at $Re < 2$, $C_0 = 12/Re$, and Eq. (2) coincides with the Stokes formula.

For $2 \times 10^5 > Re > 10^3$, C_0 is constant and is equal to the value of C_0 which corresponds to a Reynolds number of 1000.

At $Re = 100$, $C_0 = 0.25$ (2).

C_0 is a variable for intermediate values of the Reynolds number.

F is the projected area of the body in the direction of its motion (main [maximum] cross section), $m.^2$; ρ_g is the density of the gaseous medium, kg. $cm.^2/m.^4$; and U is the relative velocity of the particle, m./sec., which is equal to $C' - W$.

The equality of the force of resistance and the force of gravity is expressed by the following equation:

This article first published in *Izvest. Akad. Nauk Azerbaidzhan. SSR* No. 9, 11-19 (1957).

$$C_0 F \rho_g U^2 = \frac{\pi d_p^2}{4} \rho_p g \qquad (3)$$

where ρ_p is the density of the substance composing the particle, (kg.)(sec.^{2})/m.^{4}; d_p is the mean diameter of the particle, m.; and g is the acceleration due to gravity, m./sec.^{2}.

We assume that the particle has a spherical shape, and that all of the conclusions refer to a region in which the values of the Reynolds number vary, including industrial conditions, from 10^3 to 2×10^5; C_0 is a constant over these limits.

Then $F = \pi d_p^3/4$, and $C_0 = 0.25$,

and the relative velocity of the particle is determined from the expression:

$$U = \sqrt{\frac{8}{3} g \frac{\rho_p}{\rho_g} d_p}$$

Substituting for the ratio of the densities of the solid particle and the gas the ratio of their specific gravities, we finally obtain:

$$U = \sqrt{\frac{8}{3} g \frac{\gamma_p}{\gamma_g} d_p} \qquad (4)$$

Thus, by substituting values for all of the variables which appear in Eq. (4), we can determine the magnitude of the relative velocity of the particle U, and for given values of C′ (the velocity of the medium) we can determine the magnitude of slippage σ from Eq. (1).

Since the shape of the solid particles actually can differ from the spherical, the assumed value of the coefficient C_0 taken as 0.25 will be found to be insufficiently accurate.

In case of need, this circumstance could be taken into account in experimental verification of the computational formulae presented by us (see below) by the introduction of a correction factor.

ACTUAL CONCENTRATION OF THE PARTICLES IN THE STREAM

In studying moving two-phase systems, it becomes necessary to determine the concentrations of the phases, the fractions of the cross section occupied by each of the phases, and so on.

Existing experimental methods for determining the concentration of mixtures by weighing sections of a tube, with the aid of sampling devices or by means of simultaneous and rapid closing of two valves, involve certain difficulties.

In this paper we derive a formula for determining the actual concentration by means of calculations.

Determining the nominal concentration at the time the investigation is performed, does not involve particular difficulties. The inequality of the nominal and actual concentrations of the particles in a vertical stream makes it necessary to establish a relation between them. This relationship may be found as follows.

Let us assume that the particles have spherical shapes, the same diameters, and a uniform distribution throughout the entire volume of the gaseous medium.

We designate the areas of the cross sections of the streams of solid particles and gas over a cross section of the tube as follows: by f_p and f_g under the conditions where slippage is absent, i.e., where W = C, and by f'_p and f'_g in the presence of slippage (see the Figure).

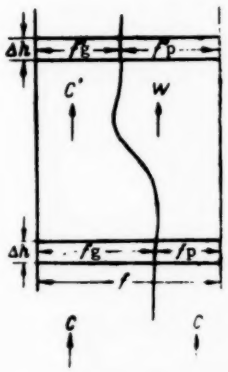

Then, we can write for the steady state regime:

$$G_p = f_p \cdot C \cdot \gamma_p = f'_p \cdot W \cdot \gamma_p \qquad (5)$$

$$G_g = f_g \cdot C \cdot \gamma_g = f'_g \cdot C' \cdot \gamma_g \qquad (6)$$

where G_p and G_g are the flow rates of the particles and the gas, kg./sec.; γ_p and γ_g are the densities [Translator's Note: the Russian text states "specific gravities", however, units of density are given] of the substances making up the particles and the gas, kg./m.^{3}; and C is the average gas velocity, m./sec.

Eq. (5) is written with the assumption that the cross section of the stream f_p is completely filled by solid particles, i.e., no allowance is made for the volume of any free spaces between them. However, considering that the difference between the densities of the components is sufficiently large, and that the ratio f_g/f_p will be very small within the limits of the stream concentrations which we are likely to encounter in practice when considering densely distributed particles, the volume of the gas in the spaces between the solid particles in the stream will be insignificant as compared to the volume of the stream of particles; hence, we will assume that the density of the stream having cross section f_p will be equal to γ_p.

We will use weight concentrations so that the results will be readily comprehended.

The weight concentrations of the solid particles in the stream is the ratio of the weight of the particles to the weight of the gas in the volume under consideration, i.e.:

$$K_G = \frac{f_p \cdot \Delta h \cdot \gamma_p}{f_g \cdot \Delta h \cdot \gamma_g} = \frac{f_p \cdot \gamma_p}{f_g \cdot \gamma_g} \tag{7}$$

where K_G is the weight concentration for the conditions under which slippage is absent, i.e., it is the nominal weight concentration (kg. of solid substance)/(kg. of gas).

When slippage is present, the weight concentration will be equal to:

$$K'_G = \frac{f'_p \cdot \gamma_p}{f'_g \cdot \gamma_g} \tag{8}$$

Dividing Eq. (5) by (6), we obtain:

$$\frac{G_p}{G_g} = \frac{f_p \cdot C \cdot \gamma_p}{f_g \cdot C \cdot \gamma_g} = \frac{f_p \cdot \gamma_p}{f_g \cdot \gamma_g} = K_G$$

and thus:

$$K_G = \frac{f'_p \cdot W \cdot \gamma_p}{f'_g \cdot C' \cdot \gamma_g} = K'_G \cdot \frac{W}{C'} \tag{9}$$

where K'_G is the actual weight concentration, (kg. of solids)/(kg. of gas).

From Eq. (9) we have:

$$\frac{K'_G}{K_G} = \frac{C}{W} \tag{10}$$

but $\sigma = U/C'$ and $U = C' - W$, or $W = C' - U$, so that:

$$\frac{K'_G}{K_G} = \frac{C'}{C' - U} = \frac{1}{1 - \frac{U}{C'}} = \frac{1}{1 - \sigma}$$

and

$$K'_G = \frac{1}{1 - \sigma} \cdot K_G \tag{11}$$

i.e., the actual concentration of the solid particles in the stream is directly proportional to the nominal concentration, where the coefficient of proportionality depends on the amount of slippage.

We see from Eq. (11) that

1. at $\sigma = 0$, i.e., at $C' = W$, $K'_G = K_G$, i.e., the actual concentration is equal to the nominal concentration.

2. at $\sigma = 1$, i.e., at $W = 0$, $K'_G = \sim$*; in this case, the particles are not being carried away by the gas stream.

To determine the actual gas velocity, we write:

*Translator's Note: *sic.* The symbol used denotes "approximately" and is meaningless in this context.

$$f_p + f_g = f \tag{12}$$

and

$$f'_p + f_g = f \tag{13}$$

where f is the cross-sectional area of the tube (pipe), m.^{2}.

From Eqs. (7) and (8), we obtain:

$$f_p = K_G \cdot f_g \cdot \frac{\gamma_g}{\gamma_p}$$

and

$$f'_p = K'_G \cdot f'_g \cdot \frac{\gamma_g}{\gamma_p}$$

Then

$$f = f_g + K_G \cdot f_g \cdot \frac{\gamma_g}{\gamma_p} = f_g \cdot \left(1 + K_G \frac{\gamma_g}{\gamma_p}\right)$$

and

$$f = f'_g + K'_G \cdot f'_g \cdot \frac{\gamma_g}{\gamma_p} = f'_g \left(1 + K'_G \frac{\gamma_g}{\gamma_p}\right).$$

Equating the right hand members of the latter equations, we have:

$$f_g \left(1 + K_G \frac{\gamma_g}{\gamma_p}\right) = f'_g \left(1 + K'_G \frac{\gamma_g}{\gamma_p}\right)$$

or

$$\frac{f'_g}{f_g} = \frac{1 + K_G \frac{\gamma_g}{\gamma_p}}{1 + K'_G \frac{\gamma_g}{\gamma_p}} \tag{14}$$

From Eq. (6) we obtain:

$$\frac{f'_g}{f_g} = \frac{C \cdot \gamma_g}{C' \cdot \gamma_g} = \frac{C}{C'}$$

Substituting this value into Eq. (14), we find:

$$\frac{C'}{C} = \frac{f_g}{f'_g} = \frac{1 + K' \frac{\gamma_g}{\gamma_p}}{1 + K_G \frac{\gamma_g}{\gamma_p}}$$

and

$$C' = C \frac{1 + K'_G \frac{\gamma_g}{\gamma_p}}{1 + K_G \frac{\gamma_g}{\gamma_p}} \tag{15}$$

Eliminating the value of C' from Eqs. (1) and (15), we have:

$$\sigma = \frac{U}{C \cdot \frac{1 + K'_G \frac{\gamma_g}{\gamma_p}}{1 + K_G \frac{\gamma_g}{\gamma_p}}} \tag{16}$$

Substituting for K'_G in Eq. (16) its value as taken from Eq. (11), we find:

$$\sigma = \frac{U}{C \cdot \dfrac{1 + \dfrac{K_G \dfrac{\gamma_g}{\gamma_p}}{1 - \sigma}}{1 + K_G \dfrac{\gamma_g}{\gamma_p}}} \tag{17}$$

Solving this equation for σ, we have:

$$\sigma = \frac{\left(1 + K_G \frac{\gamma_g}{\gamma_p}\right)(C + U) \pm \sqrt{\left[\left(1 + K_G \frac{\gamma_g}{\gamma_p}\right)\left(C + U\right)\right]^2 - 4UC\left(1 + K_G \frac{\gamma_g}{\gamma_p}\right)}}{2 \cdot C}$$

Designating:

$$\frac{\gamma_g}{\gamma_p} = a \tag{18}$$

and

$$\left(1 + K_G \frac{\gamma_g}{\gamma_p}\right)(C + U) = A \tag{18'}$$

We then find that the expression for σ can be reduced to:

$$\sigma = \frac{A \pm \sqrt{A^2 - 4UC(1 + aK_G)}}{2 \cdot C} \tag{19}$$

Using this formula, it is possible to determine the amount of slippage from given values of the nominal concentration and other parameters of a two-phase system.

Thus, by calculating a, U, and A in accordance with Eqs. (18), (4), and (18'), respectively, and substituting these values into Eq. (19), we may calculate the magnitude of slippage. Knowing the value of σ, it thus becomes possible to determine the magnitude of the actual concentration K'_G using Eq. (11), and we can subsequently calculate the actual gas velocity by using Eq. (15).

It is easier to find the latter without calculating K'_G, directly after determining σ, namely, by using Eq. (1):

$$C' = \frac{U}{\sigma} \tag{20}$$

The derivations of the computational formulas presented above are associated with the need for establishing quantitative relationships when studying two-phase systems with solid heat transfer agents as encountered in heat exchange apparatus used in petroleum refining.

However, the stated formulae may also be used for solving a number of problems associated with thermokinetic and hydrodynamic processes with two-phase mixtures.

The most frequently encountered expression for the concentration is the ratio of the weight of the particles of the solid phase to the volume of the gas, or (the ratio of) the weight of the particles to the volume of the mixture.

The transition from the concentrations as determined from Eq. (11) to the concentrations just mentioned can be made rather simply.

The weight of the solid particles per cubic meter of gas is equal to

$$K_1 = K'_G \cdot \gamma_g, \text{ kg of solid particles/m.}^3 \text{ of gas}$$

while the weight of the particles per cubic meter of the mixture amounts to

$$K_2 = \frac{K'_G \cdot \gamma_g}{1 + K'_G \dfrac{\gamma_g}{\gamma_p}}, \text{ kg of solid particles/m.}^3 \text{ of mixture} \tag{22}$$

where $K'_G\left(\frac{\gamma_g}{\gamma_p}\right)$ is the volume of solid particles present per m.^{3} of gas.

We illustrate the application of the foregoing equations using the following example.

Let us consider the motion of a two-phase mixture heated to 200°C in a vertical tube, flowing upward. The carrier phase is air and the substance being transported consists of finely divided solid particles. We assume the shape of the particles to be spherical.

We are given:

$t_{mixture} = 200°C$, $d_p = 0.0002$ m, $\gamma_p = 1200$ kg./m.^{3}
$K_G = 20$ kg. solids/kg. air, $C = 6$ m./sec.,
and $\gamma_g = 0.723$ kg./m.^{3}

First, we determine the values of a, U, A using Eqs. (18), (4), and (18'), respectively:

$$a = \frac{0.723}{1200} \quad 0.0006025$$

$$U = \sqrt{\frac{8}{3} \cdot 9.81 \cdot \frac{1200}{0.723} \cdot 0.0002} = 2.946 \text{ m./sec.}$$

and

$$A = (1 + 0.0006025 \cdot 20)(6 + 2.946) = 9.054$$

Then, according to Eq. (19), we have:

$$\sigma = \frac{9.054 \pm \sqrt{9.054^2 - 4 \cdot 6 \cdot 2.946(1 + 0.0006025 \cdot 20)}}{2 \cdot 6}$$

$$= \frac{9.054 \pm 3.228}{12}$$

$$\sigma_1 = \frac{9.054 - 3.228}{12} = 0.486$$

$$\sigma_2 = \frac{9.054 + 3.228}{12} = 1.06$$

Since slippage cannot exceed unity, a negative sign must be taken for the root in the equation for σ, i.e.,

$$\sigma = \sigma_1 = 0.486$$

From Eq. (11) we determine the actual concentration to be:

$$K'_G = \frac{1}{1 - 0.486} \cdot 20 = 1.943 \cdot 20 = 38.9 \frac{\text{kg. of solids}}{\text{kg. of gas}}$$

Finally, the actual gas velocity is found with the aid of Eq. (1):

$$C' = \frac{2.946}{0.486} = 6.06 \text{ m./sec.}$$

LITERATURE CITED

1. Armand, A. A., "Issledovanie mekhanizma dvizheniya dvukhfaznoi smesi v vertikal'noi trube" (A study of the Mechanism of Motion of a Two-Phase Mixture in a Vertical Tube), *Izvest. Vsesoyuz. Teplotekh. Inst. im. Feliksa Dzerzhinskogo*, No. 2 (1950).
2. Brounshtein, B. I., and Todes, O. M., "Giradvlika sloya tverdykh chastits vzveshennykh v voskhodyashchem potoke vozdukha" (Hydraulics of a Bed of Solid Particles Suspended in an Ascending Stream of Air), *Neft. Khoz.* No. 4 (1951).
3. "Tekhnicheskaya entsiklopediya" (*Technical Encyclopedia*), Vol. 1.
4. Khvol'son, O. D., "Kurs fiziki" (*A Course in Physics*), Vol. 1.

F. Mihail
F. Gherghel
M. Stănescu
S. Kornbaum

ROMANIA

Chlorination of Low-Pressure Polyethylene and its Compounding with Polyvinyl Chloride

Recent work in Romania on chlorination of polyethylene to produce appropriate elastomers for the elasticization of polyvinyl chloride, plus data on the compounding of the two polymers.

In our country, as well as on a world scale, research organizations are at present paying considerable attention to work connected with increasing the fields of use, and with improving the characteristics of plastic materials already in use. The present work fits also within the framework of this field of endeavor. The synthesis of chlorinated polyethylene, which was the object of our research, led to an elastomer which, by compounding with PVC, gives the latter superior properties, especially as far as low-temperature impact resistance is concerned.

The problem of improving the impact resistance of PVC—much investigated during recent years all over the world—was solved, in general, in two ways:

1. Internal plasticization by copolymerization which, however, in the majority of cases, leads only to a slight bettering of the impact resistance.
2. Elasticization with macromolecular products,

This article first published in *Revista de Chimie*, 12, No. 5, p. 275-281 (1961).

by the preparation of polymer mixtures, a modern process which leads to considerable improvement in the impact resistance. In general, elastomeric compounds are used for preparation of the mixtures: chloroprene, butadiene rubbers (butadiene-acrylonitrile, butadiene-styrene), polyurethane, and chlorinated and sulfochlorinated polyolefins.

Centering of research on the compounding of PVC with chlorinated polyethylene is justified by the fact that this procedure presents a series of advantages compared to other possibilities for the elasticization of PVC. These advantages are: the high compatibility of these two polymers, good resistance to temperature, light, ultraviolet radiation, and aging, compared to mixtures prepared with chloroprene, butadiene, and polyurethane rubbers (1).

The research was oriented in two directions: on the one hand, the chlorination of polyethylene to produce appropriate elastomers for the elasticization of PVC and, on the other hand, study of the compounding of the two polymers.

In the chlorination of polyethylene, the only basis of our work was patents (4); we had available no systematic study of the synthesis and properties of chlorinated polyethylene. We also lacked clear-cut information on processes for production of mixtures differing from this type, describing the quality and proportion of chlorinated polyethylene and the compounding method.

CHLORINATED POLYETHYLENE

Chlorination of Polyethylene

Our work was concerned with chlorination of low-pressure polyethylene with gaseous chlorine in solution and in suspension (in an organic liquid and in water) and with SO_2Cl_2 in solution.*

Chlorination brings about a structural modification in the polyethylene which leads to a transformation from a thermoplastic polymeric state to an elastomeric state. This phenomenon takes place gradually, as the degree of chlorination increases, and the elastomeric characteristics reach maximum values in the region of 35-45% chlorine content; outside these limits, the elastomeric character decreases in both directions. This phenomenon can be explained by the fact that introduction of chlorine into the highly-crystalline polyethylene macromolecule destroys this crystallinity, as it forms an asymmetric molecular element. As the chlorine content increases, the crystallinity increases accordingly, and the elastomeric characteristics are accentuated up to the region of 35-45% chlorine. With a continued increase of the percentage of chlorine, its value approaches 56%, corresponding to the chlorine content of PVC; in this case, distribution of the chlorine atoms in the macromolecule approaches the symmetrical distribution of PVC, the polar intermolecular forces (through hydrogen bonds with chlorine atoms) increase, and the product becomes rigid like unplasticized PVC.

The intensity of the elastomeric character of the chlorinated polyethylene and, implicitly, the elasticization capacity of PVC are conditioned by a series of factors, namely:

1. The linear, or branched, nature of the base polyethylene, produced by ionic catalysis at low pressure, or by radical catalysis at high pressure, is retained also after chlorination; the chlorinated polyethylene with a linear structure possesses higher physical and mechanical properties and better resistance to solvents than the branched chlorinated polyethylene produced from high-pressure polyethylene.

2. A second determining factor for the structure of chlorinated polyethylene derives from the chlorination procedure. The main methods of chlorination—in solution, in suspension, and in a fluidized bed—determine the degree to which the crystalline structure of polyethylene is affected by chlorination, as a function of the dispersion of the polymer in the reaction medium. At a certain degree of chlorination, the initial crystalline structure is totally destroyed in the case of solution chlorination, but only partially destroyed for suspension and fluidized-bed chlorination. The more advanced the destruction of the polymer crystallinity, the more its elasticity increases; the solution-chlorinated polyethylenes are much more elastic than those produced in suspension. For the latter, the chlorination takes place superficially, the crystalline interior of the particle remains unaltered, and the chlorination product is more rigid.

The chlorination procedure also determines the distribution of the chlorine atoms in the polymer chain. Solution chlorinations lead to a very uniform distribution of the chlorine (a maximum of 3-4 adjacent CH_2 groups). By suspension chlorination, one obtains long fragments, or "blocks," of chlorinated chains, in the vicinity of unchlorinated blocks.

These effects combine to determine the differences between the properties of the chlorinated polyethylenes produced by the two methods: the solution-chlorinated polyethylene has a lower softening point than the suspension-chlorinated polyethylene, higher elasticity and elongation, lower rigidity and tenacity, and higher solubility.

On the basis of the results derived from the

*Another ICECHIM collective has investigated the chlorination of high-pressure polyethylene (M. Taizs).

variation in the nature of polyethylene (low or high-pressure) on the one hand, and of the chlorination procedure (in solution or suspension) on the other hand, and in order to obtain appropriate products for the elasticization of PVC, we decided to concentrate our study on the chlorination of low-pressure polyethylene with gaseous chlorine in solution.

The chlorination was performed in a 6% solution of polyethylene in tetrachlorethane or in chlorobenzene, in a batch and in a continuous system.

The batch method was of particular use in establishing the kinetics of chlorination under various conditions. Thus, we followed the rate of change of chlorination as a function of: the molecular weight of polyethylene, the initial conditions, the chlorine flow-rate, and the chlorination temperature.

It was found that the degree of chlorination decreases with the molecular weight of polyethylene (Fig. 1).

Initiation can take place by chemical action with initiators that cause evolution of free radicals (porofor, benzoyl peroxide), as well as photochemically, in light (Fig. 2). Initiation with light leads to results similar to chlorination in darkness in the presence of porofor. In addition, porofor and benzoyl peroxide produce similar degrees of chlorination under identical conditions. It is found that the degree of chlorination does not vary with percentage of initiator, within the range of 0.1-2.5% porofor.

In darkness and in light, without initiators, the influence of temperature, within the temperature range 90-120°C, is negligible; in the presence of initiators in the light, the reaction rate decreases with temperature, undoubtedly because of the thermal degradation of the initiator which loses some of its activity at higher temperatures (Fig. 3).

The degree of chlorination normally increases with the amount of chlorine introduced, that is to say, with the flow-rate of the chlorine and the duration of the chlorination (Figs. 1 and 2).

In our laboratory, we studied also the continuous chlorination of polyethylene, a procedure which is

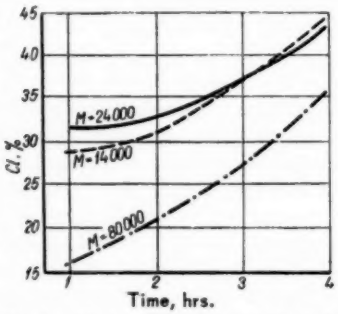

Fig. 1. Variation in chlorine content of chlorinated polyethylene with chlorination time, as a function of the molecular weight of polyethylene.

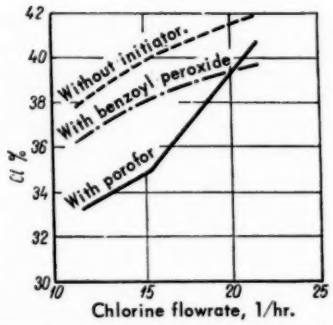

Fig. 2. Variation of chlorine content of chlorinated polyethylene with chlorine flowrate, as a function of the mode of initiation.

not mentioned in the literature.

By investigation of the continuous chlorination of polyethylene, we tried to establish a more advantageous method than the batch process, both from a technical as well as from an economic point of view. The following advantages would be obtained:

1. Increased plant capacity (6 kg./hr. of product in 100-liter capacity apparatus, for continuous polymerization, as compared to 0.9 kg./hr. for 100-liter capacity apparatus in the batch process).

2. Continuous uniform quality of the product, compared to batch chlorination, for which perfect reproducibility from batch to batch cannot be guaranteed.

The continuous chlorination method is suggested as a final model for pilot-plant production of chlorinated polyethylene.

The laboratory study of continuous chlorination of polyethylene covered the variation in degree of chlorination as a function of contact time and of the ratio chlorine : polyethylene.

There was found a normal increase of degree of chlorination with these two parameters.

In order to follow the variation in the degree of chlorination, we set up in the analytical laboratory of the Institute a rapid analysis method based on combustion of the chlorine.

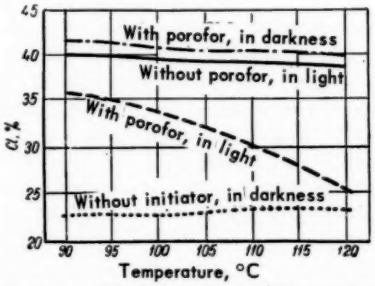

Fig. 3. Variation in chlorine content of chlorinated polyethylene with the experimental temperature, as a function of the mode of initiation (Cl:PE = 1.15 g.:1g.).

Finally, for rapid production control, the variation in chlorine content of the chlorinated polyethylene was followed also by measuring the refractive indices of the chlorinating solutions; for this purpose, the variation curve of the refractive indices as a function of percent chlorine in the product was constructed.

For isolation of the chlorinated polyethylene from the chlorination solutions, there was set up, after various tests on precipitation from solution, an optimum laboratory method, namely, precipitation of the polymer by pouring the solution as a thin stream into boiling water, under agitation, the solvent being continuously entrained with the water vapor. In the pilot stage, we shall set up a precipitation procedure based on injection of the chlorinated polyethylene solution under pressure into a bath of boiling water.

Properties of Chlorinated Polyethylene

The chlorinated polyethylene appears as an elastomer whose physical and mechanical properties vary as a function of the chlorine content, the elastomeric properties being at a maximum within the range of 34-45%. Table 1 lists the physical and mechanical properties of chlorinated polyethylene (with 41% Cl), compared to those of other non-vulcanized elastomers.

From a chemical standpoint, the chlorinated polyethylene was analyzed (5) by rapid determination of the chlorine, preceeded by purification through reprecipitation with alcohol from a benzenic solution. The chlorinated polyethylene does not exhibit a precise softening point; at 140-150°C, there begins a gradual softening of the polymer, which also turns yellow; at 200-230°C, it decomposes.

With respect to chemical agents, the chlorinated polyethylene has a behavior intermediate between that of polyethylene and that of polyvinyl chloride. It is perfectly resistant to acids and alkalies in dilute and concentrated form, to benzenes, alcohols, and acetone. However, it dissolves readily at room temperature, to the extent of 25-30%, in chlorinated solvents, aromatic hydrocarbons, and cyclohexanone.

Table 1

Physical and mechanical properties of chlorinated polyethylene compared with those of other elastomers

Properties	Units	Natural Rubber	Styrene Rubber	Nitrile Rubber	PEC (41% Cl)
300% elongation modulus	kgf./cm.²	3.0	3.3	5.7	6.3
Tensile strength	kgf./cm.²	3.4	4.1	6.6	14.5
Relative breaking elongation	%	700	1,400	2,800	1,000
Residual elongation	%	17	15	26	12

The mechanical properties of chlorinated polyethylene vary as a function of the degree of chlorination; the elastomeric character is at a maximum between 34-45% chlorine.

The thermal stability of chlorinated polyethylene is poor; it can be improved, however, by addition of stabilizers.

POLYMER MIXTURE OF POLYVINYL CHLORIDE—CHLORINATED POLYETHYLENE (PVC-PEC).

Compounding of Polyvinyl Chloride with Chlorinated Polyethylene

Polyvinyl chloride can be mixed with chlorinated polyethylene either on rolls, or before the separation of the polymers (the chlorinated polyethylene solution can be mixed with an emulsion or suspension of polyvinyl chloride).

1. Compounding on rolls. Polyvinyl chloride obtained by suspension polymerization, with K = 70, was used for the compounding. Laboratory rolls were used, at a temperature of 150-155°C, in the presence of 2% stabilizer; total kneading time was 10 minutes.

In the initial tests it was found that, by simultaneous introduction of the polymers on the rolls, there were obtained breakable sheets with a very low impact resistance. Therefore, a new compounding method was tried, which consisted of the addition of the chlorinated polyethylene into the mixture after a preplasticization of the polyvinyl chloride on the rolls for 5 minutes; the kneading is continued for another 5 minutes. This procedure ensures a homogeneous mixing of the two polymers, which in this way can form solid solutions. This results in mechanical properties, especially impact resistance at low temperatures and transparency, which are superior to those obtained by simultaneous mixing. The explanation of this phenomenon is based on the fact that, in simultaneous mixing, as a result of the lower softening point of the chlorinated polyethylene, this latter, at the kneading temperature, covers the particles of polyvinyl chloride with a film which does not permit homogeneous dispersion of the two polymers. By preplasticization, once the chlorinated polyethylene is introduced, the polyvinyl chloride is in a fluid state; this enables homogenization and forming of a solid solution.

2. Concomitant precipitation of the two polymers was tried in various ways, by mixing the solution

Table 2

Variation of the mechanical properties of the PVC-PEC (80-20) mixture as a function of the mixing method

PEC/%Cl	Tensile strength, kg./cm.²		Breaking elongation, %		Impact resistance (unscalped)*	
	I	II	I	II	I	II
32.8	280	370	10	28	0	10
34.07	245	380	12.5	24	0	10
36.75	325	415	23	28.5	0	

I—Compounding by simultaneous addition to rolls.
II—Compounding by preplastification of PVC.
*Impact resistance expressed as the number of standard test samples that did not break, out of 10 test samples struck with a 40 kgf./cm.² hammer.

from the chlorination of the polyethylene with an emulsion or suspension of PVC. Isolation of the polymers was then performed in a manner similar to that for chlorinated polyethylene, by introduction of the mixture into hot saline water—which precipitates the polymer mixture—and entraining of the solvent with vapor. From all the mixing variants tried, there were obtained agglomerated and friable granules. The mechanical properties of the material obtained are poor, especially its impact resistance at low temperatures (Table 2); this procedure is, therefore, inappropriate.

Properties of the Polymer Mixture PVC-PEC

The properties of the mixture polyvinyl chloride-chlorinated polyethylene are determined by the following factors: the compounding method, the quality of the chlorinated polyethylene used (molecular weight of the polyethylene, chlorination procedure, chlorine content), and the ratio PVC-PEC in the mixture.

In the laboratory study, we investigated the variation of these parameters in order to obtain a compound with optimum physical and mechanical properties (especially impact resistance at low temperatures).

The influence of the method used in mixing the polymers, previously discussed, is illustrated by the data in Tables 2 and 3.

The molecular weight of the polyethylene used for chlorination does not have any considerable influence. At close values of chlorine content, the mechanical properties of mixtures with chlorinated polyethylene obtained from polyethylene with molecular weights of 14,000 or 80,000 do not differ considerably. One observes only a slight improvement in the impact resistance at low temperatures (— 16°C) for the heavier polyethylene (80,000). This slight advantage, however, does not compensate for the disadvantages of using high molecular-weight polyethylene in the chlorination process, so that the use of polyethylene having a lower molecular weight (14,000-24,000) remains preferable.

With regard to the method of chlorination, chlorination in solution proved best, since polyethylenes chlorinated in suspension yield compounds having reduced impact resistance.

The chlorine content of the chlorinated polyethylene determines, in the first place, its elastomeric character. The region of maximum elasticity (in the range 34-45% Cl), corresponds to the quality of the chlorinated polyethylene, for the increase in impact resistance, especially at low temperatures, of polyvinyl chloride. The chlorinated polyethylenes containing 40-45% Cl are to be preferred for compounding, since they confer on the products obtained from the appropriate mixture a maximum degree of transparency.

In order to exhibit the improvement in impact

Table 3

Variation in mechanical properties of the PVC-PEC mixture (70-30) as a function of the mixing method

Properties	Mixture obtained on rolls with preplasticization	Mixture obtained by concomitant precipitation
Tensile strength, kgf./cm.²	290	245
Breaking elongation, %	70	180
Bending resistance, kgf./cm.²	555	330
Elastic bending modulus, kgf./cm.²	20,000	17,000
Brinell hardness, 10"/60", kgf./cm.²	700/650	600/520
Impact resistance (unscalped test samples) at 20°C, kgf.cm./cm.²	FR	FR
Impact resistance (unscalped test samples) at 0°C, kgf.cm./cm.²	FR	30-60
Impact resistance (unscalped test samples) at −10°C, kgf.cm./cm.²	FR	8-48
Impact resistance (unscalped test samples) at −20°C, kgf.cm./cm.²	FR	16-44
Impact resistance (unscalped test samples) at −30°C, kgf.cm./cm.²	65-FR	15-22
Impact resistance (scalped test samples) at 20°C, kgf.cm./cm.²	60-FR	6-50
Impact resistance (scalped test samples) at 0°C, kgf.cm./cm.²	2-18	2
Vicat thermal stability, °C	69	65

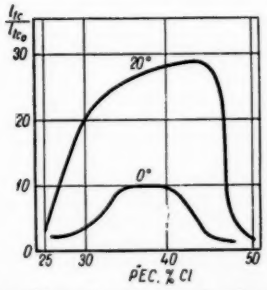

Fig. 4. Variation of impact resistance (scalped test samples) of mixture of PVC-PEC (80-20) with chlorine content of PEC. (Impact resistances expressed as multiples of the impact resistance of hard polyvinyl chloride).

resistance resulting from the elastifying action of the chlorinated polyethylene on polyvinyl chloride, Figs. 4 and 5 show the impact resistances of a mixture of the two polymers (80 PVC-20 PEC) as multiples of the impact resistance of hard, unplasticized polyvinyl chloride.

Fig. 6 exhibits the variation curves for the other mechanical properties of the mixtures as a function of the chlorine content of the chlorinated polyethylene.

The content of chlorinated polyethylene determines the rigidity of the polymer mixture, whose elastic modulus is lower the richer it is in chlorinated polyethylene (Table 4).

The thermal stability is lower for the compound than for the polyvinyl chloride; it can be improved satisfactorily, according to processing needs, by the addition of stabilizers.

The PVC-PEC mixture combines the high resistance to chemical corrosion of the component polymers, being stable in the presence of water, acids, bases, aliphatic hydrocarbons, acetone, alcohols, etc. (3).

Table 4

Physical and mechanical properties of PVC-PEC mixture, compared with those of imported polyvinyl chloride-polyethylene mixture

Properties	Units	PVC-PEC mixture (ICECHIM)				PVC-PEC mixture, imported			Hard PVC (suspension polymerized, K70)	Polyethylene (polymerized at low pressure, MW 24,000)
		PEC content (43% Cl), %				Types				
		10	15	20	30	I	II	III		
Tensile strength	kgf./cm.²	525	480	320	290	450	350	230	560	250-350
Breaking elongation	%	36	43	45	70	30	50	100	25	800
Bending resistance	kgf./cm.²	980	785	670	555	750	550	200	1,130	280-300
Elastic bending modulus	kgf./cm.²	32,000	24,700	22,300	20,000	13,800	11,300	5,100	37,000	2,000-5,000
Brinell hardness, 10"/60"	kgf./cm.²	1,100/1,025	500/860	–/700	700/650	900/850	750/700	350/300	170/1,100	330/300
Impact resistance (unscalped test samples) at 20°C	kgf.cm./cm.²	FR	FR	FR	FR	FR	FR	FR	25...FR	FR
Impact resistance (unscalped test samples) at 0°C	kgf.cm./cm.²	FR	FR	FR	FR	FR	FR	FR	20...FR	
Impact resistance (unscalped test samples) at –10°C	kgf.cm./cm.²	FR	FR	FR	FR	–	–	–	–	
Impact resistance (unscalped test samples) at –20°C	kgf.cm./cm.²	65...FR	FR	FR	FR	60...FR	FR	FR	6...45	
Impact resistance (unscalped test samples) at –30°C	kgf.cm./cm.²	30...130	30...FR	40...FR	65...FR	–	–	–	–	
Impact resistance (scalped test samples) at 20°C	kgf.cm./cm.²	2...6	5...55	40...60	60...FR	40	50	50...FR	2	8
Impact resistance (scalped test samples) at 0°C	kgf.cm./cm.²	2...3.5	2...4.5	1.5...3	2...18	8	10	20	2	
Vicat thermal stability	°C	86	78	78	69	80	75	55	90	

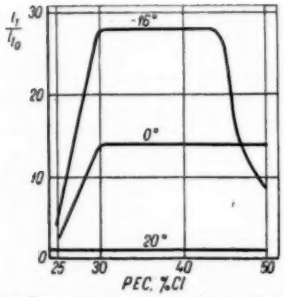

Fig. 5. Variation of impact resistance (unscalped test samples) of mixture of PVC-PEC (80-20) with chlorine content of PEC. (Impact resistance expressed as multiples of the impact resistance of hard polyvinyl chloride.)

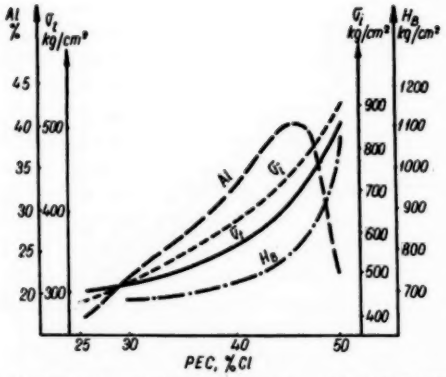

Fig. 6. Variation in mechanical properties of the PVC-PEC polymer mixture (80-20) with the chlorine content of the chlorinated polyethylene.

σ_t – Tensile strength
A_l – Breaking elongation
σ_i – Bending resistance
H_B – Brinnell hardness

Processing of Mixtures

Processing of the mixtures of PVC-PEC into final objects was carried out by all the customary methods for PVC: compression molding, extrusion, injection molding, etc.

At ICECHIM we produced extruded tubing, straight and wavy sheets, pressed objects for common use, injection-molded objects, etc., having superior mechanical properties, especially as regards impact resistance at low temperatures.

Use of PVC-PEC Mixtures

Commercial application of PVC-PEC mixtures can be carried out by uses in various fields: calendered sheets for resistant packaging in the food industry, vacuum-formed sheets, covers, plane or undulated sheets made by compression molding, water piping with very high impact resistance at low temperatures, various profiles, electrical insulation for non-inflammable and high-chemical-resistance cables, bottles and hollow vessels for the food and chemical industries, etc.

In all these areas, the mixture offers remarkable advantages over its base polymers; polyvinyl chloride and polyethylenes. Compared to polyvinyl chloride, a considerable improvement in impact resistance is evident in the mixture, especially at low temperatures; the tensile strength and bending resistance, and the modulus of elasticity are not affected appreciably for end-use needs. As compared to polyethylene, it is seen that the mixtures with 20-30% chlorinated polyethylene have similar tensile strengths, and higher bending resistances and elastic moduli; the impact resistances for unscalped test samples are similar to those of polyethylene, and are definitely superior for scalped test samples (Table 4). There arises, therefore, the possibility of using spun items made of a PVC-PEC mixture, which would eliminate the need for adhesives, and would solve the problem of preparing fiber combinations.

LITERATURE CITED

1. Frey, H. H., *Kunststoffe*, 49, p. 50 (1959).
2. Krenzel, B. A., *Zhur. Prikl. Khim.*, 32, No. 6, p. 1404 (1959).
3. Dolezel, B., *Chem. Průmsyl*, No. 2, p. 106 (1961).
4. *French Patents* 1198579, 1198421, 1195730, 1197716, 1180397/1959, 1145459/1957.
5. Miss, A. and Coppel, P., *Revista de Standardizare*, No. 3, p. 142 (1959).

Vendelín Macho

CZECHOSLOVAKIA

Effect of Sulfur and Some of its Compounds on the Oxo Process

An investigation of the effect of sulfur, carbon disulfide, ethyl mercaptan, tetrahydrothiophene, and thiophene on the oxonation of C_6-C_7 *olefins to* C_7-C_8 *aldehydes.*

RAW materials usually employed in the Oxo process may contain various sulfur impurities; for example, propylene obtained by cracking may contain organic sulfur, especially in the form of ethyl mercaptan, and higher olefins also sulfides and disulfides (1, 2). Benzene used as solvent may be contaminated with thiophene and other sulfur compounds.

The general opinion held in the literature (3, 4) is that the Oxo process, unlike the Fischer-Tropsch process, is not sensitive to sulfur. V. N. Hurd and B. H. Gwynn (5) report that although sulfur does not poison the Oxo catalyst, its absence leads to a better quality of the final product. A patent (6) protects the use of elemental sulfur as a promoter for the Oxo process, and the recommendation is made to act with hydrogen sulfide, carbon disulfide, or a solution of sulfur on cobalt before its use in the Oxo process, which is presumed to make the catalyst insensitive to oxygen and sulfur (7). V. L. Hughes and J. Kirshenbaum (8), in connection with the testing of amides and other additives for their effect on the rate of the Oxo process, found that an addition of thiophene results in a slight increase in reaction rate (by a factor of 1.1). P. W. Sherwood (9) states, on the other hand, that the presence of sulfur hinders the hydrogenation of the aldehydes formed to alcohols during the first stage of the Oxo process. In this connection, we may also mention the preparation of cobalt hydrotetracarbonyl (this compound is probably the actual Oxo catalyst) from pyrophoric cobalt, carbon monoxide, and hydrogen sulfide at 150°C (10), in which it is correctly pointed out that it is necessary to operate in a copper-clad autoclave, which binds the sulfur of hydrogen sulfide. The importance of this fact will be even more evident after a reading of the present article, in which we describe an investigation of the effect of sulfur, carbon disulfide, ethyl mercaptan, tetrahydrothiophene, and thiophene on the oxonation of C_6-C_7 olefins to C_7-C_8 aldehydes.

No detailed reports have been published thus far in the literature on the effect of sulfur and sulfur compounds on the Oxo process. Fragmentary reports, which are for the most part cited in this article, produce the general impression that sulfur and its compounds have no effect on the Oxo process itself. Our results, however limited in their scope, are in agreement with these views, and we thus regard their publication as desirable.

This article first published in *Chem. Zvesti*, No. 15, 181-190 (1961). The author is associated with the Petrochemical Research Institute, Nováky, Czechoslovakia.

EXPERIMENTAL PART

Raw Materials Used

Gasoline (from Fischer-Tropsch synthesis), fraction 51-92.5°C at 743 mm., d_4^{20} 0.6744, n_D^{20} 1.3868, iodine number 79.3, i.e., containing 28.2% by weight of C_6-C_7 olefins (calculated as $C_{6.5}$), from bromine number determined by the bromide-bromate method.

Cobalt (II) stearate, prepared from stearic acid and reagent grade cobalt (II) carbonate, containing 8.971% by weight of cobalt. Cobalt in cobalt (II) stearate as well as cobalt dissolved in the products in the form of carbonyls and other complex compounds was determined polarographically (11).

A mixture of carbon monoxide and electrolytic hydrogen (synthesis gas), in a 1:1 volume ratio, after purification contained 0.3% by volume of carbon dioxide and 0.04 ± 0.01% by volume of oxygen. Carbon dioxide was determined by absorption in 50% potassium hydroxide, and oxygen with a continuous polarographic analyzer (12).

Sulfur and carbon disulfide, reagent grade.

Ethyl mercaptan (redistilled), boiling point 37°C, n_D^{25} 1.4348.

Thiophene (redistilled), boiling point 83.4-84.1°C, n_D^{20} 1.5241.

Tetrahydrothiophene (prepared by the contact method from tetrahydrofuran and hydrogen sulfide over alumina, and rectified), boiling point 118.5-119°C at 748 mm., n_D^{20} 1.5041.

Procedure

A half-liter stainless-steel rotating autoclave was charged with cobalt stearate and an ampoule

with a weighed amount of sulfur or sulfur compound was introduced. The autoclave was then closed and air was purged from it by carefully passing through hydrogen. By means of hydrogen pressure, 50 g. of gasoline (i.e., 14 g. of C_6-C_7 olefins), likewise previously purged with hydrogen, was then forced into the autoclave using a special pipette. Finally, synthesis gas was forced in up to a pressure of 110 atm. gauge. While rotating the autoclave, the contents were heated with the aid of a resistance winding to the desired reaction temperature of 150°C in about 45 minutes. This temperature was maintained to within ±2°C until the end of the reaction, detected as the instant when pressure ceased to decrease. Temperature and pressure were read at 15-minute intervals. The time when the temperature of the autoclave reached 150°C was taken as the start of the measurements, and corresponds to zero time in the figures.

RESULTS AND DISCUSSION

Effect of Elemental Sulfur on Oxo Synthesis

The course of experiments with different amounts of sulfur and without it in the presence of 0.2% by weight of cobalt, based on the weight of the olefins in each experiment, is represented in Fig. 1.

Pressure p_0 was calculated from the measured values in atm. gauge with the aid of the equation of state for ideal gases, neglecting compressibility because we are dealing with a comparison of the course of the reactions under the conditions used.

For clarity, Fig. 1 does not include the results of all the experiments in the presence of sulfur, but the other results can be seen in Fig. 2, which shows conversion of olefins as a function of the amount of sulfur added. Conversion was followed by the decrease in the amount of olefins determined analytically in the product after the conclusion of the reaction, and not from the amounts of the C_7-C_8

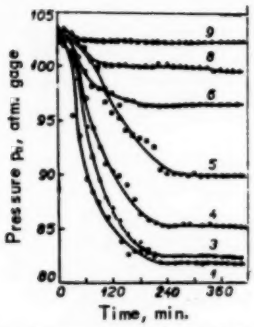

Fig. 1. Kinetics of oxonation of C_6-C_7 olefins to C_7-C_8 aldehydes as a function of amount of sulfur added. 1) 0.000% S by wt.; 3) 0.0074% S; 4) 0.050% S; 5) 0.082% S; 6) 0.100% S; 8) 0.178% S; 9) 0.200% S.

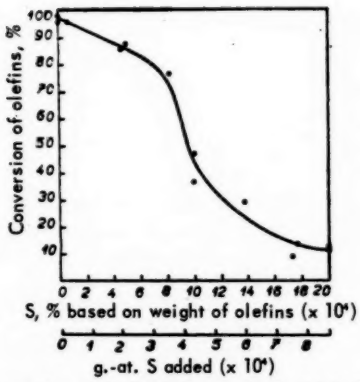

Fig. 2. Conversion of C_6-C_7 olefins to C_7-C_8 aldehydes as a function of amount of sulfur added.

aldehydes and alcohols formed which, soon after their formation, undergo partial acetalization, aldol addition, and other changes which lower the yields of aldehydes. This procedure is possible because hydrogenation and polymerization of olefins under the conditions of the Oxo process is practically negligible, and any by-products are formed with the same consumption of the reaction components as in the formation of the aldehydes themselves.

Fig. 1 shows that, although the Oxo reaction in the presence of sulfur has a very brief induction period, practically inevitable for the formation of cobalt carbonyls from the cobalt stearate, it is retarded and soon stops, as if complete conversion were reached. For this reason we determined in the resulting product (which was withdrawn after cooling the autoclave), in addition to iodine number, also the amount of cobalt carbonyls, of which especially dicobalt octacarbonyl is readily soluble in the reaction product.

It was found (Fig. 3) that as the amount of sulfur added is increased, the total amount of soluble cobalt carbonyls (expressed as Co in Fig. 3) in the product decreases. The balance of the cobalt settled on the walls and bottom of the autoclave, largely in the form of sulfide. The decrease in the amount of cobalt in gram-atoms is almost directly proportional to the gram-atoms of sulfur added. It

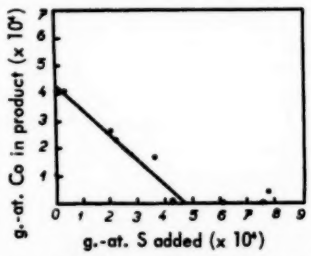

Fig. 3. Amount of cobalt in product in the form of soluble cobalt carbonyls as a function of amount of sulfur added.

is seen that when 4.36×10^{-4} g.-at. of sulfur is added (Expts. 6 and 7) and when the amount of cobalt used in the reaction is 4.78×10^{-4} g.-atoms, the resulting product contains no soluble cobalt carbonyls.

The differences between the amount of cobalt added and that found in the product from the reference experiment without sulfur was due largely to traces of oxygen present in the synthesis gas and possibly to elemental cobalt in equilibrium with cobalt carbonyls which were left in the autoclave, further by losses in the form of cobalt hydrotetracarbonyl, etc.

Experiments were also carried out with a constant amount of sulfur (0.10% by weight based on olefins, i.e., 4.36×10^{-4} g.-at.) and with different amounts of cobalt added. The results are summarized in Table 1.

It is seen from Table 1 that while at 4.78×10^{-4} g.-at. of cobalt, i.e., 0.2% by weight based on the weight of olefins, in the presence of 4.36×10^{-4} g.-at. of sulfur the conversion was 47.35%, with 0.4% by weight of cobalt, conversion was already 90% and the final product also contained soluble cobalt carbonyls.

In order to verify still better the behavior of cobalt carbonyls in the reaction system in the presence of sulfur, an experiment was carried out using 100 g. of a solution of dicobalt octacarbonyl in toluene (0.0619% by weight of Co, i.e., corresponding to 1.05×10^{-3} g.-at. of cobalt and 0.31% by weight of Fe present as $Fe(CO)_5$), to which was added 0.0560 g. of sulfur, i.e., 1.74×10^{-3} g.-at. The reaction conditions were the same as in the preceding experiments, with the only difference that no olefin was used. A study was thus made of the kinetics of the disappearance of cobalt carbonyls from the solution. It was found that even before the autoclave temperature reached 150°C, the original 1.05×10^{-3} g.-at. of cobalt was reduced to only 2.85×10^{-4} g.-at., and after heating for a further 4 hours at 150°C, the amount of cobalt dropped to 1.32×10^{-4} g.-at.

The detrimental effect of elemental sulfur on the Oxo process is largely the same as that of oxygen (13).

Table 1

Effect of different amounts of cobalt in the presence of a constant amount of sulfur

Expt. No.	Added S, g.-at. (x 10^4)	Added Co, g.-at. (x 10^4)	Conversion of olefins, %	Co in product, g.-at. (x 10^4)
18	4.36	2.97	40.30	0.00
6	4.36	4.78	47.35	0.00
19	4.36	9.57	90.25	2.19

It is evident from the results obtained that under the conditions of the Oxo process, sulfur reacts with cobalt carbonyls, which are the actual oxonation catalyst, or with very active cobalt, from which these carbonyls are formed, most likely according to

$$2Co + 8Co \rightleftharpoons [Co(CO)_4]_2 + H_2 \rightleftharpoons 2HCo(CO)_4$$
$$\downarrow + S$$
$$Co_xSy^*$$

The equilibrium is shifted in the direction of the decomposition of dicobalt octacarbonyl and cobalt hydrotetracarbonyl.

It follows from Fig. 3 that if the amount of elemental sulfur in the system is represented by Y (in gram-atoms) and the amount of cobalt in the solution of X (also in gram-atoms), cobalt is not found in the solution after the experiment, when $Y \geq X$ or $Y/X \geq 1$.

Effect of Carbon Disulfide and Ethyl Mercaptan on the Oxo Process

The course of the oxonation of C_6-C_7 olefins in the presence of different amounts of carbon disulfide and a cobalt concentration of 0.2% based on the weight of olefins is shown in Fig. 4. The similarity of this figure to Fig. 1 is striking. Even the decrease in the amount of carbonyls in the resulting

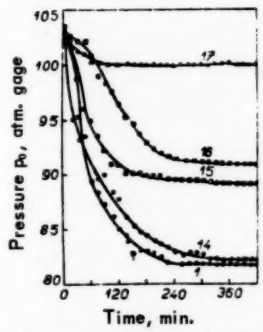

Fig. 4. Kinetics of oxonation of C_6-C_7 olefins to C_7-C_8 aldehydes as a function of the amount of carbon disulfide added. 14) 0.0735% by wt. CS_2; 15) 0.1170% CS_2; 16) 0.1820% CS_2; 17) 0.4314% CS_2.

product was similar to that in experiments in which elemental sulfur was present. It follows from this that even carbon disulfide under the conditions of the Oxo process binds cobalt or cobalt carbonyls and thus destroys their catalytic action, which in the final result (Fig. 5) is reflected in the Oxo reaction stopping before the conversion of olefins to aldehydes is complete.

*Translator's Note: *sic*.

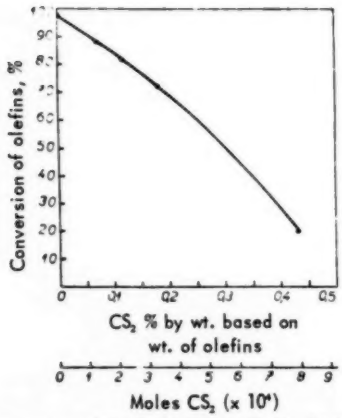

Fig. 5. Conversion of C_6-C_7 olefins to C_7-C_8 aldehydes as a function of the amount of carbon disulfide added.

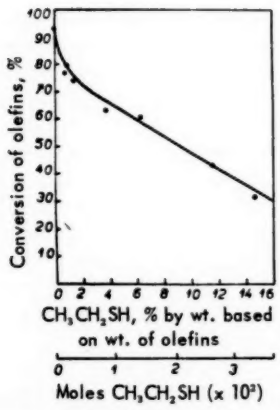

Fig. 6. Conversion of C_6-C_7 olefins to C_7-C_8 aldehydes as a function of added ethyl mercaptan.

Fig. 6 shows that ethyl mercaptan also is detrimental to the Oxo reaction, lowers conversion and, even though to a much lesser degree than elemental sulfur or carbon disulfide, nevertheless attacks cobalt carbonyls or active cobalt. This is probably the result of the relatively strongly acidic character of ethyl mercaptan (14), which is due to the lower strength of the bond between hydrogen and sulfur in the sulfhydryl group. A further possibility lies in the ability of the RS group of mercaptans to replace the carbonyl group in dicobalt octacarbonyl (15) according to

$$Co_2(CO)_8 + C_2H_5\text{-}SH \rightarrow Co_2(CO)_2(C_2H_5S)_2 + H_2 + CO$$

The likelihood of the two alternatives may serve as confirmation for the observation that the product of the Oxo reaction from an experiment carried out in the presence of 14.16% by weight of ethyl mercaptan (3.3×10^{-2} moles) and 4.78×10^{-4} g.-at. of Co was not free from soluble cobalt compounds (contained 1.04×10^{-4} g.-at. of Co), even though the conversion attained was only 31.85%. When such a low conversion was obtained in the presence of elemental sulfur, the products were completely free from soluble cobalt compounds.

The detrimental effect of elemental sulfur, carbon disulfide, and ethyl mercaptan on the course of oxonation can, on the basis of the results obtained, be expressed quantitatively by the following expression (assigning a value of 100 to the detrimental effect of sulfur):

$$S : CS_2 : C_2H_5SH = 100 : 71 : 1.6$$

In calculating this relationship, the amount of sulfur and its compounds in g.-atoms or moles at which a 40% conversion of C_6-C_7 olefins is obtained, was used as the basis.

Using a larger amount of cobalt carbonyls or other metals and compounds which can react with sulfur and its compounds (copper, carbonyls of iron and other metals, etc.) will diminish these differences. When larger amounts of cobalt carbonyls are used, their detrimental effect on the reaction rate of the Oxo reaction as well as conversion may not be detected at all. A similar effect is obtained especially when the process is conducted in autoclaves whose walls are coated with cobalt from previous experiments, or in copper-clad autoclaves.

Effect of Tetrahydrothiophene and Thiophene on the Oxo Process

Tetrahydrothiophene was selected for the experiments primarily because it is a completely saturated compound with firmly bound organic sulfur. Experiments revealed that it neither inhibits nor retards the Oxo process. The products obtained likewise contained soluble cobalt carbonyls.

In this connection, it was also of interest to determine the effect of thiophene, which contains two conjugated double bonds, since it is known that some diolefins and more highly unsaturated olefins inhibit oxonation (4, 16). The results obtained with the use of thiophene and tetrahydrothiophene are summarized in Table 2.

It is evident from Table 2 that the presence of thiophene and tetrahydrothiophene in an amount of 5-7% by weight based on olefins had practically no effect on conversion. This points to their stability under the conditions of the two-stage Oxo process, which lies in the ability of tetrahydrothiophene and thiophene to react with cobalt carbonyls or with catalytically active forms of cobalt. The presence of conjugated double bonds likewise had none of the usual effect. This is probably due primarily to the strongly aromatic character of thiophene and thus a limited relation to conjugated diolefins. This is confirmed especially by the studies of I. Wender, H. Greenfield, and their co-workers (17, 18), who

Table 2

Expt. No.	Co, % by wt. based on olefins	Substance added	Amount of substance added		Conversion of olefins, %
			% by wt. based on olefins	moles (x 10^3)	
21	0.200	tetrahydrothiophene	0.494	0.790	91.49
22	0.200	tetrahydrothiophene	0.860	1.374	91.37
24	0.200	tetrahydrothiophene	1.744	2.789	97.54
36	0.200	tetrahydrothiophene	4.241	6.782	92.86
25	0.200	thiophene	0.752	1.267	96.72
31	0.200	thiophene	0.989	1.657	92.79
26	0.200	thiophene	3.003	5.032	94.65
28	0.200	thiophene	6.775	11.350	93.66

found that thiophene fails to oxonate even under the conditions of the one-stage Oxo process, i.e., at a temperature of about 190°C and a pressure of the synthesis gas of about 400 atm. but undergoes only homogeneous hydrogenation with the formation of tetrahydrothiophene.

Thus our experiments with thiophene and tetrahydrothiophene, like the results obtained by H. Adkins and G. Krsek (19) with phenyl sulfide, show that thioether sulfur has no effect on the course of the Oxo process.

SUMMARY

Sulfur has a retarding effect on the Oxo process and reduces conversion of olefins to aldehydes. For example, when 0.20% by weight of cobalt, based on the weight of C_6-C_7 olefins, is used in the presence of 0.1% by weight of sulfur, conversion is about 42%, and with 0.2% of sulfur, conversion is no more than 12%. Using an equimolar amount of sulfur with respect to the cobalt present in the reaction medium, not only is conversion of olefins about 45%, but the product obtained contains no soluble cobalt carbonyls. By increasing the amount of cobalt, reaction rate and conversion increase linearly. Since sulfur restricts the formation of cobalt carbonyls, the optimum amount of the catalyst is determined also by the purity of the raw materials. The purer are the latter, the greater, up to a certain point, will be the rate and conversion of the Oxo reaction under otherwise identical conditions, or the smaller will be the amount of catalyst required to produce the same conversion.

An effect similar to that of elemental sulfur is shown by carbon disulfide. Oxonation is affected much less by ethyl mercaptan. Quantitative calculation of the relative adverse effects of sulfur, carbon disulfide, and ethyl mercaptan (on mole basis) gives the approximate relationship

$$S : CS_2 : C_2H_5SH = 100 : 71 : 1.6$$

Tetrahydrothiophene and thiophene, even when present in an amount of 5-7% based on the weight of olefin, do not retard or inhibit oxonation and do not lower conversion, and it may thus be concluded that compounds containing only thioether sulfur have practically no adverse effect on the Oxo process. Successful oxonation is hindered by elemental sulfur and sulfur compounds which are capable of attacking cobalt carbonyl under the reaction conditions of the Oxo process.

LITERATURE CITED

1. Alekseeva, K. A., Rudkovskii, D. M., Ryskin, M. I., and Trifel, A. G., *Khim. i Tekhnol. Topliv i Masel* 5, p. 14-17 (1959).

2. Johnson, F. B., Smith, W. M., and Moise, J. E., U. S. Patent 2,778,859.

3. Schuster, C., *Fortschr. chem. Forsch.* 330, (1951).

4. Orchin, M., in *Chemistry of Petroleum Hydrocarbons* (a Russian translation), Vol. III, p. 292, Moscow (1959).

5. Hurd, V. N., and Gwynn, B. H., *Oil Gas J.* No. 24, 199, (1959).

6. Field, E., U. S. Patent 2,683,177.

7. Hagemeyer, H. J., Jr., U. S. Patent 2,691,045.

8. Hughes, V. L., and Kirshenbaum, J., French Patent 1,173,397.

9. Sherwood, P. W., *Petroleum Refiner*, C-26, (March, 1958).

10. Orchin, M., and Schroeder, W. C., in Groggins, P. H., "Unit Operations in Organic Synthesis" (a Czech translation), Prague (1958).

11. Šingliar, M., and Kokladalová, J., Petrochemical Research Institute, Nováky (to be published).

12. Kapišinský, Z., "Polarografický analyzátor kyslíka" (Polarographic Oxygen Analyzer), Final Report, Research Institute of Acetylene Chemistry, Nováky (1958).

13. Čĥa, M., Macho, V., and Střesinka, J., *Chem. Zvesti* 13, 530-535 (1959).

14. Marko, M., *Organická chémia*, p. 187, Bratislava (1955).

15. Hieber, W., and Spacu, P., *Z. anorg. allgem. Chem.* 233, p. 353 (1937).

16. Brit. Patent 747,493 (1956).

17. Wender, J., Levine, R., and Orchin, M., *J. Am. Chem. Soc.* 72, p. 4375 (1950).

18. Greenfield, H., Metlin, S., and Orchin, M., *J. Org. Chem.* 23, p. 1054 (1958).

19. Adkins, H., and Krsek, G., *J. Am. Chem. Soc.* 71, p. 3051 (1949).

A. A. Berlin
L. I. Boguslavski
R. Kh. Burshtein
N. G. Matveeva
A. I. Sherle
N. A. Shurmovskaya

USSR

Some Electrophysical Properties of Polymer Complexes of Tetracyanethylene with Metals

Results of research aimed at commercial production of coatings and plastics based on polymeric chelate compounds of tetracyanethylene with metals.

It was shown earlier that interaction of tetracyanethylene with metal powders and salts of metals results in formation of polymeric chelate compounds which apparently have an azoporphyrin structure (1). Polymeric chelate compounds of tetracyanethylene with metals are not soluble in common organic solvents, alkalies and dilute acids. These compounds do not melt, are able to withstand heating at 500°C for many hours, possess notable magnetic properties, and show band (600-800 oersted) and line spectra of electromagnetic flux. The infusibility and insolubility of polymeric chelates of tetracyanethylene as well as of other polychelate compounds (2) make their investigation and processing difficult. A measure of theoretical and practical importance, in this connection, should be attached to the recently proposed method for the production of coatings and plastics based on polymeric chelates of tetracyanethylene and its mixtures with di- and tetranitriles (3).

The data reported in the present communication were obtained in a study of the electrophysical properties of films consisting of polymeric chelate compounds of tetracyanethylene with metals. These films, chemically bound to the metal, were obtained by treating plates of copper, iron, nickel and other metals with tetracyanethylene vapor.

EXPERIMENTAL PROCEDURE

Degreased, and in some cases also electropolished and etched metal plates, were placed in a vessel filled with tetracyanethylene. The air was next pumped out of the vessel until the pressure had been reduced to 10^{-5} mm. Hg. The reaction was carried out at 150°C to 400°C and lasted 5-20 hours. As a result, a film of the polymer complex formed on the surface of the plate, which was firmly bound to the metal.

The samples obtained in this manner were further studied, without any additional treatment. The thickness of a film was determined on the basis of its weight as well as the specific gravity of the polymer. In experiments with iron, the thickness of polymer complex films varied depending on surface treatment, from 5×10^{-6} to 3×10^{-5} cm. The films burned with great difficulty. As a consequence, microanalytical combustion data are slightly low with respect to carbon content. For the polychelate complex of copper:

Found %: C, 43.66; Cu, 20.62
Calculated %: C, 45.66; Cu, 19.88.

Examination of the infrared spectrum of a film* deposited on copper (Fig. 1) revealed a total absence of absorption maxima in the range 800-2,300 $cm.^{-1}$. The inference that seems to suggest itself is that the polymer obtained had a "parquet" structure, most likely of the type shown below.

ELECTROPHYSICAL PROPERTIES

The electrophysical properties of the films were studied with the aid of an a.c. bridge, with capacitor and resistor connected in parallel, ranging 200 cycles to 0.2 megacycles.

This article first published in *Doklady Akademii Nauk SSSR, Otdel. Fiz. Khim.*, Vol. 136, No. 5, 1127-1129 (1961). The authors are associated with the Institute of Chemical Physics, Academy of Science, USSR, and the Institute of Electrochemistry, Academy of Sciences, USSR.

*The authors wish to express their sincere thanks to Yu. Sh. Moshkovski and N. D. Kostrova, who photographed and analyzed the infrared spectrum.

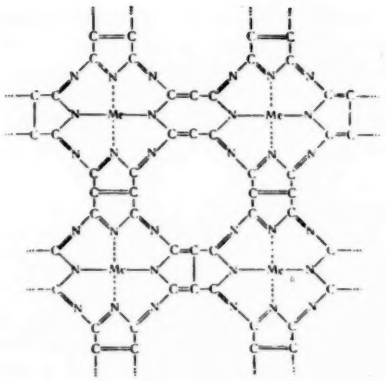

A test tube was tapered to a ground end, into which two wire leads were soldered. Mercury was poured into the test tube, and a plate coated with the polymer complex was immersed into the mercury. One of the leads was attached to the plate, the other connected the mercury to the measuring outfit. The polymer complex film therefore acted as a dielectric in a condenser, with metal plate and mercury functioning as condenser plates.

Measurements were carried out at a pressure of 10^{-5} mm. Hg. The presence of air, as a rule, materially affects the results of measurements, and will be the subject of another study.

The resistivity and capacitance of polymer complex films were determined as functions of temperature, heating time, and surface treatment of the metal. When iron plates were heated in tetracyanethylene vapor for 3 hours at 250°C, the polymer complex films obtained were relatively thin (3×10^{-6} cm.). They had a resistivity of the order $3 \times 10^{-9}(\text{ohm}^{-1})(\text{cm.}^{-1})$ and an effective dielectric constant = 7, which was calculated from the formula for a flat condenser, with a frequency of 3,000 cycles. When iron plates coated with polymer film were heated for 3 more hours under the same conditions, the resistivity rose to $3 \times 10^{-8}(\text{ohm}^{-1})(\text{cm.}^{-1})$ and the effective dielectric constant increased to 36. If the temperature at which the films were produced was raised from 250°C to 450°C, while the length of treatment remained the same, the resistivity rose from $5 \times 10^{-8}(\text{ohm}^{-1})(\text{cm.}^{-1})$ to $5 \times 10^{-6}(\text{ohm}^{-1})(\text{cm.}^{-1})$, and the effective dielectric constant reached the value of 70. The polarity of the thermal e.m.f. indicated that the films had the p-type of conductivity.

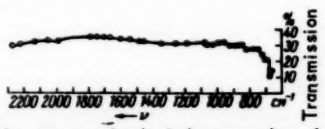

Fig. 1. Infrared spectrum of polychelate complex of copper.

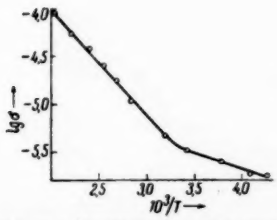

Fig. 2. Resistivity as a function of inverse temperature for a polymer complex film on etched iron, 300°C, 10 hrs.

Fig. 2 shows resistivity as a function of reciprocal temperature for polymer complex films on iron. The measurements were performed in the temperature interval −40°C to +220°C. The curve is seen distinctly to be composed of two straight line portions.

tions. The first portion, lying between −40°C and +30°C corresponds to an activation energy range of 0.07-0.12 ev. The second portion lies in the temperature interval between 30°C and 250°C, and corresponds to an activation energy range of 0.21-0.28 ev. The observed functional relationship between the logarithm of resistivity and reciprocal temperature is analogous to the relationship between 1/T and the resistivity of semiconductors, which exhibit additive conductivity.

Additional measurements were performed to determine the change in the effective dielectric permeability and resistance with the logarithm of a.c. frequency in the range 400 cycles - 0.2 megacycles.

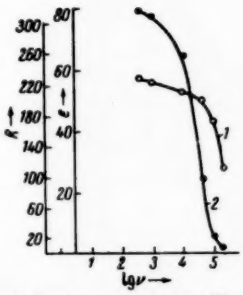

Fig. 3. Effective dielectric permeability (1) and resistance (2) as functions of the log a.c. frequency, for a polymer complex film on etched iron, 250°C, 10 hrs.

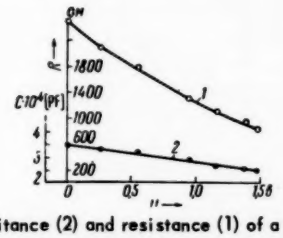

Fig. 4. Capacitance (2) and resistance (1) of a polymer complex film as functions of superimposed d.c. voltage (film deposited on air-oxidized iron), 250°C, 20 hrs.

The curves are presented in Fig. 3. It should be noted that the capacitance and resistance of the samples decreased when d.c. voltage was superimposed as seen from Fig. 4.

It should be pointed our further that significant results were obtained with iron plates coated with polymer complex film. When a direct current was passed through an alcoholic solution of copper sulfate, copper was deposited on the polymer film with which the iron plate was coated. The copper adhered firmly to the surface of the polymer complex. The relatively high values of the effective dielectric constant indicated that a polarization of the "conducting" macromolecules may have been involved.

To ascertain the nature of the electrophysical properties characterizing these films, and to determine, specifically, the significance of their nonhomogeneous structure, it is necessary to measure the effective dielectric constant of the given complex at higher frequencies. Arrangements are now being made for an experimental study of this kind.

REFERENCES CITED

1. Berlin, A. A., Matveeva, N. G., Sherle, A. I., *Izvestia Akademii Nauk SSSR, OKhN*, No. 12, 2261 (1959).
2. Berlin, A. A., Matveeva, N. G., *Uspekhi Khimii*, No. 3, 277 (1960); see also Berlin, A. A., *Uspekhii Khimii Polimerov*, No. 3 (1960).
3. Berlin, A. A., Matveeva, Sherle, A. I., Authors Certificate No. 126612, April 7, 1959.

Ryszard Chudzikiewicz

POLAND

Factors Affecting the Degree of Granular Materials

A theoretical treatment of mixing of granular solids. If the experimentally obtained standard deviation, s, is divided by the average concentration, $\bar{x}$, the results are independent of the relative concentration of the component in the mixture.

In the recent past, many branches of technology have demonstrated an immense growth of interest in granular materials. The essential tasks of this broad problem are: analysis of the mixing process, and development of a method for determining the degree of mixing.

In bulk mixers, Lacey (1) distinguishes three basic processes:

1. transfer of groups of particles, adjacent to one another, from one mixing spot to another—convection mixing,
2. distribution of particles over the newly developed surface—diffusion mixing,
3. setting (guiding) of sliding streams separated from the bulk of the mixture—shearing mixing.

In mixers, one, two or even all three of the above-mentioned processes can take place, depending on the type of the particular mixer. Convection mixing is predominant in paddle mixers with spirals or paddles. In the case of ordinary drum mixers, diffusion occurs through a surface rotating through the mixture. In continuous roll-mixers, the mixed materials form a continuous stream along the rim of the mixing bowl (disk) and are guided by spiral paddles into the center of the bowl, from where they escape to the outside through an appropriate opening. Here we observe mixing by shearing, which is similar to the flow of liquids at low Reynolds numbers (laminar). As in the case of a liquid, the mixing depends partially on diffusion perpendicular to the sliding streams.

The mixing of bulk materials is a relatively little investigated process. For this reason, the determination of the degree of mixing can be based only on statistical methods. Nearly all the methods for determining the degree of mixing are based on evaluating the quality of the mixture, which in turn is based on an analysis of randomly selected samples (2). If the mixture is entirely random, then the distribution of the components of the samples conforms to the two-dimensional Bernoulli distribution. If the mixed materials consist of various size grains, then the Manning formula, given by Buslik (1), can be used for determining the standard deviation of

This article first published in *Przem. Chem.*, 40, 48-51 (1961).

any component:

$$\sigma = \sqrt{\frac{p\,(1-p)\,\bar{\gamma}}{g}} \qquad (1)$$

where:

p - the actual relative concentration of the component,
$\bar{\gamma}$ - average weight of a particle in the mixture,
g - weight of the sample.

The above leads to the following two practical conclusions:

1. the scatter of the concentration of any component in the samples is a function of g.
2. the scatter of the concentration of a component is a function of p.

To determine the quality of mixing, in earlier work (4), the following was applied:

1. mixing quality factor Q
2. degree of mixing M

The method of Gesell (5) for determining the degree of mixing by comparing the value of $\bar{x}$ (average concentration of any component in the samples) with the value of p (actual concentration of the component in the mixture):

$$G = \frac{\bar{x}}{p} \qquad (1a)$$

cannot be applied in this case, since it does not provide any measure of scattering and cannot therefore be applied to statistical quality control. Furthermore, the value of p can be unknown.

The ratio of $\bar{x}$ and p provides a qualitative picture of the entire mixing process, i.e., the three factors which constitute the total process:

—mixed components,
—method of mixing,
—mixer characteristics.

When p is known, the mixing quality factor is introduced to determine the quality of the process:

$$Q = \frac{\bar{x}}{p} \qquad (2)$$

The above factor is not a measure of the scatter of the component concentration in the mixture. It is possible that in mixing the same mixture under different conditions the same degree of mixing with a different mixing quality factor will be obtained. The above difference indicates certain irregularities in the process, such as the presence of large dead areas and a tendency of one of the components to be held up in them, or a batching error (for example, short weight of a component), or a systematic error in measurement or analysis.

To determine the degree of mixing, a variance coefficient was applied in earlier work (4). This coefficient is sometimes used in mathematical statistics for determining the random variable scatter. It is the ratio of the standard deviation of the variable x to its average, $\bar{x}$, and is expressed as follows:

$$V = \sqrt{\frac{\Sigma\,(x_i - \bar{x})^2}{n-1}} \Big/ \bar{x} = \frac{s}{\bar{x}} \qquad (3)$$

where:

x_i - concentration of the component in sample i,
$\bar{x}$ - average concentration of the component in the samples,
n - number of samples.

The value of the standard deviation, s, is not a measure of the scatter, since it depends upon the actual content, p, and the size of the samples.

The advantage of the above method for determining the degree of mixing is that it is independent of p. M, determined by this method, depends only upon the size of the samples.

Thus, the degree of mixing in mixtures with different component concentration can be compared. For similar mixture components, (e.g., salt and sand) we obtain, after an hour's mixing in a laboratory roll mixer, the same degree of mixing at various values of p (1, 5, 10 and 50 percent), using equal weight samples, g = 2.0 grams). The selection of the variance coefficient as the yardstick of the degree of mixing has been thoroughly explained in an earlier work (4).

The method for determining the degree of mixing proposed by this writer

$$M = \frac{s}{\bar{x}} \qquad (3a)$$

does not call for a knowledge of p. It permits the determination of the degree of mixing when p is unknown or when it varies within certain limits, specifically in continuous mixing, and in all cases where fluctuations of the component concentration in mixer batching is observed. I wish to place particular emphasis on the fact that, in the laboratory as well as in industrial practice, the determination of p is far more difficult than it might appear. Out of several hundred measurements on the degree of mixing conducted in a laboratory mixer, only a few confirmed that x = p. If the mixture contains water or some volatile component, then p is not constant during the mixing process. Its value changed due to evaporation of the volatile component.

Classification of Factors Affecting the Degree of Mixing

Published data, as well as industrial practice, shows that the factors affecting the degree of mixing of granular materials can be divided into three groups which depend on:

— the mixing apparatus,
— the mixing method,
— and the type of the mixed materials.

The first group includes the following factors: type of mixer, its size and extent of filling, design features, and speed of rotation.

In the second group it is difficult to mention all the factors, due to the fact that quite unexpected circumstances may arise. In any case, the following factors affect the mixing process: sequence of introducing the mixture components, method and place of introduction of the individual components into the mixer (6), method of mixing (dry, wet, with simultaneous cooling or heating, etc).

The third group of factors includes: volume, particle shape and surface of each component, density of each component, relative concentration of each component (9), physical properties of each component and the variation of these properties during mixing.

Let us discuss briefly the effect of the respective factors upon the mixing process.

The type of mixer is determined by the mixing mechanism, i.e., diffusion, convection, or shearing mixing. The mixing depends essentially on whether the operation is continuous or intermittent (8).

The capacity of mixer, and the degree of its filling in particular, affects the requirements. It is known that if the nominal capacity is exceeded as the mixer is being filled, the mixing becomes less efficient.

The design features, such as the shape of the paddles or the size and weight of the rolls, affect the mixing process to a much greater extent than is usually assumed.

The mixing time which depends on the speed of the mixers, and which in turn determines the capacity of the mixer motor is also of interest.

Daily industrial practice confirms the importance of the sequence and method of introducing the respective components into the mixer (6). Frequently, the desired results depend only on these factors. It is known, for example, that mixing of dry components with subsequent wetting produces different results than the mixing of initially wet components.

The third group of factors is relatively little affected by mixing. The concentration of the respective components is determined by technological specifications and the weight of the components cannot be affected at all. In certain cases it is possible to control the particle size of the individual components through preliminary refining and subsequent screening. During mixing and in the presence of moisture, certain physical properties of the components change and affect to a considerable extent the mixing process.

Technique of Measuring the Degree of Mixing

The sampling of mixtures must be conducted at random, but under the same conditions. It is most convenient to determine certain points in the mixer from which equal volume samples are taken at appropriate time intervals during the investigation. The component of interest should not affect the conditions of the mixing. The determination of the number of samples is a statistical problem. The validity of the obtained results depends upon this number. In general, from five to ten samples are taken. In practice, the volume of the samples limits the accuracy of the analysis of their chemical composition. The samples should be as small as possible, not, however, smaller than a size which theoretically make the achievement of $x_i = p$ possible (3).

A number of measurements were conducted to investigate the effect of various factors upon the degree of mixing. The tests were carried out with Simpson laboratory roll mixers. The basic component of the mixture consisted of quartz sand screened through a No. 30* sieve. The component investigated was either rock salt or zinc oxide.

Effect of Filling Upon the Degree of Mixing

A series of mixing operations was conducted with the laboratory mixer using, the same charge: 99% quartz sand, 1% zinc oxide and 5% water (with respect to the dry components). The degree of filling the mixer was varied, the charge was 9.3 and 6 kg. respectively. After a five-minute mixing period, the mixing quality indices were obtained (Table 1) for measurements designated with the letters P, R, S:

$$Q = 0{,}99;\ 1.26;\ 1.07$$

and the following degrees of mixing

$$M = 0.045;\ 0.131;\ 0.0525$$

The results indicate that the 6 kg. capacity of the laboratory mixer (in conformance with the RN-55/MPM-22047 Standard) is not the optimum capacity from the viewpoint of mixing quality. The "dead space" is almost constant, and exerts a considerable effect in the case of the small charge. This is reflected in the charge of v = 3 kg. by a low mixing quality index Q = 1.26, and a low degree of mixing M = 0.131. Optimim conditions for the mixing process are obtained when the mixer is filled with v = 9 kg.

*Size of sieve mesh 0.60 mm.; the screening (sieving) was carried out in conformance with the RN-55/MPM-22077 standard.

Table 1

Composition of mixture: 99% quartz sand, 1% ZnO (converted to dry components), 5% water; p = 1%;
Simpson laboratory mixer: weight of samples, 2 grams

Measurement	Mixing time, min.	x_1 (%)	x_2 (%)	x_3 (%)	x_4 (%)	x_5 (%)	x_6 (%)	$\bar{x}$ (%)	$\frac{\Sigma (x-\bar{x})^2}{5}$	$\frac{s}{\bar{x}}$
P	5	0.976	1.040	0.939	0.953	1.052	0.983	0.991	0.002111	0.045
R	5	1.138	1.196	1.237	1.578	1.213	1.143	1.261	0.027329	0.131
S	5	1.086	1.170	1.040	1.023	1.025	1.095	1.073	0.003191	0.0525
T	2 × 2.5	1.136	1.162	1.043	1.157	1.154	1.172	1.137	9.002363	0.0427
U	5	1.052	1.085	0.683	1.275	1.080	0.977	1.025	9.037824	0.189

P – 9 kg. of dry components
R – 3 kg. of dry components
S – 6 kg. of dry components
T – 6 kg. of dry components
U – 6 kg. of dry components

Table 2

Composition of mixture: 5.94 kg. of quartz sand and 0.06 kg. salt; pv = 1%;
Simpson laboratory mixer; samples 0.5; 2 and 10 grams, collected by syringe

Time, min.	Sample, grams	x_1 (%)	x_2 (%)	x_3 (%)	x_4 (%)	x_5 (%)	$\bar{x}$ (%)	$\frac{\Sigma (x-\bar{x})^2}{4}$	$\frac{s}{\bar{x}}$
0.5	0.5	0.92	0.64	0.57	0.97	0.54	0.73	0.0409	0.277
	2.0	0.59	0.63	0.61	0.73	1.09	0.73	0.0434	0.285
1	0.5	0.97	0.72	0.79	0.53	0.66	0.73	0.0263	0.222
	2.0	0.88	0.74	0.73	0.88	0.67	0.78	0.0091	0.122
5	0.5	0.75	0.79	0.72	0.88	0.85	0.80	0.0045	0.084
	2.0	0.75	0.74	0.69	0.78	0.69	0.73	0.0016	0.055
15	0.5	0.60	0.66	0.75	0.75	0.76	0.70	0.0051	0.102
	2.0	0.74	0.81	0.66	0.73	0.73	0.73	0.0029	0.074
60	0.5	0.68	0.64	0.83	0.84	0.75	0.75	0.0079	0.118
	2.0	0.67	0.73	0.69	0.69	0.73	0.70	0.0007	0.0363
$Z_{gran.}$	0.5	0.76	0.77	0.66	0.72	0.73	0.73	0.0019	0.06
	2.0	0.64	0.74	0.76	0.77	0.74	0.73	0.0027	0.071
	10.0	0.746	0.702	0.711	0.763	0.756	0.738	0.000752	0.0274

Table 3

Composition of mixture: 5.70 kg. of quartz sand and 0.30 kg. salt; pv = 5%;
Simpson laboratory mixer; samples 0.5; 2 and 10 grams, collected by syringe

Time, min.	Sample, grams	x_1 (%)	x_2 (%)	x_3 (%)	x_4 (%)	x_5 (%)	$\bar{x}$ (%)	$\frac{\Sigma (x-\bar{x})^2}{4}$	$\frac{s}{\bar{x}}$
0.5	0.5	3.79	3.98	3.91	3.78	6.61	4.42	1.5141	0.263
	2.0	4.12	2.79	3.19	6.26	7.81	4.83	4.5702	0.443
1	0.5	5.09	4.93	4.36	4.48	5.72	4.92	0.2941	0.11
	2.0	4.69	4.53	4.41	4.86	4.87	4.67	0.0409	0.0433
5	0.5	4.47	5.09	4.37	4.38	5.23	4.71	0.1742	0.0885
	2.0	4.76	4.76	4.57	4.91	4.95	4.79	0.0223	0.0312
15	0.5	4.38	4.27	5.28	4.86	5.71	4.89	0.3584	0.122
	2.0	4.78	4.53	4.61	4.67	5.50	4.82	0.1537	0.0815
60	0.5	8.56	4.98	4.91	4.53	4.63	5.52	2.9194	0.309
	2.0	4.79	4.76	4.73	4.49	4.93	4.74	0.0254	0.0333
$Z_{gran.}$	2.0	4.67	4.50	4.80	4.56	4.78	4.66	0.0174	0.0282
	10.0	4.69	4.76	4.76	4.83	4.81	4.77	0.0030	0.0115

Effect of Certain Mixer Design Elements Upon the Degree of Mixing

The measurement U (Table 1) was carried out after removal of the rolls. Only two gathering arms remained as mixing elements in the mixer. Let us compare the mixing results obtained with and without rolls:

Measurement	S	U
Q =	1.073;	1.025
M =	0,0525;	0.189

(4)

In analyzing the above results, we see that the removal of the rolls reduced the volume of "dead space", which in turn improved the mixing quality index from Q = 1.073 to Q = 1.025. The removal of the rolls reduced the degree of mixing from M = 0.0525 to M = 0.189.

Effect of Mixer Batching Upon the Degree of Mixing

In conducting measurement T (Table 1) the charge was first mixed for 2.5 minutes, then removed from the mixer, poured again, and mixed for another 2.5 minutes. As a result, the mixing degree M = 0.0427 was obtained. This was an improvement over measurement S, where M was 0.0525 and the mixing was conducted for 5.0 minutes.

The importance of the initial mixing of components is not sufficiently appreciated in industrial practice. This is of particular advantage in those cases where one of the components occurs in small quantities, about 1% or less.

Effect of Concentration Upon the Degree of Mixing

Sand was mixed with 1, 5, 10 and 50 percent of salt. The results are presented in Tables 2, 3, 4, 5. The results confirm theoretical calculations. The extent of the variance (including standard deviations) is a function of the concentration of the component in the mixture.

Table 5

Composition of mixture: 3.00 kg. of quartz sand and 3.00 kg. salt; pv = 50%; Simpson laboratory mixer; samples 0.5; 2 and 10 grams, collected by syringe

Time, min.	Sample, grams	x_1 (%)	x_2 (%)	x_3 (%)	x_4 (%)	x_5 (%)	$\bar{x}$ (%)	$\frac{\Sigma (x-\bar{x})^2}{4}$	$\frac{s}{\bar{x}}$
0.5	0.5	52.8	49.6	42.4	46.8	47.15	47.75	14.70250	0.0805
	2.0	46.35	58.85	49.15	45.85	50.15	50.07	27.3970	0.1046
1	0.5	53.8	51.6	26.40	51.4	48.30	46.3	127.59	0.244
	2.0	50.5	52.7	48.45	48.25	52.25	50.43	4.2858	0.041
5	0.5	48.9	47.4	50.8	50.35	38.95	47.26	23.4613	0.1025
	2.0	46.85	48.85	49.3	49.8	50.1	49.48	0.3283	0.0116
15	0.5	49.1	40.4	49.4	49.2	50.8	47.78	17.4930	0.0875
	2.0	48.7	48.85	48.1	50.9	49.65	49.24	1.1668	0.022
$Z_{gran.}$	2.0	48.3	–	48.4	48.6	49.15	48.61	0.1080	0.00677
	10.0	48.60	49.20	50.15	50.1	50.05	49.64	0.4788	0.0139

Table 4

Composition of mixture: 5.40 kg. of quartz sand and 0.60 kg. salt; pv = 10%; Simpson laboratory mixer; samples 0.5; 2 and 10 grams, collected by syringe

Time, min.	Sample, grams	x_1 (%)	x_2 (%)	x_3 (%)	x_4 (%)	x_5 (%)	$\bar{x}$ (%)	$\frac{\Sigma (x-\bar{x})^2}{4}$	$\frac{s}{\bar{x}}$
0.5	0.5	7.21	10.24	6.36	7.61	6.86	7.66	2.2979	0.198
	2.0	9.01	13.15	6.02	6.23	8.72	8.63	6.2788	0.29
1	0.5	9.65	9.72	7.98	8.91	10.41	9.33	0.8550	0.099
	2.0	9.89	9.28	9.38	10.11	9.66	9.66	0.1196	0.0355
5	0.5	9.20	9.41	9.13	10.06	9.75	9.51	0.1527	0.041
	2.0	9.68	9.33	9.66	9.59	9.22	9.50	0.0434	0.022
15	0.5	8.86	8.70	8.67	9.40	9.56	9.04	0.1712	0.0458
	2.0	9.21	9.33	9.36	9.55	9.59	9.41	0.0252	0.0168
60	0.5	8.54	9.02	9.86	8.89	10.01	9.26	0.4089	0.069
	2.0	9.41	9.56	9.52	12.28	9.49	10.05	1.5543	0.124
$Z_{gran.}$	2.0	9.43	9.76	9.51	9.35	8.90	9.41	0.0782	0.0296
	10.0	9.31	9.03	8.71	8.47	9.08	8.92	0.1091	0.037

Conclusions

The theory of mixing is not sufficiently advanced to permit technological "planning" of mixing processes. Under such circumstances, it is convenient to accept the thesis that the mixing process should be investigated by statistical methods.

The degree of mixing could be determined by the standard deviation (or variance) of the concentration. In analyzing the results of the measurements (Tables 2 to 5) we see that the absolute value of the variance S^2 (and consequently of the standard deviation s) is a function of average concentration $\bar{x}$. The measurement results confirm the correctness of the variance coefficient selected by the author as a measure of the degree of mixing. If we divide the experimentally obtained standard deviation, s, by the average concentration $\bar{x}$, the results become independent of the relative concentration of the same component in the mixture.

The results presented in Tables 2-5 confirm the theoretical expectation that the variance (and consequently the standard deviation) of the concentration of the component in the samples is a function of the volume of the sample. In the light of theoretical considerations and experimental data it becomes quite clear that in determining the degree of mixing, the volume of the samples should be indicated. In conducting measurements for the sake of comparison, samples of identical volume should be used.

REFERENCES CITED

1. Buslik, D., *Bull Amer Soc. Test. Mat.*, 66 (1960).
2. Chudzikiewicz, R., *Przem. Chem.*, 38, 419, (1959).
3. Chudzikiewicz, R., *Pomiary, Automatyka, Kontrola*, 6, 185 (1960).
4. Chudzikiewicz, R., *Przegl. Odlewn.*, 10, 212 (1960).
5. Gesell, W., *Giesserei*, 44, 397 (1957).
6. Greathead, J. A. A., Simmonds, W. H. C., *Chem. Eng. Prog.*, 53, 194 (1957).
7. Lacey, P. M. C., Jr., *J. Applied Chem.*, 4, 257 (1954).
8. Reich, H. F., *Chem. Ind.* (Düsseldorf), 12, 276 (1954).
9. Work, L. T., *Chem. Eng. Prog.*, 50, 476 (1954).

Yu. N. Vol'nov
B. V. Ozimov

USSR

Reflection Spectra and Their Application to the Study of Sorption Processes

An attempt at application of reflection spectra to the study of sorption of certain organic liquids by hydrated chromic oxide. Liquids investigated were ethanol, benzene, acetoacetic ester, ethanolamine.

RECENTLY, a number of papers have appeared in which reflection spectra were used for studying adsorption phenomena (1-3), and the effect of optical factors on reflection spectra (4-7) was investigated. The present paper attempts to apply reflection spectra to the study of sorption of certain organic liquids by hydrated chromic oxide.

EXPERIMENTAL PART

Hydrated chromic oxide was prepared by precipitating a $CrCl_3$ solution with a stoichiometric amount of NaOH. The precipitate was washed with hot water until it gave a negative test for chloride and hydroxyl ions, and then dried to constant weight at 120°C. The organic liquids used were ethanol, benzene, acetoacetic ester, and ethanolamine. Water was used in the control experiments. The organic liquids were triply distilled and dehydrated. Their constants corresponded to the literature data. Solid $Cr_2O_3 \cdot nH_2O$ was passed through a sieve - particle size 0.20-0.25 mm. The prepared samples of hydrated chromic oxide were calcined for a period of 2 hours at 120, 200, 360, 600, and 800°C. Reflection spectra were taken of all the samples, both dry samples and samples mixed with the solvent (100 g. $Cr_2O_3 \cdot nH_2O$ + 50 ml. of solvent). The measurements were made in an infinitely thick layer on

This article first published in *Zhur. Vsesoyuz. Khim. Obshchestva im. D. I. Mendeleeva*, 5, No. 5, 591-592 (1960). The authors are associated with the Leningrad Technological Institute of the Refrigeration Industry.

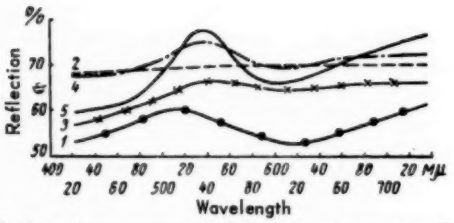

Fig. 1. Data of measurements of the reflection spectra: 1) 120°C; 2) 200°C; 3) 360°C; 4) 600°C; 5) 800°C.

the SF-2 spectrophotometer. The measurement data are depicted in Fig. 1. The reflection spectra of $Cr_2O_3 \cdot nH_2O$ change with the calcining temperature, this being undoubtedly due to the change in hydration and structure of the $Cr_2O_3 \cdot nH_2O$.

Samples prepared at the cited temperatures were studied in the media: ethanol, acetoacetic ester, ethanolamine, benzene, and ethanol vapors. In order to determine the sorption of ethanol vapors, the $Cr_2O_3 \cdot nH_2O$ samples were placed for 48 hours in a desiccator containing anhydrous ethanol. Table 1 compares experimental data for various samples, Table 2 compares the refractive indices of the binding media, % reflection for $\lambda = 589$ mμ, and wavelengths corresponding to the maximum and minimum

Table 1

Weight gain, increase in % reflection for $\lambda = 600$ mμ of $Cr_2O_3 \cdot nH_2O$ samples calcined at various temperatures

Calcining temp., °C	Weight gain after sorption of ethanol vapors, %	Increase in % reflection after sorption, compared to original sample
120	10	15
200	5	9
360	6	10
600	1	2
800	0.5	1

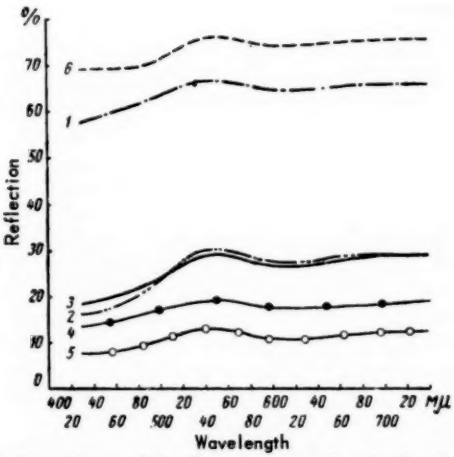

Fig. 2. Dependence of % reflection on wavelength: 1) without solvent; 2) ethanol; 3) water; 4) acetoacetic ester; 5) ethanolamine; 6) ethanol vapors.

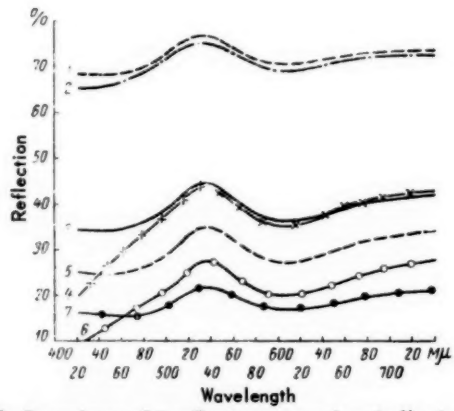

Fig. 3. Dependence of % reflection on wavelength: 1) ethanol vapors; 2) without solvent; 3) ethanol; 4) water; 5) acetoacetic ester; 6) ethanolamine; 7) benzene.

Table 2

Refractive indices of the binding medium, % reflection for $\lambda = 589$ mμ by samples, and wavelengths of the maxima and minima of reflection

Medium	Refractive index n_D	t = 120°C			t = 200°C			t = 360°C			t = 600°C			t = 800°C		
		% Reflection for $\lambda = 589$ mμ	Maximum	Minimum	% Reflection for $\lambda = 589$ mμ	Maximum	Minimum	% Reflection for $\lambda = 589$ mμ	Maximum	Minimum	% Reflection for $\lambda = 589$ mμ	Maximum	Minimum	% Reflection for $\lambda = 589$ mμ	Maximum	Minimum
Water	1.333	53	516	610	52	–	–	17	550	–	34	538	605	35	534	600
Ethanol	1.363	47	514	610	45	–	–	19	548	–	35	536	610	37	536	600
Acetoacetic ester	1.421	40	514	620	36	–	–	15	545	–	28	538	607	29	536	602
Ethanolamine	1.454	–			27.5	–	–	–	545	–	20	536	610	19	534	608
Benzene	1.501	26	520	620	20	–	–	12.5	545	–	17	538	605	37	537	610

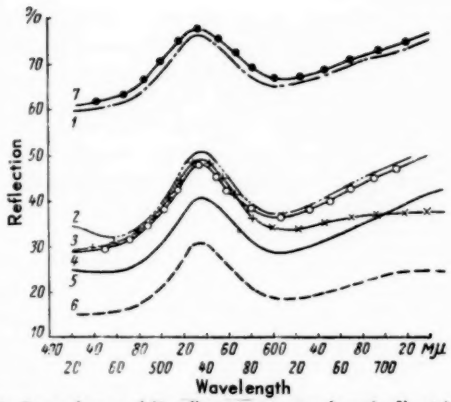

Fig. 4. Dependence of % reflection on wavelength: 1) without solvent; 2) ethanol; 3) water; 4) benzene; 5) acetoacetic ester; 6) ethanolamine; 7) ethanol vapors.

reflection of the above samples. The data obtained confirm the fact that the optical properties of the binding medium have a substantial influence on the percent reflection.

Figs. 2-4 show percent reflection vs. wavelengths curves for certain $Cr_2O_3 \cdot nH_2O$ samples obtained at corresponding temperatures in organic liquids. The experimental data cited enable us to assume that the optical properties of $Cr_2O_3 \cdot nH_2O$ depend on the binding medium. The displacement of the maxima and minima of the percent reflection according to wavelength of $Cr_2O_3 \cdot nH_2O$ in organic liquids is governed by physical and chemical causes, one of which is solvation.

REFERENCES CITED

1. Sidorov, A. I., and Terenin, A. N., *Izvest. Akad. Nauk. SSSR, Otdel. Khim. Nauk* No. 2, 152 (1950).

2. Sidorova, A. I., *Doklady Akad. Nauk SSSR* 72, 327 (1950).

3. Vedeneeva, N. E., *Zhur. Fiz. Khim.* 21, 881 (1947).

4. Zhidkova, Z. V., *Zhur. Eksptl. i Teoret. Fiz.* 27, 458 (1954).

5. Zhidkova, Z. V., *Sbornik Leningrad. Gosudarst. Univ.* (1957).

6. Girin, O. P., and Stepanov, B. I., *Zhur. Eksptl. i Teoret. Fiz.* 27, 467 (1954).

7. Chekalinskii, Yu. I., *Trudy Akad. Nauk Beloruss. SSR* 1, (1956).

8. Rozhdestvenskaya, I. D., and Balandin, A. A., *Referaty Dokladov VIII Mendeleevskogo S'ezda* (Abstracts of Reports of the VIII Mendeleev Conference), Moscow, (1958).

I. A. Uskov
Yu. G. Tarasenko
T. A. Kusnitsyna

UKRAINE, USSR

Compounding of Dissolved Polymethylmethacrylates with Fillers

Development of a method for incorporating fillers into polymethylmethacrylates for increased hardness, higher flow temperature.

INCORPORATION of aminated bentonite into methylmethacrylate by means of a vibration mill during polymerization of the monomer leads to the formation of a filled polymeric material, which possesses improved physical-mechanical characteristics (1). It has been further shown (2) that vibration milling does not produce the same results as chemical grafting of the polymer on the surface of organophilic bentonite during polymerization. The reinforcing effect of the filler in this case is due solely to the intermolecular interaction of macromolecules of the polymer with the surface of filler particles, which is covered with aliphatic amino groups.

It may be assumed, therefore, that it is possible to incorporate the filler directly into the polymer, without affecting its reinforcing effect adversely. The procedure should yield a colloidally reinforced polymeric material, with indices quite as high as those obtained by introducing the filler into a system undergoing polymerization, provided a sufficiently close interaction is obtained between mixture components.

Incorporation of the filler into melted polymethylmethacrylate entails considerable technical difficulties, since it requires thorough mixing of a highly viscous mass at an elevated temperature, to obtain a homogeneous mixture. It is difficult, under such conditions, to avoid destruction of the polymer by thermal oxidation. The effect of prolonged heating on the filler whose surface has been modified, may likewise lead to undesirable consequences, namely, oxidation and decomposition of the organic bentonite complex (in cases where organophilic bentonite is used as an active filler).

Seymour (3) proposed introducing organosols of silica into solutions of organic resins in organic solvents. Subsequent evaporation of the solvent yields resins which contain colloidal silica. However, removal of the solvent from bulky polymer samples is a lengthy process. What is more, uniform distribution of the filler throughout the volume of the polymer is not always possible.

In our experiments the polymer was dissolved and the filler introduced into it while in a dissolved state, so that the filled polymeric material could be separated by precipitation with a suitable agent.

A typical plastic, polymethylmethacrylate, was used to test the proposed method of polymer filling. Chalk (a known inert filler) and octadecylammoniated bentonite, prepared by the method described in (2), were employed as fillers. Sodium-bentonite, which had been subjected to vibration milling in a methylmethacrylate medium, was also used. As shown previously (4), bentonite under such conditions will have a grafted copolymer content, which in our case amounted to approximately 20%.

A weighed sample of the filler was placed in a thick-walled jar together with a measured volume of benzene. The whole was shaken for 30 min. To achieve higher dispersion of the filler, several dozen steel balls 3-5 mm. in diameter were placed in the jar. The suspension obtained was poured into a solution of polymethylmethacrylate in benzene, and the whole was stirred until a homogeneous mixture was obtained. A double amount of methanol was next added to the mixture, with vigorous stirring. A quantitative precipitation of both polymer and filler resulted. The precipitate was washed twice with methanol, dried at 55°C, and ground to powder. The latter appeared perfectly homogeneous on visual examination.

Differential thermographic analysis (5), we believed, might furnish some indications as to the degree of compatibility between the polymer and the filler. Simultaneously, some effect of the filler on the destruction of the polymer might be disclosed. Filler particles, it seemed, might conceivably act

This article first published in *Vysokomolek. Soed.*, 3, No. 1, 37-40 (1961). The authors are associated with the Shevchenko State University, Kiev.

as centers from which the chain reaction of destruction was initiated (6). If that were true, the position of the exothermic peak in the thermograph of the filled polymer should be displaced.

A Kurnakov pyrometer (7) was used in performing the differential thermographic analysis, with magnesium oxide calcined at 800°C taken as a standard. To eliminate the distorting effect of the layer of air between the thermocouple with its adhering polymer matter, and the crucible walls (in the region of the viscous-fluid state), the powdered polymer used for the experiments was mixed with magnesium oxide.

In Fig. 1 are shown thermographs of polymethylmethacrylate, pure and filled with aminated bentonite. The filler is also shown. The destruction of the polymer is accompanied by combustion of the methylmethacrylate formed, which corresponds to a sharp exothermic peak on the curve. The destruction of pure polymethylmethacrylate begins at 330°C and is practically completed at 380°C. The thermograph of the filled polymethylmethacrylate is quite similar to the thermograph of the pure polymer, except that the initial destruction proceeds with lesser intensity and the exothermic peak lies at a higher temperature: 400°C. The oxidation of the organic part of aminated bentonite begins at 165°C, and its combustion is essentially completed at 285°C.

According to thermographic data, introduction of a filler, far from depressing the temperature level of initial destruction, will actually raise somewhat the temperature range in which the exothermic peak is located. This peak represents the combustion of the monomer formed in the course of destruction. On the other hand, an exothermic peak at 285°C, corresponding to combustion of the organic part of the filler, is conspicuously absent in the thermograph of the filled polymer. This suggests a dense screening of the filler surface by

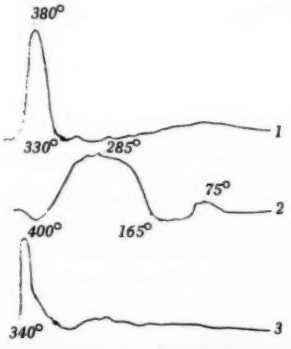

Fig. 1. Thermographs of pure polymethylmethacrylate (1) octadecylammoniated bentonite (2) and polymethylmethacrylate containing 10% octadecylammoniated bentonite (3).

macromolecules of the polymer. It may be said, therefore, that the compounding of the filler with the polymer has been accomplished.

As shown by hardness tests, by a previously used method (1), the filled material obtained is characterized by increased hardness when in a vitreous state. The value 26.9 kg./mm.^{2} obtained for the polymer containing 20% filler, as compared with 24.3 kg./mm.^{2} for the pure polymer, indicates a relative strengthening by 11%.

A still greater effect is noted when the incorporated filler consists of bentonite with some polymethylmethacrylate grafted on it. A 10% concentration of such filler increases the hardness to 28.5 kg./mm.^{2}, i.e., improves it by 17%.

An altogether different picture is observed when an inert filler is introduced into the polymer. Incorporation of chalk in a 10% concentration, under the same conditions as stated above, leads to a decrease of hardness to 23.5 kg./mm.^{2}, i.e. by slightly better than 3%.

The cited data substantiated the view held by Rebinder (8), who thought that to render the filler active so as to obtain a reinforced filled polymeric material, it was sufficient to secure interaction between the filler surface and the polymer, an interaction engendered by forces of intermolecular attraction.

Further experiments were concerned with the behavior of the polymeric material obtained when subjected to deformation at different temperatures. Thermomechanical curves were plotted by the method of Kargin and Sogolova (9). The punch load amounted to 200 g./mm.^{2}, the load action lasting 5.4 sec.

The thermomechanical curves obtained are shown in Fig. 2. Pure polymethylmethacrylate, precipitated by methanol from a benzene solution, has a vitrification temperature of 123°C and a flow temperature of ~230°C. Introduction of 10% aminated bentonite causes only a slight rise of vitrifi-

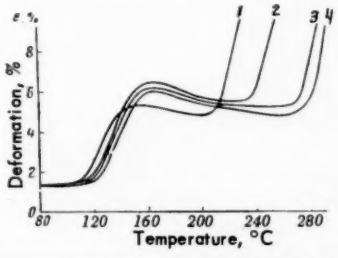

Fig. 2. Thermomechanical curves obtained for: (1) polymethylmethacrylate containing 10% chalk; (2) pure polymethylmethacrylate; (3) polymethylmethacrylate containint 10% bentonite with some polymethylmethacrylate grafted on the latter; (4) polymethylmethacrylate containing 10% octadecylammoniated bentonite.

cation temperature but strongly affects the flow temperature, which is raised nearly 50%, reaching 280°C.

Introduction of bentonite which contains some grafted polymer produces a like effect, the flow temperature reaching 270°C. Chalk, on the contrary, will lower both vitrification (113°C) and flow (205°C) temperatures, as compared with the values obtained for pure polymethylmethacrylate.

It is evident from the reported data that in the case of organophilic bentonites we are dealing with active fillers which are sufficiently well compounded with polymethylmethacrylate. Polymer materials obtained by the proposed method are reinforced colloidally, and are characterized by a higher flow temperature and improved hardness in the vitreous state. The surface of the inorganic filler must be properly modified if the filler mixed with a dissolved polymer is to be effectively compounded with the latter.

CONCLUSIONS

1. With modified bentonites and polymethylmethacrylate as experimental material, a method was developed for incorporating the filler into a dissolved polymer. Separation of the filled polymer followed by way of coprecipitation with a suitable precipitating agent.

2. It was shown by differential thermal analysis that the proposed procedure for the incorporation of the filler results in dense screening of the filler surface by macromolecules of the polymer, provided the components are compatible.

3. The hardness of the filled polymer materials, in the vitreous state, is improved as compared with the pure polymer, and its flow temperature is considerably higher. This is due to the reinforcing action of the fillers, which are active with respect to a given polymer.

REFERENCES CITED

1. Uskov, I. A., *Vysokomolek. Soed.* 2, 200 (1960).
2. Uskov, I. A., Kusnitsyna, T. A., *Vysokomolek. Soed.* 2, 728 (1960).
3. Seymour, R. B., *U. S. Pat.* 2467340-2467342 (1949).
4. Uskov, I. A., *Vysokomolek. Soed.* 2, 926 (1960).
5. Berg, L. G., Nikolaev, A. V., Rode, E. A., *Termografiya, Izd. AN SSSR*, (1944).
6. Bresler, S. E., Os'minskaya, A. T., Popov, A. G., Seminskii, E. M., Frenkel, S. Ya., *Kolloidn. Zhur.* 20, p. 403 (1958).
7. Tzurinov, G. G., *Pyrometer of N. S. Kurnakov*, Publ. Ac. Sci. USSR, Moscow, (1953).
8. Rebinder, I. A., Margaritov, V. B., *Zhur. Rezinovoi Promyshlennosti* 12, 991 (1935).
9. Kargin, V. A., Sogolova, T. I., *Zhur. Fiz. Khim.* 5, 530 (1949).

Journals currently received and monitored

SOVIET UNION

1. **Avtomatika i Telemekhanika** (Automation and Remote Control), Subscription.
2. **Darbai Lietuvos TSR Mokslu Akademijos** (Proceedings of the Academy of Sciences of the Lithuanian SSR), Exchange.
3. **Doklady Akademii Nauk SSSR** (Proceedings of the Academy of Sciences of the USSR), Subscription.
4. **Energetika i Avtomatika** (Power Engineering and Automation), Subscription.
5. **Gazovaya Promyshlennost** (Gas Industry), Subscription.
6. **Inzhenerno-Fizicheskii Zhurnal** (Engineering Physics Journal), Subscription.
7. **Izvestiya Vysshykh Uchebnykh Zavedenii Khimii i Khimicheskaya Tekhnologiya** (Bulletin of Higher Schools of Chemistry and Chemical Technology), Subscription.
8. **Izvestiya Akademii Nauk Kazakhskoi SSR, Seriya Khimicheskaya** (Bulletin of the Academy of Sciences of the Kazakhstan SSR, Chemical Series), Exchange.
9. **Izvestiya Sibirskogo Otdeleniya Akademii Nauk SSSR** (Bulletin of the Siberian Branch of the USSR Academy of Sciences), Exchange.
10. **Izvestiya Akademii Nauk Tadzhikskoi SSR, Otdelenie Geologo-Khimicheskikh i Tekhnicheskikh Nauk** (Bulletin of the Academy of Sciences of the Tajik SSR, Section of Geochemical and Technical Sciences), Exchange.
11. **Kinetika i Kataliz** (Kinetics and Catalysis), Exchange.
12. **Khimicheskaya Promyshlennost** (Chemical Industry), Exchange.
13. **Khimicheskie Volokna** (Chemical Fibers), Subscription.
14. **Khimicheskoe Mashinostroenie** (Chemical Machinery Manufacture), Exchange.
15. **Khimiya i Tekhnologiya Topliv i Masel** (Chemistry and Technology of Fuels and Oils), Subscription.
16. **Khimiya i Khimicheskaya Tekhnologiya** (Chemistry and Chemical Technology), Subscription.
17. **Khimiya i Tekhnologiya Polimerov** (Chemistry and Technology of Polymers), Subscription.
18. **Koks i Khimiya** (Coke and Chemistry), Exchange.
19. **Metallurgiya i Toplivo** (Metallurgy and Fuels), Subscription.
20. **Neft i Gaz** (Oil and Gas), Subscription.
21. **Pishchevaya Tekhnologiya** (Food Technology), Subscription.
22. **Plasticheskie Massy** (Plastics), Subscription.
23. **Trudy Akademii Nauk LSSR, Serii B** (Proceedings of the Academy of the Lithuanian SSR, Series B), Exchange.
24. **Trudy Instituta Yadernoi Fiziki Kazakhskoi SSR** (Proceedings of the Institute of Nuclear Physics of the Kazakhstan SSR), Exchange.
25. **Trudy Akademiya Nauk Tadzhikskoi SSR, Institut Khimii, Issledovaniya v Oblasti Khimii Uglya** (Proceedings of the Academy of Sciences of the Tajik SSR, Institute of Chemistry, Research in the field of Chemistry of Coal), Exchange.
26. **Trudy Instituta Khimicheskikh Nauk, Kazakhskaya SSR** (Proceedings of the Institute of Chemical Sciences, Kazakhstan SSR), Exchange.
27. **Vestnik Moskovskogo Universiteta** (Bulletin of the University of Moscow, Series in Chemistry), Subscription.
28. **Vil'nyuskoe Soveshchanie Elektrokhimikov** (Vilna Conference on Electrochemistry), Exchange.
29. **Vysokomolekulyarnye Soedineniya** (High Molecular Compounds), Subscription.
30. **Zhurnal Prikladnoi Mekhaniki i Tekhnicheskoi Fiziki** (Journal of Applied Mechanics and Engineering Physics), Subscription.
31. **Zhurnal Prikladnoi Khimii** (Journal of Applied Chemistry), Exchange.
32. **Zhurnal Fizicheskoi Khimii** (Journal of Physical Chemistry).
33. **Zhurnal Strukturnoi Khimii** (Journal of Structural Chemistry), Exchange.

34. **Zhurnal Vsesoyuznogo Khimicheskogo Obshchestva im. D. I. Mendeleeva** (Journal of the D. I. Mendeleev All-Union Chemical Society), Exchange.

POLAND

1. **Bulletin de l'Academie Polonaise des Sciences** (Bulletin of the Polish Academy of Sciences), Exchange.
2. **Chemia** (Chemistry), Exchange.
3. **Chemia Stosowana** (Applied Chemistry), Exchange.
4. **Nukleonika** (Nucleonics), Exchange.
5. **Przemysl Chemiczny** (Chemical Industry), Subscription.
6. **Roczniki Chemii** (Annals of Chemistry), Subscription.
7. **Wiadomosci Naftowe** (Petroleum News), Subscription.
8. **Wiadomosci Chemiczne** (Chemical News), Subscription.
9. **Wlokiennictwo** (Textile Industry), Exchange.

CZECHOSLOVAKIA

1. **Chemický Průmysl** (Chemical Industry), Exchange.
2. **Chemické Zvesti** (Chemical Reports), Subscription.
3. **Jaderna Energie** (Nuclear Energy), Subscription.
4. **Paliva** (Fuels), Subscription.
5. **Papir a Celulosa** (Pulp and Paper), Exchange.
6. **Prumysl Potravin** (Food Industry), Exchange.

ROMANIA

1. **Bulletinul Institutului Politehnic Bucarest** (Bulletin of the Polytechnical Institute of Bucarest), Exchange.
2. **Bulletinul Societatii de Chimie din Romania, Studii si Cercetary in Stiintifice Acad. R. P. F. Ser. V, Fiz. si Stiinte Tehnice** (Bulletin of the Romanian Chemical Society, Research Reports, Series V, Physics and Technology Section), Subscription.
3. **Bulletinul Societatii de Chimie din Romania, Studii si Cercetari in Stiintifice Acad. R. P. F., Ser V1, Chimie** (Research Reports, Series V1, Chemistry), Subscription.
4. **Revista de Chimie** (Chemical Review), Exchange.

HUNGARY

1. **Magyar Kémiai Folyóirat** (Hungarian Journal of Chemistry), Subscription.
2. **Magyar Kémikusok Lapja** (Journal of the Hungarian Chemical Society), Subscription.
3. **Magyar Tudományos Akadémia Kémiai Tudományok Osztályanak Közleményei** (Proceedings of the Department of Chemical Sciences of the Hungarian Academy of Sciences), Subscription.
4. **Vegyipari Kutát Intézetek Közlémenyei** (Proceedings of the Research Institutes), Subscription.
5. **Nehézvegyipari Kutáto Intezét Közleményei** (Proceedings of the Research Institute for the Basic Chemical Industries), Subscription.
6. **Magyar Technika** (Hungarian Technology), Subscription.
7. **Gepeszeti Ertesito** (Reports on Machinery), Subscription.

YUGOSLAVIA

1. **Bilten Dokumentacije, Serija D1, Hemija i hemiska industrija** (Chemistry and Chemical Technology), Subscription.
2. **Bilten Dokumentacije, Serija D3, Silikatna industrija** (Silicate Industry), Subscription.
3. **Bilten Dokumentacije, Serija D5, Goriva i maziva** (Fuels and Oils), Subscription.
4. **Chemija u Industrij** (Chemistry and Industry), Exchange.

BULGARIA

1. **Abstracts of Bulgarian Scientific Literature** (Exchange).
2. **Bulletin of the Chemical Institute** (Exchange).

Information retrieval

The key words and abstracts which follow are intended for use with the concept coordination system of information storage and retrieval. For complete details, see the *Chemical Engineering Thesaurus*, available from the American Institute of Chemical Engineers.

Choice of a catalyst for cracking residual petroleum fractions and an investigation of catalyst poisoning in the process—Int. Chem. Eng. Oct. '61, p. 1.

Key Words: 1, Cracking (chemical)-H, Catalysts-H, Catalysts-J, Catalysts-I, Petroleum-A, Residues-A, Gasolines-B, Gases-B, Kaolins-D, Clays-D, Silicon Dioxide-D, Aluminum Oxide-D, Oxides (inorganic)-D, Powdered-, Spherical-, Natural-, USSR-, Porosity-F, Stability-G, Activity-G. 2. Kaolins-D, Clays-D, Silicon Dioxide-D, Aluminum Dioxide-D, Oxides (inorganic)-D, Poisoning-H, Deactivation-H, Catalysts-I, Sulfur-C, Resins-C, Chlorides-C, Metals-C, Vanadium-C, Nickel-C, Metal Organics-C, Coke-C, Tar-C, Asphaltenes-C, Natural-, USSR-.

Abstract: Catalytic cracking of residual petroleum fractions may be carried out over a natural microspherical catalyst, despite poisoning of the catalyst with metals contained in the raw material. There are recommended simple natural catalysts from high-alumina refractory clays with a kaolin base.

Status of crystallization in the Soviet Union—Int. Chem. Eng. Oct. '61, p. 6.

Key Words: 1. Crystallization-H, Crystals-I, Soviet Union-, Education-H, Research-H, Unit Operations-H, Solid State Physics-H, Piezoelectricity-H, Ferroelectricity-H, Ferromagnetism-H, Luminescence-H, Photoelectricity-H, Semiconductors-H, Metallurgy-H, Ceramics-H, Virology-H, Kessel-Strauskii Theory-J, Frank Theory-J, Supersaturation-F, Temperature-F, Supercooling-F, Diffusion-H, Evaporation-H, Mixing-H, Precipitation-H, Fractionation-H, Crystallization-I, Literature-H, Crystallization-G, Ultrasonics-F.

Abstract: An up-to-date, exhaustive survey of current Soviet work in the field of Crystallization, including 118 literature references of importance to many facets of chemical engineering.

Influence of the gaseous medium on the course of physicochemical processes in semiconductor oxides at high temperatures—Int. Chem. Eng. Oct. '61, p. 13.

Key Words: 1. Stoichiometry-H, Reactivity-H, Adsorption-F, Semiconductors-I, Temperature-F, Gaseous-, Activities-H, Conductivity-H, Refractories-I, Zinc Oxide-I, Oxides (inorganic)-I, Chromium Oxide-I, Catalysis-I, Kinetics-H, Dynamics-H, Mechanics-H, Titanium Dioxide-I, Thorium Oxide-I, Zirconium Oxide-I, Uranium Oxide-I, Vacuum-E, Argon-E, Carbon Monoxide-E, Oxides (inorganic)-E, Reactivity-G, Activities-G.

Abstract: Experimental confirmation of the general nature of the influence of the gaseous medium on the progress of certain physico-chemical processes. Kinetics of these processes is controlled by deviation of the composition of semiconductor oxides from the stoichiometric ratios, by dissociation of the oxides, or by absorption of oxygen.

Polymerization of acetone—Int. Chem. Eng. Oct. '61, p. 17.

Key Words: 1. Condensation (chemical)-H, Condensation (chemical)-F, Condensation (chemical)-I, Polymerization-H, Polymerization-F, Polymerization-I, Acetone-A, Acetone-I, Entropy-G, Entropy-H, Thermodynamics-H, Liquid Phase-, Theory-J, Ketones-A, Ketones-I, Acetaldehyde-A, Acetaldehyde-I, Liquids-I, Catalysts-J, Magnesium-D, Bond Energy-F, Aldehydes-A, Aldehydes-I.

Abstract: Using acetone as an example, it is shown that, by applying the principle of preliminary ordering of monomeric molecules in the reaction system, it is possible to polymerize substances which are incapable of polymerization under normal conditions.

Thermo-oxidative degradation of polypropylene: A study of the comparative effectiveness of some antioxidants—Int. Chem. Eng. Oct. '61, p. 19.

Key Words: 1. Inhibitors-H, Degradation-H, Polypropylene-I, Hydrocarbons-I, Polymers-I, Oxidation-H, Temperature-F, Pressure-F, Concentration-F, Stabilizers-J, Amines-D, Aromatic-, Phenols-D, Alcohols-D, Reactions-H, Cyclohexylbenzene-D, Thioura-D, 2,4-Dinitrophenylhydrazine-D, 2,5-Di-tert-butylhydroquinone-D, Diphenylamine-D, Benzidine-D, Polygard-D, 2,4,6-Tri-tert-butylphenol-D, Hydroquinone monobenzyl ether-D, Ionol (2,6-di-tert-butyl-4-methylphenol)-D, Propyl gallate-D, Neozone D (phenyl-β-naphthylamine)-D, Diphenyl-p-phenylenediamine-D, Polyhydric Alcohols-D, Esters-D, Degradation-I, Antioxidants-F, Stability-G, Antioxidants-J, Stabilizers-F, Polypropylene-B, Stabilizers-I, Antioxidants-I.

Abstract: Experimental data on the effect of thirteen different antioxidants on the stability of polypropylene relative to thermo-oxidative degradation.

The equilibrium solid-liquid-gas in the system melamine-ammonia-CO_2—Int. Chem. Eng. Oct. '61, p. 22.

Key Words: 1. Equilibrium-H, Melamine-I, Amines-I, Ammonia-I, Carbon Dioxide-I, Oxides (inorganic)-I, Temperature-F, Critical-, Pressure-F, Phase Diagram-H, Phases-H, Ammonium Carbamate-I, Urea-I, Amides-I, Carbamates (esters)-I, Cyanocarbons-I, Thermodynamics-H, Enthalpy-H, Solubility-H, Equilibrium-I, Solubility-I.

Abstract: An empirical and theoretical investigation of the solubility of melamine in liquid and gaseous carbon dioxide at temperatures to 250°C and pressures to 400 kg./cm.^{2}.

The solubility of melamine in solutions of dicyandiamide in liquid ammonia—Int. Chem. Eng. Oct '61, p. 24.

Key Words: 1. Solubility-H, Solubility-G, Melamine-I, Melamine-C, Ammonia-E, Dicyandiamide-I, Concentration (composition)-F, Temperature-F, Mutual-, Heat of Solution-G, Entropy-G, Enthalpy-G, Properties (chemical)-F.

Abstract: Data on solubility of melamine in solutions of dicyandiamide in liquid ammonia are essential to design of processes for synthesis of melamine from dicyandiamide.

Peculiarities of the catalytic oxidation of naphthalene: Investigation of the oxidation of naphthalene in deep beds of vanadia catalysts—Int. Chem. Eng. Oct. '61, p. 26.

Key Words: 1. Vanadium Pentoxide-D, Oxides (inorganic)-D, Catalysts-J, Yield-G, Productivity-G, Selectivity-G, Oxidation-H, Naphthalene-I, Naphthalene-A, Hydrocarbons-I, Temperature-F, Catalysis-H, Kinetics-H, Reactions-H, Phthalic Anhydride-B, Maleic Anhydride-B, Anhydrides-B, Air-A, Silica Gel-E, Catalysts-I, Vapor phase-, Naphthoquinone-B, Carbon Monoxide-B, Carbon Dioxide-B, Oxides (inorganic)-B, Vanadium Sulfate-D, Sulfates (inorganic)-D, Maleic Anhydride-I, Phthalic Anhydride-I, Anhydrides-I.

Abstract: Data from an industrial reactor show that a combination charge of vanadia catalysts is superior to an industrial vanadium pentoxide catalyst in the catalytic production of phthalic and maleic anhydride from naphthalene.

Peculiarities of the catalytic oxidation of naphthalene: Kinetics of the oxidation of naphthalene in deep beds of vanadia catalysts—Int. Chem. Eng. Oct. '61, p. 31.

Key Words: 1. Oxidation-H, Oxidation-I, Naphthalene-A, Catalysts-J, Catalysts-I, Vanadium Pentoxide-D, Naphthoquinone-B, Phthalic Anhydride-B, Maleic Anhydride-B, Carbon Dioxide-C, Carbon Monoxide-C, Depth-F, Temperature-G, Temperature-F, Selectivity-G, Productivity-G, Beds-I, Conversion-G, Kinetics-H, Diffusion-F.

Abstract: Kinetic equations for the individual reactions taking place in oxidation of naphthalene on vanadia catalysts. Rates of formation determined for phthalic anhydride, maleic anhydride, naphthoquinone, products of severe oxidation.

Polymerization of ethylene under the influence of free radicals. Kinetics of ethylene polymerization in benzene and heptane solution—Int. Chem. Eng. Oct. '61, p. 35.

Key Words: 1. Polymerization-H, Kinetics-H, Ethylene-I, Ethylene-A, Hydrocarbons-I, Olefins-I, Vinyl Compounds-I, Benzene-E, Heptane-E, Azoisobutyronitrile-D, Pressures-F, Activation Energy-G, Reactions-H, Hydrocarbons-A, Catalysts-J, Polyethylene-B, Concentration-F, Molecular weight-G, Polyethylene-I.

Abstract: Kinetics of ethylene polymerization in solution in benzene and in heptane under the influence of azoisobutyronitrile (diniz) under pressures up to 100 atm.

Kinetic relationships in the reaction of olefins with sulfuric acid—Int. Chem. Eng. Oct. '61, p. 39.

Key Words: 1. Reactions-H, Unsaturated-, Hydrocarbons-A, Sulfuric Acid-D, Acids (inorganic)-D, Adsorption-H, Propylene-A, Olefins-A, Vinyl Compounds-A, Reactors-J, Pressure-F, Velocity-F, Kinetics-H, Solubility-F, Diffusion-H, Mass Transfer-H, Rates-H, Concentrations-F, Absorption-H, n-Butylenes-A, Isobutylene-A, Catalysts-J, Adsorption-I, Adsorption-G.

Abstract: Kinetic equations derived which describe, for dispersers of various diameters, the dependence of the rate of propylene adsorption in a grid-plate reactor, on pressure, degree of olefin conversion, and feed rate.

Empirical equilibrium distribution equations for liquid-liquid systems—Int. Chem. Eng. Oct. '61, p. 50.

Key Words: 1. Equilibrium-H, Extraction-H, Batch-, Continuous-, Statics-H, Dynamics-H, Phases-H, Solvents-I, Temperature-F, Liquids-I, Distribution-H, Phases-I, Equations-J, Azeotropes-H, Solubility-H, Solutions (Mixtures)-I, Solutes-I.

Abstract: Possibilities for maximum recovery established independently of the nature of the process (batch or continuous extraction, or extraction with a different relative flow direction of the phases, with or without removal of the mixture).

Kinetic aspects of the catalytic cracking of heavy distillate stocks—Int. Chem. Eng. Oct. '61, p. 55.

Key Words: Cracking (chemical-H, Cracking (chemical)-I, Petroleum-A, Petroleum-I, Catalysts-J, Areas (surface)-F, Diffusion-I, Rates-G, Rates-F, Activation Energy-G, Conversion-G, Space Velocity-F, Temperature-F, Kinetics-H.

Abstract: It is shown that the heavy stock cracking reaction occurs in the transition region between internal and external diffusion, which permits use of low-index catalysts with poorly developed surface area.

A method for the determination of the rates and kinetic constants of complex chemical reactions in a flowing system—Int. Chem. Eng. Oct. '61, p. 58.

Key Words: 1. Rates-G, Reactions-H, Temperature-F, Conversion-G, Catalysis-H, Activation Energy-G, Pressure-F, Reactors-J, Heterogeneous-, Homogeneous-, Kinetics-H, Determination-H, Rates-I, Catalysis-I, Reactions-I, Rates-H.

Abstract: From the magnitude of the activation energy of a heterogeneously catalyzed process, and the temperature dependence, an idea can be obtained concerning the region in which the process is taking place.

Determination of effective diffusion coefficients in porous sorbents—Int. Chem. Eng. Oct. '61, p. 61.

Key Words: 1. Sorption-H, Adsorption-H, Porous-, Diffusion-H, Transport-H, Kinetics-H, Fick's Law-J, Convection-F, Mixing-F, Concentrations-F, Sorption-G, Adsorption-G.

Abstract: Mathematical analysis of the sorption of vapors and gases by porous adsorbents.

Combustion of gas flowing at the surface of a plate—Int. Chem. Eng. Oct. '61, p. 64.

Key Words: 1. Boundries-H, Layers-H, Combustion-H, Gases-I, Heterogeneous-, Homogeneous-, Surfaces-H, Rates-H, Reactions-I, Velocity-F, Temperature-F, Concentration-F, Combustion-G, Equations-J, Laminar Flow-H, Flow-H, Differential-, Steady-State-, Energy-H, Enthalpy-H, Kinetic Energy-H, Diffusion-H, Thermal Conductivity-G, Pressure-F, Density-F, Temperature-F, Viscosity-F, Arrhenius Equation-J, Activation Energy-F, Heat Transfer-H, Fluxes-H, Molar-, Dorodhitsyn Variables-J, Blasius Problem-J, Transcendental-, Hysteresis-H, Ignition-H, Extinction-H, Heat of Friction-F, Adiabetic-, Equilibrium-H, Exothermic-, Critical-, Prandtl Number-J, Turbulent-.

Abstract: Analysis of surface conditions and corresponding velocity, temperature, and concentrations in the boundry layer for combustion of gas flowing at the surface of a plate.

Maintaining optimum temperature conditions in chemical reactors—Int. Chem. Eng. Oct. '61, p. 68.

Key Words: 1. Design-H, Reactors-I, Catalysts-J, Kinetics-H, Homogeneous-, Heterogeneous-, Conversion-G, Synthesis-H, Hydrocarbons-I, Hydrocarbons-B, Carbon Monoxide-A, Hydrogen-A, Temperature-F, Activation Energy-F, Velocity-F, Pressure-F, Recirculation-F, Gases-I, Rectification-I, Distillation-I, Heat Exchange-J, Heat Transfer-J, Mixtures-H, Packings-J, Reactions-H, Reflux-F, Binary-, Flows-H, Heat of Reaction-F, Evaporation-G, Distribution-G, Rates-F.

Abstract: Rectification and distillation heat exchange procedures used to maintain the desired temperature distribution in chemical reactors.

Hydrodynamic conditions on open-grid (turbogrid) trays—Int. Chem. Eng. Oct. '61, p. 74.

Key Words: 1. Trays-I, Perforated-, Grids-I, Columns-I, Towers-I, Absorption-I, Distillation-I, Hydrodynamics-H, Plates-I, Liquid Level-G, Diameter-F, Cross-section-F, Pressure Gradient-G, Hold-up-G, Rates-F, Resistance-G, Throughput-G, Liquid-I, Gases-I, Velocities-F, Friction-F, Interfaces-G, Bubbling-G, Foaming-G, Aeration-F, Turbulence-G, Distribution-H, Design-H, Equipment-I, Sieve Plates-I, Mass Transfer-H, Phases-H, Bubble Plates-I, Oscillation-H, Optimization-H, Showering-F, Showering-, Spraying-F, Spraying-, Ripple Plates-I, Correlations-H.

Abstract: The hydrodynamic processes occurring on grid plates, and determination of optimum operating conditions.

Oxidation of n-butane in the liquid phase under pressure—Int. Chem. Eng. Oct. '61, p. 79.

Key Words: 1. Oxidation-H, Liquid Phase-, Hydrocarbons-I, Hydrocarbons-A, Butane-I, Butane-A, Reactions-H, Costs-H, Production-I, Temperature-F, Phases-H, Acetic Acid-B, Acids (carboxylic)-B, Methylethyl Ketone-B, Ketones-B, Ethyl Acetate-B, Acetates (esters)-B, Esters-B, Formaldehyde-B, Aldehydes-B, Acetaldehydes-B, Methanol-B, Alcohols-B, Ethanol-B, Acetone-B, Formic Acid-B, Air-A, Solvents-J, Critical-, Rates-H, Oxidation-I, Reactors-J, Autoclaves-J, Catalysts-J, Titanium-D, Condensers (process equipment)-J, Reflux-, Solubilities-H, Stratification-H, Peroxides-C, Pressure-F, Conversion-G, Chain Reactions-H, Concentrations-G.

Abstract: Optimum conditions determined for oxidation of n-butane by air to acetic acid, under pressure and in the presence of a solvent.

Investigations of polyacrylonitrile fibers obtained at various drafts—Int. Chem. Eng. Oct. '61, p. 85.

Key Words: 1. Physical Properties-G, Physical Properties-H, Fibers-I, Spinning-F, Spinning-J, Acrylonitrile-I, Acrylic Compounds-I, Cyanides-I, Nitriles-I, Vinyl Compounds-I, Drawing-H, Electron Microscope-J, Baths-J, Plasticizing-, Precipitating-, Polymers-I, Diffraction-J, Temperature-F, Strength-G.

Abstract: Investigation of changes in fiber texture caused by changes in draft and temperature, and quantitative data on structure of acrylonitrile fibers.

The movement of a bed of solid particles in rotary kilns—Int. Chem. Eng. Oct. '61, p. 88.

Key Words: 1. Particles-I, Solids-I, Kilns-I, Kilns-J, Rotary-, Rates-H, Dimensional Analysis-J, Movement-H, Design-H, Scale-up-H, Velocity-F, Movement-G, Density-F, Viscosity-F, Size-F, Diameter-F, Angle of Repose-F, Cross-section-F, Reynolds Number-J, Froude Number-J, Gallileo Criterion-J, Flow-H, Steady State-, Temperature-F, Beds-J.

Abstract: Dimensional analysis used to investigate role of various factors affecting a moving bed of solid particles in a rotary kiln, and determination of scale-up conditions.

Graft copolymerization in the presence of benzoyl peroxide-dimethyl aniline with the aid of irradiation—Int. Chem. Eng. Oct. '61, p. 93.

Key Words: 1. Polymerization-H, High Energy-, Irradiation-J, Free Radicals-J, Mechanism-H, Polymerization-I, Reactions-H, Water-E, Methanol-E, Alcohols-E, Bonds (chemical)-F, Polymers-B, Polymers-I, Copolymerization-H, Graft Polymerization-H, Polyvinyl Chloride-A, Chlorinated Hydrocarbons-A, Halogenated Hydrocarbons-A, Plastics-A, Thermoplastics-A, Vinyl Chloride Plastics-A, Vinyl Compounds-A, Polyethylene-A, Hydrocarbons-A, Membranes-I, Benzoly Peroxide-D, Dimethyl Aniline-D, Aniline-D, Amines-D, Initiators-J, Activators-J, Methyl Methacrylate-A, Acrylic Compounds-A, Esters-A, Methacrylates-A, Vinyl Acetate-A, Acetates (esters)-A, Styrene-A, Graft Polymers-B, Concentrations-F, Temperature-F, Graft Polymerization-G, Intensities-F, Time-F, Refractive Index-J.

Abstract: Experimental data on use of initiator-activators for graft copolymerization with irradiation, and determination of optimum initiator-activator concentrations at which grafting is relatively large and separation of homopolymers from the membrane is still possible.

Study of bubble formation in glass melting under vacuum—Int. Chem. Eng. Oct. '61, p. 99.

Key Words: 1. Bubbles-G, Bubbles-H, Glasses-B, Glasses-I, Corrosion-H, Refractories-I, Porosity-G, Reactions-H, Temperature-F, Composition-F, Optical-, Vacuum-E, Furnaces-J, Electric-, Nitrogen-C, Carbon Dioxide-C, Oxides (inorganic)-C, Oxygen-C, Nitrates (inorganic)-F, Carbonates (inorganic)-F, Pressure-F, Viscosity-F, Sorption-H, Supersaturation-G.

Abstract: Most probable cause of bubble formation in molten glass under vacuum is supersaturation of the glass melt with gases. Variation of the pressure in industrial furnaces does not appear to influence bubble formation.

Determination of solid phase concentration in a two-phase medium in upward motion in a vertical tube—Int. Chem. Eng. Oct. '61, p. 106.

Key Words: Velocities-H, Phases-H, Flows-H, Flows-I, Two-phase-, Tubes-I, Vertical-, Cross-section-F, Flows-G, Rates-H, Slippage-G, Suspending-H, Particles-I, Gases-I, Densities-F, Volume-F, Heat Transfer-H, Heat Exchange-H.

Abstract: In a two-phase liquid-solids system, the phenomenon of slippage leads to the condition that the fraction of the cross section occupied by each of the components does not correspond to the value that would be obtained by a calculation based on the feed rates for the gaseous and solid substances.

Chlorination of low-pressure polyethylene and its compounding with polyvinyl chloride—Int. Chem. Eng. Oct. '61, p. 110.

Key Words: 1. Plastics-I, Synthesizing-H, Polyethylene-A, Polyethylene-I, Hydrocarbons-I, Polymers-I, Thermoplastics-I, Elastomers-I, Chlorination-H, Chlorinated Polyethylene-B, Physical Properties-G, Impact Resistance-G, Plasticization-H, Copolymerization-H, Polymerization-H, Reactions-H, Elasticization-H, Mixtures-H, Chloroprene-I, Butadiene-I, Styrene-I, Vinyl Compounds-I, Polyurethane-I, Sulfo-Chlorinated Polyolefins-I, Rubber-I, Chlorine-D, Halogens-D, Crystallinity-G, Fluidized Beds-J, Free Radicals-J, Porofor-D, Benzoyl Peroxide-D, Initiators-J, Temperature-F, Thermal Stability-G, Transparency-G, Compounding-H, Polyvinyl Chloride-I, Polyvinyl Chloride-A, Tensile Strength-G, Elasticity-G, Stabilizers-J, Molecular Weight-F, Mixing-H.

Abstract: Work on chlorination of polyethylene to produce appropriate elastomers for elasticization of polyvinyl chloride, plus data on compounding of the two polymers.

Effect of sulfur and some of its compounds on the Oxo process—Int. Chem. Eng. Oct. '61, p. 117.

Key Words: 1. Oxo Process-I, Oxo Process-H, Oxo Process-G, Catalysts-J, Promoters-J, Sulfur-J, Rates-G, Reactions-H, Hydrogenation-H, Aldehydes-B, Alcohols-B, Oxonation-H, Olefins-A, Hydrocarbons-A, Sulfur-C, Carbon Disulfide-C, Sulfides (inorganic)-C, Ethyl Mercaptan-C, Mercaptans-C, Thiophene-C, Tetrahydrothiophene-C, Gasoline-A, Cobalt Stearate-D, Stearates (salts)-D, Temperature-F, Pressure-F, Conversion-G, Kinetics-H, Equilibrium-H.

Abstract: Investigation of effect of sulfur, carbon disulfide, ethyl mercaptan, tetrahydrothiophene, and thiophene on the oxonation of olefins to aldehydes in the Oxo process.

Some electrophysical properties of polymer complexes of tetracyanethylene with metals—Int. Chem. Eng. Oct. '61, p. 122.

Key Words: 1. Tetracyanethylene-A, Tetracyanethylene-I, Polymers-I, Chelation-H, Reactions-H, Coatings-B, Plastics-B, Films-B, Metals-A, Metals-I, Copper-I, Iron-I, Nickel-I, Physical Properties-G, Electrical Properties-G, Resistivity-G, Capacitance-G, Temperature-F, Heating Time-F, Surfacing-F, Polarization-H, Plates-I.

Abstract: Results of research aimed at commercial production of coatings and plastics based on polymeric chelate compounds of tetracyanethylene with metals.

Factors affecting the degree of mixing of granular materials—Int. Chem. Eng. Oct. '61, p. 124.

Key Words: 1. Theory-H, Mixing-H, Mixing-I, Bulk Materials-I, Granular-, Particles-I, Convection-J, Diffusion-J, Shearing-J, Mixers-J, Paddle-, Drum-, Roll-, Concentrations-F, Scattering-H, Deviation-J, Variance-J, Design-H, Mixing-G, Volume-F, Density-F, Surface-F.

Abstract: A theoretical treatment of mixing of granular solids. If the experimentally obtained standard deviation, s, is divided by the average concentration, $\bar{x}$, the results are independent of the relative concentration of the component in the mixture.

Reflection spectra and their application to the study of sorption processes—Int. Chem. Eng. Oct. '61, p. 129.

Key Words: 1. Reflection Spectra-J, Adsorption-H, Sorption-H, Shromic Oxide-D, Ethanol-I, Benzene-I, Acetoacetic Ester-I, Ethanolamine-I, Temperature-F, Reflection Spectra-G.

Abstract: An attempt at application of reflection spectra to the study of sorption of certain organic liquids by hydrated chromic oxide. Liquids investigated were ethanol, benzene, acetoacetic ester, ethanolamine.

Compounding of dissolved polymethylmethacrylate with fillers—Int. Chem. Eng. Oct. '61, p. 132.

Key Words: 1. Methyl Methacrylate-I, Acrylic Compounds-I, Esters-I, Methacrylates-I, Vinyl Compounds-I, Polymerization-H, Fillers-F, Physical Properties-G, Polymers-A, Bentonite-D, Clays-D, Fillers-D, Chalk-D, Mixing-H, Hardness-G, Deformation-F, Compounding-H.

Abstract: A method of incorporating fillers into polymethylmethacrylates for increased hardness, higher flow temperatures.